AN INVESTIGATION INTO THE EFFECTS OF METABOLIC DISTURBANCE ON
MONOCYTE INFLAMMATORY RESPONSE AND REGULATION

JUSTIN WILLIAM KILLICK
Doctor of Philosophy

ASTON UNIVERSITY

September 2015

Aston University

AN INVESTIGATION INTO THE EFFECTS OF METABOLIC DISTURBANCE ON MONOCYTE
INFLAMMATORY RESPONSE AND REGULATION

Justin William Killick

Doctor of Philosophy

2015

The presence of chronic inflammation is associated with increased nutrient availability during obesity or type 2 diabetes which contributes to the development of complications such as atherosclerosis, stroke and myocardial infarction. The link between increased nutrient availability and inflammatory response remains poorly understood. The functioning of monocytes, the primary instigators of the inflammatory response was assessed in response to obesity and increased glucose availability.

Monocyte microRNA expression was assessed in obese individuals prior to and up to one year after bariatric surgery. A number of microRNAs were identified to be dysregulated in obesity, some of which have previously been linked to the regulation of monocyte inflammatory responses including the microRNAs 146a-5p and 424-5p. Weight loss in response to bariatric surgery lead to the reversal of microRNA changes towards control values.

In vitro treatments of THP-1 monocytes with high concentrations of D-glucose resulted in decreased intracellular NAD^+:NADH ratio, decreased SIRT1 deacetylase activity and increased P65 acetylation. However the increased osmotic concentration inhibited LPS induced inflammatory response and TNFα mRNA expression.

In vitro treatment of primary human monocytes with increased concentrations of D-glucose resulted in increased secretion of a number of inflammatory cytokines and increased expression of TNFα mRNA. Treatment also resulted in decreased intracellular NAD^+:NADH ratio and increased binding of acetylated P65 to the TNFα promoter region. *In vitro* treatments of primary monocytes also replicated the altered expression of the microRNAs 146a-5p and miR-424-5p, as seen in obese individuals.

In conclusion a number of changes in monocyte function were observed in response to obesity and treatment with high concentrations of D-glucose. These may lead to the dysregulation of inflammatory responses contributing to the development of co-morbidities.

Key words

> Monocytes
> High Glucose
> Inflammation
> Bariatric Surgery
> MicroRNA

Dedications

This thesis is dedicated in loving memory of my Dad, Anthony Killick, whose constant love, support and understanding is sorely missed.

Abbreviations

2-NBDG - 2-(N-(7-Nitobenz-2-oxa-1,3-diazol-4-yl) Amino)-2-Deoxyglucose

ADP - Adenosine diphosphate

AGO - Argonaute

AID – Activation-induced cytidine deaminase

AKT – Protein Kinase B

ANOVA – Analysis of variance

AR - Aldose reductase

ATCC – American Tissue Culture Collection

ATP - Adenosine triphosphate

BCA – Bicinchoninic acid

BMI – Body mass index

BSA - Bovine serum albumin

CD14 - Cluster of differentiation 14

CD16 - Cluster of differentiation 16

CD36 – Cluster of differentiation 36

ChIP- Chromatin immunoprecipitation

COPD – Chronic obstructive pulmonary disease

CpG - Cytosine-phosphate-guanine

CR3 – Complement receptor 3

Ct- Cycle threshold

CVD – Cardiovascular disease

DAMPs - Danger-associated molecular patterns

DMSO- Dimethylsulphoxide

cDNA- Copy Deoxyribonucleic acid

DGCR8 - DiGeorge Critical Region 8

DNA- Deoxyribonucleic acid

DnMT - DNA methyltransferases

ECACC – European Collection of Authenticated Cell Cultures

EDTA- Ethylenediaminetetraacetic acid

EGF- Epidermal growth factor

EGTA- Ethylene glycol tetraacetic acid

ERK1/2 - Extracellular signal-regulated kinases 1/2

FBS- Foetal bovine serum

FCCP- Carbonyl cyanide-4-phenylhydrazone

FGF-2 – Fibroblast growth factor 2

Flt-3L – FMS-like tyrosine kinase 3 ligand

G-CSF – Granulocyte colony-stimulating factor

GLUT- Glucose Transporter

GLP-1 – Glucagon-like peptide-1

GIP – Gastric inhibitory peptide

GM-CSF – Granulocyte macrophage colony stimulating factor

GRB10 - Growth factor receptor-bound protein 10

GRO – Growth Regulated Oncogene

HAT – Histone acetyltransferase

HCl – Hydrochloric acid

HDAC – Histone deacetylase

HOMO-IR – Homeostatic model assessment for insulin resistance

HSE – Health survey for England

IDF - International Diabetes Federation

IFNα2 – Interferon alpha 2

IFN-γ – Interferon gamma

IL-1α – Interleukin 1 alpha

IL-1β – Interleukin 1 beta

IL-1RA - Interleukin

IL-2 – Interleukin 2

IL-3 – Interleukin 3

IL-4 – Interleukin 4

IL -5 – Interleukin 5

IL-6- Interleukin 6

IL-7 – Interleukin 7

IL-8 – Interleukin 8

IL-9 – Interleukin 9

IL-10- Interleukin 10

IL-13 – Interleukin 13

IL-15 – Interleukin 15

IL-17 – Interleukin 17

ICAM-1 - Intercellular adhesion molecule 1

IKKβ - IκB kinase-β

IP-10 - Interferon gamma-induced protein 10

IRAK - Interleukin-1 receptor-associated kinase

IR - Insulin receptor

IRS- Insulin receptor substrate

JNK1- Jun Kinase 1

LPS- Lipo-polysaccharide

LFA1 - Lymphocyte function associated antigen 1

MAPK – Mitogen-activated protein Kinase

MCP-1 - Monocyte chemoattractant protein-1

MCP-3 - Monocyte chemoattractant protein-3

MDC – Macrophage derived chemokine

MHC-II - Major histocompatibility complex class 2

MIP-1α – Macrophage inflammatory protein 1 alpha

MIP-1β - Macrophage inflammatory protein 1 beta

MMP2 – Matrix metalloproteinase-2

MMP9 - Matrix metalloproteinase-9

mOsm - Milliosmole

miRNA - Micro-ribonucleic acid

mRNA - Messenger-ribonucleic acid

MSR1 – Macrophage Scavenger Receptor 1

MTT- 3-(4,5-dimethylthiazol-2-yl)-2,5-diphenyltetrazolium bromide

NaBu – Sodium Butyrate

NAD^+ – Nicotinamide adenine dinucleotide

NADH – Reduced nicotinamide adenine dinucleotide

NADPH - Nicotinamide adenine dinucleotide phosphate

NaOH – Sodium Hydroxide

NFI-A - Nuclear factor 1 A-type

NF-κB - Nuclear factor kappa-light-chain-enhancer of activated B cells

NICE – The National Institute for Health and Care Excellence

OPD- o-phenylenediamine dihydrochloride

p53 – Tumour protein 53

PAMPs – Pathogen-associated molecular patterns

PBMC - Peripheral blood mononuclear cells

PBS - Phosphate buffered saline

PCIA - Phenol chloroform isoamyl alcohol

PDGF -AA – Platelet derived growth factor AA

PDGF -BB - Platelet derived growth factor BB

PMA - Phorbol 12-myristate 13-acetate

PPAR - Peroxisome proliferator-activated receptor

Pri-miRNA – Primary miRNA

Pre-miRNA – Precursor miRNA

PS – Phosphatidylserine

PSGL-1 - P-selectin glycoprotein ligand 1

PTP1B - Protein tyrosine phosphatase

qPCR - Quantitative polymerase chain reaction

RISC - RNA-induced silencing complex

RNA - Ribonucleic acid

RNA Pol – RNA polymerase

ROS - Reactive oxygen species

RPMI media - Roswell Park Memorial Institute media

sCD40L – Soluble cluster of differentiation 40 ligand

SD – Standard deviation

SDS - Sodium dodecyl sulphate

SEM - Standard error of the mean

SIRT - Sirtuin

SLAN - 6-sulfo LacNAc

T2DM – Type 2 Diabetes mellitus

TAE- Tris acetate EDTA buffer

TGFα – Transforming growth factor alpha

TGF-β1 - Transforming growth factor β1

TIR - Toll-interleukin-1 receptor

TMB - Tetramethylbenzidine

TNFα - Tumour necrosis factor alpha

TNFβ – Tumour necrosis factor beta

TLR - Toll like receptor

TRAF6 - TNF receptor-associated factor 6

PVDF - Polyvinylidene difluoride

VCAM - Vascular cell adhesion molecule

Table of Contents

List of Figures

List of tables

1   Introduction

1.1   Metabolic diseases

Metabolic disorders include a wide variety of conditions which lead to a disruption in normal metabolism. Many of these are inherited genetic disorders such as Wilson's disease and phenylketonuria which are caused by genetic mutations of the ATP7B (Bull, Thomas et al. 1993) and phenylalanine hydroxylase (PAH) (DiLella, Kwok et al. 1986) genes respectively. Genetic mutations of the ATP7B gene results in ineffective biliary secretion of excess dietary copper leading to accumulation. Mutations in the PAH gene leads to reduced enzymatic activity resulting in decreased or inhibited conversion of phenylalanine to tyrosine which can cause a variety of neurological disorders. However, this thesis focused on acquired metabolic disorders. Acquired metabolic disorders describe conditions that mainly arise as a consequence of environment such as the viral destruction of the beta pancreatic cells in type 1 diabetes mellitus, or those that arise as a consequence of poor diet and/or lifestyle such as type 2 diabetes mellitus, obesity and metabolic syndrome. The development of acquired metabolic disorders is subject to many risk factors such as diet, lifestyle, genetics, increasing age and birth weight. Prenatal nutritional availability is believed to influence the development of epigenetic marks leading to "foetal programming" which can increase the risk of developing metabolic diseases such as type 2 diabetes and metabolic syndrome (Godfrey, Sheppard et al. 2011, Brenseke, Prater et al. 2013). The Barker hypothesis, also known as the thrifty phenotype hypothesis, suggests that low foetal growth due to low maternal nutrition leads to an increased risk of developing disorders such as type 2 diabetes, hypertension, stroke and coronary heart disease (Hales and Barker 1992). Evidence of this effect was shown by the Dutch famine birth cohort studies. The Dutch famine occurred during World War 2 when food supplies were cut off from the populace by the occupying German army as punishment for Dutch opposition (Painter, de Rooij et al. 2006). Individuals born during this period had a low birth weight and were shown to have an increased risk of developing the aforementioned metabolic disorders later in life. Poor maternal nutrition during pregnancy experienced by the developing foetus is postulated to cause "foetal programming" resulting in the child having an adaption to a low nutrient environment (Hales and Barker 1992). Increased maternal nutritional availability has also been shown to result in an increased risk of developing metabolic syndrome and type 2 diabetes later in life (Boney, Verma et al. 2005). These studies suggest that nutritional availability can have a profound effect on epigenetic modifications leading to increased risk of developing metabolic diseases.

1.1.1 Diabetes

Diabetes is a metabolic disease characterised by prolonged elevation of blood glucose. The World Health Organisation defines type 2 (T2) diabetes as a fasting plasma glucose level of ≥7.0mmol/l or random venous plasma glucose concentration ≥ 11.1 mmol/l (WHO/ International Diabetes Federation (IDF),2006). In 2014 the number of worldwide cases of diabetes was estimated at 387 million (IDF, 2014),90% of which were classified as type 2 diabetes (Shi and Hu 2014). Approximately 6% of the UK population has been diagnosed with T2 diabetes (Gatineau Mary 2014). T2 diabetes is characterised either by reduced insulin secretion by pancreatic beta cells or cellular desensitisation to secreted insulin which neutralises its ability to regulate blood glucose concentration. A number of risk factors which contribute to the development of T2 diabetes have been identified. These include: increasing age; genetic makeup; high blood pressure; a dietary intake high in sugar and fat; being overweight and ethnicity. Due to high incidence of long term complications associated with diabetes, management of the condition is costly, with approximately 10% of the NHS annual budget spent on treatment of diabetes and its complications with this predicted to rise to 17% by 2035 (Hex, Bartlett et al. 2012). Diabetes can result in a number of debilitating complications including micro- and macro-vascular complications. Microvascular complications can include retinopathy, nephropathy and neuropathy which can result in blindness, renal failure and nerve damage. Macrovascular complications include coronary heart disease, stroke and peripheral vascular complications which can result in limb amputation and hypertension (Amos, McCarty et al. 1997).

1.1.2 Management of type 2 diabetes

T2 diabetes requires a multifaceted approach to management to monitor and avoid the development of further complications. This includes the patient implementing lifestyle changes such as reducing weight, increasing physical activity and lowering dietary intake of saturated fats. Blood glucose levels should be monitored and self-managed by the patient through implementation of the aforementioned lifestyle changes, and where appropriate, the use of medication in addition to this. Depending on the aetiology of the diabetes, the patient may be treated with insulin, insulin sensitising drugs (such as rosiglitazone) or metformin. Weight reduction through changing dietary intake, increasing levels of physical activity (Lim, Hollingsworth et al. 2011) and bariatric surgery have all been reported as effective methods of reversing obesity induced T2 diabetes (Brethauer, Aminian et al. 2013).

1.1.3 Obesity

1.1.3.1 Epidemiology

The WHO reports that currently worldwide 39% of adults over 18 are overweight and 13% obese (Shanthi Mendis and Cecile Mace 2014). The 2013 Health Survey for England (HSE) recorded that 26% of men and 24% of women were obese (BMI > 30) and 41% of men and 33% women were overweight (BMI > 25) (Mindell 2014, NICE 2014). Obesity currently costs the NHS £6 billion annually in direct medical treatment, expected to rise to between 10 and 12 billion by 2030 (Richard Dobbs 2014). Being obese or overweight is commonly considered a major risk factor for a number of non-communicable diseases such as diabetes and CVD a number of studies have challenged this. A recent meta-analysis by Flegal, Kit et al. (2013) assessed data from 97 studies with a combined sample size of 2.88 million individuals including more than 270,000 deaths in order to establish the association between mortality and BMI. The meta-analysis found that individuals who were overweight (BMI: 25 - < 30) or had grade one obesity (BMI: 30 - < 35) had either a lower risk or no increased risk of mortality when compared to normal weight individuals (BMI: 18.5 - < 25). Since its publication this paper has been criticised and several other papers published that refute its claims that being overweight or grade one obese results in no increase in mortality. The main criticism levelled against this paper is the inclusion of individuals who were smokers, frail due to old age or had chronic medical conditions associated with weight loss such as cancer into the normal weight group (Tobias and Hu 2013, Willett, Hu et al. 2013). Other publications that eliminated weight loss due to disease or smoking found all-cause mortality to increase with BMI and the optimum BMI to be between 20 – 24.9 (Berrington de Gonzalez, Hartge et al. 2010, Wormser, Kaptoge et al. 2011).

A number of studies have assessed the prevalence of obesity within families, mono- and di- zygotic twins. These studies have discovered obesity to have a high degree of heritability, between 40%-70% (Turula, Kaprio et al. 1990, Magnusson and Rasmussen 2002, Wardle, Carnell et al. 2008) not observed in adopted individuals (Stunkard, Sorensen et al. 1986), suggesting a potential genetic background. In the years since these studies were published a number of genetic contributors of obesity have been identified including inherited mutations in a variety of genes. A number of these genes appear highly expressed in the CNS and the hypothalamus and play a role in appetite and satiety. Several mutations have been discovered that interfere with the leptin signalling pathway, leptin being a hormone responsible for stimulating the feeling of satiety in response to food, which affect either leptin production, secretion (Montague, Farooqi et al. 1997, Fischer-Posovszky, Funcke et al. 2015) or the leptin receptor (Clement, Vaisse et al. 1998). These mutations cause the individual

to feel constantly hungry which results in them eating more in an attempt to satisfy the hunger resulting in obesity. Another example of genetic mutations resulting in obesity can be observed in mutations within the MC4R receptor (Huszar, Lynch et al. 1997, Vaisse, Clement et al. 1998, Loos, Lindgren et al. 2008). The MC4R receptor is a G protein coupled receptor predominately expressed within the hypothalamus and the CNS which has a role in regulating appetite (Yang 2011). Several genome wide association studies have been undertaken identifying 97 individual loci to be associated with the development of obesity (Locke, Kahali et al. 2015).

1.1.3.2   Obesity management

Bariatric surgery is becoming a more commonly employed means of treating obesity. Bariatric surgery describes a range of surgical procedures performed on people with obesity with the aim of causing weight reduction. Bariatric surgery is believed to result in weight loss and increased glycaemic control through a variety of mechanisms. Surgically restricting the size of the stomach or bypassing the duodenum and upper jejunum causes decreased calorie intake and increased weight loss. This restriction of calorie intake and weight loss leads to improved glucose control (Dixon, O'Brien et al. 2008, Isbell, Tamboli et al. 2010) and rapid improvements in hepatic insulin sensitivity followed by later improvements in insulin sensitivity of peripheral tissues (Bojsen-Moller, Dirksen et al. 2014).

The evidence base in support of bariatric surgery as a treatment to aid weight loss has grown substantially in recent years, with it now being seen as an effective means of treating obesity and its associated co-morbidities, especially type 2 diabetes (Sjostrom, Narbro et al. 2007, Brethauer, Aminian et al. 2013). Bariatric surgery has also been shown to be more effective than conventional weight loss methods at reducing weight, improving mortality in addition to being more effective at improving glycaemic control during type 2 diabetes than currently prescribed medication (Mingrone, Panunzi et al. 2012, Schauer, Kashyap et al. 2012). Guidelines set out by NICE state that bariatric surgery should be available for individuals with a body mass index (BMI) greater than 35 who have failed to lose weight through medical weight loss programs (NICE 2014). Recent additions (November 2014) to the NICE guidelines state that obese individuals (BMI > 30) with recently diagnosed type 2 diabetes should receive expedited assessment for bariatric surgery.

A study comparing patients prescribed medication to aid weight loss, (incretin analogues, anti-hypertensive and lipid lowering medications) and given lifestyle advice and dietary adjustments with patients who received bariatric surgery in addition to the aforementioned treatment found that

those who received bariatric surgery lost significantly more weight and achieved greater glycaemic control (Schauer, Kashyap et al. 2012). These individuals' homeostasis model assessment of insulin resistance (HOMO-IR) also improved significantly compared to individuals who did not receive bariatric surgery. Furthermore, participants who had bariatric surgery reduced the medication they took over the 12 month period since receiving surgery from an average of 2.5 diabetic medications to 0.9, whereas those only receiving the intensive medical therapy started on an average of 2.8 diabetic medications which increased to 3.0 over the 12 month period (Schauer, Kashyap et al. 2012). The reduction in use of diabetic medications in those receiving bariatric surgery in addition to being beneficial to the patient is also beneficial to the healthcare service through the reduction in the cost of condition management which is cumulative. This is supported by a number of systematic reviews which concluded that bariatric surgery, whilst initially expensive, reduces healthcare spending over the long term due to reduced incidence of co-morbidities associated with obesity such as type 2 diabetes and cardiovascular disease(Picot, Jones et al. 2009, Terranova, Busetto et al. 2012, Borisenko, Adam et al. 2015).

1.1.4 Ageing as a risk factor of metabolic disease

The process of ageing is associated with decreased glucose tolerance, insulin sensitivity and an increased risk of developing metabolic disorders such as type 2 diabetes, CVD and metabolic syndrome. Reaven, Gold et al. (1979) first demonstrated that aged rats had decreased β-cell insulin secretion in response to stimulation with glucose when compared to younger controls. Rowe, Minaker et al. (1983), compared young (22-37 year olds) non obese participants with old (63-77 year olds) non-obese participants and found that the old participants had decreased insulin sensitivity, resulting in a reduced rate of glucose uptake by peripheral tissue. The study also showed that there was no impairment of secreted insulin's ability to bind to the insulin receptor, suggesting that the decreased insulin sensitivity was due to a defect in the insulin signalling pathway downstream of receptor binding. Through assessing non-obese participants, the study demonstrated that increased age, independent of dietary intake or obesity, resulted in an increased risk of developing metabolic disease.

Development of metabolic disease has also been attributed to accelerated ageing. Wang et al. 2006, showed that insulin resistance in diabetic mice models led to increased muscle atrophy. The authors found that this was due to decreased PI3K activity resulting in decreased inhibition of E3 ubiquitin conjugating enzymes, causing increased activation of the ubiquitin proteasome proteolytic pathway (UPP) which resulted in muscle protein degradation. Muscle wastage is a large contributing factor to age related frailty. The chronic inflammation associated with metabolic diseases is also believed to

contribute to accelerated ageing and insulin resistance (Shoelson, Lee et al. 2006, Franceschi, Capri et al. 2007).

1.2   Insulin signalling and obesity induced resistance

1.2.1   Insulin signalling

Insulin is a peptide hormone, 51 amino acids in length, produced and secreted by the beta cells of the islets of Langerhans, the endocrine cells of the pancreas. Insulin is secreted in response to a number of stimuli including: free fatty acids; the amino acids arginine and leucine; the incretins glucagon-like peptide-1 (GLP-1) and gastric inhibitory polypeptide (GIP); cephalic stimulation in anticipation of food, and most importantly elevated blood glucose (Wilcox 2005). Insulin has many functions in the body although perhaps its most significant being in the maintenance of blood glucose and fatty acid concentrations. Elevated blood glucose results in increased glucose uptake by the beta cells of the pancreas which in turn stimulates the secretion of insulin. Secreted insulin causes many cellular metabolic and mitogenic changes, resulting in increased cell growth and division and causing a metabolic shift away from glycogen breakdown and glucose production to increased cellular glucose uptake and storage, thus restoring blood glucose to within normal range. Although many tissues respond to secreted insulin the majority of insulin's systemic effects are mediated by the skeletal muscle, the liver and adipose tissues. The skeletal muscle is essential for insulin's rapid effect on reducing blood glucose concentration, as it has the capacity to take up and store large quantities of glucose quickly.

Insulin signalling begins at the plasma membrane when secreted insulin binds to the insulin receptor (IR). The IR is a heterotetrameric complex consisting of two extracellular alpha subunits responsible for ligand binding and two transmembrane beta subunits with intracellular tyrosine kinase activity, which upon ligand binding propagate the signal into the cell causing the associated cellular insulin response (figure 1.2.1). The beta subunits' tyrosine kinase activity is repressed prior to ligand binding by the alpha subunit. Upon ligand binding, the alpha subunits' imposed kinase repression is removed and the beta subunits auto-phosphorylate tyrosine residues located within their cytoplasmic tails. Auto-phosphorylation causes the beta subunits to undergo a conformational change resulting in increased kinase activity allowing tyrosine phosphorylation of intracellular substrates. The activated IR has been shown to phosphorylate a number of intracellular proteins including those belonging to the insulin receptor substrate (IRS) family of proteins (IRS I, II, III and IV), DOK 4/5, GAB1, Cbl, Shc and APS proteins. The phosphorylated substrate proteins form signalling complexes with effector

proteins via Src homology 2 (SH2) domains resulting in the activation of several signalling pathways (Avruch 1998, Taniguchi, Emanuelli et al. 2006).

The majority of insulin's effects result from the activation of the phosphatidylinositol 3-kinase (PI3K) and mitogen activated protein kinase (MAPK) pathways. The summation of these activated pathways is increased translocation of additional glucose transporters (GLUT) proteins to the cell membrane increasing glucose uptake. Insulin stimulates an increase in cellular storage of glucose as glycogen, decreased gluconeogenesis, increased breakdown of glucose by glycolysis and increased fatty acid synthesis and storage as triglycerides. This results in the cells switching from an energy usage metabolic state to an energy storage state (White 1997).
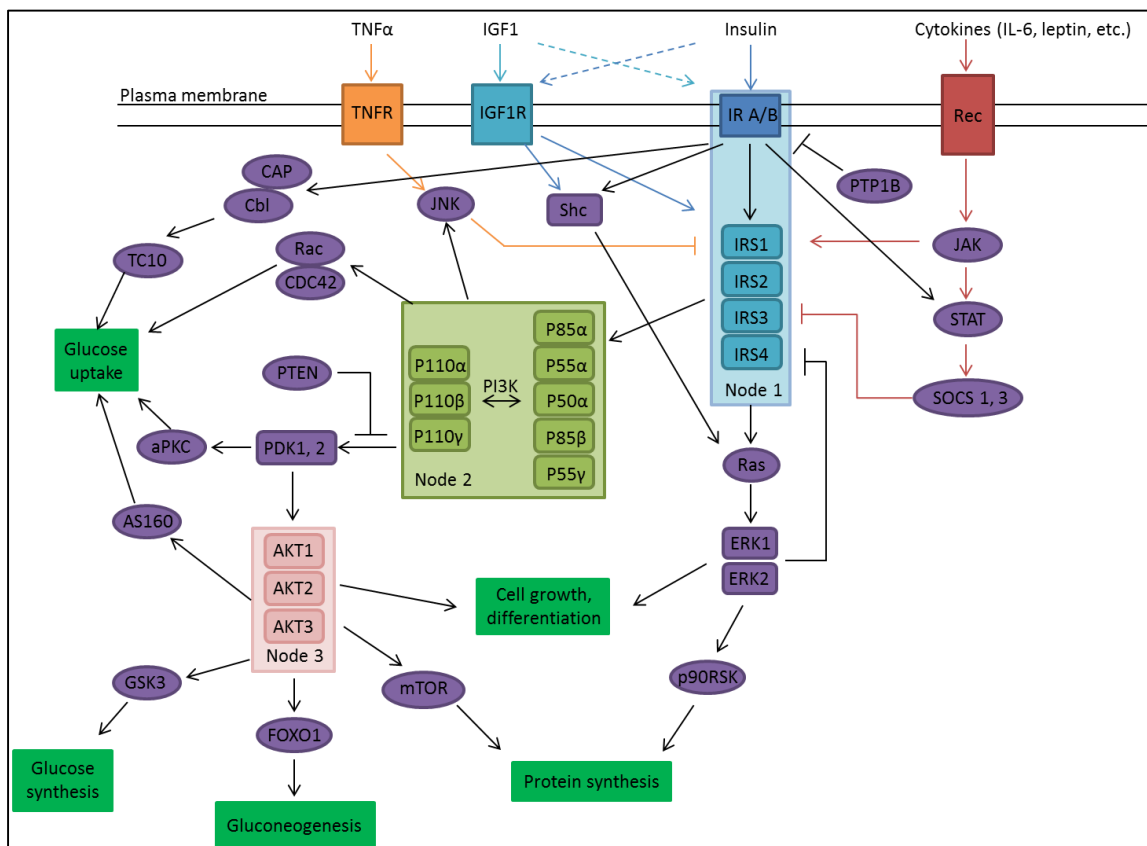
Figure 1.2.1: Insulin signalling pathways,

Adapted from Taniguchi, Emanuelli et al. (2006). Figure displays the critical nodes of the insulin signalling pathway. Critical nodes downstream of the insulin receptor are denoted by black arrows and downstream of the Insulin growth factor receptor in blue. Pathways activated by cytokines TNFα, IL-6 and by leptin interfere with the insulin signalling pathway (Red and orange lines). Three important nodes of insulin signalling are shown within this figure, the insulin receptor and insulin receptor substrates (light blue box), phosphatidylinositol 3-kinase signalling (light green box) and AKT/protein kinase B signalling (pink box).

1.2.2   Insulin resistance in obesity

Insulin resistance is defined as a decrease in cellular response to beta cell secreted insulin which results in insufficient glucose uptake and storage, decreased suppression of hepatic glucose production, and increased lipolysis and free fatty acid (FFA) secretion by adipose tissue. The summation of this leads to dysregulation of glucose and lipid homeostasis, which the beta cells attempt to compensate for by increasing insulin secretion and eventually leads to beta cell death. The resulting elevated concentration of circulating glucose and lipids lead to gluco- and lipo-toxic effects and aid in progressing complications of diabetes such as atherosclerosis. It has long been established that a causal link exists between obesity and insulin resistance, with several potential mechanisms being identified (Kahn, Hull et al. 2006, Qatanani and Lazar 2007). A relationship between the ectopic deposit of lipids in insulin sensitive tissues and development of insulin resistance was first shown in studies by Randle, Garland et al. (1963). They established that when rat heart and diaphragm muscle were treated with fatty acids they showed a decreased uptake of glucose in response to insulin. Randle et al (1963) believed that the accumulation of these lipids within the muscle tissue decreased glycolysis thus decreasing glucose uptake. It has since been shown that lipid-induced insulin resistance in muscle cells is due to impaired insulin signalling and insulin-stimulated glucose uptake, rather than glycolysis. The increased accumulation of lipids within these tissues has been proposed to result in increased intracellular metabolites such as fatty acids, diacylglycerol (DAG), ceramides and acyl-CoAs; these metabolites have been shown to interfere with the insulin signalling pathway. Yu, Chen et al. (2002) observed that increased intracellular acyl-CoA and DAG resulted in activation of serine protein kinase C (PKC) which they showed to phosphorylate IRS1 preventing IRS1 activation of the PI3-kinase preventing induction of the normal insulin signalling pathway.

Obesity has also been associated with systemic chronic low grade inflammation resulting from an increase in circulating inflammatory cytokines. The increased presence of inflammatory cytokines and markers such as TNFα, IL-6 and CRP has been found to predict development of insulin resistance and type 2 diabetes (Dandona, Aljada et al. 2004, Shoelson, Lee et al. 2006). It has been observed in both mice and humans that obesity results in the accumulation of macrophages to the stromal vascular fraction of white adipose tissue (Weisberg, McCann et al. 2003, Xu, Barnes et al. 2003). Studies have shown that the increased presence of inflammatory cytokines interferes with insulin signalling through activation of Jun kinase 1 (JNK1) and IκB kinase-β (IKKβ) which phosphorylates inhibitory serine residues on IRS1 disrupting the insulin signalling pathway (Kanety, Feinstein et al. 1995, Yuan, Konstantopoulos et al. 2001, Gao, Zhang et al. 2004). Inhibition of macrophage recruitment to adipose tissue using MCP-1 and CCR2 knock out mice ameliorated insulin resistance

which occurred as a result of being fed a high fat diet (Kanda, Tateya et al. 2006, Weisberg, Hunter et al. 2006).

1.3   Inflammatory signalling

The Gram negative bacterial cell wall component, LPS, induces an inflammatory response through binding to the TLR4 receptor (Poltorak, He et al. 1998). When LPS is present it is bound by the LPS binding protein (LBP) which subsequently binds to the membrane protein CD14; together this complex binds to and activates signal transduction through TLR4. TLR4 signal transduction can be divided into either myeloid differentiation primary response gene 88 (MyD88) dependent or independent pathways observed to be responsible for activating gene expression of pro-inflammatory cytokines (Kawai, Adachi et al. 1999) or interferons respectively (Kawai, Takeuchi et al. 2001). Upon LPS recognition and binding, TLR4 recruits the adaptor protein MyD88 to its intracellular toll-interleukin-1 receptor (TIR) domain. MyD88 proceeds to recruit the proteins interleukin-1 receptor-associated kinase 1 (IRAK-1) and IRAK-4 which it activates (Suzuki, Suzuki et al. 2002). IRAK-4 subsequently activates IRAK-1 (Lye, Mirtsos et al. 2004). Both IRAK-1 and IRAK-4 dissociate from the MyD88 protein and bind to TNF receptor-associated factor 6 (TRAF6) resulting in its ubiquitination. Ubiquitinated TRAF6 subsequently activates the protein transforming growth factor-β-activated kinase 1 (TAK1) which proceeds to phosphorylate and activate the kinases IKKβ and MAPK leading to activation of the NF-κB and MAPK pathways (Sato, Sanjo et al. 2005).

The NF-κB pathway has been shown to play a key role in the induction of inflammation in response to a number of stimuli including bacterial antigens such as LPS and inflammatory cytokines such as TNFα and IL-1. The NF-κB protein family consists of five members, P65, P52, P50, RelB and c-Rel, the NF-κB complex is comprised of a dimer of these members. Many variations of the NF-κB complex exist comprised of dimers of these subunits, however the P65:P50 complex is believed to be the primary mediator of the canonical NF-κB pathway. In the absence of an inflammatory stimulus NF-κB is sequestered in the cytoplasm where it is bound by IκB proteins resulting in functional inhibition. Upon the introduction of an inflammatory stimulus, a signalling cascade occurs that results in the activation of the IκB kinase (IKK). IKK phosphorylates the NF-κB bound IκB proteins which results in the IκB proteins being ubiquitinated by ubiquitin ligase and degraded by proteasome complexes. The unbound NF-κB translocates to the nucleus where it binds to target gene promoter regions resulting in transcription of inflammatory genes. This process of nuclear translocation is dependent on phosphorylation of the NF-κB complex by protein kinase A (PKA) and A kinase interacting kinase 1 (AKIP1) at serine 276 (Zhong, Voll et al. 1998, Chen, Williams et al. 2005). Phosphorylation of serine

276 has been shown to promote and increase binding of the acetyltransferase protein p300 which results in acetylation of P65 at various sites. Acetylation of P65 has been shown to occur at a number of lysine residues modulating NF-κB transcriptional activity. Acetylation of lysine 221 has been reported to increase DNA binding and prevents newly expressed IκB binding to, and inhibiting NF-κB (Chen, Mu et al. 2002). Acetylation of P65 lysine-310 has been observed to be necessary for full transcriptional activity(Chen, Mu et al. 2002).

A number of cytokines including IL-6 and IL-10 elicit their respective responses through the Janus Kinase (JAK) signal transducer and activator of transcription (STAT) pathway. The binding of the cytokine results in cell membrane receptor dimerisation leading to recruitment of JAK kinases which auto-phosphorylate and phosphorylate the receptor cytoplasmic tail. This allows the binding of proteins belonging to the STAT family which are subsequently phosphorylated by the recruited JAK kinases. Phosphorylation of STAT results in its dimerisation and translocation to the cell nucleus (Decker and Kovarik 2000). The transcriptional activity of STAT once translocated to the nucleus has been shown to be influenced by its acetylation status (Wieczorek, Ginter et al. 2012). The histone acetyltransferase proteins p300 and CREB-binding protein have been reported to acetylate STAT proteins at multiple lysine residues which results in increased DNA binding and STAT transcriptional activity (Wang, Cherukuri et al. 2005, Yuan, Guan et al. 2005). Histone deacetylase proteins including SIRT1 have been shown to deacetylate STAT proteins resulting in decreased STAT transcriptional activity and decreased translocation of STAT to the nucleus (Nie, Erion et al. 2009).

1.4   Monocytes

Monocytes form between 2% and 8% of the total leukocyte population and are mononuclear, with a characteristic kidney shaped nuclei. Monocyte cells are a type of leukocyte belonging to the innate immune system. They perform several roles in the body, primarily instigation of inflammation and recruitment of other immune cells to sites of infection or tissue damage. They are also phagocytic and antigen presenting so can digest invading pathogens at sites of infection and present the antigen, activating cells of the adaptive immune system. Monocytes also use their phagocytic activity to remove apoptotic and necrotic cells from the sites of infection and inflammation, aiding in the resolution of inflammation (Devitt and Gregory 2008). Monocytes also migrate to a variety of tissues replenishing resident macrophages and dendritic cells.

Monocytes can be divided into several subpopulations depending on their expression of cell surface receptor proteins and their cytokine secretion profiles. The current belief is that monocytes can be divided into at least three subpopulations: a "classical" or "Mon 1" monocyte, a "non-classical" or

"Mon 3" monocytes and a third "intermediate" or "Mon 2" population (Shantsila, Wrigley et al. 2011). In humans the total monocyte population consists of 80% - 90% Mon 1 classical monocytes, 5% - 7% Mon 2 intermediate monocytes and 6% - 8% Mon 3 non-classical monocytes (Cros, Cagnard et al. 2010, Cornwell, Vega et al. 2013).

Mon 1 monocytes are characterised by high cell surface expression of CD14 and negative expression of CD16 (CD14^{++}, CD16^{-}), Mon 2 monocytes express low levels of both CD14 and CD16 (CD14^{+}, CD16^{+}) and Mon 3 monocytes express low levels of CD14 and high levels of CD16 (CD14^{+}, CD16^{++}) (Ghattas, Griffiths et al. 2013).

Recently the presence or absence of 6-sulfo LacNAc (SLAN) modified P-selectin glycoprotein ligand 1 (PSGL-1) has been observed to allow further separation of the CD16 positive Mon 2 and Mon 3 sub-populations (Hofer, Zawada et al. 2015). Whereby the Mon 2 monocytes are SLAN negative and the Mon 3 monocytes SLAN positive (Hofer, Zawada et al. 2015). The presence of the SLAN modification has been shown to block the recognition of PSGL-1 to P- and E- selectin thereby influencing the trafficking of the individual monocyte sub-populations (Schakel, Kannagi et al. 2002). The monocyte sub-populations mon 1, and at lower concentrations mon 2, have both been observed to express cell surface C-C chemokine receptor type 2 (CCR2) (Shantsila, Wrigley et al. 2011). This receptor recognises the chemokine MCP-1 which is secreted from a variety of tissues in response to inflammation or tissue damage. MCP-1 secreted from inflamed, infected or damaged tissues form a chemotactic gradient which CCR2 expressing monocyte populations can follow allowing trafficking and recruitment of these monocytes to the site of MCP-1 secretion (Maus, Henning et al. 2002).

Several studies have attempted to further characterise each sub-population to identify the roles they perform within the context of innate immunity, inflammation and disease. These studies have identified each sub-population to display a unique gene expression profile, with the CD16 positive Mon 2 and Mon 3 populations having the more similar gene expression profile (Frankenberger, Sternsdorf et al. 1996, Belge, Dayyani et al. 2002, Wong, Tai et al. 2011). The results of the genome wide analysis on monocyte sup-populations by Wong, Tai et al. (2011) identified the classical Mon1 monocytes to express genes related to angiogenesis and wound healing perhaps suggesting a role in tissue repair. The authors identified the Mon 2 intermediate sub-population to have increased expression of genes related to antigen presentation whilst the Mon 3 non-classical sub-population expressed genes related to cyto-skeletal rearrangement suggesting potential specialisations towards antigen presentation and phagocytosis respectively. The cytokine secretion profiles also differ between the monocyte sub-populations. CD16 positive Mon 2 and Mon 3 monocytes have been

observed *in vitro* to secrete higher concentrations of TNFα and IL-1β basally and upon stimulation with various TLR ligands, whereas Mon 1 monocytes secrete higher concentrations of IL-10, IL-6 and IL-8 (Frankenberger, Sternsdorf et al. 1996, Belge, Dayyani et al. 2002, Cros, Cagnard et al. 2010, Wong, Tai et al. 2011). These populations have been shown to shift during certain chronic inflammatory conditions such as rheumatoid arthritis and sepsis, both of which result in expansion of the CD16 positive Mon 2 population (Poehlmann, Schefold et al. 2009, Rossol, Kraus et al. 2012). These studies also showed that expression of these population markers vary within the subpopulations themselves producing a spectrum of expression between the groups, meaning that although it is convenient to divide monocyte populations into three distinct groups in reality it appears to less defined.

Upon tissue recruitment monocytes differentiate into resident macrophages. Macrophages as a cell type are often classified into two individual subtypes, "M1" or "M2". Although as with monocytes, macrophages exist as a spectrum of phenotypes dependent on the environment and cytokines they are exposed to rather than two individual well defined populations (Murray, Allen et al. 2014). Macrophages with a more M1 phenotype are described as "classically activated" and secrete high concentrations of inflammatory cytokines and reactive oxygen species. Macrophages with a more M2 phenotype direct inflammatory resolution and tissue repair (Verreck, de Boer et al. 2006).

1.5 LPS induction of an inflammatory response through TLR4

1.5.1 Toll-like receptors

The Toll receptor was first discovered in Drosophila where it was identified to play a role in embryonic development (Hashimoto, Hudson et al. 1988) and activation of the innate immune system (Lemaitre, Nicolas et al. 1996). Since then a total of 13 Toll receptor homologues, Toll-like receptors, have been discovered, 10 of which are present in humans. Toll-like receptors are a family of proteins responsible for the recognition of invading pathogens and necrotic or apoptotic cells through recognition of conserved molecules entitled Pathogen-associated molecular patterns (PAMPs) or Danger-associated molecular patterns (DAMPs). Viral and bacterial components such as viral double stranded RNA, bacterial flagellum and cell wall components such as lipoteichoic acid (LTA) and lipopolysaccharide (LPS) are examples of PAMPs recognised by TLR-3 (Alexopoulou, Holt et al. 2001), TLR-5 (Hayashi, Smith et al. 2001), TLR-2 (Schwandner, Dziarski et al. 1999), and TLR4 (Poltorak, He et al. 1998) respectively.

1.5.2 TLR4 signalling

LPS is a cell wall component found in gram negative bacteria that induces an inflammatory response through binding to the TLR4 receptor (Poltorak, He et al. 1998). When LPS is present it is bound by the LPS binding protein (LBP) which subsequently binds to the membrane protein CD14; together this complex binds to and activates signal transduction through TLR4. TLR4 signal transduction can be divided into either myeloid differentiation primary response gene 88 (MyD88) dependent or independent pathways, observed to be responsible for activating gene expression of pro-inflammatory cytokines (Kawai, Adachi et al. 1999) or interferons respectively (Kawai, Takeuchi et al. 2001).

Upon LPS recognition, TLR4 recruits the adaptor protein MyD88 to its intracellular toll-interleukin-1 receptor (TIR) domain. MyD88 proceeds to recruit the proteins interleukin-1 receptor-associated kinase 1 (IRAK-1) and IRAK-4, which it activates (Suzuki, Suzuki et al. 2002). IRAK-4 subsequently activates IRAK-1 (Lye, Mirtsos et al. 2004). Both IRAK-1 and IRAK-4 dissociate from the MyD88 protein and bind to TNF receptor-associated factor 6 (TRAF6) resulting in its ubiquitination. Ubiquitinated TRAF6 subsequently activates the protein transforming growth factor-b-activated kinase 1 (TAK1) which proceeds to phosphorylate and activate the kinases IKKβ and MAPK leading to activation of the NF-κB and MAPK pathways (Sato, Sanjo et al. 2005).

Figure 1.5.1: MyD88 dependent and independent TLR4 signalling pathways

Adapted from Lu, Yeh et al. (2008). Figure displays canonical MYD88 independent and dependent TLR4 signalling pathways.

1.5.3   Monocyte recruitment and role in inflammatory response

The recruitment of monocytes to sites of infection from the circulation can be divided into three stages: rolling, adhesion and transmigration. Typically, the first leukocytes to reach sites of infection and tissue damage are neutrophils; upon reaching the site they proceed to phagocytose invading pathogens and secrete pro-inflammatory cytokines and chemokines which in turn stimulates the adjacent endothelium to express adhesion molecules on their luminal surface and attract monocytes to the site of infection(Wantha, Alard et al. 2013). The inflamed endothelium displays increased luminal surface expression of the adhesion molecules P-selectin, E-selectin and L-selectin (Kansas 1996). The first stage of monocyte transmigration, rolling, occurs when circulating monocytes

approach the inflamed endothelium, upon which they bind to the endothelial expressed selectins via P-selectin glycoprotein ligand 1 (PSGL-1) (McEver and Cummings 1997). These interactions allow the monocytes to adhere to the inflamed endothelium.

The inflamed endothelium also expresses integrins which are involved in slowing the rolling speed of the monocytes, allowing stronger adherence to the endothelium. The monocyte expressed integrin CD18 is integral to the rolling process, forming complexes with CD11a to form lymphocyte function associated antigen 1 (LFA1) and CD11b to form macrophage receptor 1 (MAC1) (Dunne, Ballantyne et al. 2002, Salas, Shimaoka et al. 2004). These both interact with endothelial expressed intercellular adhesion molecule 1 (ICAM-1) (Lo, Lee et al. 1991, Chesnutt, Smith et al. 2006). The binding of these integrins stops the monocytes rolling and provides a firm adherence to the endothelium allowing transmigration to the site of inflammation. The cells can pass through the endothelium via two routes, either the paracellular or transcellular route. The paracellular route involves cells passing through the inter-endothelial junctions and the transcellular route which involves the monocytes passing through the endothelial cells (Feng, Nagy et al. 1998).

Upon recruitment to the site of inflammation the monocytes begin to phagocytose invading pathogens or apoptotic cells, engulfing them into phagosomes. Vesicles called lysosomes contain antimicrobial enzymes and have NADPH oxidase localised within their membranes, a protein capable of producing reactive oxygen species (ROS). These lysosomes migrate to the phagosome, fuse with it, and in the process secrete into the phagosome the antimicrobial enzymes and ROS. The result of this is the digestion of the engulfed pathogen. This allows the monocyte to display digested antigen on cell surface major histocompatibility complex class II (MHC-II) receptors. The antigen presenting monocytes can pass into the lymphatic system, reaching lymph nodes where they can present the antigen engaging the adaptive immune response. During the process of phagocytosis, monocytes and resident macrophages secret pro-inflammatory cytokines and chemokines such as TNFα and monocyte chemoattractant protein-1 (MCP-1) and MCP-3 which propagate the inflammatory response and recruit additional cells of the immune system.

Monocytes are one of the cell populations most responsible for propagating the inflammatory response in addition to playing a role in its resolution through the clearance of apoptotic cells. Upon apoptosis phosphatidylserine (PS) is externalised to the outer plasma membrane where it is recognised and bound by monocyte and macrophage CD14; this interaction allows the recognition and clearance of apoptotic cells (Devitt, Pierce et al. 2003). Co-culture of apoptotic lymphocytes and neutrophils with LPS stimulated monocytes inhibits the secretion of the pro-inflammatory cytokine

TNFα and stimulates the secretion of the anti-inflammatory cytokines interleukin 10 (IL-10) and transforming growth factor β1 (TGF-β1) (Voll, Herrmann et al. 1997).

1.5.4   The effects of obesity and diabetes on monocyte function

The hyperlipidaemic and hyperglycaemic environments found as a result of obesity and type 2 diabetes have been observed to lead to aberrant monocyte and macrophage function, contributing to the development of these metabolic conditions and their complications. Elevated free fatty acids (Gordon 1960, Reaven, Hollenbeck et al. 1988) and oxidised LDL (Njajou, Kanaya et al. 2009, Kelly, Jacobs et al. 2010) present during obesity and type 2 diabetes contribute to the development of complications such as atherosclerosis through immuno-modulation of monocytes and macrophages. Oxidised LDL and free fatty acids have been observed to be recognised and internalised by monocytes and macrophages via recognition and interaction with a variety of scavenger receptors including CD36 and Macrophage Scavenger receptor 1 (MSR1). Both CD36 and MSR1 have been found to be the primary mediators of oxidised LDL and free fatty acid uptake and internalisation within monocytes and macrophages (Endemann, Stanton et al. 1993, Baillie, Coburn et al. 1996, Kunjathoor, Febbraio et al. 2002). The contribution of CD36 to lipid uptake, foam cell formation and plaque formation has been established in a number of CD36 knockout studies (Febbraio, Podrez et al. 2000, Zhao, de Beer et al. 2005, Kuchibhotla, Vanegas et al. 2008). The MRS1 receptor has also been observed to contribute to the internalisation of both oxidised and acetylated LDL contributing to atherosclerotic plaque formation (Suzuki, Kurihara et al. 1997, Babaev, Gleaves et al. 2000). Exposure of primary human monocytes to oxidised LDL has recently been observed to result in epigenetic reprogramming to induce long term changes in the expression of proatherogenic genes (Bekkering, Quintin et al. 2014). The authors treated primary human monocytes with oxidised LDL for 24 hours followed by a six day washout period. The treated monocytes were shown to have increased histone H3K4 trimethylation (a marker of active transcription) in specific promoter regions resulting in increased expression of a number of proatherogenic genes including TNFα, IL-6, IL-8, MCP-1, MMP2, MMP9, CD36 and MSR1 (Bekkering, Quintin et al. 2014).

Oxidised LDL has been observed to be an activator of PPARγ mediated gene expression (Nagy, Tontonoz et al. 1998) which has been shown in turn to promote the differentiation of monocytes to macrophages (Tontonoz, Nagy et al. 1998). This increase in PPARγ activation has also been observed to upregulate the expression of cell surface CD36 which in turn increases uptake of oxidised LDL (Han, Hajjar et al. 1997, Feng, Han et al. 2000). Increased expression of CD36 has itself been shown to

induce inflammation through the formation of a TLR4-TLR6 heterodimer through which lipids are proposed to cause an inflammatory response leading to increased secretion of inflammatory cytokines (Stewart, Stuart et al. 2010). The culmination of this process is the continued recruitment of additional monocytes to the inflamed endothelium, differentiation of these cells into macrophages and foam cells and the formation of an atherosclerotic plaque.

The increased availability of glucose during diabetes has also been shown to have an immuno-modulatory effect on monocytes, increasing pro-inflammatory cytokine secretion and monocyte recruitment to the endothelium and adipose tissue. Primary monocytes isolated from individuals with either type 1 or type 2 diabetes had higher expression of TNFα, IL-6, IL-1α and IL-8 mRNA compared to control participants (Giulietti, van Etten et al. 2007). This has also been observed *in vitro* after treatment of THP-1 monocytes with high concentrations of glucose over a 72 hour period (Shanmugam, Reddy et al. 2003). The authors observed increased mRNA expression of a number of inflammatory cytokines and chemokines including TNFα IL-1β and MCP-1. The increased secretion of inflammatory cytokines has been found to disrupt insulin signalling pathways through increased activation of the JNK1 and IKKB kinases which phosphorylate IRS1 leading to its inhibition attenuating, insulin signalling pathways (Kanety, Feinstein et al. 1995, Yuan, Konstantopoulos et al. 2001, Gao, Zhang et al. 2004). Mouse models lacking the IKKB protein were protected from high fat diet and age induced insulin resistance (Arkan, Hevener et al. 2005). The importance of inflammatory cytokines, particularly TNFα, in the development of insulin resistance has been highlighted in a number of studies. Rodent models of obesity including mice and Zucker rats either genetically lacking the gene for TNFα or treated with infliximab, an anti-TNFα antibody, show increased insulin sensitivity in response to obesity (Cheung, Ree et al. 1998, Cheung, Wang et al. 2000, Qin, Qiu et al. 2007). Patients suffering from chronic inflammatory conditions such as rheumatoid arthritis and psoriasis, both of which are associated with insulin resistance, displayed improved insulin sensitivity upon treatment with anti-TNFα antibodies (Gonzalez-Gay, De Matias et al. 2006, Pina, Armesto et al. 2015). Treatment of the THP-1 monocytic cell line and primary monocytes with high concentrations of glucose over a 72 hour period has been shown to increase cell surface expression of TLR2 and TLR4 as well as NF-κB signalling (Dasu, Devaraj et al. 2008). The same research group also noted this effect was increased when the cells were co-incubated with increased concentrations of glucose and the fatty acid palmitate (Dasu and Jialal 2011). Increased expression of TLR2 and TLR4 has been observed to contribute to and be associated with increased insulin resistance in a variety of cell types (Song, Kim et al. 2006, Caricilli, Nascimento et al. 2008). Under hyperglycaemic conditions monocyte adhesion and transmigration through a number of cell types (Meng, Park et al. 2010, Nandy,

Janardhanan et al. 2011) has been observed to increase due to increased endothelial expression of the adhesion molecules ICAM-1 and vascular cell adhesion molecule (VCAM-1) (Manduteanu, Voinea et al. 1999). Increased recruitment of monocytes to the endothelium is a significant contributing factor to the development of atherosclerosis. Several studies have observed increased monocyte recruitment to the adipose tissue occurring during obesity and diabetes (Lumeng, Deyoung et al. 2007, Oh, Morinaga et al. 2012). A recent study introduced hyperglycaemic conditions in human participants over a three hour period via a hyperglycaemic clamp which resulted in increased recruitment of monocytes to the subcutaneous abdominal adipose tissue (Tencerova, Kracmerova et al. 2015). The increased recruitment of monocytes and differentiated macrophages to the adipose tissue has been observed to reduce insulin sensitivity and glucose uptake in adipocytes through inflammatory cytokine mediated suppression of IRS-1 and GLUT4 (Lumeng, Deyoung et al. 2007). The authors observed that decreased IRS-1 expression resulted in decreased Atk phosphorylation leading to reduced insulin induced GLUT4 translocation to the membrane (Lumeng, Deyoung et al. 2007). This results in disruption of insulin signalling and impairment of glucose uptake.

1.6   Epigenetic modifications and micro RNAs

The meaning of Epigenetics has undergone many changes since the term was coined by Waddington (1942). Originally Waddington used the term to explain differentiation of cells from a totipotent state to a defined one. The definition of epigenetics has since undergone several iterations, being defined as:

 "…*the study of mitotically and/or meiotically heritable changes in gene function that cannot be explained by changes in DNA sequence" by Arther Riggs (Bird 2007) or as "stably heritable phenotype resulting from changes in a chromosome without alterations in the DNA sequence"* (Berger, Kouzarides et al. 2009*).*

These definitions stipulate that the epigenetic changes must be heritable and stable, which would exclude several modifications currently classed as changes to the epigenome such as histone modifications. Other definitions take this into account; Adrian Bird (2007) defined epigenetics as:

 "…*the structural adaptation of chromosomal regions so as to register, signal or perpetuate altered activity states."*

and the definition given by the NIH "Roadmap Epigenomics Project," which described epigenetics as:

"*…epigenetics refers to both heritable changes in gene activity and expression (in the progeny of cells or of individuals) and also stable, long-term alterations in the transcriptional potential of a cell that are not necessarily heritable.*"

The latter definitions consider epigenetics to be modifications which result in altered cellular gene expression independent of gene sequence, which may or may not be heritable. Considering the broader definitions of epigenetics, many types of modifications can fall under this classification. Epigenetic modifications generally fall under three broad groups: DNA methylation, Histone modifications and microRNAs.

1.6.1   DNA methylation

The DNA of higher organisms, especially of vertebrates, is subject to the addition of methyl groups by DNA methyltransferases (DnMT) to the 5' carbon of cytosine residues existing as part of cytosine-phosphate-guanine (CpG) di-nucleotides. DNA methylation is essential in development, playing a fundamental role in developmental processes such as X-chromosome inactivation and genomic imprinting (Ideraabdullah, Vigneau et al. 2008, Panning 2008). Addition of methyl groups is primarily carried out by proteins belonging to the DnMT family, and can be described as "maintenance" methylation or "de novo" methylation. Maintenance methylation is the process by which existing methylation is copied onto newly replicated DNA and is performed by the DnMT1 methyltransferase. De novo methylation is performed by the methyltransferases DnMT3a and DnMT3b and is the addition of methyl groups to previously unmodified DNA. Regions of the genome containing a high concentration of CpG residues called CpG islands exist in the promoter regions of approximately 70% of genes; these regions are inherently unmethylated, although can be methylated altering gene expression (Illingworth and Bird 2009). How DNA methylation alters gene expression is still the focus of ongoing research. Current belief is that proteins capable of binding to methylated cytosine, such as the protein MeCP1, bind to the methylated CpG islands and in doing so either block the promoter region from being bound to by polymerases, preventing gene transcription, or form a complex with proteins that have histone deacetylase activity altering the chromatin conformation, restricting gene expression (Nan, Campoy et al. 1997). Methylation of cytosine nucleotides was believed to increase the chance of spontaneous deamination occurring converting the cytosine to a thymine nucleotide (Bird 1980). This is believed to explain the discrepancy between the observed and expected frequency of CpG nucleotides within the genome (Salser 1978, Bird 1980). Although it is now believed that the process of deamination of 5-methylcytosine to thymine is mediated by the deaminase enzymes (activation-induced cytidine deaminase) AID (Morgan, Dean et al. 2004) and

(apolipoprotein B mRNA editing enzyme, catalytic polypeptide) APOBEC (Guo, Su et al. 2011, Wijesinghe and Bhagwat 2012) and plays a role in the removal of methylation modifications to restore gene expression. Deamination of 5-methylcytosine to thymine produces a T-G mismatch which results in DNA repair proteins removing and replacing the segment of DNA (Rai, Huggins et al. 2008).

1.6.2   Histone modifications

Nucleosomes, the functional units of chromatin, are formed from genomic DNA wrapped around histone core protein complexes. The core histone protein complexes are octomers made up of pairs of proteins belonging to four distinct histone protein families: H2A, H2B, H3 and H4. Each of the histone proteins has a pair of N-Terminal tails which act as the primary site for histone post translational modifications. The structuring of genomic DNA in this way is advantageous for a number of reasons: the core histone protein complexes provide structural support, facilitating DNA replication; wrapping the genomic DNA around the histone protein complexes compacts the DNA allowing it to fit within the cell nucleus and the histone protein complexes being modifiable also provides an additional level of gene regulation.

There are several distinct types of histone modifications which have been shown to alter chromatin confirmation and gene expression which include methylation, acetylation, phosphorylation, ubiquitination, SUMOylation, citrullination and ADP- Ribosylation.

1.6.2.1   Histone acetylation

Histone acetylation is the addition of acetyl groups to lysine residues located within the histone proteins N-terminal tails, a process which has been shown to regulate gene expression. The acetyl groups are covalently bonded to the histone proteins by histone acetyltransferase (HAT) proteins which utilise acetyl-coenzyme A as a source of acetyl groups. The antagonistic process deacetylation is performed by histone deacetylase (HDAC) proteins which remove the acetyl groups which are subsequently transferred to coenzyme A. Histone acetylation is thus a dynamic and reversible process with acetyl addition mediated by HAT enzymes, and acetyl removal by HDAC enzymes allowing the cell to alter gene expression to changing conditions. Histone acetylation is generally considered to result in gene activation and deacetylation to result in gene silencing.

The mechanism by which histone acetylation results in altered gene expression has not yet been fully elucidated although there have been several suggestions as to how this occurs. One of the more basic proposed mechanisms is that acetylation alters the interaction between the DNA and the histone proteins. Acetylation neutralises the lysine residues positive charge, weakening the interaction between these positively charged residues and the negatively charged phosphate backbone of the DNA (Zentner and Henikoff 2013). This relaxes the tight chromatin structure exposing the gene promoter to RNA polymerases allowing gene transcription and aiding in elongation. It has also been suggested that proteins containing bromo-domains, a domain with acetyl-lysine recognition and binding ability binds to the acetylated residues and subsequently recruits additional chromatin remodelling proteins (Chen, Ghazawi et al. 2010).

1.6.2.2   Histone deacetylase enzymes and the regulation of histone and protein acetylation

Histone deacetylase (HDAC) enzymes like HAT enzymes are also believed to be highly conserved between mammals and yeast. At the time of writing, at least 18 HDAC enzymes have been discovered and separated into four distinct classes based on their homology to yeast HDAC proteins. HDACS belonging to class I, II (a and b) and IV are all closely related and have zinc dependant catalytic sites, whereas class III HDACs do not. Class III HDACs contain the sirtuin family of deacetylase proteins which are nicotinamide adenine dinucleotide (NAD^+) dependent and share homology with the yeast silent information regulator 2 (Sir2) deacetylase protein (Dokmanovic, Clarke et al. 2007).

The yeast Sir2 histone deacetylase protein was first discovered to have a role in regulating the ageing process by Sinclair and Guarente (1997). Overexpression of Sir2 in yeast results in an approximate 30% increase in budding yeast cellular lifespan whereas Sir2 knockout yeast cells showed a 50% decrease in cellular lifespan. Yeast cells subjected to reduced glucose availability (caloric restriction) also experienced increased cellular lifespan via upregulation of the Sir2 protein. Calorie restriction has also been shown to increase lifespan in worm, fly and mice models via invertebrate and mammalian Sir2 homologs (Weindruch, Walford et al. 1986, Lakowski and Hekimi 1998, Lipman, Smith et al. 1998, Lin, Kaeberlein et al. 2002). The mammalian homologs of yeast Sir2 belong to the sirtuin family of proteins which contains 7 proteins (SIRT1 – 7). SIRT1 is the most closely related of the sirtuins to sir2. SIRT1 is a NAD^+ dependent deacetylase protein which recognises and deacetylases both histones and several other proteins and transcription factors (Haigis and Sinclair 2010).

As SIRT1 is NAD$^+$ dependent, intracellular NAD$^+$ availability is a deacetylation rate limiting factor. NAD$^+$ availability is believed to be increased during low nutrient availability due to increased flux through the NAD$^+$ salvage pathway. The NAD$^+$ salvage pathway consists of the proteins nicotinamide phosphoribosyltransferase (NAMPT) and nicotinamide mononucleotide adenylyltransferase (NMNAT). NAMPT converts nicotinamide (NAM), the product of NAD$^+$ dependent deacetylation, to nicotinamide mononucleotide (NMN) which is subsequently converted to NAD$^+$ by NMNAT. Thus SIRT1 deacetylase activity is limited by cellular NAD$^+$ availability and the activity of the enzymes involved in the NAD$^+$ salvage pathway; NAD$^+$ availability providing a link between metabolism and histone, protein deacetylation. In contrast with this, increased glycolysis due to increased nutrient availability is believed to result in increased pyruvate and subsequently increased intracellular acetyl-CoA, a substrate necessary for acetylation, thus increased nutrient availability results in increased acetyl-CoA substrate for histone acetylation increasing acetylation frequency (Haigis and Sinclair 2010).

SIRT1 has many targets (figure 1.6.1) which it recognises and deacetylates such as histone proteins as well as several other proteins and transcription factors. SIRT1 deacetylases the histone proteins H3 and H4 at lysine residues K9 and K16 respectively as well as several proteins and transcription factors including: the peroxisome proliferator gamma co-activator 1 alpha (PGC-1α) (Rodgers, Lerin et al. 2005); the NF-κB subunit P65 (Yeung, Hoberg et al. 2004); the FOXO proteins FOXO1 and FOXO3 (Brunet, Sweeney et al. 2004), P53 (Vaziri, Dessain et al. 2001); protein tyrosine phosphatase 1B (PTP1B) (Sun, Zhang et al. 2007) and the insulin receptor substrate IRS2 (Zhang 2007). PGC-1a is a transcription co-activator that interacts with several different transcription factors increasing glucose and fatty acid metabolism and mitochondrial biogenesis. SIRT1 deacetylates PGC-1a at specific lysine residues increasing PGC-1a activity. PGC-1a activation causes increased gluconeogenesis and glycolysis in liver cells as well as increased fat mobilisation in white adipose tissue. SIRT1 has also been identified as a suppressor of inflammation in several tissue types by inhibiting the NF-κB pathway. Upon activation the NF-κB complex translocates to the cell nucleus where it is acetylated by the protein acetyltransferase p300 and activated causing transcription of several genes responsible for the inflammatory response such as cytokine secretion. SIRT1 deacetylates and binds to the P65 subunit of the NF-κB complex preventing acetylation and activation (Yeung, Hoberg et al. 2004). SIRT1 deacetylates and inhibits the PTP1B enzyme, a negative regulator of the insulin signalling pathway, thereby increasing insulin sensitivity (Sun, Zhang et al. 2007).

SIRT1 has also been observed to inhibit mammalian target of rapamycin (mTOR) signalling through interacting with its upstream regulators. The mTOR protein is a serine/threonine kinase shown to

respond to intracellular nutrient availability regulating protein synthesis, adipogenesis, autophagy and senescence (Laplante and Sabatini 2012). It has been demonstrated to become dysregulated in obesity increasing adiposgenesis (Gagnon, Lau et al. 2001, Zhang, Huang et al. 2009) and plays a role in cellular ageing and senescence. Mice treated with the mTOR inhibitor, rapamycin have been observed to have increased longevity (Harrison, Strong et al. 2009) and remain lean when fed a high fat diet (Polak, Cybulski et al. 2008). SIRT1 deacetylates the upstream activator of mTOR signalling liver kinase B1 (LKB1) which promotes its ubiquitination and subsequent degradation (Zu, Liu et al. 2010). SIRT1 has also been shown to interact with TSC2 component of the TSC1-TSC2 mTOR inhibitor complex promoting its inhibition of the mTOR activator the GTPase Rheb resulting in mTOR signalling inhibition (Ghosh, McBurney et al. 2010).

By acting in response to cellular nutrient availability and subsequently altering biological processes such as inflammatory response, fatty acid and glucose metabolism, mitochondrial biogenesis, DNA repair pathways and cellular ageing, SIRT1 may form a potential link between metabolism, inflammation and cell ageing.
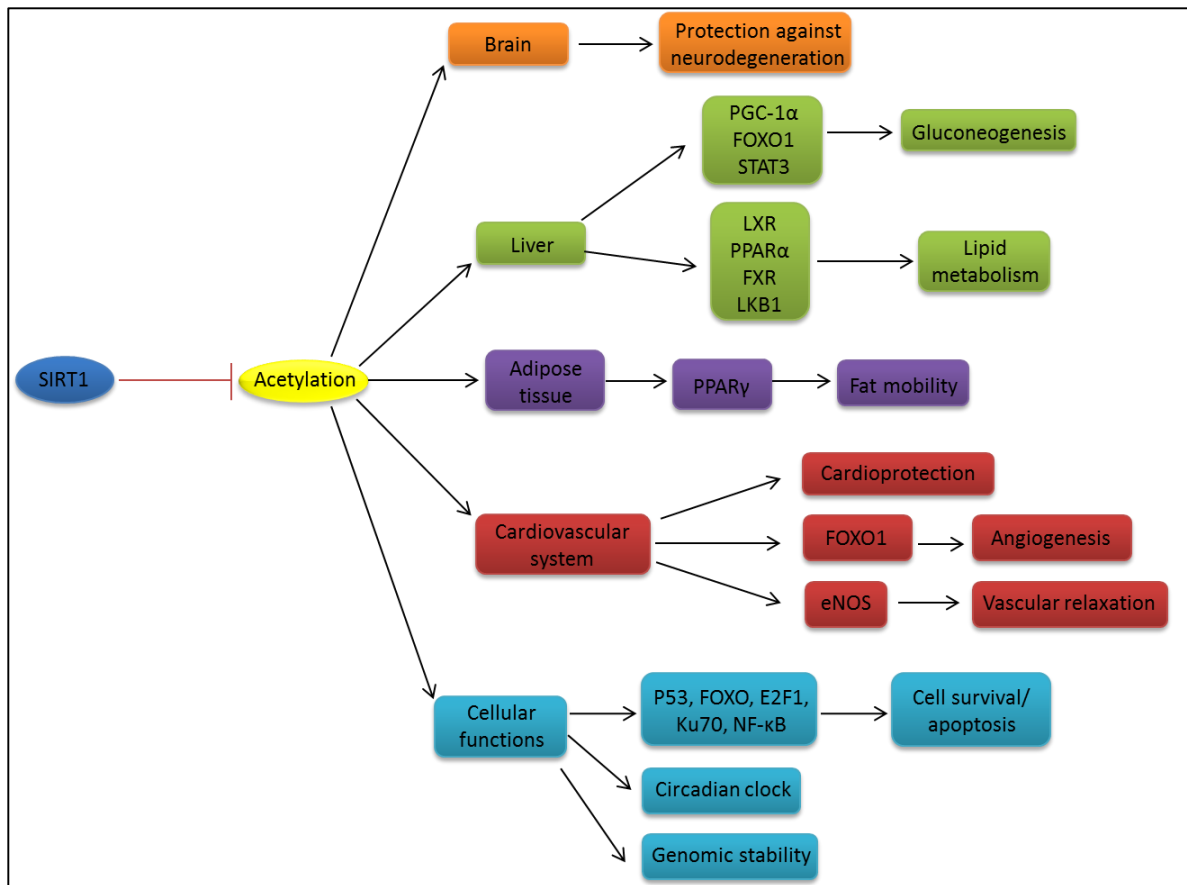
Figure 1.6.1: Sirtuin 1 Interactions and Functions,

Adapted from Bao and Sack (2010). Figure displays a summary of the known targets of SIRT1 deacetylase activity in a variety of different tissue types and the resulting consequence of SIRT1 mediated protein deacetylation.

1.6.3   MicroRNAs

MicroRNAs are small non-coding single stranded RNA molecules between 18 to 23 nucleotides in size that were first discovered in Caenorhabditis elegans by Lee, Feinbaum et al. (1993). Since their discovery, miRNAs have been the focus of much scrutiny due to their ability to regulate post translational gene expression through binding to messenger RNAs leading to their degradation or by inhibiting their translation. Their binding to mRNA does not require perfect complementarity, which potentially allows a single miRNA to target multiple mRNAs (Lim, Lau et al. 2005).

1.6.3.1   MicroRNA biogenesis

The biogenesis of microRNAs is a complex process, with the initial miRNA called the primary miRNA (pri-miRNA) going through several stages before becoming functional mature miRNA (figure 1.6.2). The process of miRNA biogenesis begins in the nucleus with transcription by either RNA polymerase II (Pol II) or RNA polymerase III (Pol III) to produce the pri-miRNA transcript. Although miRNAs can be

transcribed by both RNA Pol II and Pol III, the majority are transcribed by RNA Pol II receiving 5'
methylated caps and 3' polyadenylated tails (Lee, Kim et al. 2004, Borchert, Lanier et al. 2006). Pri-
miRNA transcripts consist of a hairpin stem, a terminal loop and two single stranded flanking regions
upstream and downstream of the hairpin. The pri-miRNA transcripts are cleaved within the nucleus
by a protein complex consisting of the proteins Drosha and DiGeorge critical region 8 (DGCR8)
together termed the Microprocessor complex (Lee, Ahn et al. 2003, Han, Lee et al. 2004, Landthaler,
Yalcin et al. 2004). The double-stranded stem and the unpaired flanking regions of the pri-miRNA are
essential for DGCR8 binding and Drosha RNase cleavage. The microprocessor complex cleaves the
pri-miRNA approximately 11 nucleotides from the hairpin base, removing the flanking single
stranded regions leaving a 2 nucleotide overhang at the hairpin stems 3' end (Lee, Ahn et al. 2003,
Han, Lee et al. 2004). The resulting hairpin stem transcript is now termed precursor miRNA (pre-
miRNA) and is exported from the nucleus to the cytoplasm by a complex of Exportin-5 and Ran-GTP
(Yi, Qin et al. 2003). Exportin-5 binds preferentially to pre-miRNA transcripts with a double stranded
stem region within a defined length and the presence of the 3' two nucleotide overhang; in this way
Exportin-5 only transports pre-miRNA transcripts which have undergone correct cleavage by the
microprocessor complex (Zeng and Cullen 2004, Lund and Dahlberg 2006). The exported pre-miRNA
undergoes further cleavage in the cytoplasm by the RNase III enzyme Dicer. The Dicer protein is
characterised as having a helicase, a PAZ dsRNA binding and two RNase III domains. The PAZ dsRNA
binding domain has been shown to bind to the pre-miRNA 3' two nucleotide overhang (Ma, Ye et al.
2004). The Dicer protein forms a complex with the protein TAR RNA-binding protein (TRBP) which
aids in stabilising Dicer's binding to the pre-miRNA transcripts (Koscianska, Starega-Roslan et al.
2011). The Dicer RNase cleaves the pre-miRNA transcript removing the terminal loop leaving a
miRNA duplex of approximately 22 nucleotides in length; cleavage leaves a two nucleotide overhang
at both 3' ends of the miRNA duplex. The Dicer-TRBP complex dissociates from the miRNA duplex
which is then bound by a complex of proteins called the RNA-induced silencing complex (RISC) which
consists of Dicer, TRBP and Argonaute (AGO) (Rana 2007). When bound to the RISC complex the
miRNA duplex is unwound by a helicase and the guide strand. The strand of the miRNA duplex with
gene inhibitory activity is bound to the RISC complex whilst the other strand of the duplex, the
passenger strand, is degraded. The RISC complex bound guide strand allows the RISC complex to
recognise its target mRNA whereby the AGO protein can cleave the mRNA strand or engage cofactor
proteins to stimulate mRNA transcript de-adenylation to encourage mRNA degradation (Meister,
Landthaler et al. 2004, Pillai, Artus et al. 2004).

Micro RNAs are proposed to direct the RISC complex to its target mRNAs via complementarity
binding between its "seed sequence", the sequence between the 2nd and 8th nucleotides of the 5'

extremity and regions of the target mRNA (Lewis, Burge et al. 2005). The miRNAs bind via this seed sequence to target mRNAs at either 3' untranslated regions (UTR), 5'UTR sequences or coding regions (Lim, Lau et al. 2005, Lytle, Yario et al. 2007, Fang and Rajewsky 2011). Micro RNA mediated translational repression has been shown to occur via a variety of mechanisms. These include the promotion of mRNA degradation via induction of mRNA 3' deadenylation and 5' decapping or by interference with mRNA transcription (Mathonnet, Fabian et al. 2007, Boutet, Cheung et al. 2012). MicroRNAs interfere with mRNA transcription by causing ribosomal dissociation and by causing premature termination of mRNA transcription (Chendrimada, Finn et al. 2007, Fabian, Sonenberg et al. 2010).
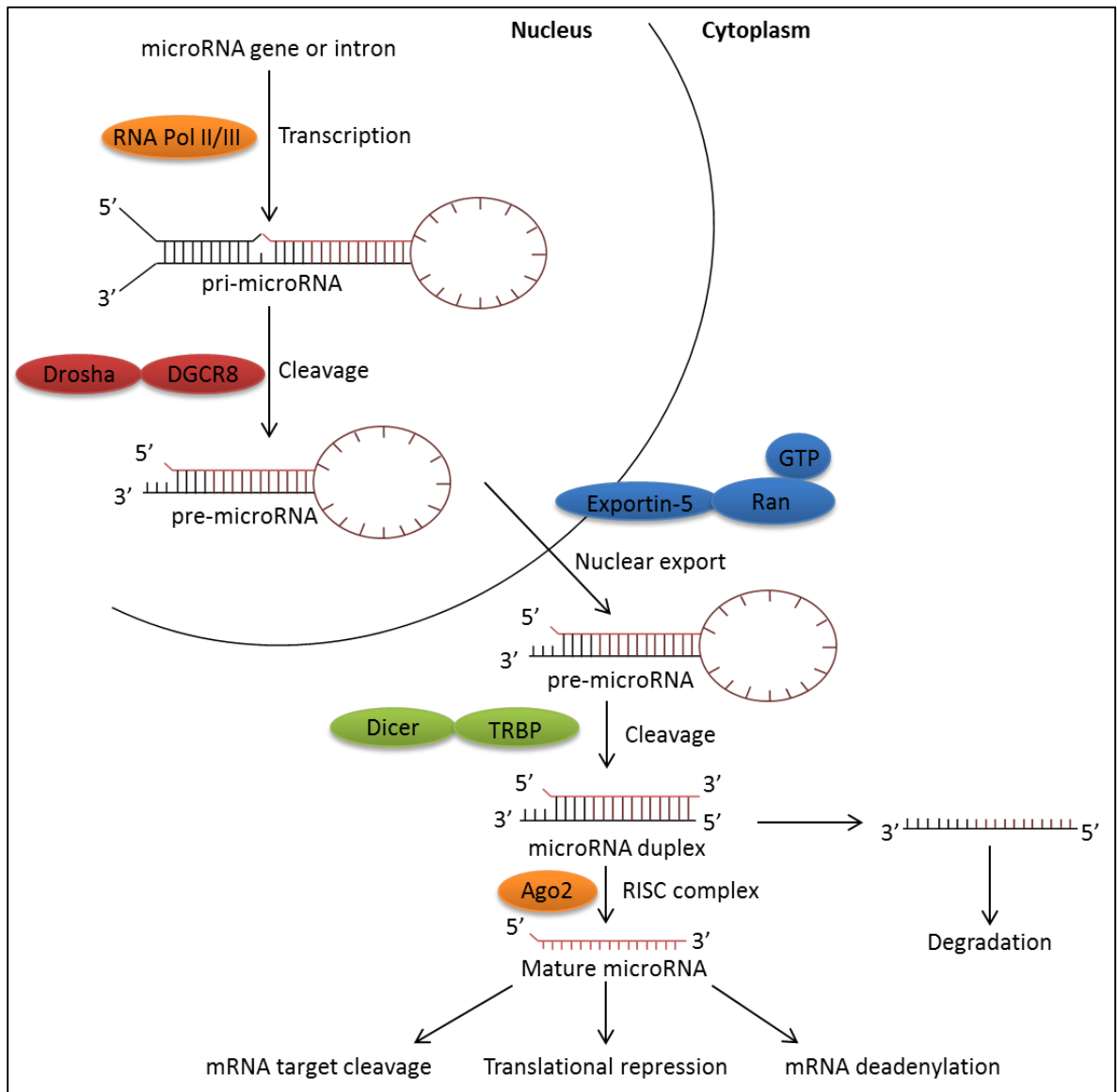
Figure 1.6.2: MicroRNA biogenesis

Adapted from Winter, Jung et al. (2009). This figure displays the canonical mechanism of mature miRNA biogenesis. This includes the transcription of the primary (pri-) miRNA by either RNA polymerase II or III. The cleavage of the transcribed pri-miRNA to pre-miRNA by the microprocessor Drosha-DGCR8 complex. The cleaved pre-miRNA is exported from the nucleus to the cytoplasm via the Exportin-5-Ran-GTP transporter. The exported pre-miRNA is further cleaved by the Dicer-TRBP complex to remove the stem loop leaving the double stranded miRNA duplex. The functional strand of the miRNA duplex interacts with the Ago2 protein to form the RNA-induced silencing complex (RISC). The functional strand directs the RISC complex to its target mRNA resulting in its translational silencing.

1.6.3.2   MicroRNAs in immune function, inflammation and metabolic disease

Dysregulation of miRNA expression has been shown to result from a number of diseases as well as being causal for their pathogenesis. The first observed example of miRNA dysregulation resulting in a disease was the dysregulation of miR-15 and miR-16 which resulted in development of chronic

lymphocytic leukaemia (Calin, Dumitru et al. 2002). Since this discovery miRNAs have been shown to have a role in a number of diseases including many types of cancers, where the majority of research has focused, heart disease and obesity as well as a role in the inflammatory response. Many specific miRNAs have been identified to regulate the function and differentiation of cells belonging to both the adaptive and innate immune systems. B-cell proliferation and survival has been shown to be promoted by increased expression of the miR-17-92 cluster (Xiao, Srinivasan et al. 2008) whereas expression of miR-150 has been observed to impair B-cell differentiation and responses (Zhou, Wang et al. 2007). The miRNA, miR-181a is required for T-cell development of tolerance whereby inhibition of miR-181a expression results in decreased sensitivity of the T-cell receptor (Li, Chau et al. 2007).

Several miRNAs have been identified as playing a regulatory role in the inflammatory response of cells belonging to the innate immune system, specifically monocytes and macrophages. Target prediction analysis of 613 genes involved in regulation of innate immunity found that potentially 285 genes were under direct regulation of miRNAs (Asirvatham, Gregorie et al. 2008). Screening of miRNA expression in cells belonging to the THP-1 monocytic cell line treated with the TLR4 ligand LPS identified increased expression of three miRNAs, miR-146a, miR-155 and miR-132 (Taganov, Boldin et al. 2006). The miRNA 146a has been found to directly interact with the mRNA of TRAF6 and IRAK1, two key molecules belonging to the TLR4 signalling pathway (Gao, Wang et al. 2015, Lu, Cao et al. 2015). It is believed that miR-146a expression results in a negative feedback response, limiting TLR4 signalling and inflammatory response. Dysregulation of miR-146a expression has been shown to contribute to a number of diseases including T2DM (Balasubramanyam, Aravind et al. 2011) (Baldeon, Weigelt et al. 2014) and chronic obstructive pulmonary disease (COPD) (Sato, Liu et al. 2010). Fibroblast samples taken from patients with COPD were shown to have reduced expression of miR-146a compared to healthy controls, this was shown to contribute to the inflammatory nature of COPD by increasing production of prostaglandin E2. The authors were also able to directly correlate reduced expression of miR-146a to increased severity of the COPD (Sato, Liu et al. 2010). A number of inflammatory conditions have also been associated with increased expression of miR-146a including psoriasis(Sonkoly, Wei et al. 2007), diabetic nephropathy (Alipour, Khamaneh et al. 2013) and rheumatoid arthritis (Pauley, Satoh et al. 2008). However it is not known whether this increase in expression is contributing to these disease states or is a protective measure in an attempt to limit the inflammatory response.

Dysregulation of several miRNAs have been observed to contribute to the development of metabolic diseases such as obesity and T2DM. As previously stated, miR-146a expression has been observed to be dysregulated in type two diabetes (Balasubramanyam, Aravind et al. 2011). The authors observed

that PBMCs taken from participants with T2DM expressed significantly lower levels of miR-146a compared to healthy controls. The authors were also able to negatively correlate miR-146a expression with insulin resistance, glycated haemoglobin, TRAF6 and NFKB mRNA expression and circulating levels of TNFα and IL-6 cytokines (Balasubramanyam, Aravind et al. 2011). Patients with type two diabetes were observed to overexpress the miRNA miR-199a compared to healthy controls (Yan, Li et al. 2014). The microRNA miR-199a was shown to target GLUT4 mRNA reducing GLUT4 expression; the authors suggested this may contribute to the development of type two diabetes(Yan, Li et al. 2014). Obese individuals were observed to have decreased expression of miR-26a compared to lean controls(Fu, Dong et al. 2015). The authors also showed that obese mice models developed decreased insulin sensitivity which was restored in response to miR-26a restoring insulin sensitivity. A large amount of evidence currently exists for the role of these miRNAs, along with several others, in the regulation of immune cell development and function, inflammatory response and in the development of metabolic diseases and their associated complications making miRNAs viable targets for intervention of, or as biomarkers of diseases.

Dysregulation of several miRNAs have been observed to contribute to the development of metabolic diseases such as obesity and T2DM. The miR-146a-5p expression is dysregulated in type two diabetes, (T2DM) (Balasubramanyam, Aravind et al. 2011). These authors observed that PBMCs taken from participants with T2DM expressed significantly lower levels of miR-146a-5p compared to healthy controls. The authors also found a negative correlation between miR-146a-5p expression with insulin resistance, glycated haemoglobin, TRAF6 and NF-κB mRNA expression and circulating levels of TNFα and IL-6 cytokines (Balasubramanyam, Aravind et al. 2011). The miR-146a-5p has been shown to directly interact with the mRNA of TRAF6 and IRAK1, two key molecules belonging to the TLR4 signalling pathway (Gao, Wang et al. 2015, Lu, Cao et al. 2015). It is believed that miR-146a-5p expression results in a negative feedback response, limiting TLR4 signalling and inflammatory response. Dysregulation of miR-146a-5p expression has been shown to contribute to a number of diseases including T2DM (Balasubramanyam, Aravind et al. 2011, Baldeon, Weigelt et al. 2014) and chronic obstructive pulmonary disease (COPD) (Sato, Liu et al. 2010).

1.7   Research aims

The overarching aim of the work presented in this thesis was to assess the effects of increased nutritional availability present in obesity and diabetes on monocyte inflammatory response.   The specific aims of each chapter are as follows:

1.7.1   Chapter three:

Currently only a small number of studies have assessed microRNA dysregulation occurring as a result of obesity and type 2 diabetes (Baldeon, Weigelt et al. 2015, Li, Zhou et al. 2015). Between these few studies a number of dissimilarities in the results exist highlighting the need for more research in this area. In addition to this only a few studies have assessed the effect of bariatric surgery on obesity induced microRNA dysregulation. As of writing the current literature has assessed changes in miRNA content in serum of obese human and mice models pre- and post- bariatric surgery, however the literature is yet to assess the effects of weight reduction surgery on miRNA expression within primary human monocytes (Lirun, Sewe et al. 2015, Wu, Li et al. 2015). Monocytes play a key role in the chronic inflammation present during obesity which leads to the development and propagation of a number of related co-morbidities such as atherosclerosis. For this reason, assessing the impact of bariatric surgery on monocyte miRNA expression is of a high importance due to a potential role of miRNA dysregulation as a contributor to the chronic inflammation present in obesity.

1.7.1.1   Chapter three aims:

 i.   To assess the effects of obesity and type 2 diabetes on the expression of microRNAs relevant to monocyte function.
 ii.   To identify how changes in microRNA expression may relate to inflammatory response, disease progression and the development of co-morbidities.
 iii.   To assess the effectiveness of bariatric surgery as a weight loss measure to reverse obesity and diabetes induced changes in microRNA expression towards healthy control values.

1.7.2   Chapters four and five:

Although a great deal is known about the adverse effects of chronic exposure to high concentrations of glucose much less is known about the effects of elevated glucose over acute time periods. Exposure to high concentrations of D-glucose over acute time periods is of relevance to pre-diabetes whereby due to decreased insulin sensitivity and glucose tolerance much larger shifts in post-prandial glucose concentration can occur over shorter time periods. Increased glucose availability has been reported to activate the polyol pathway in a variety of tissues including in monocytes. Activation of this pathway results in the conversion of glucose to sorbitol and subsequently fructose,

this process depletes intracellular NAD$^+$, reducing its availability for other intracellular processes. Sirtuin 1, an NAD$^+$ dependent protein deacetylase and homolog of the yeast sir2 protein, has been observed to regulate a number of intracellular processes. Increasing deacetylase activity of SIRT1 has been shown to reduce inflammatory response through the deacetylation of the P65 subunit of the NF-κB complex. Increased glucose availability may result in increased NAD$^+$ reduction to NADH reducing its availability for SIRT1. This may lead to increased acetylation of the P65 subunit of the NF-κB complex resulting in increased NF-κB mediated gene transcription and an increased inflammatory response. Decreased intracellular NAD$^+$ availability and SIRT1 deacetylase activity may provide a link between increased glucose availability and Inflammatory response in monocytes.

1.7.2.1   Chapters four and five, aims:

i.   To assess whether acute increases in glucose availability would result in increased monocyte inflammatory response either independently in response to glucose, or in response to an inflammatory stimulus such as LPS.

ii. To assess whether the increased concentrations of glucose would disrupt the balance of intracellular NAD$^+$: NADH resulting in altered SIRT1 deacetylase activity, and whether this could provide a link between increased glucose availability and the increased inflammation observed in hyperglycaemia.

iii. To assess whether the leukemic THP-1 monocytic cell line responds differently to treatment with high concentrations of glucose then primary human monocytes.

2   Materials and methods

2.1   Cell culture

2.1.1   Cell Culture materials and reagents

The THP-1 human monocytic cell line was obtained from the European Collection of Authenticated Cell Cultures (ECACC) part of the Public Health England culture collections. The THP-1 cell line was cultured in Roswell Park Memorial Institute medium (RPMI 1640) supplemented with 10%v/v foetal calf serum and 1% v/v Penicillin (100 µg/ml)/ (100 µg/ml) streptomycin solution.

2.1.2   Cell line background

The human monocytic THP-1 cell line is derived from the peripheral blood of a 1 year old male with acute monocytic leukaemia. Since its establishment the cell line has become well characterised. THP-1 monocytes express both Fc and C3b receptors but lack surface and cytoplasmic immunoglobulins, they stain positive for alpha-napthhyl butyrate esterase and are phagocytic against both latex and sensitised erythrocytes. THP-1 cells can also be differentiated into macrophages by incubation with either vitamin D3 or PMA (Tsuchiya, Yamabe et al. 1980, Tsuchiya, Kobayashi et al. 1982, Schwende, Fitzke et al. 1996). Undifferentiated THP-1 monocytes have been observed to express cell surface CD14 albeit at lower concentrations than primary human monocytes and have been reported to be CD16 negative (Fleit and Kobasiuk 1991, Antal-Szalmas, Strijp et al. 1997). Differentiation with either PMA or vitamin D3 has been shown to increase cell surface expression of both CD14 and CD16 (Fleit and Kobasiuk 1991, Antal-Szalmas, Strijp et al. 1997).

2.1.3   Cell culture protocol

The THP-1 monocytes were cultured in RPMI 1640 media with stable glutamine supplemented with foetal calf serum (FCS) up to a final concentration of 10 % v/v and penicillin (100 µg/ml)/ streptomycin (100 µg/ml) solution to a 1% v/v final concentration. The THP-1 monocytes were routinely cultured in 75cm^2 flasks (Appleton woods, UK) with vented caps incubated in a humidified environment at 37°C with 5% carbon dioxide. The THP-1 cells were seeded at 3 x 10^5 cells/ml in

30ml's of media and incubated until reaching 1×10^6 cells/ml at which point they were passaged in a lamina flow hood under sterile conditions. The passaging required the cells to be harvested by centrifuging at 500xg for 8 minutes and resuspended into fresh warm RPMI media (10% FCS, 1% pen/strep) prior to being counted by trypan blue staining on a Neubauer haemocytometer and diluted to the desired cell density.

2.2 Trypan blue exclusion staining

2.2.1 Trypan blue exclusion materials and reagents

Trypan blue reagent and a Neubauer haemocytometer, cover slides

2.2.2 Cell counting by trypan blue exclusion

Trypan blue is a diazo dye which due to its inability to cross intact cell membranes allows selective staining of dead or dying cells, allowing distinction from live cells (Tennant 1964, Schanne, Kane et al. 1979). Dead or dying cells have increased membrane permeability which allows the trypan blue to pass through the membrane, bind to intracellular proteins staining them blue whereby live cells appear clear.

Cell suspensions were diluted at a 1:2 ratio with trypan blue and incubated for 1 minute at room temperature. The cells were then mixed by pipetting before loading 10µl of the cell suspension onto a Neubauer haemocytometer and counted. Cells on all 25 squares of the grid were counted and the number of cells/ml calculated using the following formula; Average of cells counted x dilution factor x 10,000. For each sample four repeat counts were performed, from each the number of viable/dead and total number of cells recorded.

2.3 Measurement of cellular viability by MTT assay

2.3.1 3-(4,5-Dimethylthiazol-2-yl)-2,5-diphenyltetrazolium bromide (MTT) assay materials and reagents

The assay reagent was prepared by dissolving (3-(4,5-dimethylthiazol-2-yl)-2,5-diphenyltetrazolium bromide in PBS at 12mM (5mg/ml). SDS cellular lysis buffer consisted of 0.7M SDS dissolved in 50% v/v dimethyl formamide (DMF), the solution was adjusted to pH 4.7 with glacial acetic acid.

2.3.2 MTT assay

The MTT assay is a microplate colourimetric assay used to determine cellular viability first described by Mosmann (1983). The principle of the assay is that (3-(4,5-Dimethylthiazol-2-yl)-2,5-diphenyltetrazolium bromide (MTT), a yellow tetrazolium salt is reduced to insoluble purple formazan crystals. The MTT salt is reduced by oxidoreductase enzymes such as succinate dehydrogenase and by intracellular NADH in several cellular compartments such as the mitochondria, exosomes and the cytoplasm. The resulting colour change is measured to give an indication of cellular metabolic activity itself an indicator of cellular viability.

2.3.3 MTT assay protocol

Cell suspensions (100µl) were taken 4 hours before the treatment endpoint and transferred to a 96 well plate. The cells were mixed with 25µl MTT solution (5mg/ml in PBS) and subsequently placed in a cell incubator (37°C, 5% CO_2, humidified) in the dark for the remaining 4 hours of the treatment. The cells were subsequently lysed with 200µl SDS cell lysis buffer and incubated overnight. Absorbance was read at a wavelength of 570nm on a microplate reader. As a negative control, cellular suspensions were treated with the mitochondrial uncoupling agent carbonyl cyanide 4-(trifluoromethoxy) phenylhydrazone (FCCP); by inhibiting mitochondrial function FCCP prevents MTT reduction. Cellular viability was expressed as a percentage of control cells.

2.4 Determination of protein concentration by BCA assay

2.4.1 BCA assay materials and reagents

The assay requires a bicinchoninic acid solution (containing, bicinchoninic acid, sodium carbonate, sodium tartrate and sodium bicarbonate at pH 11.25), copper(II) sulphate pentahydrate (4% w/v) solution and BSA (1mg/ml) protein standard solution all purchased from sigma-aldrich.

2.4.2 BCA assay

The protein content of lysed cells was determined using the bicinchoninic acid assay (BCA) (Smith, Krohn et al. 1985). The BCA assay relies upon the conversion of Cu^{2+} to Cu^{+} under alkaline conditions resulting in a purple colouration change from green which can be detected colourimetrically by measuring absorbance on a spectrophotometer at 570nm. The Cu^{2+} reduction to Cu^{+} has been shown to be dependent on the presence of protein peptide bonds as well as the amino acids cysteine, cystine, tryptophan, and tyrosine (Wiechelman, Braun et al. 1988). The amount of Cu^{2+} reduction although proportional to the amount of protein present is dependent on the amino acid composition of the protein.

2.4.3 BCA assay protocol

Prior to lysis the cells were collected by centrifugation at 500xg for 5 minutes and washed with sterile PBS to prevent media constituents such as FCS or high concentrations of glucose interfering with the BCA assay (Smith, Krohn et al. 1985). The cells were lysed as described previously in methods section 2.7. The cell lysates were diluted at a 1:5 ratio and 10µl loaded onto a clear, flat bottomed 96 well plate in triplicate. Assay standards were made by diluting 1mg/ml BSA solution aliquots (Sigma, UK) to 1mg/ml, 0.8mg/ml, 0.6mg/ml, 0.4mg/ml, 0.2mg/ml and a BSA negative. The BCA solution was mixed in a 50:1 ratio with copper (II) sulphate solution and 200µl added to each standard and sample well. The plate was incubated at 37°C for 30 minutes prior to measurement of absorbance at 570nm on an absorbance microplate reader.

2.5 Enzyme-linked immunosorbent assays (ELISA) for the detection of TNFα and HMGB1

2.5.1 ELISA materials and reagents

Human TNFα and HMGB1 ELISAs were purchased from Peprotech, UK and Antibodies Online, US respectively, o-phenylenediamine (OPD), NUNC-Immuno Maxi Sorp 96 well plates, hydrogen peroxide, BSA, citrate phosphate buffer (50mM citric acid, 100mM sodium phosphate), 2N Sulphuric acid and Tween-20 were all purchased from Sigma-Aldrich, UK.

2.5.2 ELISA background

Both the TNFα and HMGB1 ELISAs are examples of a sandwich ELISA method. The sandwich ELISA method consists of coating the base of wells of 96 well microplates with a capture antibody specific for an analyte of interest. The plate is then incubated with a sample containing the analyte of interest, after which a biotin-conjugated detection antibody and subsequently a streptavidin-conjugated horseradish peroxidase (HRP) enzyme is added. If the analyte being assessed is present in the sample then it will have been bound by the capture antibody allowing the further binding of the detection antibody and the HRP enzyme. A HRP enzyme chromogenic substrate such as OPD is then added which the HRP enzyme using H_2O_2 as an oxidising agent oxidises resulting in a colourimetric change measurable using a spectrophotometer. The resulting absorbance values are compared to known standards in order to quantify the analyte of interest.

2.5.3 TNFα ELISA protocol

The supplied anti-TNFα capture antibody was diluted to 100µg/ml in sterile water and 100µl added to each well on a Nunc-ImmunoSorb 96 well plate, the plate was incubated overnight at room temperature. The following day the plate was washed using a prepared wash buffer (PBS, 0.05% v/v Tween-20) 4 times and dried on blotting paper after which 300µl of block buffer (PBS, 1% w/v BSA) was added to the wells. The plate was incubated for 1 hour to block any non-specific antibody binding. The wells were washed and dried as previously described and 100µl of prepared standards (0 – 2ng/ml TNFα) and the samples were added to respective wells, the plate was incubated for 2 hours at room temperature. The plate was again washed and wells incubated with 100µl of biotin conjugated detection antibody (100µg/ml) for 2 hours at room temperature. The plate was washed again and 100µl of streptavidin-HRP added to each well and incubated for 45 minutes at room

temperature. The plate was washed again and 100µl of *o*-phenylenediamine (OPD) HRP substrate dissolved in 30ml citrate phosphate buffer with 10µl hydrogen peroxide added to each well. The plate was covered and incubated until sufficiently developed approximately 15 - 20 minutes. To stop colour development 100µl of 2N sulphuric acid was added to each well, absorbance was read on a microplate reader at 460nm.

2.5.4 HMGB1 ELISA protocol

HMGB1 secretion by glucose treated primary monocytes was measured by HMGB1 ELISA purchased from Antibodies online, UK. The purchased ELISA kit provided a 96 well plate pre-coated with anti-HMGB1 antibody, lyophilised HMGB1 standard, detection reagent, avidin-conjugated HRP solution, tetramethylbenzidine (TMB) ELISA substrate, standard and assay diluent, wash buffer and stop solution. The lyophilised standards were reconstituted in 1ml standard diluent and added to the ELISA plate (0 - 4000pg/ml). The samples (100µl) were added to the plate and subsequently sealed and incubated at 37°C for 2 hours. The liquid was removed from the wells by inverting the plate and blotting onto absorbent paper. To each well 100µl of provided detection reagent was added and the plate sealed and incubated for 1 hour at 37°C. The plate was inverted to remove the well contents and 350µL of wash buffer added to each well; the plate was incubated for 3 minutes and the wash buffer removed, this was repeated a further two times. The plate was dried by blotting onto absorbent paper and 100µl of provided avidin-conjugated HRP solution added to each well. The plate was incubated for 30 minutes at 37°C. The plate was washed as described previously 5 times and 90µL of the provided TMB substrate solution added to each well. The plate was incubated at 37°C for approximately 20 minutes until adequate colorimetric development had occurred after which 50µl of a provided stop solution was added to halt the development. Absorbance was measured on a microplate reader at 450nm.

2.6   Quantification of glucose uptake

2.6.1   Materials and reagents

Glucose (hexokinase) quantification assay purchased from Sigma Aldrich (UK) includes: glucose standard (10mg/ml) and a lyophilised glucose assay reagent

2.6.2 Background

Glucose removal from the media over a period of time was measured using a hexokinase glucose assay adapted for use on a 96 well plate. The concentration of glucose removed by the cells was calculated by subtracting the final glucose concentration of the media from the initial concentration. The assay consists of a sterile glucose standard solution and an assay reagent containing NAD^+, ATP, hexokinase and glucose-6-phosphate dehydrogenase. Glucose in the sample and ATP are converted by the hexokinase enzyme to glucose-6-phosphate and ADP, the glucose-6-phosphate with NAD^+ is subsequently converted to 6-phosphogluconate and NADH by glucose-6-phosphate dehydrogenase. The NADH concentration increases as glucose is converted to 6-phosphogluconate, NADH concentration is measured by reading absorbance at 340nm allowing an indirect quantification of glucose concentration.
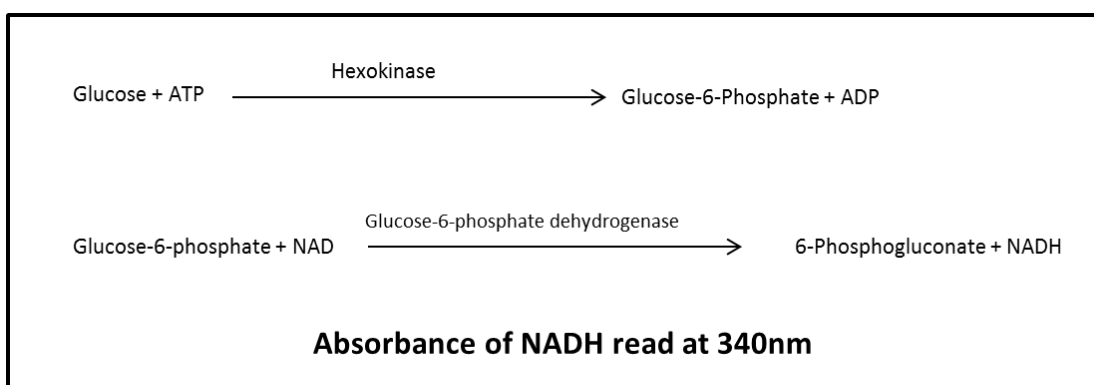
Figure 2.6.1: Explanation of the Hexokinase glucose quantification assay.

Hexokinase catalyses the phosphorylation of glucose to glucose- 6-phosphate utilising available ATP. Glucose-6-phosphate dehydrogenase catalyses the oxidation of glucose-6-phosphate to 6-phosphogluconate a process that results in oxidised NAD^+ being reduced to NADH. The resulting NADH is measured by an increase in absorbance at 340nm.

2.6.3 Protocol

The lyophilised glucose assay buffer was reconstituted with 20ml of distilled water. Glucose standards (0.05mg/ml – 5mg/ml) and samples (50µl) were added to a 96 well plate. The reconstituted glucose assay buffer (100µl) was added to each well. The plate was incubated for 15 minutes at room temperature prior to measuring absorbance at 340nm on a microplate reader.

2.7   Cell lysis

2.7.1   Materials and reagents

Radioimmunoprecipitation assay (RIPA) buffer (150 mM sodium chloride, 1.0% triton-X, 0.5% sodium deoxycholate, 0.1% SDS, 50mM Tris, pH 8.0), protease inhibitor cocktail (Sigma-Aldrich, UK), 21 gauge needle, 1ml syringes (Appleton woods, UK)

2.7.2   Protocol

Treated cells were harvested by centrifugation at 1000xg for 5 minutes and washed with ice cold PBS and centrifuged. The pellet was lysed in 50µl RIPA buffer supplemented with 0.5µl protease inhibitor cocktail before lysis and incubated for 30 minutes on ice. The DNA in the lysate was then sheared using a 21 gauge needle attached to a syringe and centrifuged at 16,000xg for 30 minutes at 4°C to remove cellular debris.

2.8   SDS polyacrylamide gel electrophoresis

2.8.1   Materials and reagents

Buffer 1 (1.5M Tris-Base, 0.4%w/v SDS in distilled water, adjusted to pH 8.4), Buffer 2 (0.5M Tris-base, 0.4%w/v SDS in distilled water, adjusted to pH 6.8), SDS-Polyacrylamide gel electrophoresis (PAGE) running buffer (24.8mM Tris-base, 191.3mM glycine, and 3.5mM SDS), tetramethylethylenediamine (TEMED), 10%w/v ammonium persulphate (APS) in distilled water, 30% w/v acrylamide solution, Laemmli buffer (Sigma-Aldrich, UK), precision plus protein standards (Bio-Rad, UK), gel electrophoresis tank, gel casting system.

2.8.2   SDS gel electrophoresis background

SDS polyacrylamide gel electrophoresis (SDS PAGE) is a technique employed to separate proteins by their molecular weight (Davis and Ornstein 1959, Raymond and Weintraub 1959). The proteins to be separated need to be first boiled in Laemmli buffer, which contains 2-mercaptoethanol that reduces the protein di-sulphide bonds to sulphhydryl groups, so linearising the protein. This allows the SDS in the Laemmli buffer to uniformly bind to the linear protein, providing it with a negative charge.

The separating gel contains acrylamide which when polymerised forms pores which provide resistance to the migrating proteins. The higher the acrylamide content, the smaller the pore size providing greater resistance to the migrating protein and greater separation. The linearised proteins are loaded onto the acrylamide gels. An electrical field is applied across the gel causing the negatively charged proteins to migrate from the negative (cathode) electrode towards the positive (anode) electrode. This causes the proteins to separate based on their size which is relative to the molecular weight, therefore larger proteins migrate slower and smaller proteins quicker.

2.8.3   SDS gel electrophoresis protocol

The gels were cast in two parts, the first larger part being the resolving gel this being topped with the stacking gel. The resolving gel was made by mixing 4.4ml water, 3ml Buffer 1 and 4.4ml acrylamide solution. When ready to be cast, 45µl of APS solution was added with 5µl TEMED which facilitates acrylamide polymerisation. The resolving gel solution was transferred to the gel casting system and overlaid with methanol to prevent the gel drying whilst it sets. The stacking gel solution was made by mixing 4.87ml water, 1.87ml buffer 2, 750µl acrylamide solution, 75µl APS solution and 10µl TEMED. After the resolving gel had set, the methanol was poured off and remaining methanol removed using blotting paper. To the set resolving gel the stacking gel solution was poured and a 10 well comb inserted. Subsequent to the stacking gel setting the gel was transferred to an electrophoresis tank containing running buffer. The comb was removed from the gel to allow samples to be transferred into the wells. A protein standard (5µl) was loaded onto the first and last well on the gel. Subsequent to cell lysis and protein concentration determination, the lysates were boiled in Laemmli buffer in a 1:1 ratio for 10 minutes at 95°C. 35µl of the prepared lysates were loaded into the wells of the SDS gel. The loaded protein standard and prepared samples were separated by electrophoresis at 115V for 1 hour 45 minutes.

2.9   Western blot

2.9.1   Materials and regents

Electrophoresis protein transfer tank, Ice pack, gel holder cassette, foam pads, blotting paper, polyvinylidene difluoride (PVDF) membrane (GE healthcare, UK), methanol , western blot protein transfer buffer (Tris-base 24.8mM, glycine 192mM, 20%v/v (300ml) methanol, with 1200ml distilled H_2O) and Tris buffered saline (TBS; 200mM sodium chloride, 50mM Tris-base, pH adjusted to 7.4).

2.9.2   Background

After cell lysate protein has been separated by SDS-PAGE electrophoresis, the proteins can be transferred to a solid state membrane allowing antibody staining and assessment of specific proteins. Several different types of membranes are used, the most common being comprised of either nitrocellulose or PVDF. Both of these membranes are porous with pore sizes ranging from 0.05 to 10μm in diameter, the smaller the pore size the larger the protein binding surface and the greater the protein binding capacity. PVDF membrane was used because of its greater durability which allows the membrane to be stripped and re-probed. It also has greater protein binding capacity, although this can also result in PVDF membranes giving greater background signal compared to nitrocellulose membranes. The PVDF membrane is placed on top of the acrylamide gel and held in place with blotting paper and foam pads in a cassette. The cassette is placed in an electrophoresis tank, with the acrylamide gel facing towards the cathode (negative) electrode and the PVDF membrane towards the anode (positive) electrode. As the protein is negatively charged the proteins migrate laterally towards the anode electrode where they become embedded in the PVDF membrane. The PVDF membrane can now be stained with antibodies to determine the presence of specific proteins in the lysate.
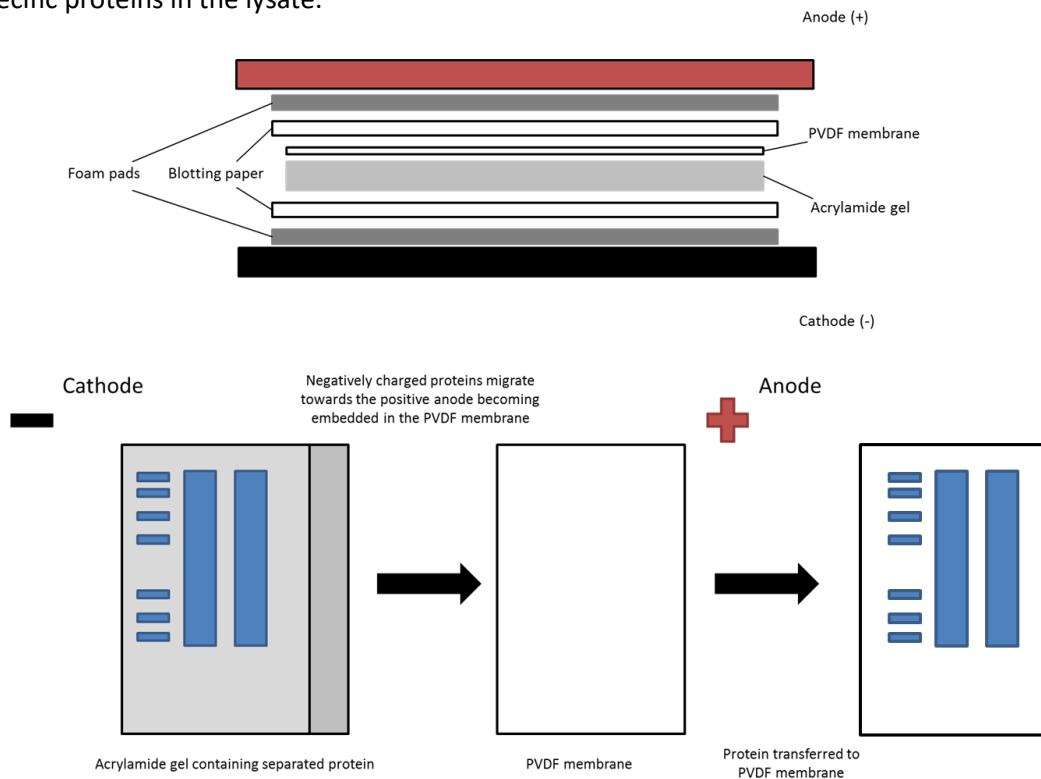
Figure 2.9.1: Electrophoresis transfer of proteins to PVDF membranes

This figure displays the arrangement of the protein containing acrylamide gel with the PVDF membrane in a blotting cassette in addition to describing the procedure of an application of a charge to induce protein transfer to the PVDF membrane.

2.9.3   Protocol

The components required for transfer, the gel foam holders and blotting paper are soaked in the transfer buffer prior to being placed onto the gel holder cassette as shown in figure 2.9.2. The acrylamide gel containing the separated protein is removed from the glass plates used during SDS-PAGE transfer and placed on top of the blotting paper towards the negative side of the cassette. The PVDF membrane is cut to the required size and soaked in methanol for 30 seconds prior to use, as the membrane is very hydrophobic soaking in methanol is required to allow binding of the protein. The membrane is never handled directly, being handled with tweezers to prevent unwanted protein being absorbed from skin or gloves. The membrane is then soaked in transfer buffer for 5 minutes to equilibrate it and place the membrane on top of the acrylamide gel. Pressure is placed onto the membrane to hold it in place and a roller used to remove any air bubbles between the membrane and gel. The blotting paper and gel foam pad is placed on top of the membrane, the cassette closed and placed in the electrophoresis tank. The tank is filled with transfer buffer and an ice pack to keep the buffer cold to prevent overheating during electrophoresis. The transfer conditions used were a constant current of 115 milliamps for 1 hour 45 minutes. After this the membrane was washed in TBS containing 0.05%v/v Tween-20 (TBST) every 5 minutes for 30 minutes (total of six washes) to remove any residual transfer buffer. The membrane could then be stained with antibodies for the proteins of interest.

2.10 Assessment of intracellular NAD^+:NADH ratio

The NAD^+:NADH ratio was assessed using an NAD^+:NADH quantification kit purchased from Abcam, UK (ab65348). Treated cells were collected by centrifugation at 500xg and washed with ice cold sterile PBS. The cells were centrifuged again and the pellet lysed in 400μl of kit supplied extraction buffer. The lysate was freeze-thawed twice to aid cellular lysis. The cell lysates were centrifuged through a 19kDa filter in order to remove proteins from the lysate which may utilise the NAD^+. To measure total NAD^+ and NADH 50μl of the lysate was loaded directly to a 96 well plate. To measure NADH 200μl of the filtered lysate was heated for 30 minutes at 60°C and 50μl transferred to the 96 well plate; 100μl of assay buffer was added to each sample and standard well. The plate was incubated at room temperature for 5 minutes before the addition of a developer solution. The developer solution produced a measurable colorimetric response to NAD^+. The total NAD^+ and NADH were quantified by measuring the absorbance at 450nm on a microplate reader. To determine the

quantity of available NAD$^+$ in the lysate the measured NADH was subtracted from the total NAD and NADH. The determined NAD$^+$ was then divided by the NADH to determine the NAD$^+$:NADH ratio.

2.11 Sirtuin 1 deacetylase activity assay

2.11.1 Materials and reagents

SIRT1 deacetylase activity assay (Sigma-Aldrich, UK), nuclear lysis buffer A (10mM HEPES, 1.5mM MgCl$_2$, 10mM KCl, 0.5mM DTT and 0.05% v/v Triton X-100, adjusted to pH 7.9), nuclear lysis buffer B (5mM HEPES, 1.5mM MgCl$_2$, 0.2mM EDTA, 0. 5mM DTT and 26% v/v glycerol, adjusted to pH 7.9), protease inhibitor cocktail (Sigma-Aldrich, UK)

2.11.2 Cell lysis and nuclear fraction collection

The treated monocytes were collected by centrifuging at 500xg for 5 minutes and washed with ice cold PBS. The cell pellet was resuspended in 500µl of nuclear lysis buffer A (10mM HEPES, 1.5mM MgCl$_2$, 10mM KCl, 0.5mM DTT and 0.05% v/v Triton X-100, adjusted to pH 7.9) supplemented with 5µl protease inhibitor cocktail to lyse the cells leaving the nucleus intact. The lysate was kept on ice for 10 minutes followed by the centrifugation at 800xg for 10 minutes at 4°C to pellet the intact nuclei. The pellet was resuspended in 374µl nuclear lysis buffer B (5mM HEPES, 1.5mM MgCl$_2$, 0.2mM EDTA, 0. 5mM DTT and 26% v/v glycerol, adjusted to pH 7.9) supplemented with 4µl protease inhibitor cocktail and 26µl 4.6M NaCl. The lysate was homogenised and the DNA sheared by passing through a 25-gauge needle and incubated on ice for 30 minutes. The cell lysates were centrifuged at 16,000xg for 30 minutes at 4°C to remove cellular debris. The supernatants were retained for quantification by BCA assay and for the SIRT1 deacetylase assay.

2.11.3 SIRT1 deacetylase activity assay

Sirtuin 1 (SIRT1) deacetylase activity was measured with a SIRT1 activity assay purchased from Sigma-Aldrich (CS1040). The kit supplies a SIRT1 specific substrate, an acetylated lysine residue conjugated to a fluorophore, upon deacetylation by SIRT1 the substrate is cleaved by a developer solution causing the release of a highly fluorescent group. Treated THP-1 monocytic cells were lysed and the nuclear fraction extracted. The protein content of the nuclear lysate was quantified by BCA assay as

previously described. Nuclear lysate containing 15µg of protein was assessed using the activity assay with fluorescence being measured by excitation at 340-380nm and emission 430-460nm.

2.12 Measurement of mitochondrial reactive oxygen species using mitoSOX red superoxide stain

2.12.1 Materials and reagents

MitoSOX red reagent (Invitrogen, UK), DMSO (Sigma-Aldrich, UK), PBS solution, flow cytometer

2.12.2 Background

The mitochondria generate energy primarily through the electron transport chain. This process can result in the generation of superoxide anions. MitoSOX red a derivative of dihydroethidium localises to the mitochondria where it can be oxidised to 2-hydroxyethidium in response to superoxide anions. The produced 2-hydroxyethidium produces fluorescence at an excitation peak at ~400nm which can be measured at ~590nm in order to determine relative generation of superoxide anions.

2.12.3 Protocol

The MitoSOX reagent was dissolved in DMSO to a final concentration of 5mM (50µg MitoSOX reagent dissolved in 13µl DMSO). Treated THP-1 monocytes were harvested by centrifuging at 500xg for 5 minutes and washed with PBS. The cells were again pelleted by centrifugation, resuspended in PBS and incubated at 37°C for 5 minutes prior to addition of 2.5µM MitoSOX reagent. The cells were covered with foil and incubated for 30 minutes at 37°C and subsequently analysed by flow cytometry.

2.13 Isolation of primary monocytes

2.13.1 Isolation of primary monocytes materials and reagents

Lymphoprep (Axis Shield, UK), Sigmacote silicanizing agent (Sigma-Aldrich, UK), monocyte isolation buffer (Ca^{2+} and Mg^{2+} free PBS containing 0.1%w/v BSA and 2mM EDTA), Dynabeads untouched human monocyte kit (Invitrogen, UK).

2.13.2 Background

The isolation of primary monocytes from whole blood can be separated into two individual processes, first the isolation of the peripheral blood mononuclear cells (PBMCs) from the blood followed by the isolation of the monocytes from the PBMC population.

The PBMCs population, which consists of monocytes and leukocytes were isolated by density gradient centrifugation by layering the diluted whole blood onto a commercially available isosmotic media called Lymphoprep (Boyum 1968). The principle is that the Lymphoprep solution has a density of 1.077g/ml which is higher than the vast majority of mononuclear cells, whereas erythrocytes and polymorphonuclear (PMN) cells have a greater density. This result of this is that upon centrifugation the erythrocytes and PMN cells pass through the Lymphoprep solution and form a pellet whereas the PBMCs form a "buffy coat" layer on top of the media from which they can be collected.

The monocytes were then negatively isolated from the collected PBMCs. A negative isolation consists of removing all other contaminating cells leaving only the monocyte population. The isolated PBMC population is incubated with magnetic beads conjugated to antibodies specific against the contaminating cells, therefore the unwanted cells will be bound to the beads and removed leaving only the monocytes. A negative isolation method was chosen to reduce the possibility of activating the monocytes through direct interaction with membrane surface proteins.

2.13.3 Isolation of primary monocytes protocol

2.13.3.1 Isolation of peripheral blood mononuclear cells

30ml whole blood was collected from healthy, consenting volunteers into evacuated EDTA collection tubes by venepuncture from the median cubital vein. The EDTA in the collection tubes chelates calcium ions preventing the coagulation of the blood. The collected whole blood was then diluted in

a 1:1 ratio with sterile PBS (0.1% w/v BSA). The diluted blood is then layered onto 11ml of Lymphoprep solution in a 50ml conical centrifuge tube. After layering the whole blood the solution is centrifuged at room temperature at 180xg for 20 minutes with the deceleration removed to prevent the layers mixing upon the centrifugation ending. The upper 5ml of plasma was then removed using a Pasteur pipette to remove the platelets. The solution was again centrifuged at 380xg for 20 minutes, again with deceleration removed, to form the "buffy coat" the PBMC layer at the interface between the Lymphoprep solution and the plasma. This layer was collected using a Pasteur pipette with care taken to avoid disturbing the Lymphoprep solution. The isolated PBMCs were then washed in sterile PBS (0.1% w/v BSA) three times. For the first wash, the PBMC suspension was centrifuged at 500xg for 8 minutes with the subsequent washes being centrifuged at 350xg again for 8 minutes. The initial wash was centrifuged at a greater speed to take into account the possibility of any Lymphoprep being present in the cell suspension which may interfere with the formation of a cell pellet. The cell pellet was then re-suspended in isolation buffer (magnesium/ calcium ion free PBS containing 0.1% w/v BSA, 2mM EDTA) and the number and viability of the isolated PBMCs determined by the trypan blue exclusion method as previously described.

2.13.3.2 Isolation of primary monocytes from PBMC population

The monocytes were isolated from the PBMC population by negative isolation using a Dynal Untouched Human Monocyte isolation kit (Life Technologies). The kit contains magnetic beads which are conjugated to a mixture of antibodies for specific markers of the unwanted cells (ie. B-cells, T-cells, NK cells etc.) so they can be isolated and removed leaving the CD14 positive, CD16 negative Mon 1, monocyte population. On average 10ml of whole blood would supply approximately 1×10^7 PBMCs from which approximately 1×10^6 primary monocytes could be isolated.

The PBMCs were adjusted to 5×10^7 cells in 500µL of isolation buffer, and to this 100µl of blocking buffer (aggregated gamma globulin in 0.9% NaCl, which blocks the monocyte Fc receptors) was added. The solution was incubated for 2 minutes at room temperature prior to 100µL of antibody mixture (biotinylated IgG specific for CD3, CD7, CD16, CD19, CD56, CDw123 and CD235a) added. The solution was mixed well by pipetting and incubated for 20 minutes at 4°C prior to being washed by the addition of 4ml of isolation buffer and centrifuged at 350xg for 8 minutes. The supernatant was discarded and the pellet resuspended in 500µL isolation buffer. Prior to use the magnetic beads were washed. The beads were vortexed for at least 30 seconds to resuspend them and 500µL transferred to 1ml of isolation buffer in a 1.5ml microcentrifuge tube. The tube was then left for at least 1 minute on a magnetic rack, the supernatant removed and the beads were

resuspended in 500µL of isolation buffer. The 500µL washed magnetic beads were then added to the cell suspension and incubated for 15 minutes at 4°C on a tube rotator. The PBMC and magnetic bead suspension was diluted with 4ml of ice cold isolation buffer to give a total volume of 5ml, which was transferred to 5 x 1.5ml microcentrifuge tubes (1ml in each). Each tube was left on a magnetic rack on ice for 2 minutes and the supernatants retained and transferred to fresh 1.5ml tubes. The magnetic beads were resuspended again in isolation buffer and left on the magnetic rack for a further 2 minutes and the supernatant collected into fresh 1.5ml tubes. The collected supernatants were again left on the magnetic rack for 2 minutes in order to remove any contaminating magnetic beads. The supernatants were pooled together and centrifuged at 350xg for 8 minutes and resuspended in RPMI 1640 media. Whilst optimising this procedure the purity of the monocyte isolation was determined by flow cytometry. Both the collected PBMC fraction and the subsequently negatively isolated primary monocytes were stained with fluorescently conjugated antibodies against CD3 and CD14 to determine the presence of CD3 positive T cells and CD14 positive monocytes respectively. The percentage of CD14 positive monocytes to CD3 positive T cells was determined pre and post monocyte isolation to determine an approximate monocyte purity. Using this method, the extracted monocyte purity was shown to be approximately 95%. Viability and monocyte number was determined by trypan blue exclusion. This protocol is scalable depending on the number of cells available ie. the PBMCs number can be adjusted to 2.5×10^7 cells in 250µL which would require 50µL of blocking solution and 50µL of antibody mixture. All plasticware; the tubes, Pasteur pipettes and pipette tips, used in the PBMC and monocyte isolation were coated with Sigmacote siliconising agent prior to use to prevent unwanted monocyte interaction with the plastic causing monocyte activation.
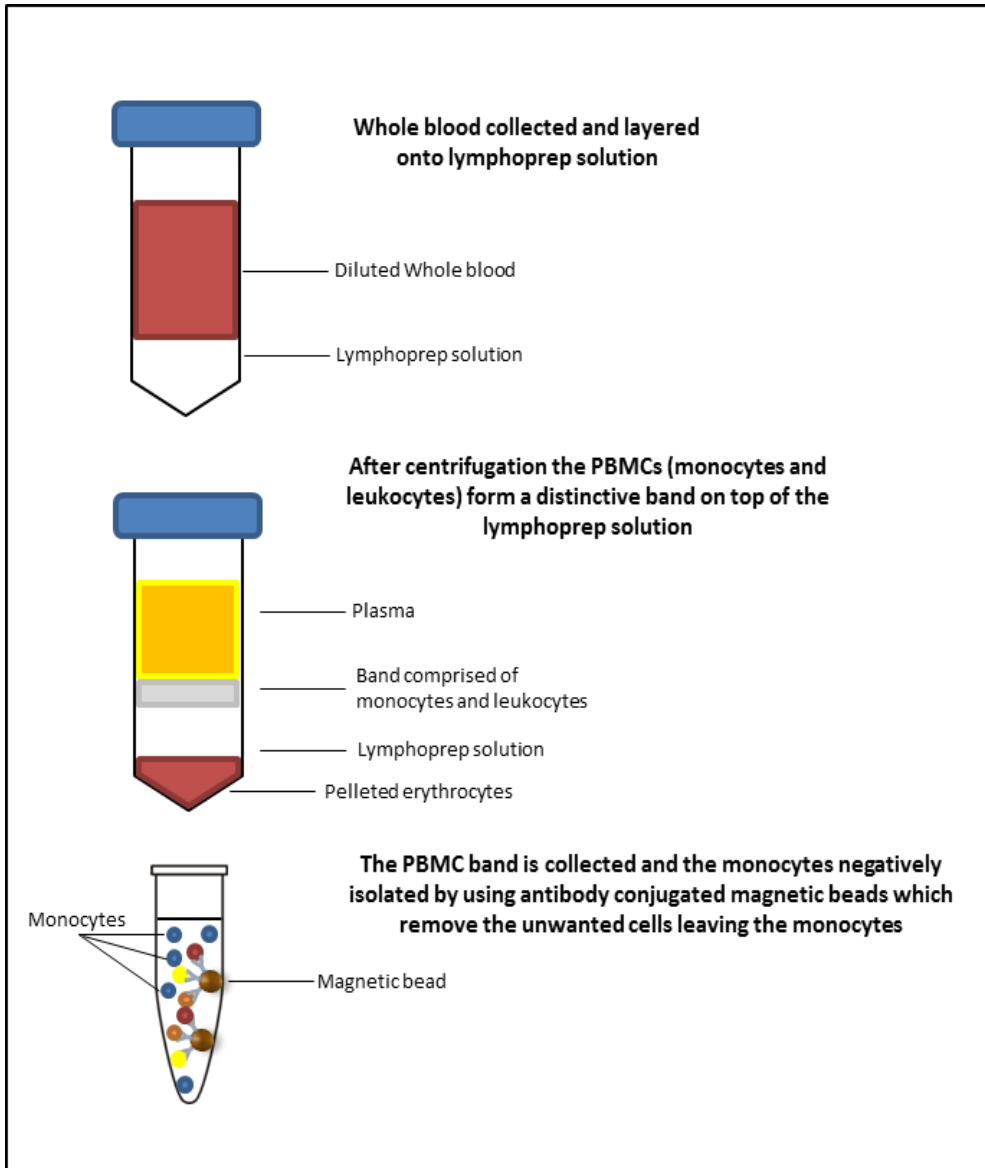
Figure 2.13.1: Isolation of primary monocytes from whole blood.

This figure displays the process used to negatively isolate primary monocytes from whole blood. The whole blood is initially diluted with PBS and layered onto a density solution, lymphoprep. The layered solution is centrifuged to allow cells with a greater density than the lymphoprep solution to pass through forming a pellet. The peripheral blood mononuclear cell (PBMC) population has a lower density than the lymphoprep solution so under centrifugation the PBMC population forms a band above the lymphoprep. The PBMC population is collected, washed with PBS and incubated with magnetic beads conjugated to antibodies specific to markers of unwanted cells. These cells are removed leaving an isolated monocyte population.

2.14 Assessment of blood glucose, HDL, LDL and total cholesterol

2.14.1 Materials and reagents

Reflotron machine (Roche), Reflotron strips to test for glucose, HDL cholesterol, LDL cholesterol and total cholesterol (Roche, UK).

2.14.2 Protocol

Subsequent to the collection of whole blood into evacuated tubes, 30µl of whole blood was placed onto the Reflotron strips to assess the content of glucose, HDL, LDL and total cholesterol. The Reflotron strips were placed into the machine and the produced result collected.

2.15 Analysis of cytokine secretion by multiplex array

2.15.1 Materials and reagents

Merck Millipore 41 analyte magnetic bead cytokine panel (HCYTMAG-60K-PX41) (Kit supplies:96 well plate, human cytokine/chemokine standards, cytokine/chemokine quality controls, pre-mixed cytokine antibody bound beads, assay buffer, wash buffer, cytokine detection antibodies and streptavidin-phycoerythrin, Luminex 200 analyser.

2.15.2 Background

Cytokine secretion was assessed using a magnetic bead-based multiplex panel designed to quantify 41 individual cytokines (2.15.1). The cytokine panel purchased from Merck Millipore utilises a mixture of 41 beads each coated with monoclonal antibodies which recognise a specific analyte. Each of the individual bead sets has a specific fluorescent signature which can be used to identify the bead. The bead mixtures are incubated with the sample, this allows binding of the analytes present in the sample to bind to the respective beads. The beads are washed and a detection antibody conjugated to biotin introduced which binds to the bead bound analytes. The fluorescent dye phycoerythrin conjugated to streptavidin is added to the beads whereby it binds to any biotinylated detection antibodies bound to the analyte-bead complexes. The beads were then analysed by the

Luminex 200 which employs methods similar to flow cytometry by using a series of laser and measuring fluorescent emission. The beads are identified by its specific fluorescent signature to determine the analyte bound to it and the quantity of analyte bound determined by fluorescence emitted by bound phycoerythrin.

2.15.3 Protocol

Wash buffer (200µl) was added to each well on the supplied 96 well plate, the plate sealed and incubated on a plate shaker for 10 minutes. The wash buffer was removed and the plate dried by inverting onto blotting paper. Prepared standards (25 µl) (10,000pg/ml – 3.2pg/ml) and quality controls (25µl) were added to appropriate wells on the 96 well plate. The samples (25µl) were added to the plate in duplicate to appropriate wells. To each well 25µl of assay buffer was added to give a well volume of 50µl. The pre-mixed magnetic beads were sonicated for 30 seconds prior to addition to each well on the 96 well plate. The plate was sealed and incubated on a plate shaker overnight at 4°C. The 96 well plate was placed onto a magnetic plate to draw the magnetic beads to the base of the wells and the plate washed twice using an automated plate washer. The detection antibodies (25 µL) were added to each well and the plate was covered with foil and incubated for 1 hour on a plate shaker at room temperature. To each well 25µl of streptavidin-phycoerythrin was added and the plate covered with foil and incubated for 30 minutes on a plate shaker. The plate was washed as described previously a further two times and 150µl of sheath fluid added to each well. The plate was incubated for 5 minutes at room temperature on a plate shaker to resuspend the magnetic beads. The plate was read on a Luminex 200 analyser with detection set to read a minimum of 50 beads per analyte.
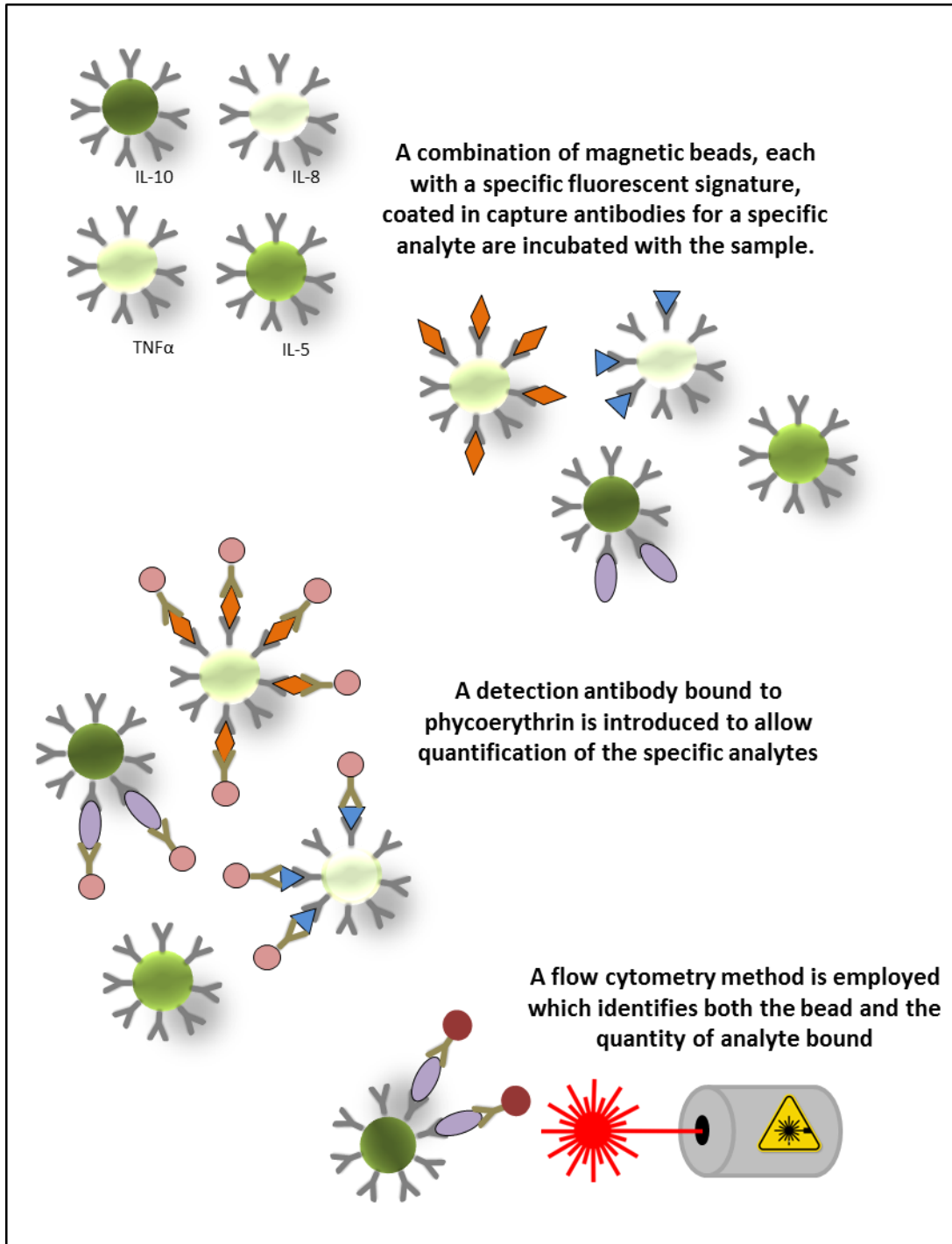
Figure 2.15.1: Multiplex assays allow the detection of multiple analytes from an individual sample.

The individual bead sets each recognise a specific cytokine and have a unique fluorescent signature that allows its identification. These beads are coated in capture antibodies that recognise and bind the target cytokine. A phycoerythrin conjugated detection antibody binds to the capture antibody bound cytokines. These beads are analysed using a piece of equipment called a luminex 200 which by using a series of lasers simultaneously identifies the bead group and quantifies the amount of bound cytokine.

2.16 Extraction of total ribonucleic acid (RNA)

2.16.1 Extraction of total RNA materials and reagents

miRNeasy Micro Kit and miRNeasy Mini kit (Qiagen, UK), RNAse away solution (Sigma-Aldrich, UK), Trizol lysis solution (Qiagen, UK), Nuclease free H_2O (Thermo-Scientific, UK), Nuclease free DNAse (Thermo-Scientific, UK).

2.16.2 Extraction of total RNA background

The cells are lysed in Trizol reagent, a phenol based lysis buffer containing guanidine thiocyanate. Guanidine thiocyanate is a chaotrophic agent meaning that the guanidine thiocyanate disrupts non-covalent molecular interactions such as hydrophobic and Van der Waals interactions, this results in the denaturing of proteins. The benefit of this is that proteins which may result in the degradation of the RNA such as RNAses are denatured (Chomczynski and Sacchi 1987). The RNA extraction kits use a spin column containing a silica gel membrane. Nucleic acids bind to silica in the presence of high concentrations of chaotrophic salts in this case guanidine thiocyanate, these salts are removed by washing allowing the elution of the nucleic acid (Chen and Thomas 1980, Marko, Chipperfield et al. 1982).

2.16.3 Extraction of total RNA protocol

The monocytes were transferred to 1.5ml micro-centrifuge tubes before being harvested by centrifugation at 1000xg for 5 minutes. The media was removed and the cells were washed in PBS, then cells were again pelleted and the supernatant removed. The cell pellet was lysed in 700µl of Trizol reagent, the pellet was vortexed until completely lysed prior to being stored at -80°C until extraction. The frozen samples were left at room temperature until thawed and briefly vortexed to ensure homogenisation. To each sample, 140µl of chloroform was added, the tube sealed and shaken vigorously for approximately 30 seconds. The mixture was centrifuged at 12,000xg 4°C for 15 minutes in order to separate the mixture into an upper aqueous phase and a lower organic phase. The upper aqueous phase was collected (approximately 350µl) and mixed with 1.5 x volume of 100% ethanol (approximately 525µl) and mixed by pipetting. A supplied RNA extraction spin column was placed into a 2ml collection tube and 700µl of the sample loaded onto the spin column. The column was centrifuged at 8000xg for 30seconds at room temperature, the flow through discarded, the rest of the sample loaded and the centrifugation repeated. The spin column was washed with 700µl of a

supplied "RWT" wash buffer and centrifuged as described above and the flow through discarded. The spin column was again washed with 500µl of a supplied "RPE" wash buffer and centrifuged as described above and the flow through discarded. 500µl of 80%v/v ethanol was added to the spin column which was subsequently centrifuged at 8000xg for 2minutes at room temperature and the flow through discarded. The spin column was placed into a clean 2ml collection tube and centrifuged with the lid open at full speed (~14,000xg) for 5minutes to dry residual ethanol from the membrane. The spin column was placed into a 1.5ml collection tube and 14µl of nuclease free water added directly to the membrane and incubated at room temperature for 1minute before being centrifuged at full speed for 1 minute at room temperature. The eluted RNA was then quantified spectrophotometrically using a Nanodrop and stored at -80°C.

2.17 Quantitative polymerase chain reaction (qPCR) of messenger RNA (mRNA)

2.17.1 Materials and reagents
SYBR green PCR master mix (Primer Design, UK), 96 well PCR plates, strip caps, nuclease free water, High capacity reverse transcription kit (Applied Biosystems, UK), PCR primers, Stratagene mx3000p qPCR thermocycler.

2.17.2 Background
Polymerase chain reaction (PCR), developed by Kary Mullis and colleagues for which he received the 1993 noble prize for chemistry, is a technique which amplifies small quantities of DNA by several orders of magnitude (Saiki, Scharf et al. 1985, Saiki, Gelfand et al. 1988). PCR involves the amplification of a specific double stranded DNA sequence through the use of heat stable DNA polymerase enzymes. The specific DNA sequence is heated to cause denaturation to produce single strands of DNA. Specific DNA oligonucleotides called primers, which share complementarity with the 5' ends of the sense and anti-sense DNA strands anneal to the DNA. A DNA polymerase recognises the primer sequence bound at the 5' ends and extends it using free nucleotides producing the complementing DNA strand. This produces copies of the both the sense and anti-sense strands which can reanneal resulting in a copy of the original DNA sequence. This cycle of denaturation, annealing and copying occurs numerous times to significantly amplify the DNA sequence. The amplification of DNA can be quantified through the addition of fluorescent dyes specific to DNA, SYBR green for example binds to double stranded DNA which as the sequence is copied the quantity of double stranded DNA increases. The rate at which the fluorescent signal increases gives an indication of the

quantity of DNA in the initial sample allowing relative quantification of the specific DNA sequence in the sample.

2.17.3 Protocol

Reverse transcription was performed using a high capacity reverse transcription kit purchased from Applied Biosystems to convert extracted mRNA to cDNA. A mastermix solution was made from the reverse transcription kit components, consisting of per sample; 2μl reverse transcriptase buffer, 0.8μl dNTP mixture (100mM), 1μl reverse transcriptase, 2μl random primers and 4.2μL nuclease free water was added. The mastermix was mixed by vortexing and 10μl added to 200μl PCR tubes. An equal volume of extracted RNA sample (containing 500ng RNA) was added to the PCR tubes. To control for possible genomic DNA contamination the samples were also incubated with a mastermix solution without the addition of the reverse transcriptase enzyme. The rationale behind this being that if the negative reverse transcriptase samples give a positive result during the qPCR stage it can be postulated that these samples have genomic DNA contamination that could negatively impact on the results. The samples were incubated in a thermal cycler set to the conditions described in table 2.1. The converted cDNA was diluted 1 in 10 with nuclease free water and stored at -20°C until needed.

The expression of specific mRNA was measured by qPCR analysis of the diluted cDNA. A qPCR reaction stock solution was made by mixing for each sample: 0.5μl of the forward and reverse primers, 4μl nuclease free water and 10μl SYBR green mastermix. To each well on a qPCR plate 15μl of the reaction stock solution was added to 5μl of the diluted cDNA. The wells were sealed with strip caps and the plate loaded onto a Stratagene mx3000p qPCR thermocycler set to the thermal profile detailed in table 2.3. The produced data was analysed using the comparative delta delta CT method (Livak and Schmittgen 2001, Schmittgen and Livak 2008). The results are normalised as a fold change relative to the 5mM D-glucose treated cells, to avoid removing the variance as a result of the normalisation the standard error of the ΔCT ($CT_{gene} - CT_{housekeeper}$) values of the 5mM D-glucose treatments are included on the datasets. Which allows more accurate statistical analysis.

Table 2.1: Thermal cycler settings for reverse transcriptase of mRNA to cDNA

	Step 1	Step 2	Step 3	Step 4
Temperature (°C)	25	37	85	4
Time	10 minutes	120 minutes	5 minutes	∞

Table 2.2: qPCR primers

Primer	Forward primer sequence	Reverse primer sequence
TNFα mRNA	CCCAGGGACCTCTCTCTAATCA	GCTACAGGCTTGTCACTCGG
SIRT1 mRNA	CTGGACAATTCCAGCCATCT	GGGTGGCAACTCTGACAAAT
18S rRNA	GTAACCCGTTGAACCCCATT	CCATCCAATCGGTAGTAGCG

Table 2.3: Thermal profile conditions for mRNA qPCR

Step	Enzyme activation	PCR		
	Hold	40 cycles		
		Denature	Anneal	Extension
Temperature (°C)	95	95	55	72
Time	10 minutes	5 seconds	5 seconds	10 seconds

2.18 qPCR of micro-RNA (miRNA)

2.18.1   Materials and reagents

Taqman miRNA reverse transcription kit (Thermo-Scientific, UK), PCR mastermix (Primer Design, UK), Taqman miRNA assays (Thermos Scientific: assays for miR-146a-5p, miR-155, miR-424 and miR-16), nuclease free water, 96 well PCR plates, strip caps, Stratagene mx3000p qPCR thermocycler.

2.18.2   Protocol

A reverse transcription mastermix was made by mixing 0.15µL dNTPs, 1µL reverse transcriptase, 1.5µL reverse transcription buffer, 0.19µL RNase inhibitor and 4.16µL nuclease free water for each sample. Reverse transcription of each individual miRNA requires a miRNA specific reverse transcription primer. To the mastermix 3µL (per sample) of a miRNA specific reverse transcription primer was added. The solution is mixed and 10µL added to PCR tubes for the number of samples to be reverse transcribed. To each tube 5µL (containing 10ng RNA) of the extracted RNA was added and the tubes loaded into a thermocycler. The miRNA was reversed transcribed using the thermocycler conditions described in table 2.4. The reverse transcribed miRNA was stored at -20°C until needed.

Quantitative PCR was performed on the reversed transcribed miRNA by adding 1.33µL of the reverse transcription product to 10µL PCR mastermix, 7.67µL nuclease free water and 1µL of miRNA specific primer and taqman probe. The final 20µL volume was transferred to a 96 well PCR plate, the plate sealed with strip caps and the plate loaded onto a stratagene mx3000p qPCR thermocycler set to the thermal profile described in table 2.5. The microRNA hsa-miR-16 was chosen as a housekeeper miRNA due to it being observed to remain stable in the microarray assessment of miRNA expression in monocytes taken from obese individuals, in addition to remaining stable during the qPCR assessment of glucose treated primary monocytes. The produced data was analysed using the comparative delta CT method (Livak and Schmittgen 2001, Schmittgen and Livak 2008). The results are normalised as a fold change relative to the 5mM D-glucose treated cells, to avoid removing the variance as a result of the normalisation the standard error of the ΔCT (CT $_{gene}$ – CT $_{housekeeper}$) values of the 5mM D-glucose treatments are included on the datasets. Which allows more accurate statistical analysis.

Table 2.4: Thermal cycler settings for reverse transcription of miRNA

	Step 1	Step 2	Step 3	Step 4
Temperature (°C)	16	42	85	4
Time	30 minutes	30 minutes	5 minutes	∞

Table 2.5: Thermal profile conditions for miRNA qPCR

	Enzyme activation	PCR	
		40 cycles	
Step	Hold	Denature	Anneal/extend
Temperature (°C)	95	95	60
Time	10 minutes	15 seconds	60 seconds

2.19 Chromatin Immunoprecipitation

2.19.1 Materials and reagents

Diagenode bioruptor, 1.5ml polymethylpentene microtubes (Diagenode, Belgium), methanol free 16% formaldehyde ampoules (Thermo-Scientific, UK), SDS lysis buffer (50mM Tris-HCl pH8.0, 10mM EDTA, 1% v/v SDS (from 10%w/v stock solution), *Added prior to use:* 20mM sodium butyrate (NaBu) and protease inhibitor cocktail, RIPA buffer (10mM Tris-HCl pH 7.5, 1mM EDTA, 0.5mM EGTA, 140mM sodium chloride, 1% Triton X-100, 0.1% SDS and 0.1% sodium deoxycholate), ChIP elution buffer (20mM Tris-HCl pH 7.5, 5mM EDTA, 50mM sodium chloride, 1% SDS, *Added prior to use:* 20mM sodium butyrate), blocking buffer (added to RIPA buffer: BSA 200µg/ml, salmon sperm 10µg/ml)

2.19.2 Background

Chromatin immunoprecipitation is a technique developed to assess interactions between proteins such as histones and transcription factors with DNA (figure 2.19.1). This allows the identification of sites of transcription factor binding or genes associated with specific histone modifications.

The technique first requires the proteins to be cross-linked to the DNA by a fixative agent such as UV light or formaldehyde. Formaldehyde is a common choice of fixative agent due to its reversibility with high temperature. The fixed chromatin is sheared by either micrococcal nucleases or sonication to approximately 500bp in length. The shearing of the chromatin allows for selection of specific proteins by immunoprecipitation in order to assess their associated genes. Subsequent to immunoprecipitation the extracted chromatin is treated with proteinase K and the crosslinking reversed leaving the DNA. The DNA is then extracted and purified for subsequent analysis by qPCR in order to identify specific genes regulated by the protein of interest.

2.19.3 Protocol

The protocol for chromatin immunoprecipitation was adapted from previously established protocols designed for use with low cell numbers (Dahl and Collas 2009, Sikes, Bradshaw et al. 2009). Isolated primary monocytes ($1x10^5$ cells) were washed with 500µl sterile PBS by centrifuging at 450xg for 5 minutes and resuspended in 500µl sterile PBS before being fixed with 1% v/v methanol-free formaldehyde (31.25µl of 16% formaldehyde) for 10 minutes at room temperature. Methanol-free formaldehyde was used as methanol increases cellular permeability making fixation conditions difficult to replicate. The formaldehyde fixation was quenched by addition of Tris (pH 7.4) to a final concentration of 750mM, the solution was incubated at room temperature for 5 minutes with gently mixing (Sutherland, Toews et al. 2008). The fixed cells were pelleted by centrifuging at 450xg at 4°C for 5 minutes. The pellet was washed three times with 500µl ice cold PBS by centrifuging at 450xg at 4°C for 5 minutes, the supernatant was removed and the cell pellet resuspended in sterile ice cold PBS. After the final wash the pellet was resuspended in 120µl 1% SDS lysis buffer (50mM Tris-HCl pH8.0, 10mM EDTA, 1% SDS with 20mM NaBu to inhibit histone deacetylase proteins thereby preventing loss of acetylation modifications during lysis, and protease inhibitor cocktail to prevent histone and transcription factor degradation). Sonication was chosen as the method of chromatin shearing as opposed to micrococcal nuclease digestion due to the bias micrococcal nucleases have for certain genomic regions resulting in uneven, non-random DNA shearing. Sonication was performed using a Diagenode Bioruptor, a water bath sonicator that emits 20kHz sonication waves. The fixed cells were sonicated for a total of 10 cycles, a cycle consisting of 30 seconds on and 30

seconds off. The samples were briefly vortexed after every 2 cycles of sonication and kept on ice. After sonication, the lysate was centrifuged at 4°C, 14,000xg for 10 minutes to clear the lysate of cellular debris. The sonicated chromatin was diluted with 1080µl RIPA buffer to reduce the SDS concentration to ~0.1% to prevent the SDS interfering with antibody binding during the immunoprecipitation process.

The samples were pre-cleared prior to immunoprecipitation by incubating 100µl of sonicated chromatin with 10µl Dynal magnetic beads for 1 hour at 4°C with rotation; this was done in order to remove chromatin from the sample that may bind non-specifically to the beads decreasing sensitivity of the assay. 10µl of protein A-conjugated magnetic beads were blocked by incubating with 100ul of blocking buffer containing salmon sperm and BSA. The blocked protein A-coated Dynal magnetic beads were conjugated to an anti-acetylated (K310) P65 antibody by incubating 3µg of antibody in a solution of 90µl RIPA buffer with 10µl magnetic beads for 2 hours at 4°C. 100µl of the chromatin samples were incubated with the antibody-bead conjugates overnight at 4°C with rotation. The samples were placed onto a magnetic rack, the supernatant discarded and 100µl of RIPA buffer added prior to incubation for 4 minutes at 4°C with rotation. This washing step was repeated a further two times before the addition of 150µl of elution buffer supplemented with 2mg/ml of proteinase K. The samples were incubated at 68°C for 2.5 hours on a heating block; the samples were manually agitated every 10 minutes to prevent the beads from sedimenting. Heating the samples aids the elution process whilst reversing the DNA cross-linking. The heated samples were placed in the magnetic rack and the supernatant collected. The beads were resuspended in an additional 150µl elution buffer and heated again at 68°C for a further 30 minutes. The samples were again placed in a magnetic rack and the supernatant collected and added to the first collected sample to give a final volume of 300µl. The eluted DNA was isolated by phenol-chloroform-isoamyl alcohol extraction followed by qPCR (see below).
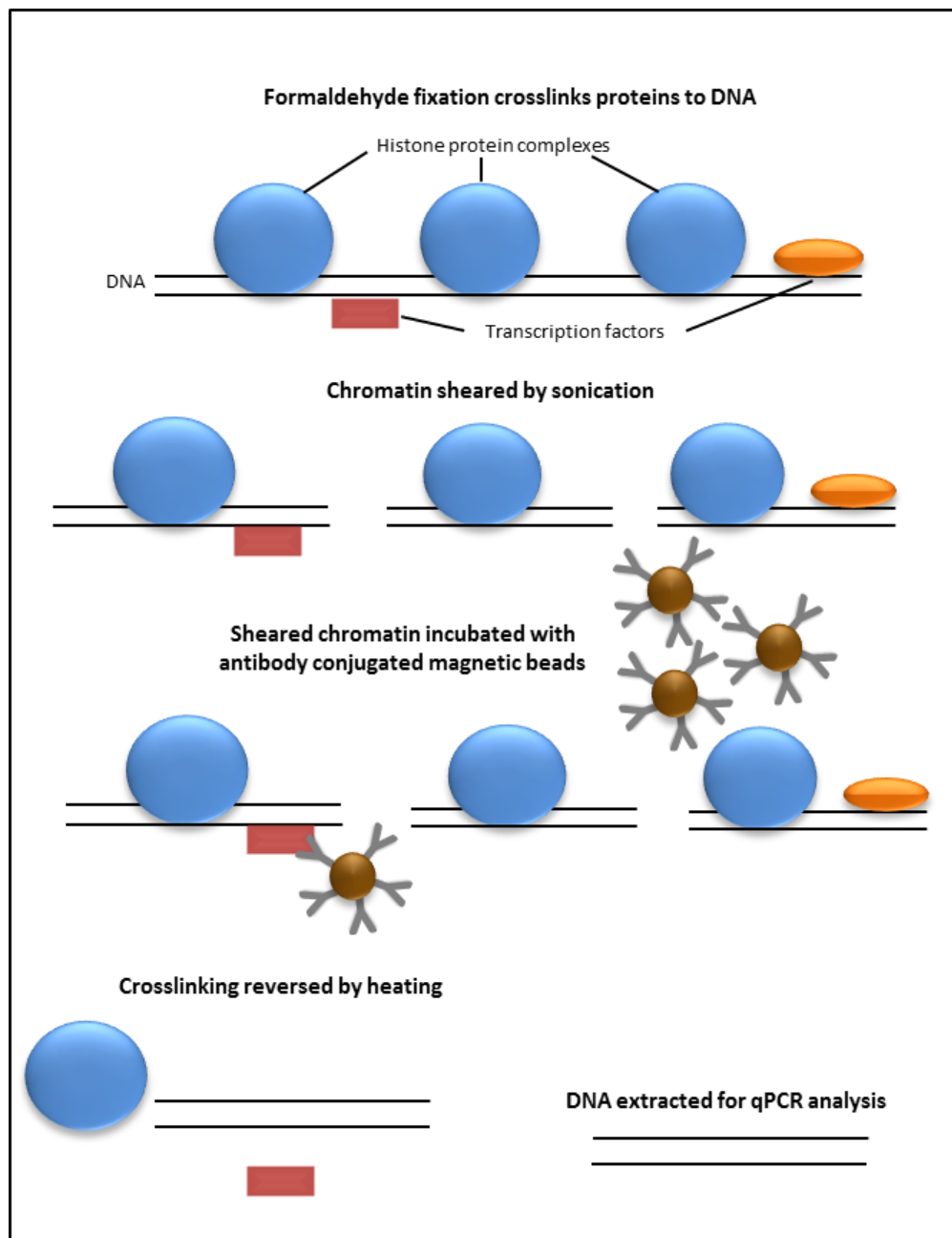
Figure 2.19.1: Background of Chromatin Immunoprecipitation method for assessment of protein -DNA interaction.

Treated cells are incubated with formaldehyde to fix the DNA associated proteins preserving the interactions of transcription factors, histone proteins and polymerases with the DNA. The cells are lysed and the DNA sheared by sonication. The sheared DNA is immuno-precipitated from the lysate based on a specific protein or protein modification. The immuno-precipitated DNA is heated to reverse the crosslinking between the protein and the DNA. The DNA is purified and assessed by qPCR to determine the DNA regions interacting with the immuno-precipitated protein.

2.20 Phenol chloroform isoamyl alcohol extraction of immunoprecipated DNA

2.20.1 Materials and reagents

ChIP elution buffer (20mM Tris-HCl pH 7.5, 5mM EDTA, 50mM sodium chloride, 1% SDS, *Added prior to use:* 20mM sodium butyrate), Phenol:Chloroform:Isoamyl alcohol (25:24:1), chloroform, ethanol, 200mM sodium chloride solution Tris-EDTA (TE) buffer, linear acrylamide (Thermo-Scientific, UK), DNA low bind 1.5ml microcentrifuge tubes (Eppendorf, UK)

2.20.2 Background

The phenol chloroform isoamyl extraction method both removes contaminating proteins and purifies DNA from an aqueous sample. The aqueous sample is mixed with the phenol:chloroform:isoamyl solution and centrifuged. The centrifugation separates the mixture into a clear upper aqueous phase which contains the DNA, a white precipitous interphase consisting of protein and a lower organic phase containing phenol. As DNA and water are both polar molecules DNA due to its negative phosphate backbone and water due to its electronegative oxygen atom, is very soluble in water so upon centrifugation the DNA is localised to the aqueous phase. As proteins are generally non-polar they localise to the phenol organic phase upon centrifugation as phenol is itself a non-polar molecule. The aqueous phase containing the DNA can be removed and the DNA precipitated by mixing with cold ethanol and a high sodium chloride salt buffer. The positively charged sodium ions interact with the DNA negative phosphate backbone disrupting the electrostatic interactions that occur between the DNA phosphate back bone and the water molecules. The added ethanol reduces the dielectric constant facilitating the salts neutralisation of the DNA phosphate backbones charge causing its precipitation from solution.

2.20.3 Protocol

The 300µl of immunoprecipitated DNA was diluted with ChIP elution buffer to a volume of 500µL in 1.5ml DNA low bind tubes and phenol:chloroform:isoamyl alcohol solution (supplied as a ratio of 25:24:1) added in a 1:1 ratio. The solution was mixed vigorously for 30 seconds, left at room temperature for 5 minutes before being centrifuged at 12,000xg for 10 minutes at room temperature. The aqueous phase containing DNA was collected without disturbing the interphase or organic phase, was then mixed in a 1:1 ratio with chloroform and again vigorously mixed. The mixture was centrifuged at 4°C 12,000xg for 10 minutes to separate into aqueous-, inter- and organic

phases. The collected aqueous phase was collected then mixed with 100% ethanol at a ratio of 1:1.75, 200mM sodium chloride (NaCl) and linear acrylamide. The mixture was incubated at -20°C overnight and then centrifuged at 14,000xg for 30 minutes at 4°C to pellet the DNA. The supernatant was then removed and the pellet washed with 70% ethanol to remove any salt and dried in a vacuum centrifuge. The pellet was then re-suspended in a Tris-HCl low EDTA buffer (to prevent any interference with subsequent qPCR analysis) and quantified spectrophotometrically using a Nanodrop.

2.21 Agarose gel visualisation of sheared DNA

2.21.1   Materials and reagents

Agarose powder (Sigma-Aldrich, UK), Tris-acetate-EDTA (TAE) buffer (40mM Tris, 20mM acetic acid and 1mM EDTA (pH8.0)), ethidium bromide solution (10mg/ml), gel casting tray, gel combs, electrophoresis tank, electrophoresis power pack, 6x DNA loading buffer and 500bp DNA ladder (Thermo-Scientific, UK)

2.21.2   Protocol

Agarose gels were made by resuspending 1%w/v of agarose powder in TAE buffer, the agarose was dissolved by heating in a microwave. The solution was mixed after every 30 seconds of microwaving until the agarose was completely melted and homologous. The solution was left to cool until the beaker could be held without burning, after which an ethidium bromide solution was added to a final concentration of 0.5µg/ml. The solution was mixed to completely disperse the added ethidium bromide and the gel poured into a casting tray to a thickness of approximately 5mm with an inserted 10 well comb. The gel was left until it had completely set and then placed into the electrophoresis chamber with the wells placed towards the negative (cathode) end. TAE buffer was poured into the electrophoresis chamber to cover the gel and the combs gently removed.

The extracted DNA was mixed with 6x DNA loading buffer (Thermo Scientific, UK) in a 1:5 ratio. A 500bp DNA ladder (5µl) was added to the first well and to the subsequent wells the prepared DNA samples (10µl) were added. The DNA was separated by applying 100V to the gel for approximately 2 hours. The gel was removed from the electrophoresis tank and the separated DNA visualised on a UV light box.

3 Reversibility of obesity induced miRNA expression in response to bariatric surgery

3.1 Preface

This chapter describes an investigation into the effects of bariatric surgery on obese individuals' monocyte microRNA expression profiles relative to those from healthy, non-obese control subjects. This was done in order to assess the reversibility of miRNA expression profiles associated with obesity and whether bariatric surgery would normalise expression of dysregulated miRNAs. Blood samples were collected from patients awaiting bariatric surgery and follow-up samples were taken 3 months and 1 year post-surgery; samples were collected from control individuals at matching time points. The monocyte population was isolated from the collected blood samples and lysed for RNA extraction miRNA expression being subsequently assessed by microRNA microarrays.

3.2 Introduction

Many studies have determined that a number of microRNAs are dysregulated in response to obesity and diabetes (Baldeon, Weigelt et al. 2015, Li, Zhou et al. 2015). A number of these are postulated to contribute to the development of obesity associated chronic inflammation and insulin resistance (Williams and Mitchell 2012, Deiuliis 2015). Due to the increased prevalence of obesity and an increased evidence base supporting its use, bariatric surgery is becoming a more commonly employed means of treating obesity. Bariatric surgery describes a range of surgical procedures performed on patients with obesity with the aim of causing weight reduction. Guidelines set out by the National Institute for Health and Care Excellence (NICE) state that bariatric surgery should be available for individuals with a body mass index (BMI) greater than 35 who have failed to lose weight through medical weight loss programs. Recent additions (November 2014) to the NICE guidelines state that obese individuals (BMI > 30) with recently diagnosed type 2 diabetes should receive expedited assessment for bariatric surgery. The evidence base in support of bariatric surgery as a weight loss measure has grown substantially in recent years with it now being seen as an effective means of treating obesity and its associated co-morbidities, especially type 2 diabetes (Sjostrom, Narbro et al. 2007, Brethauer, Aminian et al. 2013). Bariatric surgery has also been shown to be more effective than conventional weight loss methods at reducing weight, improving mortality and also being more effective at improving glycaemic control during type 2 diabetes than currently prescribed medication (Mingrone, Panunzi et al. 2012, Schauer, Kashyap et al. 2012). A study following the

progress of obese individuals treated with conventional weight loss methods against those who received bariatric surgery found that the individuals receiving bariatric surgery lost 16.1% of their body weight compared to the obese individuals who received the conventional weight loss methods gained 1.6% over the 10 year period (Sjostrom, Lindroos et al. 2004). A meta-analysis of 5000 obese patients with type 2 diabetes who received bariatric surgery found that 76.8% achieved full diabetic remission and 86% either achieved full diabetic remission or significantly improved glycaemic control (Buchwald, Avidor et al. 2004). Bariatric surgery also reduced some markers of obesity induced inflammation including plasma CRP, IL-6 and TNFα (Netto, Bettini et al. 2015). However adequate weight loss in response to bariatric surgery is not always achieved. Over a 10 year period after bariatric surgery 20.4% of morbidly obese patients and 34.9% of super morbidly obese patients failed to lose the amount of weight for the surgery to be deemed successful (Christou, Look et al. 2006).

Cellular ageing is a complex process which is strongly linked to inflammation. The inflammaging model of cellular ageing proposed by Franceschi, Bonafe et al. (2000) suggests that the ageing phenotype is caused by the accumulation of damage from a multitude of stresses such as reactive oxygen species (ROS) produced as a consequence of normal cellular metabolism, exposure to U.V radiation and bacterial and viral infections. Stressed cells employ several adaptive mechanisms such as DNA repair pathways, organelle autophagy, reducing agents such as glutathione and inflammatory responses. It is believed that over prolonged exposure to these stresses, the cells become less capable of adequately repairing this damage leading to cellular ageing. Recent studies have highlighted a link between obesity and accelerated ageing, potentially mediated through inflammation. miR analysis during ageing has highlighted a number of regulatory sequences that are in common with those seen in obesity. It is not known whether any of the age- and obesity-associated miR changes can be reversed nor whether this improves health outcomes.

Although bariatric surgery has been proven in the majority of cases to be an effective method of reducing weight, inflammation and insulin resistance, only a handful of studies have assessed its ability to reverse obesity-induced microRNA dysregulation. Continued microRNA dysregulation could result in individuals continuing to be at a higher risk of developing insulin resistance and co-morbidities associated with increased inflammation post bariatric surgery. This could impair the effectiveness of bariatric surgery as a method of weight reduction and patient outcome. Assessment of patients' miR profiles prior to surgery may also give an indication as to how successful surgery may be for them in the long term.

3.2.1　Aims and objectives

The aims of the research presented within this chapter were to assess whether obesity would result in the dysregulation of microRNAs associated with monocyte function and whether weight loss induced by bariatric surgery would result in the reversal of any observed changes in microRNA expression.

The objectives were to assess monocyte miR expression of obese individuals prior to bariatric surgery relative to healthy controls, in order to determine miRs dysregulated in response to obesity and if surgery would reverse dysregulated microRNAs. To achieve this, whole blood samples were taken from obese individuals awaiting bariatric surgery, 3 months and 1 year after receiving bariatric surgery and from control individuals at corresponding time points. From these whole blood samples the monocytes were isolated, lysed and the RNA extracted. The RNA extracted at these time points was assessed for microRNA expression by microarray analysis to determine obesity induced changes and if bariatric surgery would reverse these changes.

3.3 Methods

3.3.1 Patient sample collection and clinical values

A total of ten obese individuals awaiting bariatric surgery were recruited from Heartlands Hospital, Birmingham, by Dr Srikanth Bellary, a consultant physician in diabetes and endocrinology. Whole blood samples (30ml) were collected by venepuncture into potassium EDTA evacuated collection tubes from the patients by a clinician. The patients' blood samples were assessed for HbA1c, total cholesterol, HDL and LDL cholesterol (table 3.2). A total of six healthy control individuals were recruited from staff and student volunteers at Aston University and 30ml whole blood collected by venepuncture. The whole blood samples were collected and the monocytes isolated as described previously (methods chapter; 2.13). Approximately 1.5 million monocyte cells were extracted and lysed in a phenol based lysis regent (Trizol; Qiagen, UK). The RNA was extracted using spin columns as described previously (methods chapter; 2.16) and RNA integrity and concentration was assessed using a Bioanalyzer (Agilent, UK).

The control and obese individuals' clinical values were statistically compared by unpaired t-test to determine statistical significant differences between these groups of individuals. The obese individuals had significantly higher levels of plasma glucose and HbA1c although surprisingly they had comparable values for total, HDL and LDL cholesterol. The reason for this may be due in part to medication, lipid uptake inhibitors (Orlistat) and statins (Atorvastatin, Simvastatin) a number of the obese individuals were prescribed. A number of the obese individuals were also prescribed anti-hyperglycaemic medications such as Metformin, Liraglutide, Sitagliptin and Novorapid, which may also have reduced the observed differences in plasma glucose and HbA1c values. The clinical values of the obese individuals at the baseline time-point and the 1 year follow-up time-point were also compared to determine changes occurring as a result of the bariatric surgery. Although plasma glucose and HbA1c concentration had decreased by the 1 year post surgery time-point the change was not determined to be statistically significant.

Table 3.1: Participant gender and age information

	Bariatric participants	Control participants
Number	10	6
Sex	m= 4; f= 6	m= 2; f= 4
Average age	46.1 ± 12.66	41.5 ± 16.02

Table 3.2: Clinical values of obese individuals at baseline and 1 year post surgery time points

	Control individuals	Obese individuals	
	1 year time point	**Baseline**	**1 year post surgery follow-up**
Average weight (kg)	~	144.79 ± 35.91	119.22 ± 28.15
Average BMI	~	53.15 ± 10.16	43 ± 8.45 **(†)**
HbA1c (%)	4.96 ± 0.51	7.02 ± 1.51 **(*)**	6.56 ± 1.78
Glucose (mmol/L)	5.34 ± 0.83	8.59 ± 2.19 **(*)**	7.87 ± 2.19
Cholesterol (mmol/L)	4.54 ± 1.07	4.6 ± 0.97	4.25 ± 1.17
HDL (mmol/L)	1.11 ± 0.50	1.03 ± 0.33	1.13 ± 0.25
LDL (mmol/L)	3.21 ± 0.80	3.06 ± 1.21	2.59 ± 1.08

Significance was determined by unpaired t-test. Comparisons were made between the clinical data from the control individuals and from the obese individuals at baseline or the 1 year post surgery time-point whereby significant differences are denoted by (*), (**) and (***) representing $p<0.05$, $p<0.01$ and $p<0.001$ respectively. Comparisons were also made between the clinical data values from the obese individuals at the baseline time point with the values from the obese individuals at the 1 year post surgery time point whereby significant differences are denoted by (†), (††) or (†††) representing $p<0.05$, $p<0.01$ and $p<0.001$ respectively.

3.3.2 Isolation of primary monocytes

Described in detail in Chapter 2, Materials and methods, Section (2.3)

3.3.3 Determination of extracted RNA integrity and concentration using an Agilent Bioanalyzer

3.3.3.1 Materials and reagents

Agilent RNA 6000 nano kit (supplies: RNA nano chips, RNA ladder, RNA Dye concentrate, RNA nano marker and RNA nano gel matrix), nuclease free water, Agilent chip priming station, syringe, spin filters, Agilent 2100 bioanalyzer.

3.3.3.2   Background

The integrity and concentration of the extracted RNA samples were assessed through the use of an Agilent bioanalyzer. The bioanalyzer uses 16 well chips through which an electrophoresis gel containing a RNA specific dye has been included. This allows the RNA samples to be separated by electrophoresis providing quantification of RNA against markers and visualisation of RNA degradation.

3.3.3.3   Protocol

The supplied RNA nano gel matrix and RNA nano dye concentrate were equilibrated to room temperature for 30 minutes prior to use. The RNA gel matrix was filtered by adding 550µL of gel matrix to a spin filter and centrifuging at 1500xg for 10 minutes. The RNA nano dye concentrate was vortexed for 10 seconds prior to the addition of 1µL to 65µL of the filtered gel matrix. The gel-dye mixture was vortexed to ensure mixing and centrifuged at 13,000xg for 10 minutes at room temperature. The gel-dye mixture was loaded onto a supplied RNA nano chip which was sealed within the Agilent chip priming station, a syringe was fitted onto the chip priming station and the syringe plunger pressed down to pressurise and distribute the gel-dye matrix throughout the chip. 5µL of supplied RNA nano marker was added to the wells. An RNA ladder (1µL) was added to a designated well on the chip. The samples were denatured by heating at 70°C for 2 minutes and 1µL of each sample loaded onto the chip. The chip was placed horizontally onto a vortexer chip adaptor and vortexed for 60 seconds. The chip was inserted into the Agilent 2100 bioanalyzer and the sample RNA concentration and quality analysed.

3.3.4   microRNA microarray

3.3.4.1   Materials and reagents

Agilent technologies human miRNA microarray chips (8x60K) (included: calf intestinal phosphatase, 10x calf intestinal phosphatase buffer, T4 ligase, 10x T4 ligase buffer, cyanine 3-pCp, labelling spike in solution, hybridisation buffer, hybridisation spike in solution, DMSO, Dilution buffer, gene expression blocking agent, gene expression wash buffer 1 and 2), Hybridisation chamber and gasket slides, hybridisation oven with rotators, heat block.

3.3.4.2　Background

The concept, principles and protocols of microarrays were first conceived by Tse Wen Chang (1983) who described the use of antibody microarrays for proteomic analysis. Many varieties of microarrays exist allowing high throughput detection of a variety of substrates such as DNA, proteins or microRNAs. Microarrays consist of an array fixed to a solid substrate such as a glass slide; the microarray chips have complementary sequences or substrates bound to them which allow the binding of fluorescently tagged analytes of interest. MicroRNA microarrays for example are coated with RNA sequences complementary for the microRNAs being assessed. The microRNAs are fluorescently coated prior to hybridisation to the microarray. The arrays are washed to remove unbound microRNA and the array assessed by an array reader; bound microRNAs will produce a fluorescent signal. Each microRNA has several potential binding sites on the array so the array can give an indication of relative quantity of miRNA present in the sample compared to control samples.

3.3.4.3　Protocol

MicroRNA (miR) microarray analysis requires (a) preparation of the miR sample, (b) fluorescently labelling the miR, (c) vacuum drying the samples, (d) incubating the labelled miR with the array for hybridisation of the sample with immobilised probes, (e) washing the array slides and finally (f) quantitating the array fluorescence.

The extracted RNA samples prior to preparation were quantified and the quality assessed using an Agilent Bioanalyzer. The RNA samples were diluted to a concentration of 50ng/μL in nuclease free water. The samples were dephosphorylated by incubating 2μL (100ng) of RNA with 0.5μL supplied calf intestinal phosphatase (CIP), 0.4μL 10x CIP buffer and 1.1μL labelling spike in solution. The samples were dephosphorylated in order to remove the miR 5' phosphate groups. The labelling spike in solution controls for errors occurring as a result of the miR fluorescent dye labelling process. The RNA-CIP solution was incubated at 37°C for 30 minutes in a heat block to facilitate dephosphorylation. The samples were denatured to prevent miR self-annealing by treating with 2.8μL DMSO and incubating at 100°C for 10 minutes. The samples were immediately transferred to an ice bath to prevent the miRNA from re-annealing. The dye cyanine 3-cytidine bisphosphate (3-pCp) was then ligated to the 3' end of the miR within the samples. The samples were treated with 4.5μL of a ligation mastermix from supplied reagents including, 1μL 10x T4 RNA ligase buffer, 3μL cyanine 3-pCp and 0.5μL T4 RNA ligase. The samples were incubated for 2 hours at 16°C. The labelled miR samples were dried over a 3 hour period using a vacuum centrifuge set to 50°C. This was done in order to remove the DMSO from the sample which could adversely interfere with the hybridisation

of the miR to the microarray. The dried samples were resuspended in 17μL of nuclease-free water. To each sample a supplied 10x gene expression blocking agent (4.5μL), 2x hybridisation buffer (22.5μL) and hybridisation spike in solution (1μL) was added. Addition of the hybridisation spike-in solution controlled for any processing errors occurring during the hybridisation step. The samples were incubated for 5 minutes at 100°C followed by 5 minutes in an ice bath. The samples were pipetted onto individual chambers of an eight chamber Agilent gasket slide. The gasket slide was then sandwiched together with the microarray slide and inserted into a clasp assembly to hold the two together. The slides were incubated for 20 hours at 55°C in an incubator to allow hybridisation of the labelled miR to the microarray slide. The slides were removed from the incubator and submerged in the supplied gene expression wash buffer 1 (supplemented with 0.005%v/v triton X-102). The submerged slides were prised apart and the microarray slide transferred and submerged in fresh gene expression wash buffer 1 (0.005%v/v triton X-102) and incubated for 5 minutes. The microarray slides were transferred and submerged in the provided gene expression wash buffer 2 (preheated to 37°C prior to use) and incubated for 5 minutes. The slides were removed from the wash buffer and allowed to dry prior to placing them in an Agilent microarray slide holder which was subsequently inserted and analysed using an Agilent high-resolution scanner (G2505C).

3.3.5 MicroRNA microarray data analysis

The microarray data was uploaded into Genespring software where it was normalised using a quantile normalisation method. The array manufacturer, Agilent, recommends normalising to the 90th percentile, however, many publications have shown quantile normalisation to be the better normalisation method (Pradervand, Weber et al. 2009). Subsequent to quantile normalisation the data was baseline-normalised to the mean of all samples. The microarray produced a signal from 1398 different immobilised entities. This list was filtered on entities detected in 100% of samples in all 6 of the conditions (bariatric baseline, bariatric 3 month post-surgery, bariatric 1 year post-surgery, control baseline, control 3 month post-surgery and control 1 year post surgery) resulting in a list of 132 entities. These entities were analysed by volcano plot using a moderated T-test (ElSharawy, Keller et al. 2012), Benjamini Hochberg FDR (false detection rate) multiple comparison test (Benjamini and Hochberg 1995, ElSharawy, Keller et al. 2012). Entities were selected for further analysis based on a p value of less than 0.05 and a fold change difference of greater 2.0. Comparisons using the volcano plot were made to analyse statistical significance between bariatric baseline samples and control baseline samples in order to determine the differences in miR expression caused by obesity.

3.3.6   Identification of potential target mRNAs and subsequent pathway analysis

Messenger RNA (mRNA) interaction targets of identified miRs were assessed through searching several online databases, miRTarBase, StarBase, miRecords, human Targetscan and through Ingenuity pathway analysis software. These databases were searched for experimentally validated mRNA targets of identified miRNAs. Experimentally validated miRNA targets were chosen for further study to assess as searching for predicted targets of miRNAs based on sequence complementarity can yield a large number of predictions. The lists of experimentally-validated target mRNAs were uploaded into Ingenuity pathway analysis software which attempts to place the targeted mRNAs into known pathways in order to predict affected pathways.

3.3.7   Statistical analysis

The results produced from the microRNA microarrays was analysed using a statistical software package called Genespring. The produced data was normalised using a quantile normalisation method to reduce inter-array variation. The microarrays produced miRNA expression data on 1368 individual miRNAs. This data was first filtered by the miRNAs detectable in all of the six conditions assessed (Bariatric and control samples at baseline, 3 month follow-up and 1 year follow-up) leaving a total of 132 miRNAs. The miRNA expression of the bariatric baseline and control baseline samples were compared by volcano plot testing significance with a moderated t-test and determining miRNAs with a fold change of greater than or equal to 2.0. The miRNA expression of the bariatric baseline and bariatric one year follow-up samples were compared by volcano plot testing significance with a moderated t-test and determining miRNAs with a fold change of greater than or equal to 2.0. These comparisons were also compared using a Benjamini Hochberg multiple comparisons testing to attempt to eliminate false detection of significant changes.

3.4   Results

3.4.1   Analysis of microRNA microarray

The Volcano plots compared miRNA expression of monocytes between the bariatric and control participants at the baseline time point (figure 3.4.1, a.)) and between the bariatric baseline and bariatric 1 year follow up time points (figure 3.4.1, b.)). These comparisons were made in order to attempt to determine the differences in monocyte miRNA expression occurring as a result of obesity and in response to the weight reduction surgery within the bariatric individuals (figure 3.4.1, a.) and b.)). Comparisons made between the bariatric and control baseline samples did not identify any entities that fitted within the criteria of a $p \leq 0.05$ and a fold change difference ≥ 2.0. However comparisons made between the bariatric baseline and the bariatric 1 year follow-up samples identified 15 entities that fitted the aforementioned inclusion criteria. Some of these entities, however, appeared to be changing over time in the control subjects between the baseline and 1 year follow-up time points. To measure the difference occurring independent of the observed change over time, fold change differences between the bariatric baseline, 3 month follow-up and 1 year follow-up samples were compared with their respective control sample time points (table 3.3). The expression of four of the entities listed in table 3.3, EBV-miR-BART12, hsa-miR-1202, hsa-miR-1260a and hsa-miR-3162-5p, appeared to change over time rather than in response to bariatric surgery or weight reduction. Comparisons in the fold change of expression of these miRs between the bariatric samples and the control samples at corresponding time points indicated very low fold change differences in expression. This suggests that the expression of these miRs changed to the same degree in the control samples over the 1 year time course as was observed between the bariatric baseline and bariatric 1 year follow-up samples. Eight of these miRs, hsa-miR-130a-3p, hsa-miR-146a-5p, hsa-miR-151a-5p, hsa-miR-199b-5p, hsa-miR-2861, hsa-miR-424-5p, hsa-miR-582-5p and hsa-miR-638 appeared to have a greater fold change difference between the bariatric and control samples at the baseline time point. These observed differences were seen to be reduced when comparing the fold change differences between the bariatric and control samples at the 1 year follow-up time point. This suggests that expression is returning towards control levels in response to the weight reduction surgery. One of these entities, hsa-miR-199a-3p showed no difference in expression between the bariatric and control at baseline, although at the 3 month and 1 year follow-up expression was reduced when fold change difference was compared to the respective control samples (table 3.3). Hsa-miR-126-3p, initially showed no difference in expression between bariatric and control samples at baseline. However, comparisons in fold change of expression between the bariatric and control samples at the 3 month follow-up time point showed the bariatric individuals to

have reduced expression relative to the control samples with the fold change difference in expression returning to control levels by the 1 year follow-up time point.
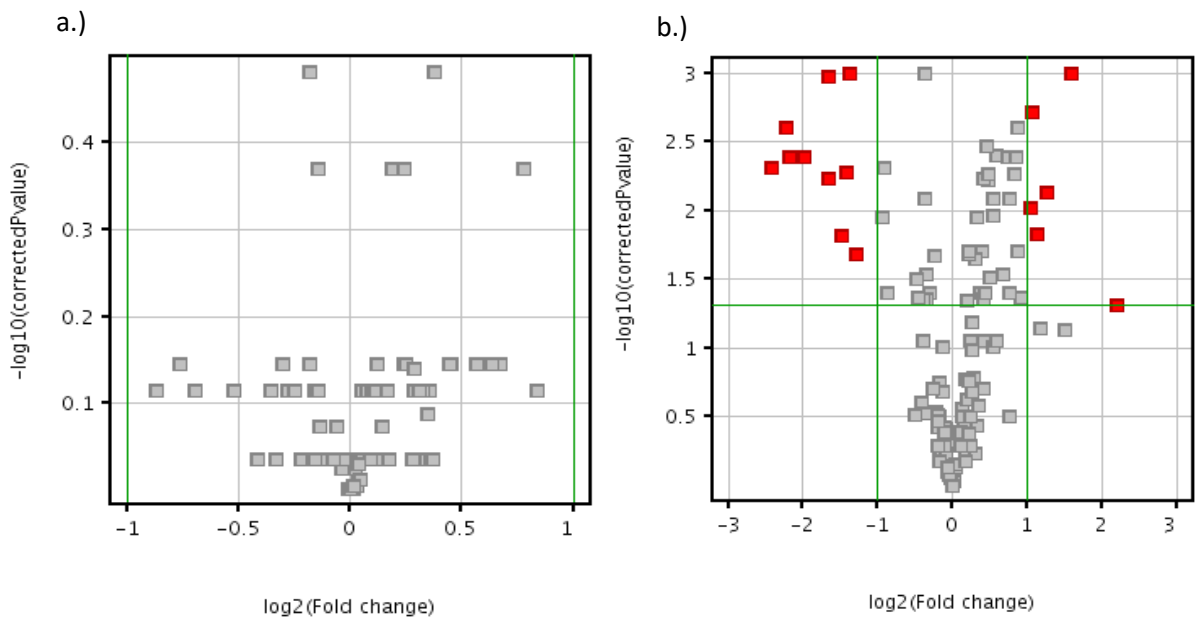
Figure 3.4.1: Comparisons between bariatric baseline and control samples (a.), and bariatric one year follow-up samples (b.) in order to determine microRNAs with a p-value ≤0.05 and a fold change difference ≥2.0.

The microRNA microarray results were analysed by volcano plot to determine statistical significance and fold change differences between two of the six experimental conditions. Significance was determined using a moderated T-Test and Benjamini Hochberg multiple comparison test. Entities were selected based on a P values of ≤0.05 and a fold change difference of ≥2.0 and denoted on the volcano blot by a red square. Comparisons were made between the control baseline and bariatric samples a.) and the bariatric baseline and the bariatric one year follow-up samples b.).

Table 3.3: List of miRNA entities determined to have a p-value <0.05 and Fold change >2.0 between Bariatric baseline and one year follow-up samples.

systematic name	Fold change difference, Bariatric baseline and Bariatric 1 year follow-up	p-value	Fold change difference, Bariatric baseline vs Control baseline	Fold change difference, Bariatric 3 month follow-up vs Control 3 month follow-up	Fold change difference, Bariatric 1 year follow-up vs Control 1 year follow-up
ebv-miR-BART12	2.58	0.001	1.11	1.08	1.12
hsa-miR-1202	3.16	0.001	1.10	1.01	1.03
hsa-miR-126-3p	4.54	0.004	-1.07	-1.53	-1.05
hsa-miR-1260a	3.02	0.001	1.01	1.13	-1.09
hsa-miR-130a-3p	2.80	0.015	-1.28	-1.28	-1.07
hsa-miR-146a-5p	3.14	0.006	-1.69	-1.61	-1.04
hsa-miR-151a-5p	3.96	0.004	-1.44	-1.54	-1.08
hsa-miR-197-3p	2.09	0.002	-1.16	-1.01	-1.04
hsa-miR-199a-3p	2.42	0.022	1.03	-1.25	-1.23
hsa-miR-199b-5p	2.39	0.007	1.37	1.22	-1.07
hsa-miR-2861	5.33	0.005	-1.83	1.23	1.25
hsa-miR-3162-5p	2.66	0.005	-1.02	1.07	1.01
hsa-miR-424-5p	2.18	0.015	1.72	1.63	-1.03
hsa-miR-582-5p	2.07	0.010	1.78	1.10	-1.33
hsa-miR-638	4.66	0.003	-1.62	-1.53	1.20
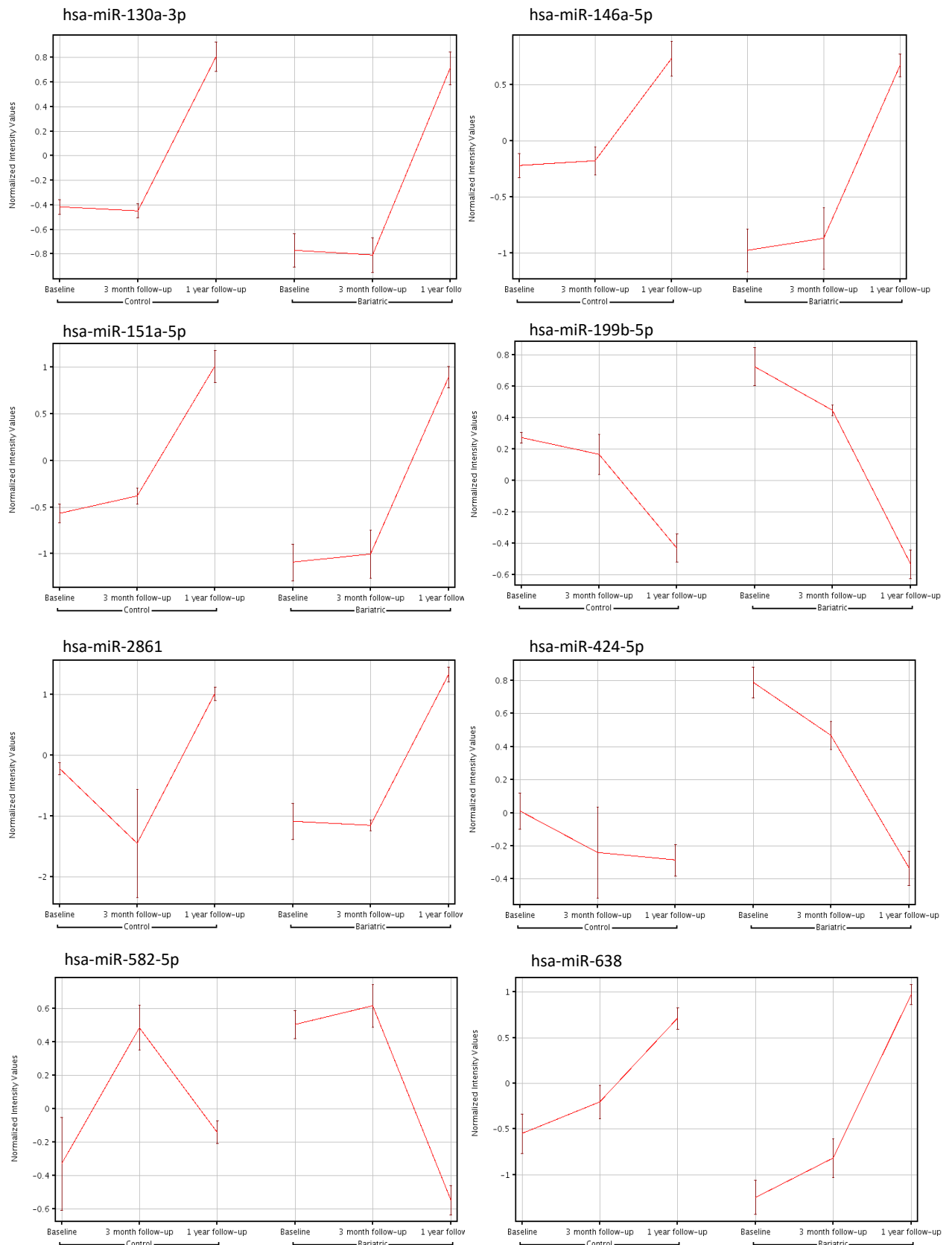
Figure 3.4.2: Line graphs displaying relative expression of microRNAs identified by volcano plot comparison of microRNA expression of bariatric baseline and one year follow up samples having a p value of ≤0.05 and a fold change difference of ≥2.0 (figure 3.4.1, b.).

Each line graph represents the relative microRNA expression as determined by microarray, of the control and bariatric samples at the baseline, three month and one year follow up time points.

3.4.2 Ingenuity pathway analysis of experimentally observed miRNA target mRNA for the determination of canonical pathways and upstream regulators

Each individual miR can potentially influence the expression of hundreds of mRNA targets (Lim, Lau et al. 2005). Many online databases exist which catalogue validated miR target mRNAs or can predict based on miR sequence their potential mRNA targets. A number of miR target databases (miRTarBase, starBase, miRecords and human Targetscan) were examined to determine the experimentally validated miR target mRNAs. A summary of the number of validated mRNA targets for each of the eight miRNAs and the database sources are listed in table 3.4 and the full list is available in the appendix, 8.3. The experimentally validated miR target mRNA were inputted into Ingenuity pathway analysis software to determine potential common pathways being affected by the altered miRs. The pathway analysis software generated a number of common pathways based on the uploaded list of experimentally validated target mRNAs. The software generates the pathways based on the degree of overlap between the miR target mRNA uploaded against the known mRNA in the specific pathway. The software determines this as a degree of overlap and uses a Fisher's exact test which applies a value of probability to each pathway. The generated pathways have been ordered by p-value and are listed in table 3.5. A number of inflammatory signalling pathways were identified by the pathway analysis including: IL-6 and IL-10 signalling, toll like receptor signalling, acute phase response signalling, NF-κB signalling.

Table 3.4: Table displaying number of experimentally observed mRNA targets of selected miRNAs (full list of mRNA targets listed in appendix 8.3)

systematic name	Number of experimentally validated mRNA targets	Sources
hsa-miR-130a-3p	9	TargetScan Human,miRecords, miRTarBase, Ingenuity Expert Findings
hsa-miR-146a-5p	77	TargetScan Human,miRecords, miRTarBase, Ingenuity Expert Findings
hsa-miR-151a-5p	4	miRTarBase
hsa-miR-199b-5p	7	TargetScan Human,miRecords, miRTarBase, Ingenuity Expert Findings
hsa-miR-2861	1	(Li, Xie et al. 2009), (Fischer, Paul et al. 2015)
hsa-miR-424-5p	187	TargetScan Human,miRecords, miRTarBase, Ingenuity Expert Findings
hsa-miR-582-5p	1	miRTarBase
hsa-miR-638	1	miRTarBase

Table 3.5: Canonical pathways determined by ingenuity pathway analysis of experimentally observed miRNA mRNA targets

Ingenuity Canonical Pathways	p-value
Role of Macrophages, Fibroblasts and Endothelial Cells in Rheumatoid Arthritis	3.06E-19
IL-6 Signalling	1.45E-18
IL-10 Signalling	2.45E-17
Toll-like Receptor Signalling	4.06E-17
PPAR Signalling	2.97E-15
p38 MAPK Signalling	7.94E-13
Dendritic Cell Maturation	6.31E-13
Hepatic Fibrosis / Hepatic Stellate Cell Activation	6.31E-13
Altered T Cell and B Cell Signalling in Rheumatoid Arthritis	3.16E-13
Communication between Innate and Adaptive Immune Cells	1.58E-13
Acute Phase Response Signalling	1.58E-13
NF-κB Signalling	1.26E-13
Role of Osteoblasts, Osteoclasts and Chondrocytes in Rheumatoid Arthritis	7.94E-12
Hepatic Cholestasis	7.94E-12
Pancreatic Adenocarcinoma Signalling	1.00E-11
Colorectal Cancer Metastasis Signalling	3.63E-10
IL-8 Signalling	3.39E-10
iNOS Signalling	3.24E-10
Cholecystokinin/Gastrin-mediated Signalling	1.10E-10
LXR/RXR Activation	1.07E-10

3.4.3 Ingenuity pathway analysis of predicted miRNA target mRNA for the determination of canonical pathways and upstream regulators

The miRNAs observed to be changing in response to bariatric surgery were uploaded into ingenuity pathway prediction software. The software contacts a number of different miRNA target prediction databases to determine potential mRNA targets. Predicted mRNA targets were placed into order of confidence and the top hundred chosen for each miRNA. The final list of 800 target mRNA was uploaded into Ingenuity pathway analysis software to determine the common pathways these target mRNA belong to. This was done in addition to examining the experimentally observed miRNA mRNA targets due to the inherent bias examining only the experimentally observed targets introduces. Only two of the examined miRNAs had over ten experimentally observed target mRNA which skews the pathway prediction towards the miR with the largest number of experimentally validated target mRNA. Also the majority of experimental work surrounding miRNAs has examined them with regards to the development of various cancers. This can also skew the pathway analysis software to select pathways related to cancer development. The results of inputting the top one hundred target mRNA for each miRNA identified a number of common pathways. This included a number of inflammatory signalling pathways: IL-6 signalling, IL-10 signalling, toll like receptor signalling, NF-kB signalling and acute phase response signalling.

Table 3.6: Table displaying the number of predicted mRNA targets of selected miRNAs

Systematic name	Number of predicted mRNA targets	Sources
hsa-miR-130a-3p	100	Ingenuity Expert Findings, TargetScan Human, miRecords
hsa-miR-146a-5p	100	Ingenuity Expert Findings, TargetScan Human, miRecords
hsa-miR-151a-5p	100	Ingenuity Expert Findings, TargetScan Human, miRecords
hsa-miR-199b-5p	100	Ingenuity Expert Findings, TargetScan Human, miRecords
hsa-miR-2861	100	Ingenuity Expert Findings, TargetScan Human, miRecords
hsa-miR-424-5p	100	Ingenuity Expert Findings, TargetScan Human, miRecords
hsa-miR-582-5p	100	Ingenuity Expert Findings, TargetScan Human, miRecords
hsa-miR-638	100	Ingenuity Expert Findings, TargetScan Human, miRecords

Table 3.7: Canonical pathways determined by Ingenuity pathway analysis of the top 100 predicted mRNA targets for each miR

Ingenuity canonical pathway	p-value
Role of Macrophages, Fibroblasts and Endothelial Cells in Rheumatoid Arthritis	4.46E-18
PPAR Signalling	4.83E-13
IL-6 Signalling	5.54E-13
Toll-like Receptor Signalling	4.81E-12
IL-10 Signalling	3.16E-11
Role of Osteoblasts, Osteoclasts and Chrondrocytes in Rheumatoid Arthritis	4.37E-11
Hepatic Fibrosis/Hepatic Stellate cell activation	2.27E-09
NF-kB Signalling	2.45E-09
Altered T Cell and B Cell signalling in Rheumatoid Arthritis	7.18E-09
Molecular mechanisms of Cancer	1.06E-08
p38 MAPK Signalling	1.32E-08
Dendritic cell maturation	2.35E-08
Acute Phase response signalling	4.96E-08
Cyclins and cell cycle response	7.42E-08
Hepatic Cholestasis	9.04E-08
Communication between Innate and Adaptive Immune cells	9.67E-08
iNOS signalling	1.08E-07
STAT3 Signalling	2.81E-07
Activation of IRF by cytosolic Pattern recognition receptors	3.87E-07
Axonal guidance Signalling	5.32E-07

3.4.4 The expression of miR-146a-5p and miR-424-5p was altered with increasing age

Primary monocytes were taken as described previously from healthy midlife (>50 years old) and young (<30 years old) participants. These monocytes were lysed and total RNA extracted for analysis of the miRNAs 146a-5p and 424-5p. This was done in order to determine whether increased age would result in a similar expression pattern of these miRNAs as was observed between the individuals awaiting bariatric surgery and control individuals in figure3.4.3. Differences in age were selected due to the predisposition of increased age towards the development of diabetes and other complications in response to obesity.

Participant blood glucose, total, HDL and LDL cholesterol was measured using a Reflotron clinical chemistry analyser as described previously in more detail (methods chapter, 2.14). Table 3.8 contains mean values ± the standard deviation. Significance in differences in resting blood glucose, total, HDL and LDL cholesterol between mid-life and young participants was determined by unpaired t-test. Total cholesterol and LDL cholesterol was determined to be significantly higher (p-values of 0.044 and 0.021 respectively) in the mid-life participants compared to the young participants.

The expression of the miRNAs 146a-5p and 424-5p in monocytes was assessed by qPCR as described previously (methods chapter, 2.18). Data was analysed using the comparative CT method and expressed as fold change difference in miRNA expression between younger and mid-life participants. Figure 3.4.4, a.) and b.) display expression of miRNA 146a-5p and miRNA 424-5p respectively. Expression of the miRNA 146a-5p was observed to be decreased in the mid-life individuals relative to the young participants. Expression of the miRNA 424-5p was observed to be increased in the mid-life individuals relative to the young participants. The expression patterns of these miRNAs follow a similar pattern of expression as was observed in figure 3.4.3 between individuals awaiting bariatric surgery and control individuals at the baseline time-point.

Table 3.8: Clinical chemistry data of young and mid-life participants

	Young participants (<30 years old)	Mid-life participants (>50 years old)
Average Age	28.33 ± 0.58	61.33 ± 8.14**
Gender	M=2, F=1	M=2, F=1
Average resting glucose (mmol/L) ± SD	4.97 ± 0.39	5.25 ± 1.19
Average Total cholesterol (mmol/L) ± SD	3.34 ± 0.17	5.12 ± 1.05*
Average total HDL cholesterol (mmol/L) ± SD	0.84 ± 0.20	1.33 ± 0.64
Average total LDL cholesterol (mmol/L) ± SD	2.33 ± 0.35	3.61 ± 0.50*

Significance was determined by unpaired t-test, whereby (*), (**) and (***) represents p<0.05, p<0.01 and p<0.001 respectively.
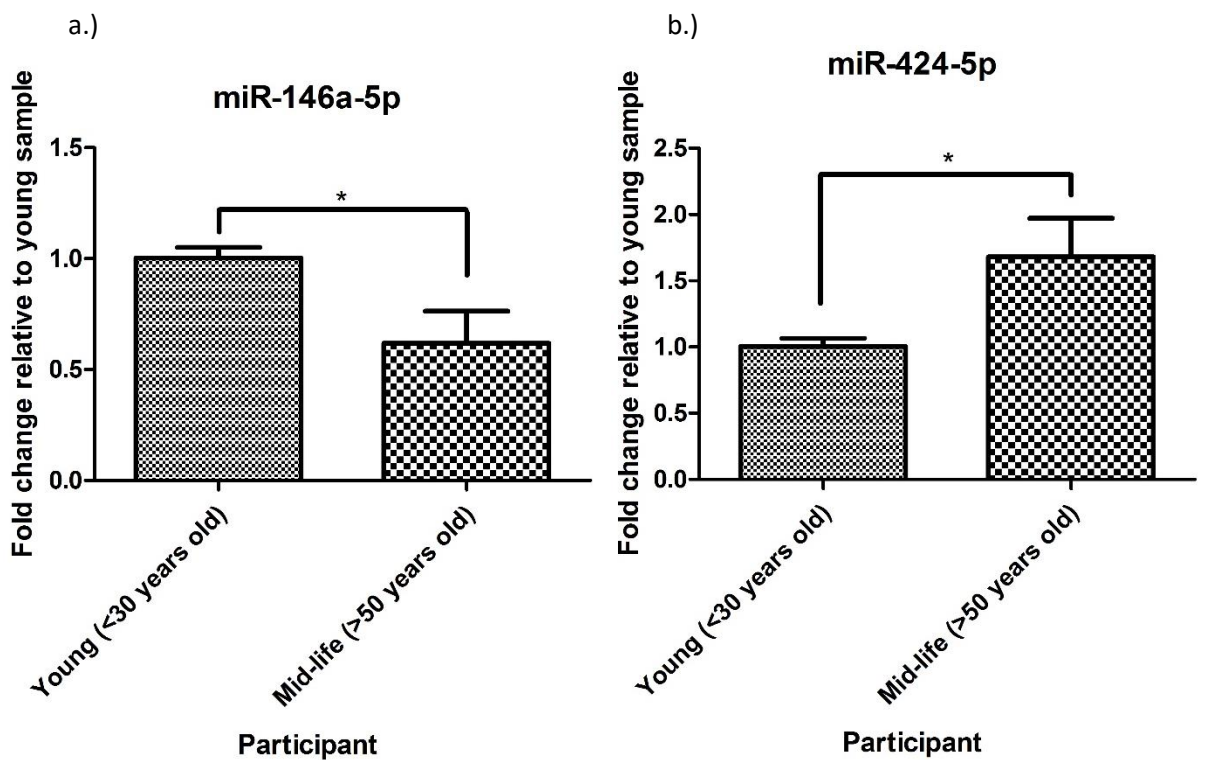
Figure 3.4.4: Increased age results in altered expression of the miRs 146a-5p and 424-5p

Human primary monocytes were isolated from whole blood taken by venepuncture from healthy volunteers who were either <30 years old (young) or >50 years old (midlife) (table 3.8). The isolated monocytes were harvested by centrifugation, washed with PBS and lysed in Trizol reagent prior to RNA extraction. The total RNA was extracted by spin columns and the RNA quantity and quality assessed by nanodrop. The expression of the miRs 146a-5p a.) and 424-5p b.) were assessed by qPCR to determine if increasing age would change expression. The micro RNA miR-16 was used as a housekeeper gene, the results were analysed using the ΔΔCT method and expressed as fold change (±SE) relative to the young (<30 years old) participants' expression. Significance was determined by unpaired t-test, whereby (*), (**) and (***) represents p<0.05, p<0.01 and p<0.001 respectively.

3.5 Discussion

The microarray study of monocyte microRNA expression identified eight miRs that were significantly different with a fold change difference of >2.0 between the bariatric baseline and bariatric 1 year follow-up samples. This included the miRs: 146a-5p, 424-5p, 130a-3p, 199b-5p, 151a-5p, 2861, 582-5p and 638. Comparisons in fold change difference in the expression of these miRs between the bariatric and control individuals identified the largest fold change difference to be occurring at the baseline time point. This fold change difference in miR expression between the bariatric and control individuals decreased at the 1 year post surgery time point. A number of these identified miR have either been reported in the literature as being dysregulated in response to obesity and T2 diabetes or have a functional role in the regulation of inflammatory signalling pathways.

The reduced expression of miR-146a-5p in obese relative to control individuals reported within this thesis has been reported previously in individuals with T2 diabetes and obesity (Balasubramanyam, Aravind et al. 2011, Baldeon, Weigelt et al. 2014). miR-146a-5p has been shown to function as a negative regulator of TLR signalling by targeting and silencing IRAK1 and TRAF6 (Ho, Yu et al. 2014, Park, Huang et al. 2015). Increased expression of miR-146a-5p has also been observed to result in decreased expression of IL-6, IL-8, IL-1β and TNFα (Pauley, Satoh et al. 2008). A study by Yang, He et al. (2011) observed expression of miR-146a-5p in THP-1 monocytes and differentiated macrophages to be reduced in response to oxidised LDL. The authors identified overexpression of miR-146a in response to a miR-146a-5p mimetic to result in decreased monocyte and macrophage uptake of LDL and cholesterol suggesting miR-146a as a target of intervention in the prevention of atherosclerosis. In patients with T2 diabetes the expression of miR-146a-5p has been negatively correlated to insulin resistance, glycated haemoglobin, NF-κB mRNA levels and circulating levels of TNFα and IL-6 (Balasubramanyam, Aravind et al. 2011).

Expression of the miR-130a-3p was observed within this thesis to be decreased in the obese relative to the control individuals at the baseline time point (table 3.3). Decreased expression of miR-130a-3p has been reported previously in diabetic mice models where it was observed to result in impaired insulin signalling (Xiao, Yu et al. 2014). The authors showed that decreased expression of miR-130a-3p resulted in increased expression of growth factor receptor-bound protein 10 (GRB10) which has been found previously to disrupt insulin signalling (Wang, Balas et al. 2007).

Expression of miR-199b-5p was observed to be increased in the obese relative to the control individuals at the baseline time point (table 3.3). Expression of miR-199b-5p has been previously reported to be increased in diabetic cardiomyocytes (Greco, Fasanaro et al. 2012). Increased

expression of miR-199b-5p has been observed to negatively regulate SIRT1 expression (Saunders, Sharma et al. 2010). The protein deacetylase SIRT1 has been observed to both inhibit inflammatory signalling through NF-κB deacetylation (Yang, Zhang et al. 2012) and protect against high fat diet induced insulin resistance (Sun, Zhang et al. 2007).

Expression of the miR-151a-5p was observed to be decreased in the obese relative to the control individuals at the baseline time point (table 3.3). Although this finding has not currently been reported in regard to obesity or diabetes, it has been observed to be significantly decreased in response to increased age in both humans and Rhesus monkeys (Noren Hooten, Fitzpatrick et al. 2013). The authors performed pathway analysis on miR-151a-5p predicted mRNA targets which identified miR-151a-5p to potentially be involved in regulation of TNFα and NF-κB signalling.

Expression of miR-424-5p was observed to be increased in the obese relative to the control individuals at the baseline time point (table 3.3). Although expression of miR-424 has not at the time of writing been linked to obesity or diabetes, high expression has been observed to result in increased differentiation of monocytes to macrophages (Rosa, Ballarino et al. 2007) which has been suggested to play a role during development of atherosclerosis (Hulsmans, De Keyzer et al. 2011).

Expression of miR-582-5p was observed to be higher and the miRs miR-638 and miR-2861 were observed to be lower in the obese relative to the control individuals at the baseline time point (table 3.3). At present, very little work has been conducted on these miRs with each of them having only a single experimentally validated target mRNA. A number of these miRs appear to contribute to the development of obesity associated inflammation and could facilitate the development of associated complications.

Expression of the miR-126-3p was observed to be increased in the obese relative to the control individuals at the 3 month post-surgery time point. The miR-126-3p has previously been reported to regulate angiogenesis (Wang, Aurora et al. 2008) and stimulate tissue repair by increasing recruitment of progenitor cells to the area of damage (Zernecke, Bidzhekov et al. 2009). The increase in miR-126-3p expression observed in the obese individuals 3 months post-surgery could be an attempt to promote tissue repair in response to surgery.

The eight identified miR appearing dysregulated in response to obesity returned towards control levels of expression by the one year post surgery time point. Although research in this area is currently limited, a number of studies have sought to assess whether bariatric surgery would have an impact on miRNA expression. The current literature has assessed the effects of bariatric surgery on the presence of serum miRs (Lirun, Sewe et al. 2015, Wu, Li et al. 2015). Both of these studies

identified a number of miRs changing in response to surgery, however, there appears to be little consensus between the results. Between the two studies a total of 33 independent miRs were observed to change in response to surgery, however, only three of these were commonly identified between the two studies with one of these having the opposite response. This illustrates the need for further research in this particular field to strengthen the knowledge base. Of the miRs identified by these papers only two, miR-146a-5p and miR-151-5p were identified in the results presented in this thesis with miR-146a-5p having the opposite response to surgery. The differences observed between these results could be due to the location of miR analysis, with some of the differences representing monocyte specific changes.

The experimentally validated and top one hundred predicted target mRNA for each miR were inputted into Ingenuity pathway analysis software. The experimentally validated and predicted target mRNA were identified to be involved in a number of inflammatory pathways including IL-6, IL-10 and toll like receptor signalling. These pathways have previously been reported to be present during obesity contributing to development of associated chronic inflammation and decreased insulin sensitivity. A number of studies have identified decreased secretion of the anti-inflammatory cytokine IL-10 (Manigrasso, Ferroni et al. 2005, Jung, Park et al. 2008, Paredes-Turrubiarte, Gonzalez-Chavez et al. 2015), increased secretion of IL-6 (Kern, Ranganathan et al. 2001, Khaodhiar, Ling et al. 2004) and increased toll like receptor induction of inflammatory cytokines (Tsukumo, Carvalho-Filho et al. 2007, Kim, Choi et al. 2012) during obesity. The miRs regulation of the target mRNAs involved in these pathways could potentially be contributing to the altered activity of these pathways in obesity.

This study, through the use of microarrays, demonstrated a number of miR appearing dysregulated in monocytes in response to obesity. Over the course of a year post bariatric surgery, a number of these miRs returned towards control levels of expression. These results add to a currently limited knowledge base.

Many theories have been suggested over the last 100 years to try to explain the process of cellular ageing. The rate of living hypothesis proposed by Raymond Pearl in 1928 suggested that a quicker basal metabolic rate results in decreased lifespan. Denham Harman built on this notion with the free radical theory of ageing which suggested that the by-products of metabolic activity such as the reactive oxygen species $OH^.$ and O_2^- results in cellular ageing. The mutation accumulation theory suggested by Peter Medawar in 1952 suggests that over the cause of the organism's lifetime, mutations accumulate in the genome causing dysregulation of genes involved in ageing and development. The process of replicative senescence was first discovered by Hayflick and Moorhead

in 1961 who described that cells had a limited number of cell divisions called the Hayflick phenomenon. This effect has been explained as being caused by the shortening of telomeres that occurs with each cell division. Recently, the strong association between altered metabolism and inflammation has been highlighted as an important underpinning ageing mechanism. The expression of miR-146a-5p was observed to decrease and miR-424-5p increase in older relative (>50 years old) to younger individuals (<30 years old). Expression of miR-146a-5p has been reported previously to decrease in response repeated passaging of HUVEC cells to induce an ageing phenotype (Vasa-Nicotera, Chen et al. 2011). Expression of miR-424-5p in bone marrow derived human mesenchymal stem cells aged through repeated passaging has been previously shown to increase (Yoo, Kim et al. 2014). The change in expression induced by increased age in these miRs could contribute to the development of increased inflammation observed with increasing age (Jenny 2012).

3.5.1 Strengths and limitations

A limitation of the data reported within this chapter is that due to time constraints there has been no validation of the microarray results by an alternative method such as qPCR. A number of studies have shown good correlation between data obtained by microarrays and qPCR for miRNA analysis, although qPCR analysis of miRNA expression has been shown to be a more sensitive and specific method (Ach, Wang et al. 2008, Chen, Gelfond et al. 2009, Pradervand, Weber et al. 2010). Future work would seek to confirm the miR changes observed within this chapter by qPCR and could also seek to assess the effects of any confirmed dysregulated miR on mRNA expression. This could be assessed by whole transcriptome analysis performed using RNA sequencing or by targeted qPCR to assess the expression of specific miR target mRNA. The effects of the dysregulated miRs could also be determined *in vitro* experiments by transfecting isolated monocytes with miR mimetics or inhibitors and assessing the resulting response to a number of inflammatory or metabolic stimuli.

A further limitation of the study presented within this chapter are as a result of the chosen monocyte isolation technique. The monocyte isolation procedure extracted only the "classical" Mon 1, CD14 positive CD16 negative primary monocytes due to the removal of CD16 positive cells. The consequence of this is that miRNA expression of the CD16 positive monocyte Mon2 "intermediate" and Mon 3 "non-classical" subpopulations were not assessed. The loss of the Mon 2 "intermediate" population in particular is important due to its identified role as the more inflammatory subpopulation and due to the expansion of this population during obesity (Frankenberger, Sternsdorf et al. 1996, Belge, Dayyani et al. 2002, Cros, Cagnard et al. 2010, Poitou, Dalmas et al. 2011, Wong,

Tai et al. 2011). Due to this population being expanded during obesity it may be the monocyte population experiencing the largest changes in miRNA expression.

Although there are some advantages to only assessing a single monocyte subpopulation. Each of the individual subpopulations have been shown to have unique gene expression profiles and role within the innate immune system (Wong, Tai et al. 2011), pooling the three populations together would potentially dilute any observable changes. An alternative method could have isolated both CD14 and CD16 positive monocyte populations and subsequently separated them by fluorescence-activated cell sorting (FACS) into each individual population for miRNA assessment.

4 Identifying mechanisms of inflammation during metabolic disturbances in treated THP-1 monocytes

4.1 Preface

The research presented in this chapter aimed to investigate whether acute treatment with high concentrations of glucose would elicit a pro-inflammatory response in monocytes and whether the mechanisms through which this occurs could be investigated *in vitro*. Treatments were performed using the THP-1 monocyte cell line. The monocytes were treated with up to 50mM D-glucose over either a 6 or 28 hour period and the effect of treatment on cytokine secretion in response to LPS assessed. Further experiments sought to explore the pathways through which glucose may modulate LPS induced cytokine secretion. This included assessment of intracellular NAD:NADH ratios, sirtuin 1 deacetylase activity and acetylation status of the NF-κB P65 subunit.

4.2 Introduction

Increased availability of glucose present during type 2 diabetes and insulin resistance is associated with increasing pro-inflammatory cytokine secretion and monocyte recruitment to the endothelium and adipose tissue (Shanmugam, Reddy et al. 2003, Giulietti, van Etten et al. 2007, Nandy, Janardhanan et al. 2011, Tencerova, Kracmerova et al. 2015). Primary monocytes isolated from individuals with either type 1 or type 2 diabetes were both shown to have higher mRNA expression of TNFα, IL-6, IL-1α and IL-8 compared to control participants (Giulietti, van Etten et al. 2007). This has also been observed following *in vitro* treatment of THP-1 monocytes with high concentrations of glucose over a 72 hour period (Shanmugam, Reddy et al. 2003). The authors observed increased mRNA expression of a number of inflammatory cytokines and chemokines including; TNFα, IL-1β and MCP-1.

Cytokine expression is regulated at several levels; initial signalling through the MAPK cascade is amplified by intracellular ROS that inactivates protein tyrosine phosphatase 1B and amplifies the MAPK signal. At the transcriptional level, post-translational modifications to IKK, the inhibitor of NF-κB, trigger release of active NF-κB which translocates to the nucleus whereas for STAT3, phosphorylation by JAK provides a regulatory nuclear localisation signal. The consensus sequence transcription factor binding sites in the nucleus can undergo variable methylation which in turn, regulates transcription factor binding or RNA polymerase association. Translation of protein and maturation in the ribosome is dependent on functional endoplasmic reticulum. However, recent evidence suggests that hyperglycaemia causes endoplasmic reticulum stress in monocytes (Komura,

Sakai et al. 2010). Failure to fold proteins affects the processing of secretory proteins which may result in monocytes being more susceptible to apoptosis due to endoplasmic reticulum stress. Secretion of cytokines proceeds via different pathways; TNF is expressed on cell surface membranes where it is released by TACE, although the efficiency of this process differs between primary cells and THP-1 tumour cells (Moreira-Tabaka, Peluso et al. 2012). Secretion is also affected by osmotic pressure with an increase in secretion being reported after hypo-osmotic shock (Frenkel, Shani et al. 2001). Many of the steps in the regulation of cytokine expression are likely to be sensitive to extracellular glucose concentration.

Increased availability of glucose has been observed to alter the intracellular balance of NAD^+: NADH leading to decreased NAD^+ availability (Travis, Morrison et al. 1971, Nyengaard, Ido et al. 2004, Fulco, Cen et al. 2008). Increased glucose availability leads to glucose being shuttled through the polyol pathway which results in its conversion to sorbitol and subsequently to fructose via the aldose reductase (AR) and sorbitol dehydrogenase enzymes respectively. The AR enzyme has a relatively high K_m for D-glucose (0.66 μm/l) which limits its ability to convert glucose to sorbitol at normoglycaemic concentrations (Inagaki, Miwa et al. 1982, Grimshaw 1986, Erbel, Rupp et al. 2016). Increased glucose availability during diabetes results in increased substrate for AR leading to increased conversion of D-glucose to sorbitol and fructose through the polyol pathway. This process utilises intracellular NAD^+ leading to a reduction in the NAD^+: NADH ratio (Sango, Suzuki et al. 2006, Takamura, Tomomatsu et al. 2008). Decreased availability of NAD+ limits the activity of NAD+-dependent deacetylases such as SIRT1. SIRT1 has been identified to act as both a suppressor of inflammation and an insulin sensitizer in several tissue types. Endogenously formed fructose has been observed to be phosphorylated by fructose-3-phosphokinase at the C-3 position to produce fructose-3-phosphate, a glycating agent (Hamada, Araki et al. 1996). Fructose-3-phosphate degrades to produce 3-deoxyglucosone a highly reactive sugar which has been reported to crosslink proteins to produce advanced glycation end products (Kato, Hayase et al. 1989, Schalkwijk, Stehouwer et al. 2004).

Upon activation, the NF-κB complex translocates to the cell nucleus where it is acetylated by the protein acetyltransferase p300 and activated causing transcription of several genes responsible for the inflammatory response such as cytokine secretion (Vanden Berghe, De Bosscher et al. 1999, Mukherjee, Behar et al. 2013). SIRT1 binds to and deacetylates the P65 subunit of the NF-κB complex thereby preventing its acetylation and activation (Yeung, Hoberg et al. 2004).

In summary, a number of studies have assessed the effects of hyperglycaemia on monocyte inflammatory response *in vitro* and *ex vivo*, finding increased secretion of inflammatory cytokines (Hancu, Netea et al. 1998, Wu, Wu et al. 2009). At present, the majority of these studies have assessed chronic exposure to high concentrations of glucose (3 – 7 days) on monocyte inflammatory response. A number of mechanisms of glucose mediated inflammatory response have been identified from these chronic treatments. These include the generation of ROS and advanced glycation end products in response to increased glucose metabolism (Brownlee 2005). This is of relevance to pre-diabetes whereby individuals with reduced insulin sensitivity and glucose tolerance may suffer from very large, acute oscillations in post-prandial glucose concentrations. Investigating the effects of acute high glucose exposure may also allow the direct effects of glucose metabolism on inflammatory response to be assessed independent of increased advanced glycation end product formation and ROS generation.

4.2.1   Aims and objectives

The aims of the research presented within this chapter were to determine whether acute treatment with high concentrations of D-glucose would result in modulation of endotoxin induced inflammatory response and assess whether the THP-1 monocytic cell line could be used as a viable model of high glucose induced inflammation.

The objectives were to identify whether treatment with high concentrations of D-glucose would modulate cytokine response to treatment with LPS and to identify potential mechanisms through which high glucose may lead to induction of an inflammatory response.

4.3 Materials and Methods

4.3.1 Treatment of THP-1 monocyte with increased concentrations of glucose prior to inflammatory stimulation

Prior to treatment, the THP-1 monocytes were harvested by centrifugation at 500xg for 5 minutes, the supernatant removed and the cells washed in glucose free RPMI media, supplemented with 10% FCS and 1% penicillin/streptomycin and pre-heated to 37°C. The cells were counted using trypan blue staining, centrifuged again and re-suspended in fresh glucose-free RPMI media. The THP-1 monocytes were loaded onto a 12 well plate at 1×10^6 cells/ml, 1ml per well. To these wells 1ml of pre-made glucose stock solutions of either 10mM D-glucose, 40mM D-glucose, 100mM D-glucose or 10mM D-glucose with 90mM L-glucose was added and mixed by pipetting. Glucose stock solutions were made by addition of a glucose solution to glucose free RPMI media; the stock solutions were stored at 4°C and were kept for up to 1 week. This gave final glucose concentrations of either 5mM D-glucose, 20mM D-glucose, 50mM D-glucose or 5mM D-glucose with 45mM L-glucose and a cell density of 5 x 105 cells/ml in a 2ml volume. The treated cells were incubated at 37°C for a period of 4 hours subsequent to which either LPS (serotype- 0111:B4) or opsonised zymosan was added to a final concentration of 10ng/ml or 250µg/ml respectively. The cells were again incubated for a further 2 or 24 hours after which supernatants, lysates and RNA were taken for further analysis.
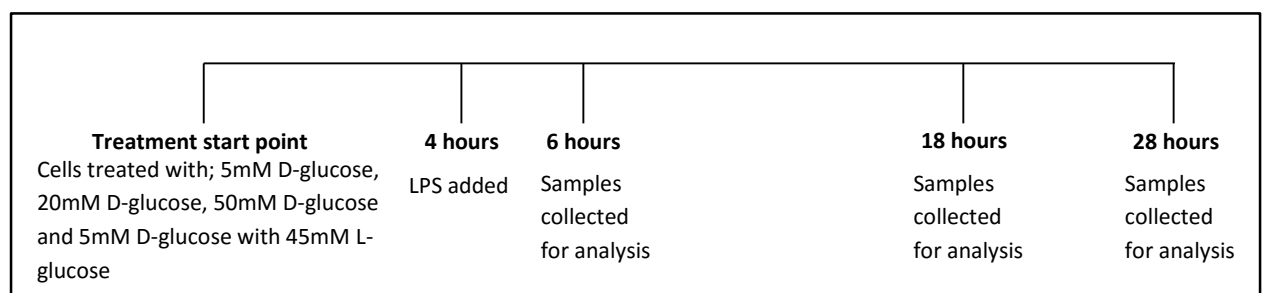
Figure 4.3.1: Schematic of monocyte treatments.

Figure displays the time-line of *in vitro* treatment of THP-1 monocytes with high concentrations of glucose. The THP-1 monocytes were treated for a period of 4 hours with either 5mM D-glucose, 20mM D-glucose, 50mM D-glucose or 5mM D-glucose with 45mM L-glucose. The cells were subsequently treated with LPS and incubated for a further 2 hours, 18 hours or 24 hours at which points samples were taken for analysis.

4.3.2   Preparation of opsonised zymosan

Opsonised zymosan was prepared by conjugating guinea pig complement (TCA Bioscience) to zymosan A (Sigma). Lyophilised guinea pig complement was reconstituted by dissolving in 20ml sterile filtered PBS prior to the addition of zymosan A. The mixture of complement and zymosan was heated at 37°C in a water bath for 1 hour with agitation to aid conjugation. Excess complement was removed by centrifuging the mixture at 1500xg, discarding the supernatant and replacing with fresh sterile PBS. Washing was repeated three times and the solution stored at 4°C and kept for up to one week before being discarded.

4.3.3   Statistical analysis

The data reported within this chapter has been expressed as the mean± the standard error of the mean (SEM) of a minimum of three independent experiments. The data was collated using Graphpad software and statistically analysed by one-way analysis of variance (ANOVA) followed by Dunnett's post-test comparing treatments against 5mM D-glucose treated cells. The significance is reported where the p-value is less than 0.05 denoted by *, >0.01 denoted by ** and >0.001 denoted by ***.

4.4 Results

4.4.1 Treatment with increased concentrations of glucose with and without concurrent LPS treatment had no effect on THP-1 viability, determined by MTT assay and trypan blue counts

THP-1 monocytes were treated with increased concentrations of glucose in order to determine any effect of treatment with or without LPS (10ng/ml) on cellular viability over a 28 hour period. Viability was determined subsequent to treatment by trypan blue staining and MTT assays as described previously (Methods chapter, sections; 2.2 and 2.3 respectively). This was done to determine whether treatment with glucose by itself or concurrent with LPS would result in cellular apoptosis.

After 24 hour incubation with increased concentrations of glucose with or without LPS, MTT reduction was analysed. As a positive control for the MTT assay cells were treated with FCCP, a mitochondrial uncoupler, which will inhibit the cells' ability to reduce MTT to formazan via mitochondrial reductases. Data are expressed as a percentage of the 5mM D-glucose treated cells. Figures, 4.4.1 a.) and b.) showed no decrease in cellular viability as a result of treatment with D-glucose at concentrations ranging from 5mM -50mM or with 5mM D-glucose with 45mM L-glucose either in the presence or absence of LPS.

Trypan blue staining was used to assess cellular viability in conjunction with MTT assays due to the MTT assay being a measurement of mitochondrial activity not a direct measure of cellular viability. THP-1 monocytes incubated with high concentrations of glucose in the presence or absence of LPS (figures, 4.4.1 c.) and d.) respectively) produced no significant change in the percentage of viable to dead cells. Total cell numbers were counted to determine whether treatment would result in a change in THP-1 monocyte proliferation. High concentrations of glucose in the presence or absence of LPS, figures, 4.4.1 e.) and f.) respectively, produced no change in the total number of cells.
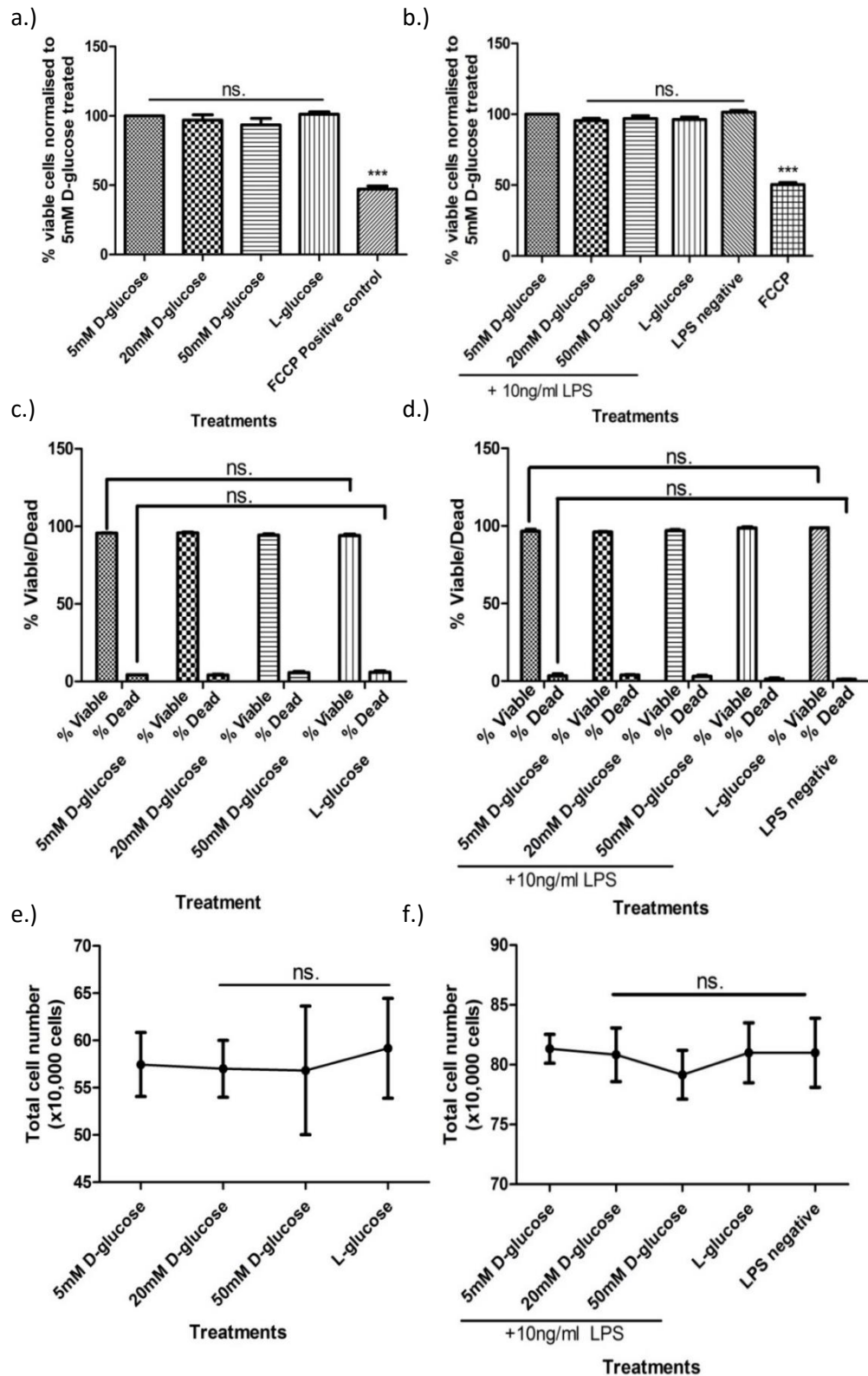
Figure 4.4.1: Treatment of THP-1 monocytes with increased concentrations of D-glucose had no effect on cellular viability

THP-1 monocytes were pre-treated with either 5mM D-glucose, 20mM D-glucose, 50mM D-glucose or 5mM D-glucose with 45mM L-glucose for a period of 4 hours. Subsequent to this the cells were incubated for a further 24 hours either with LPS (10ng/ml) (b.), d.), f.)) or without LPS (a.), c.), e.)). Cellular metabolic activity and viability was assessed by MTT assay (a.) and b.)) and trypan blue staining respectively. The trypan blue counts are expressed as a percentage of viable cells (c.) and d.)) and total cell number (e.) and f.)). Results are the mean of 3 independent experiments (± the standard error of the mean). Significance was determined by ANOVA followed by Dunnett's post-test comparing treatments to the 5mM D-glucose treated cells, whereby (*), (**) and (***) represents p<0.05, p<0.01 and p<0.001 respectively.

115

4.4.2   THP-1 monocytes treated with 50mM D-glucose remove significantly more glucose from the media than 5mM D-glucose-treated cells

To investigate whether THP-1 monocytes consumed more glucose when incubated with higher extracellular glucose concentrations, monocytes were incubated in glucose-free RMPI media (10%v/v FCS, 1%v/v Pen/Strep) supplemented with glucose (5mM D-glucose, 50mM D-glucose and 5mM D-glucose with 45mM L-glucose) and supernatants were collected at 2 hours, 18 hours and 24hours post-LPS addition. Glucose content in the media was assessed using a glucose quantification assay purchased from Sigma; the final glucose measurement was subtracted from the initial value to determine the concentration of glucose removed by the cells from the media over the 28 hour period. THP-1 monocytes incubated with 50mM D-glucose over a 28 hour period took up significantly more D-glucose over the time course compared to the 5mM treated and L-glucose-treated THP-1 monocytes.
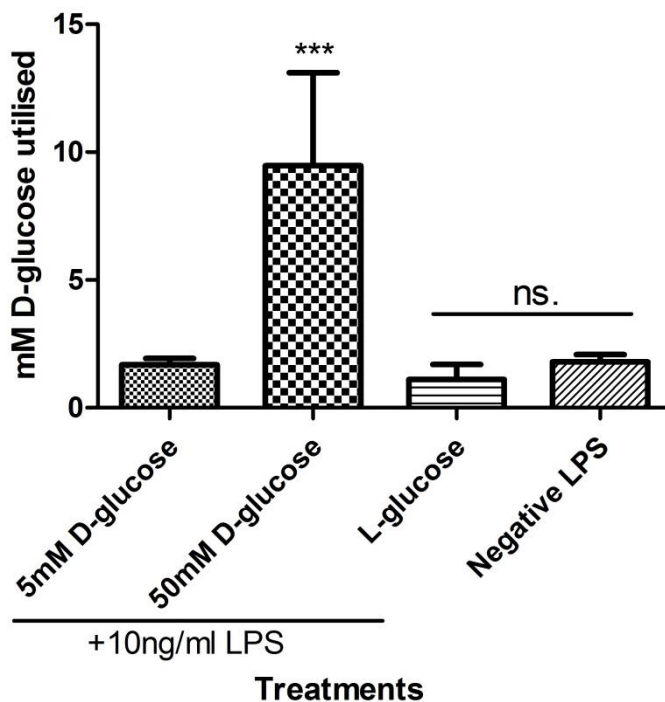
Figure 4.4.2: Treatment of THP-1 monocytes with increased concentrations of D-glucose resulted in a significant increase in D-glucose utilisation from the media.

THP-1 monocytes were treated with glucose at concentrations of either 5mM D-glucose, 50mM D-glucose or 5mM D-glucose with 45mM L-glucose for a period of 4 hours prior to the addition of LPS (10ng/ml). The supernatants were collected at the start of the treatment and at 24 hours post LPS addition and the glucose concentration of these samples determined. Glucose utilisation from the media by the monocytes was calculated by subtracting the glucose concentration of the final time point from the concentration of the initial time point. Results are the mean of 3 independent experiments (± the standard error of the mean). Significance was determined by ANOVA followed by Dunnett's post-test comparing treatments to the 5mM D-glucose treated cells, whereby (*), (**) and (***) represents $p<0.05$, $p<0.01$ and $p<0.001$ respectively.

4.4.3 THP-1 monocytes treated with increased concentrations of D-glucose over a 28 hour period did not increase the generation of reactive oxygen species

THP-1 monocytes treated with high concentrations of D-glucose over a 28 hour period were incubated with MitoSOX, a fluorescent dye used to measure mitochondrial reactive oxygen species (ROS). Fluorescence generated in response to ROS was measured by flow cytometry. This was conducted to determine whether treatment with increased concentrations of D-glucose would result in an increase in generation of mitochondrial ROS. As a positive control for measurement of mitochondrial ROS the cells were treated with FCCP, a mitochondrial electron transport chain uncoupler.

THP-1 monocytes treated with increased concentrations of D-glucose (20mM or 50mM D-glucose) did not show a significant increase in mitochondrial ROS relative to 5mM D-glucose treated cells. Treatment with 5μM FCCP resulted in a significant increase in ROS generation.
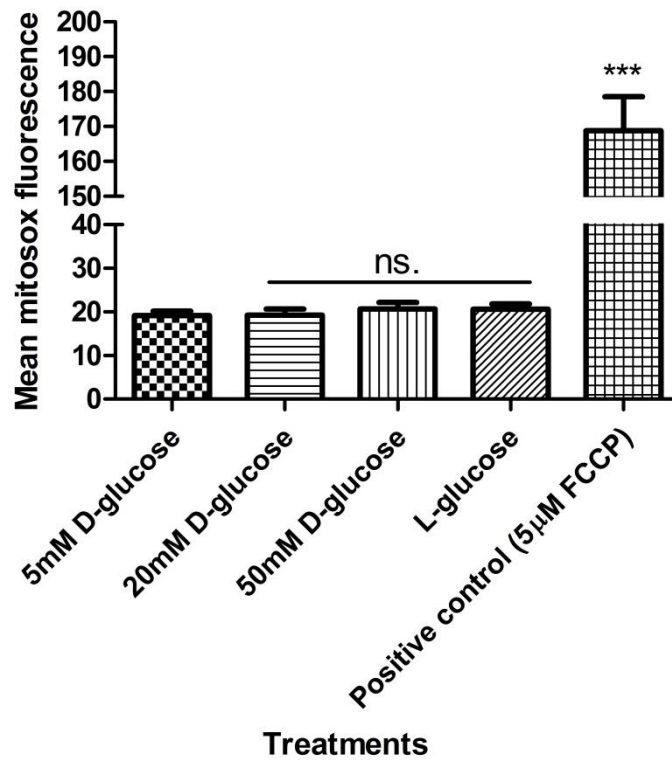
Figure 4.4.3: Treatment of THP-1 monocytes with increased concentrations of D-glucose had no effect on mitochondrial ROS generation

THP-1 monocytes were treated with either 5mM D-glucose, 20mM D-glucose, 50mM D-glucose or 5mM D-glucose and 45mM L-glucose for 28 hours. The cells were collected by centrifugation and washed with PBS prior to mitoSOX staining. The cells were resuspended in PBS and incubated with 2.5µM mitoSOX reagent for 5 minutes at 37°C prior to analysis by flow cytometry. Results are the mean of 3 independent experiments (± the standard error of the mean). Significance was determined by ANOVA followed by Dunnett's post-test comparing treatments to the 5mM D-glucose treated cells, whereby (*), (**) and (***) represents $p<0.05$, $p<0.01$ and $p<0.001$ respectively.

4.4.4 LPS induced TNFα secretion of THP-1 monocytes was reduced in the presence of high concentrations of glucose

THP-1 monocytes were treated with increased concentrations of D-glucose prior to incubation with the bacterial cell wall component LPS, which induces an inflammatory response through activation of the TLR4 receptor. This was done to assess whether an increased availability of D-glucose would alter THP-1 monocyte inflammatory response to LPS. THP-1 monocytes were treated with either 5mM, 20mM or 50mM D-glucose and to control for osmotic concentration, 5mM D-glucose was added with 45mM of L-glucose. L-glucose is an isomer of D-glucose that is taken up by the cells through glucose transporters but cannot be phosphorylated by hexokinase so does not enter the metabolic pathway. The cells were incubated at their respective glucose concentrations for 4 hours prior to treatment with LPS at 10ng/ml. Supernatants were collected and assessed for TNFα content by ELISA (Methods chapter, 2.5.3) at 2, 18 and 24 hours post-LPS addition. At all three time points, treatment with 20mM and 50mM D-glucose and 5mM D-glucose with 45mM L-glucose reduced TNFα secretion compared to the 5mM D-glucose treated monocytes. Both 2 and 18 hour post LPS addition THP-1 monocyte TNFα secretion decreased significantly with increasing concentration of glucose, ($p<0.01$) compared to the 5mM D-glucose treated cells. After 24 hours, TNFα secretion induced by LPS was significantly decreased with 50mM D-glucose and L-glucose treatments ($p<0.01$ and $p<0.001$ respectively) compared to the 5mM D-glucose treated cells. At all three time points the largest decrease in TNFα secreted in response to LPS was caused by treatment with 5mM D-glucose with 45mM L-glucose. This suggests that the decrease in TNFα secretion may be a result of the change in osmotic pressure rather than a specific effect of increased D-glucose uptake.

a.)

b.)

c.)
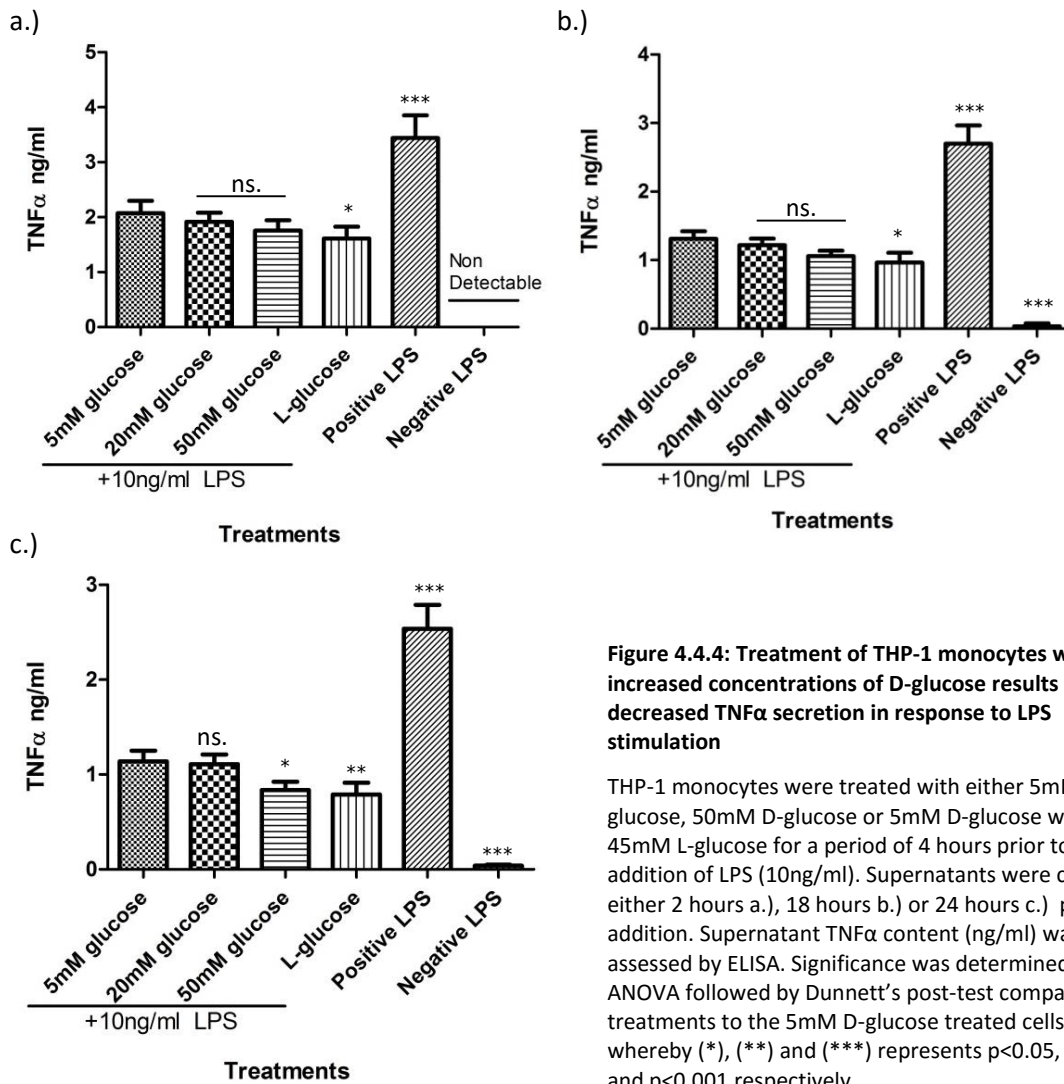
Figure 4.4.4: Treatment of THP-1 monocytes with increased concentrations of D-glucose results in decreased TNFα secretion in response to LPS stimulation

THP-1 monocytes were treated with either 5mM D-glucose, 50mM D-glucose or 5mM D-glucose with 45mM L-glucose for a period of 4 hours prior to the addition of LPS (10ng/ml). Supernatants were collected either 2 hours a.), 18 hours b.) or 24 hours c.) post LPS addition. Supernatant TNFα content (ng/ml) was assessed by ELISA. Significance was determined by ANOVA followed by Dunnett's post-test comparing treatments to the 5mM D-glucose treated cells, whereby (*), (**) and (***) represents p<0.05, p<0.01 and p<0.001 respectively.

4.4.5   Opsonised zymosan induced TNFα secretion of THP-1 monocytes was reduced in the presence of high concentrations of glucose

THP-1 monocytes were treated with increasing concentrations of D-glucose prior to incubation with opsonised zymosan inducing an inflammatory response through activation of the TLR2 and complement receptor 3 (CR3) receptors. This was done to assess whether the observed decrease in TNFα secretion by THP-1 monocytes in the presence of high glucose and treated with the inflammatory stimulus LPS, is specific to the TLR4 pathway. The THP-1 monocytes were treated with increasing concentrations of opsonised zymosan in the presence of 5mM D-glucose in order to optimise the concentration of opsonised zymosan required to elicit an inflammatory response. The cells were incubated with 5mM D-glucose for a period of 4 hours prior to the addition of opsonised zymosan ranging in concentration from 50µg/ml to 4mg/ml. TNFα secretion was measured by ELISA. The results presented in figure 4.4.5, a.) show THP-1 monocyte TNFα secretion increasing as the cells were treated with increasing concentrations of opsonised zymosan. Treatment with 250µg/ml of opsonised zymosan produced a significant inflammatory response measured as TNF-α secretion for further study. THP-1 monocytes were treated with either 5mM, 20mM or 50mM D-glucose and 5mM D-glucose with 45mM of L-glucose to control for osmotic pressure effects. The cells were incubated at their respective glucose concentrations for 4 hours prior to treatment with opsonised zymosan at 250µg/ml. The cells were incubated for a further 24 hours and THP-1 monocyte TNFα secretion was again measured by ELISA. THP-1 monocyte TNFα secretion in response to opsonised zymosan was reduced with increased concentrations of glucose. Treatment with 20mM D-glucose results in a trend to decreased TNFα secretion. Treatment with 50mM D-glucose and L-glucose resulted in a significant decrease (p<0.001) in opsonised zymosan stimulated secretion of TNFα by THP-1 monocytes. As was previously observed in figure 4.4.4 the L-glucose treatment resulted in the greatest decrease in opsonised zymosan-stimulated TNFα secretion, again suggesting that the decrease is caused by the presence of increased osmotic pressure rather than increased availability of D-glucose. Incubation with D- and L- glucose has the same inhibitory effect on inflammatory response induced through the TLR2 and CR3 pathways as observed with LPS induction of TLR4 pathway, suggesting that the inhibitory effect is occurring downstream at a point where these pathways converge.
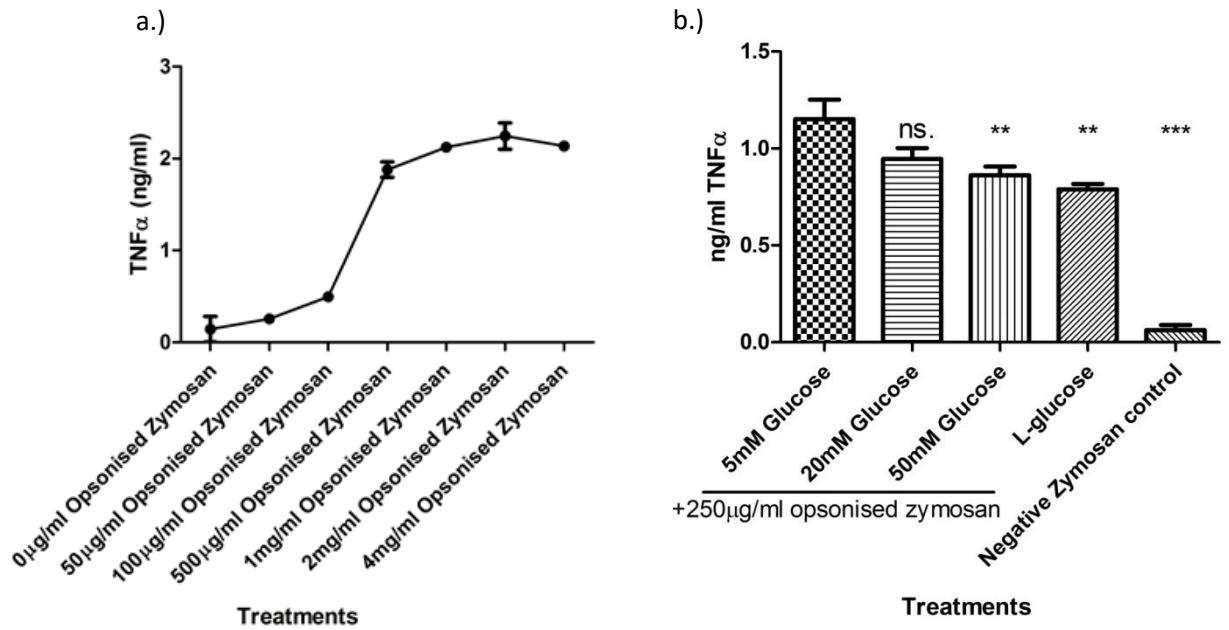
Figure 4.4.5: Treatment of THP-1 monocytes with increased concentrations of D-glucose results in decreased TNFα secretion in response to opsonised zymosan stimulation

THP-1 monocytes were treated with opsonised zymosan at concentrations of 50µg/ml up to 4mg/ml in the presence of 5mM D-glucose over a 28 hour period in order to determine the optimum concentration required to elicit a sufficient TNFα response a.). THP-1 monocytes were treated with glucose at concentrations of either 5mM D-glucose, 50mM D-glucose or 5mM D-glucose with 45mM L-glucose for 4 hours prior to the addition of opsonised zymosan (250µg/ml). The cells were incubated for a further 24 hours, the supernatants collected and the TNFα content (ng/ml) assessed by ELISA b.). Results are the mean of 3 independent experiments (± the standard error of the mean). Significance was determined by ANOVA followed by Dunnett's post-test comparing treatments to the 5mM D-glucose treated cells, whereby (*), (**) and (***) represents $p < 0.05$, $p < 0.01$ and $p < 0.001$ respectively.

4.4.6 Increased concentrations of glucose reduce the secretion of many cytokines from LPS-stimulated THP-1 monocytes

Supernatants of glucose treated THP-1 monocytes were assessed for alterations in LPS-induced cytokine secretion by multiplex array, which examined a panel of 41 individual inflammatory cytokines (Methods chapter, 2.15). This was done in order to assess whether the observed inhibitory effect of treatment with 50mM D-glucose or 5mM D-glucose with 45mM L-glucose was limited to LPS-induced TNFα secretion, or whether secretion of other cytokines would be affected. THP-1 monocytes were treated as described previously, pre-treated with different glucose concentrations for 4 hours and then stimulated with LPS (10ng/ml) for a further 24 hours. Treatment with either 50mM D-glucose or 5mM D-glucose with 45mM L-glucose resulted in the inhibition of LPS-induced secretion of a number of cytokines compared to 5mM D-glucose treated THP-1 monocytes. The treatment with 5mM D-glucose with 45mM L-glucose generally produced a greater decrease in LPS induced cytokine secretion than treatment with 50mM D-glucose or 5mM D-glucose. This suggests that the inhibitory effect of osmotic pressure on cytokine secretion is not specific to TNFα secretion and affects the secretion of many other cytokines. The only cytokine of the 41 analysed that increased with treatment with 50mM D-glucose and 5mM D-glucose with 45mM L-glucose compared to 5mM D-glucose treated THP-1 monocytes was interferon gamma-induced protein 10 (IP-10).
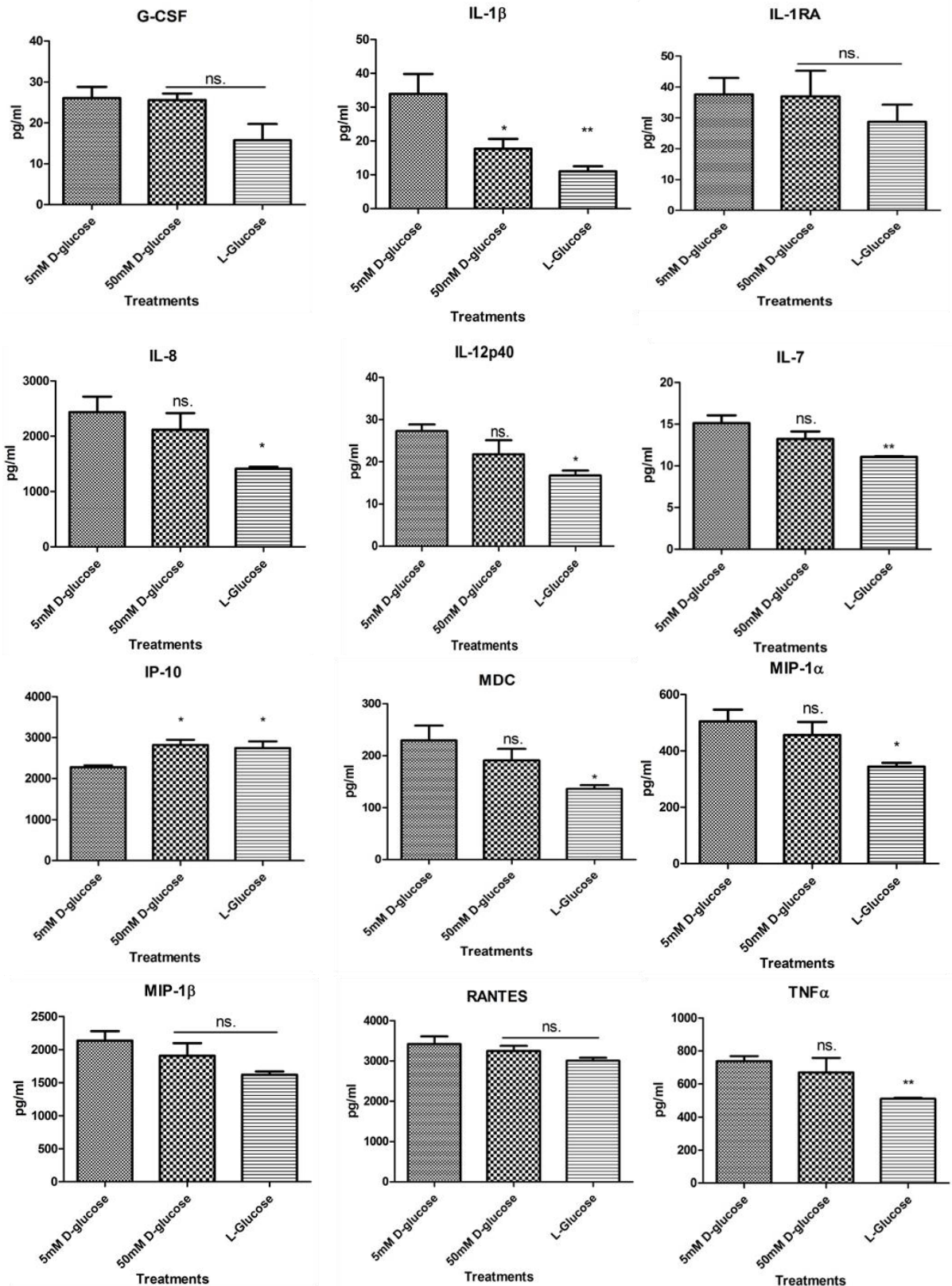
Figure 4.4.6: Treatment of THP-1 monocytes with increased concentrations of glucose resulted in decreased secretion of a number of cytokines in response to LPS

THP-1 monocytes were treated with glucose at concentrations of either 5mM D-glucose, 50mM D-glucose or 5mM D-glucose with 45mM L-glucose for a period of 4 hours prior to the addition of LPS (10ng/ml). The supernatants were collected 24 hours post LPS addition and the presence of 41 individual cytokines assessed using cytokine multiplex assays. Results are the mean of 3 independent experiments (± the standard error of the mean). Significance was determined by ANOVA followed by Dunnett's post-test comparing treatments to the 5mM D-glucose treated cells, whereby (*), (**) and (***) represents $p < 0.05$, $p < 0.01$ and $p < 0.001$ respectively.

Table 4.1: Summary of multiplex (41-plex) cytokine assay of supernatants from THP-1 monocytes treated with varying concentrations of glucose with LPS

Cytokine	Summary of change in cytokine secretion relative to 5mM D-glucose treated THP-1 monocytes	Cytokine	Summary of change in cytokine secretion relative to 5mM D-glucose treated THP-1 monocytes
EGF	Analyte concentration too low for detection	IL-10	Analyte concentration too low for detection
Eotaxin	Analyte concentration too low for detection	IL-12(p40)	Decrease; 50mM D-glucose, L-glucose
FGF-2	Analyte concentration too low for detection	IL-12(p70)	Analyte concentration too low for detection
Flt-3L	Analyte concentration too low for detection	IL-13	Analyte concentration too low for detection
Fractalkine	No change observed in response to treatment	IL-15	Analyte concentration too low for detection
G-CSF	Decrease; treatment with L-glucose	IL-17	Analyte concentration too low for detection
GM-CSF	Analyte concentration too low for detection	IP-10	Increase; treatment with 50mM D-glucose, L-glucose
GRO	No change observed in response to treatment	MCP-1	No change observed in response to treatment
IFNα2	Analyte concentration too low for detection	MCP-3	Analyte concentration too low for detection
IFN-γ	Analyte concentration too low for detection	MDC	Decrease; 50mM D-glucose, L-glucose
IL-1α	Analyte concentration too low for detection	MIP-1α	Decrease; 50mM D-glucose, L-glucose
IL-1β	Decrease; 50mM D-glucose, L-glucose	MIP-1β	Decrease; 50mM D-glucose, L-glucose
IL-1RA	Decrease; L-glucose	PDGF-AA	No change observed in response to treatment
IL-2	Analyte concentration too low for detection	PDGF-BB	Analyte concentration too low for detection
IL-3	Analyte concentration too low for detection	RANTES	Decrease; 50mM D-glucose, L-glucose
IL-4	Analyte concentration too low for detection	sCD40L	Analyte concentration too low for detection
IL-5	Analyte concentration too low for detection	TGFα	Analyte concentration too low for detection
IL-6	Analyte concentration too low for detection	TNFα	Decrease; 50mM D-glucose, L-glucose
IL-7	Decrease; 50mM D-glucose, L-glucose	TNFβ	Analyte concentration too low for detection
IL-8	Decrease; 50mM D-glucose, L-glucose	VEGF	No change observed in response to treatment
IL-9	Analyte concentration too low for detection		

4.4.7 Increased concentrations of glucose reduce the secretion of many cytokines from opsonised zymosan-stimulated THP-1 monocytes

Supernatants of glucose-treated THP-1 monocytes were assessed for alterations in opsonised zymosan-induced cytokine secretion by multiplex cytokine detection.THP-1 monocytes were treated as described previously, pre-treated with glucose for 4 hours and stimulated with opsonised zymosan (250µg/ml) for a further 24 hours. Subsequent to glucose and zymosan treatment, the supernatants were collected and analysed for the presence of 41 individual cytokines by multiplex detection.

The only cytokine secretion that was increased following opsonised zymosan stimulation in the presence of increased concentrations of glucose was IP-10. IP-10 was increased in response to treatment with either 50mM D-glucose or 5mM D-glucose with 45mM L-glucose. The secretion of many other cytokines decreased in response to increased concentrations of glucose, although these again decreased in the presence of both 50mM D-glucose or 5mM D-glucose with 45mM L-glucose. This suggests that the increase in osmotic pressure inhibited the secretion of many inflammatory cytokines except for the cytokine IP-10.
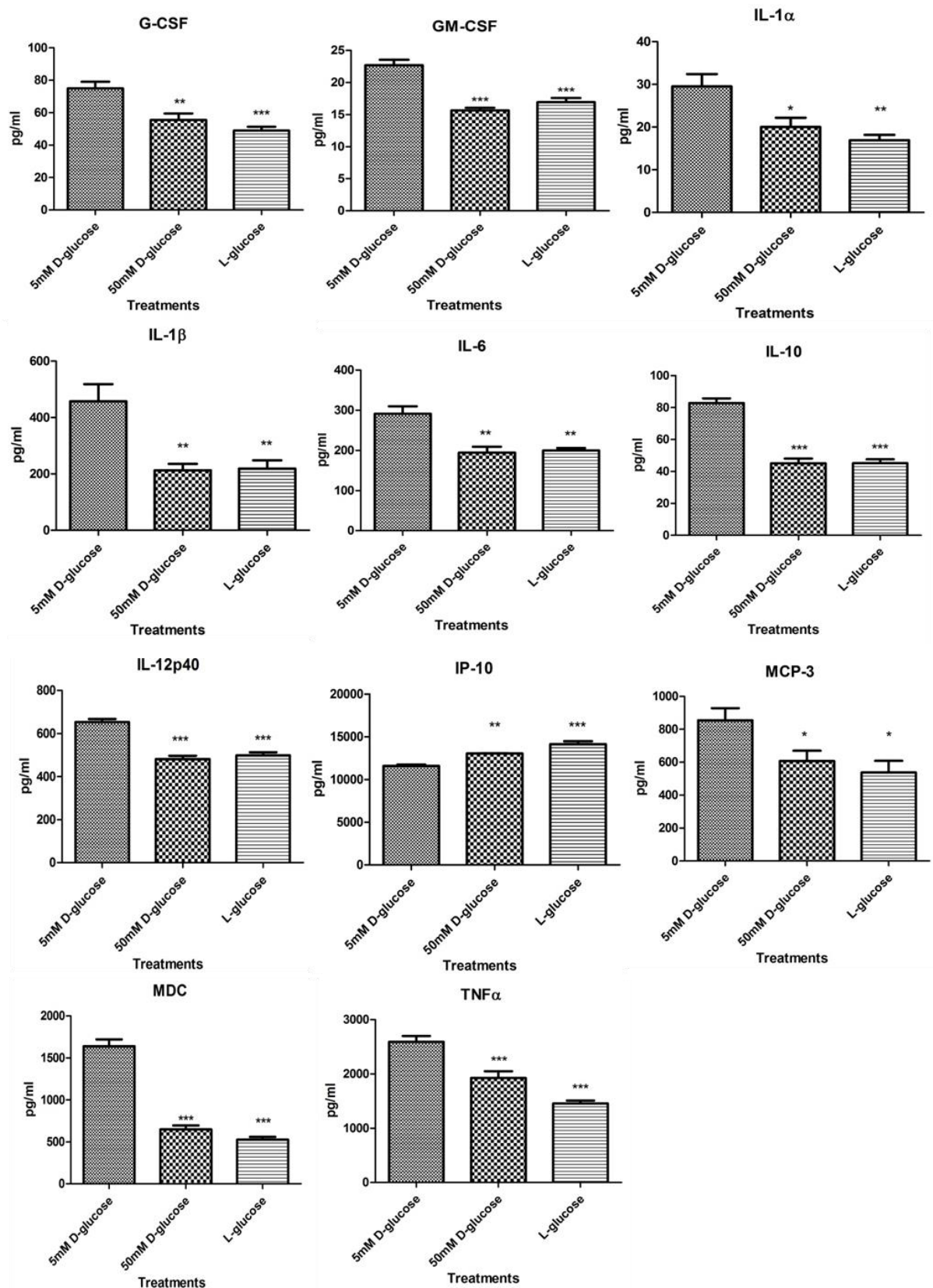
Figure 4.4.7: Treatment of THP-1 monocytes with increased concentrations of glucose resulted in decreased secretion of a number of cytokines in response to opsonised zymosan

THP-1 monocytes were treated with glucose at concentrations of either 5mM D-glucose, 50mM D-glucose or 5mM D-glucose with 45mM L-glucose for 4 hours prior to the addition of opsonised zymosan (250µg/ml). The supernatants were collected 24 hours post addition of opsonised zymosan and the presence of 41 individual cytokines assessed using cytokine multiplex assays. Results are the mean of 3 independent experiments (± the standard error of the mean). Significance was determined by ANOVA followed by Dunnett's post-test comparing treatments to the 5mM D-glucose treated cells, whereby (*), (**) and (***) represents $p<0.05$, $p<0.01$ and $p<0.001$ respectively.

127

Table 4.2: Summary of multiplex (41-plex) cytokine assay of supernatants from THP-1 monocytes treated with varying concentrations of glucose with opsonised zymosan

Cytokine	Summary of change in cytokine secretion relative to 5mM D-glucose treated THP-1 monocytes	Cytokine	Summary of change in cytokine secretion relative to 5mM D-glucose treated THP-1 monocytes
EGF	Analyte concentration too low for detection	IL-10	Decrease; treatment with 50mM D-glucose, L-glucose
Eotaxin	Analyte concentration too low for detection	IL-12(p40)	Decrease; treatment with 50mM D-glucose, L-glucose
FGF-2	Analyte concentration too low for detection	IL-12(p70)	Analyte concentration too low for detection
Flt-3L	Analyte concentration too low for detection	IL-13	Analyte concentration too low for detection
Fractalkine	No change observed in response to treatment	IL-15	Analyte concentration too low for detection
G-CSF	Decrease; treatment with 50mM D-glucose, L-glucose	IL-17	Analyte concentration too low for detection
GM-CSF	Decrease; treatment with 50mM D-glucose, L-glucose	IP-10	Increase; treatment with 50mM D-glucose, L-glucose
GRO	No change observed in response to treatment	MCP-1	Analyte concentration too high for detection
IFNα2	No change observed in response to treatment	MCP-3	Decrease; treatment with 50mM D-glucose, L-glucose
IFN-γ	Analyte concentration too low for detection	MDC	Decrease; treatment with 50mM D-glucose, L-glucose
IL-1α	Decrease; treatment with 50mM D-glucose, L-glucose	MIP-1α	Analyte concentration too high for detection
IL-1β	Decrease; treatment with 50mM D-glucose, L-glucose	MIP-1β	Analyte concentration too high for detection
IL-1RA	No change observed in response to treatment	PDGF-AA	No change observed in response to treatment
IL-2	Analyte concentration too low for detection	PDGF-BB	Analyte concentration too low for detection
IL-3	Analyte concentration too low for detection	RANTES	No change observed in response to treatment
IL-4	Analyte concentration too low for detection	sCD40L	No change observed in response to treatment
IL-5	Analyte concentration too low for detection	TGFα	Analyte concentration too low for detection
IL-6	Decrease; treatment with 50mM D-glucose, L-glucose	TNFα	Decrease; treatment with 50mM D-glucose, L-glucose
IL-7	No change observed in response to treatment	TNFβ	Analyte concentration too low for detection
IL-8	No change observed in response to treatment	VEGF	No change observed in response to treatment
IL-9	Analyte concentration too low for detection		

4.4.8 Higher osmotic concentration decreases THP-1 monocyte TNFα secretion

As observed in previous figures 4.4.6 and 4.4.7, treatment of THP-1 monocytes with both D- and L-glucose results in decreased secretion of a number of cytokines in response to both LPS and opsonised zymosan. A series of experiments were performed to determine if this effect would be observed by treatment with an alternative sugar, mannitol. Also, normalising the osmotic concentration to 50milliosmoles (mOsM) was investigated, to determine whether treatment with increased concentrations of D-glucose would result in a relative increase in LPS-induced secretion of TNFα. THP-1 monocytes were treated with increasing concentrations of the sugar mannitol in the presence of 5mM D-glucose for 4 hours prior to addition of LPS (10ng/ml) after which the cells were incubated for a further 24 hours in order to assess the effects of increased osmotic concentration on THP-1 cellular viability by MTT (figure 4.4.8, a.)) and LPS-induced secretion of the inflammatory cytokine TNFα (figure 4.4.8, b.)). Increased osmotic concentration as a result of mannitol incubation had no significant effect on THP-1 cell viability as assessed by MTT assay.

Incubation of THP-1 monocytes with 5mM D-glucose and increasing concentrations of mannitol decreased the secretion of TNFα (figure 4.4.8, b.)). Incubation of THP-1 monocytes with 5mM D-glucose and 95mM mannitol (100mOsm) resulted in a significant decrease in TNFα secretion in response to LPS stimulation. This suggests that higher osmotic concentration suppresses LPS-induced TNFα secretion by THP-1 monocytes. This result conforms with the effects of increased osmotic concentration from 5mM D-glucose and 45mM L-glucose on LPS- or opsonised zymosan-induced TNFα secretion (figures, 4.4.4 and 4.4.5).

Figure 4.4.8, c.), represents the effects of varying concentrations of D-glucose whilst the osmotic concentration remained constant at 50 milliosmoles (mOsm) on LPS induced TNFα secretion by THP-1 monocytes treated over a 28 hour period. Although not significant, 50mM D-glucose showed a trend for increased secretion of TNFα in response to LPS compared to the THP-1 monocytes co-treated with 5mM D-glucose and 45mM L-glucose. This may suggest that the presence of higher concentrations of D-glucose may induce an increase in LPS induced secretion of TNFα which is being suppressed by the presence of higher osmotic concentration. This possibility was investigated subsequently by analysing the effect of high glucose on TNFα mRNA
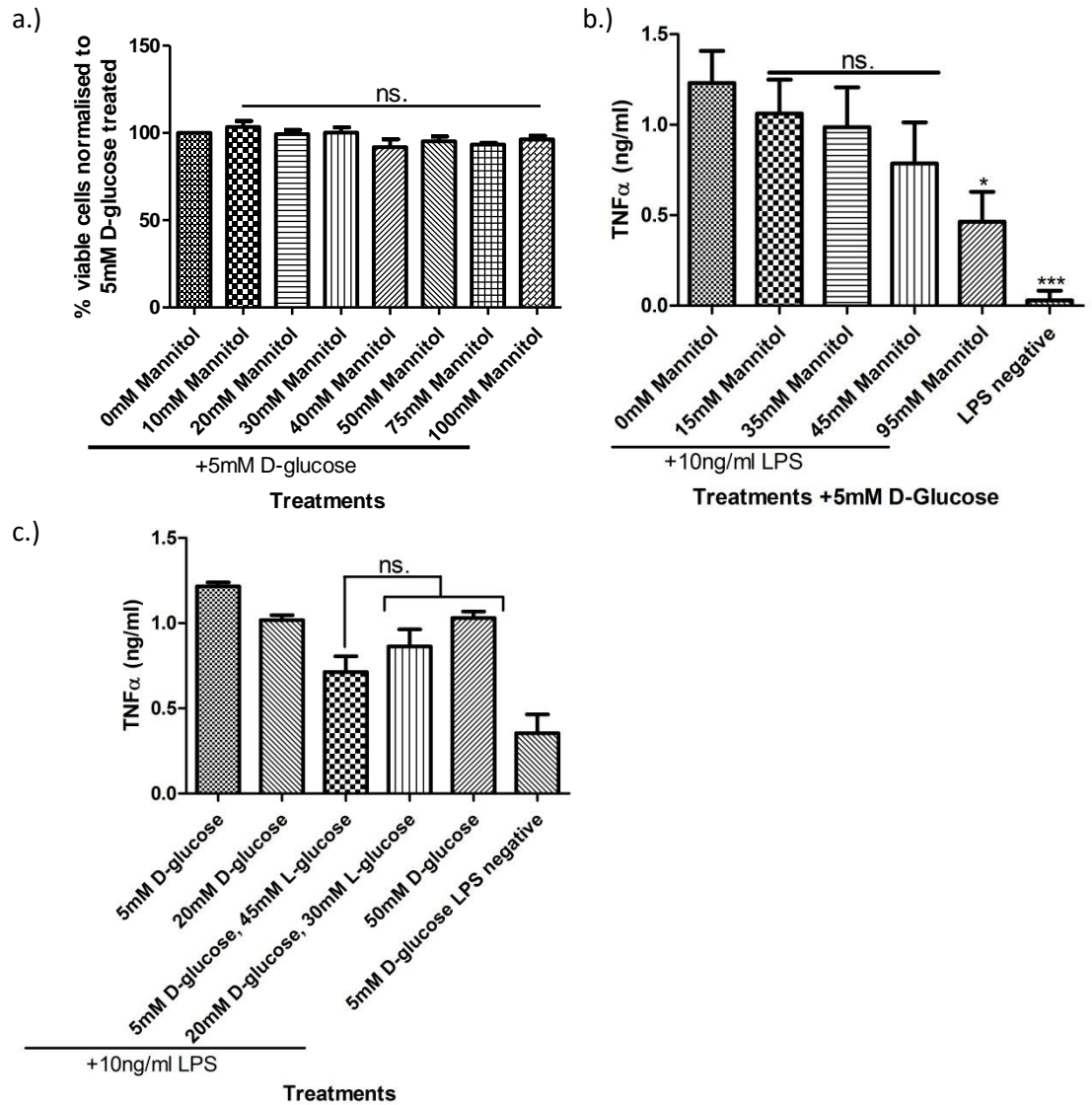
Figure 4.4.8: Increased osmotic concentration has an inhibitory effect on LPS induced THP-1 TNFα secretion independent of cellular viability

THP-1 monocytes were treated with concentrations of the sugar mannitol up to 100mM with 5mM D-glucose over a 28 hour period and cellular metabolic activity and LPS induced TNFα secretion assessed by MTT assay a.) and ELISA b.) respectively. THP-1 monocytes were also treated with increased concentrations of D-glucose with a normalised osmotic concentration of 50mOsm and LPS induced TNFα secretion assessed by ELISA c.). Results are the mean of 3 independent experiments (± the standard error of the mean). Significance was determined by ANOVA followed by Dunnett's post-test comparing treatments to the 5mM D-glucose treated monocytes, whereby (*), (**) and (***) represents p<0.05, p<0.01 and p<0.001 respectively.

4.4.9 TNFα mRNA transcription THP1 monocytes in response to LPS is reduced by increased concentrations of glucose

Due to the decrease in cytokine secretion observed in THP-1 monocytes treated with increased concentrations of glucose and stimulated with LPS, TNFα mRNA transcription was examined under the same conditions. This was to assess whether the observed osmotic effect on cytokine secretion was occurring further upstream of the cytokine secretory pathways, e.g. causing alterations in cytokine mRNA transcription.

THP-1 monocytes were treated with increased concentrations of glucose and LPS as described previously; cells were lysed for RNA extraction at 2, 18 and 24 hours post-LPS addition. The extracted RNA was quantified and quality-assessed spectrophotometrically then reverse transcribed as previously described. The data was assessed using the comparative CT method (Livak and Schmittgen 2001, Schmittgen and Livak 2008), normalising to the housekeeper gene 18S and expressing the data as fold change relative to 5mM D-glucose-treated monocytes.

The results show decreased TNFα mRNA expression in the THP-1 monocytes treated with either 50mM D-glucose or 5mM D-glucose with 45mM L-glucose in response to LPS stimulation. The reduction occurs at all three of the time points studied, with TNFα expression reduced by approximately 30% in response to 50mM D-glucose and 5mM D-glucose with 45mM L-glucose treatment.
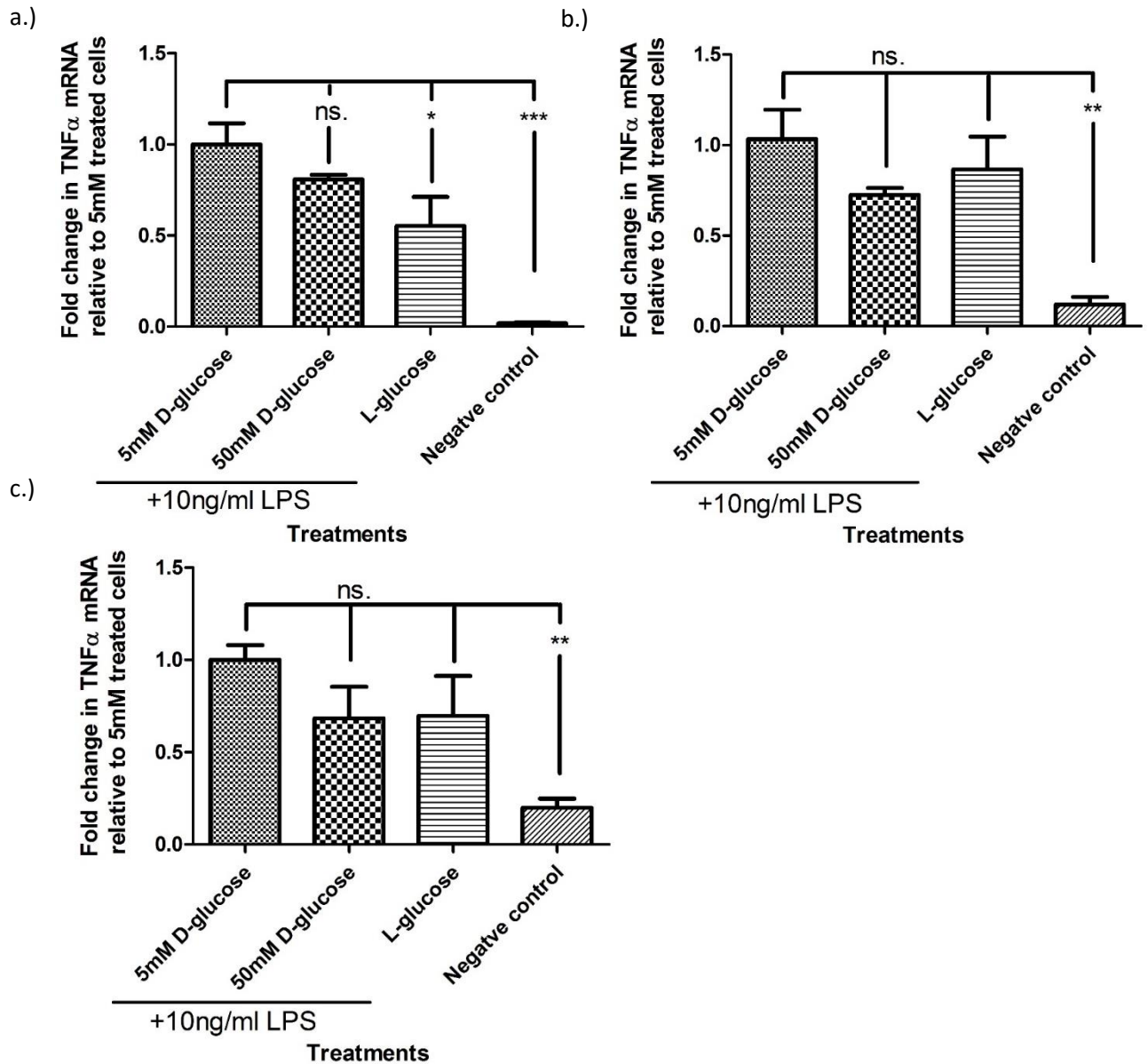
Figure 4.4.9: Treatment of THP-1 monocytes with increased concentrations of D-glucose resulted in decreased expression of TNFα mRNA

THP-1 monocytes were treated with glucose at concentrations of either 5mM D-glucose, 50mM D-glucose or 5mM D-glucose with 45mM L-glucose for 4 hours prior to the addition of LPS (10ng/ml). The negative LPS treatment group were treated with 5mM D-glucose without LPS for the duration of the treatment. The monocytes were harvested by centrifugation, washed with PBS and lysed in Trizol reagent at 2 hours a.), 18 hours b.) and 24 hours c.) post LPS addition. The total RNA was extracted using Qiagen RNA extraction spin columns and the RNA quantity and quality assessed by nanodrop. The extracted RNA was reverse transcribed to cDNA and TNFα mRNA expression assessed by qPCR at the 2 hour, 18 hour and 24 hour post LPS addition time points. The ribosomal RNA 18S was used as a housekeeper gene. The results were analysed using the ΔΔCT method, whereby the results are expressed as a fold change (± standard error of ΔCT) relative to the 5mM D-glucose treated monocytes. The results are the mean of 3 independent experiments (± the standard error of the mean). Significance was determined by ANOVA followed by Dunnett's post-test comparing treatments to the 5mM D-glucose treated cells and the 5mM D-glucose and 45mM L-glucose treated cells, whereby (*), (**) and (***) represents $p<0.05$, $p<0.01$ and $p<0.001$ respectively.

4.4.10 Treatment of THP-1 monocytes with increased concentrations of D-glucose results in a decrease in the NAD$^+$:NADH ratio

The ratio of NAD$^+$:NADH was assessed in order to determine whether treatment with increased concentrations of glucose would alter intracellular NAD$^+$:NADH ratio. This is of particular significance to proteins which require NAD$^+$ to function such as the deacetylase SIRT1.

The results show a reduction in the NAD$^+$:NADH ratio in the 50mM D-glucose-treated THP-1 monocytes compared to the 5mM D-glucose-treated and the 5mM D-glucose 45mM L-glucose-treated monocytes which was greater at 24 hours.
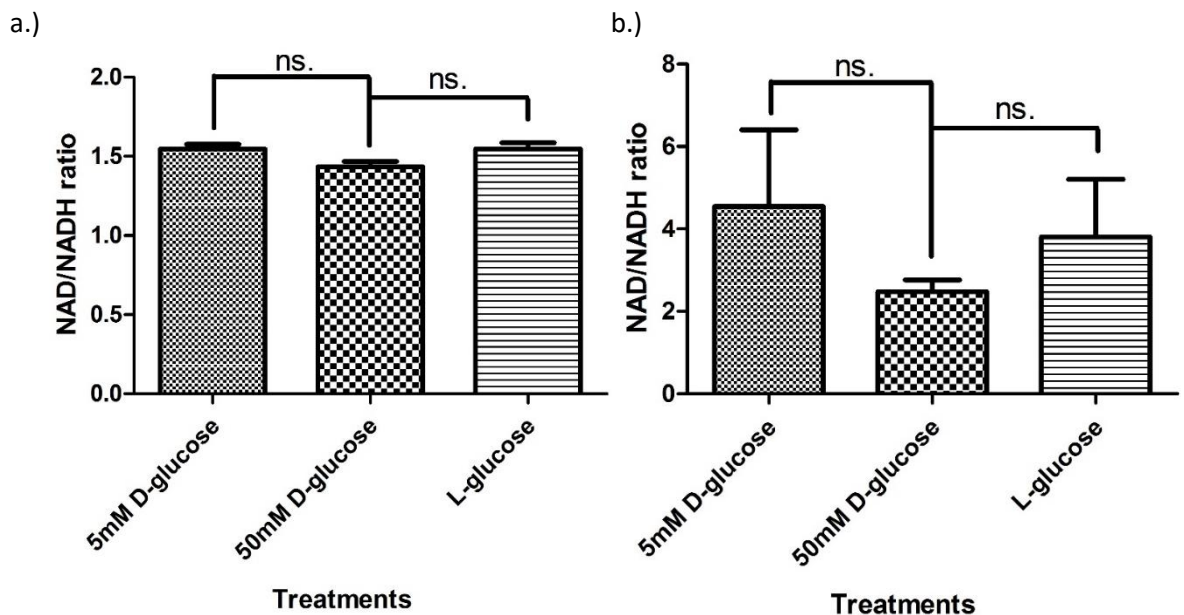
Figure 4.4.10: Treatment of THP-1 monocytes with glucose over a 6 or 24 hour period results in a decrease in the NAD$^+$:NADH ratio

THP-1 monocytes were treated with either 5mM D-glucose, 50mM D-glucose or 5mM D-glucose with 45mM L-glucose for a period of either 6 hours a.) or 28 hours b.). Subsequent to treatment the ratio of NAD$^+$: NADH was measured using a NAD$^+$:NADH quantification assay. Results are the mean of 3 independent experiments (± the standard error of the mean). Significance was determined by ANOVA followed by Dunnett's post-test comparing treatments with either the 5mM D-glucose treated monocytes or the 5mM D-glucose, 45mM L-glucose treated cells, whereby (*), (**) and (***) represents p<0.05, p<0.01 and p<0.001 respectively.

4.4.11 SIRT1 deacetylase activity of THP-1 monocytes is reduced with 50mM D-glucose

THP-1 monocytes were treated with increased concentrations of glucose over either a 6 hour or 28 hour period. The cells were subsequently lysed and the nuclear fraction retained in order to determine the effect, if any, of elevated glucose on SIRT1 deacetylase activity. SIRT1 activity was measured due to its observed role as a nutrient sensor and in the regulation of NF-κB gene transcription in response to inflammatory stimuli.

Treatment of THP-1 monocytes with 50mM D-glucose or 5mM D-glucose with 45mM L-glucose over a 6 hour period had no effect on SIRT1 deacetylase activity relative to the 5mM D-glucose treated cells. Treatment of THP-1 monocytes with 50mM D-glucose over a 28 hour period resulted in a significant decrease ($p < 0.05$) in SIRT1 deacetylase activity relative to 5mM D-glucose treated cells. However, THP-1 monocytes incubated with 5mM D-glucose and 45mM L-glucose produced no change in SIRT1 deacetylase activity relative to 5mM D-glucose treated cells. These results suggest that the observed decrease in SIRT1 deacetylase activity resulting from treatment with 50mM D-glucose occurred independent of increases in osmotic concentration. This reduction in SIRT1 deacetylase activity may be further affected by the reduction in the NAD^+:NADH ratio occurring in THP-1 monocytes treated with 50mM D-glucose over a 28 hour period.
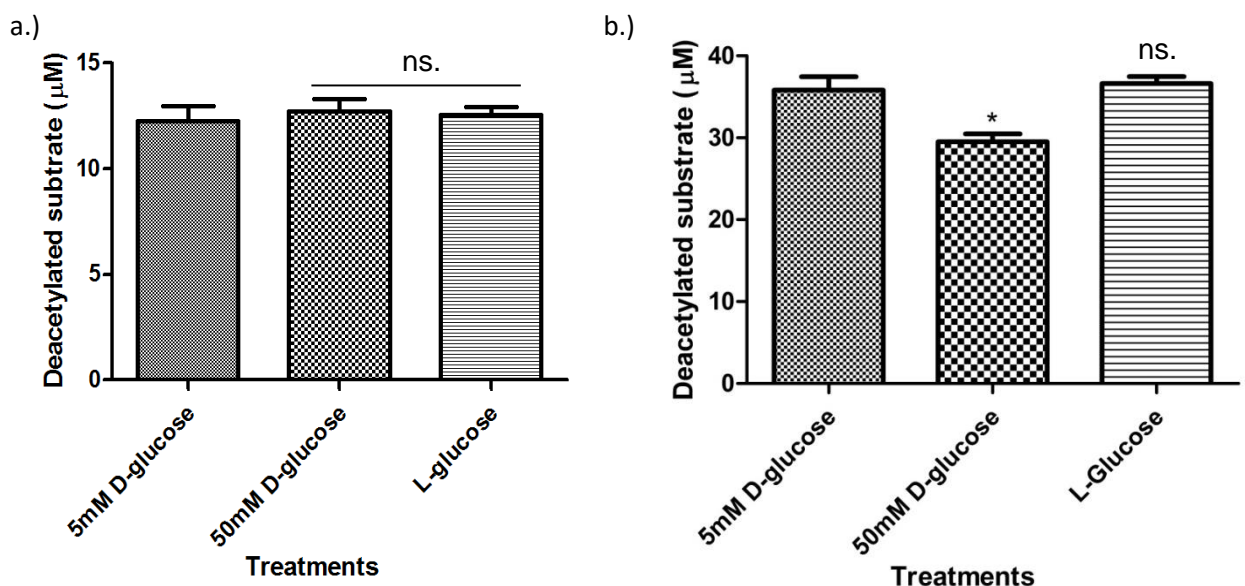
Figure 4.4.11: Treatment of THP-1 monocytes with increased concentrations of D-glucose over a 28 hour period results in decreased SIRT1 activity

THP-1 monocytes were treated with glucose at concentrations of either 5mM D-glucose, 50mM D-glucose or 5mM D-glucose with 45mM L-glucose for a period of either 6 hours a.) or 28 hours b.). Subsequent to treatment the THP-1 monocytes were harvested by centrifugation, lysed and the nuclear fraction collected. The protein concentration of the isolated nuclear fraction was assessed by BCA assay. SIRT1 deacetylase activity was measured in 15μg of nuclear lysate using the SIRT1 activity assay as described in the protocol. Results are the mean of 3 independent experiments (± the standard error of the mean). Significance was determined by ANOVA followed by Dunnett's post-test comparing treatments to the 5mM D-glucose treated cells, whereby (*), (**) and (***) represents $p < 0.05$, $p < 0.01$ and $p < 0.001$ respectively.

4.4.12 Incubation of THP-1 monocytes with increased concentration of D-glucose had no effect on SIRT1 mRNA expression

THP-1 monocytes were treated with varying concentrations of D-glucose over a 4 hour period prior to incubation with LPS (10ng/ml); the cells were again incubated for a further 2, 18 or 24 hours. The cells were collected by centrifugation washed with ice cold sterile PBS, and pelleted prior to lysis and RNA extraction. The extracted mRNA was converted to cDNA and assessed for the presence of SIRT1 mRNA by qPCR. Due to the decrease in SIRT1 deacetylase activity observed in high glucose treated THP-1 monocytes (figure, 4.4.11), changes in SIRT1 mRNA expression in response to treatment was examined by qPCR.

Treatment of THP-1 monocytes with glucose and LPS for a combined 6 or 18 hours did not result in a significant change in SIRT1 mRNA expression. Treatment of THP-1 monocytes with glucose and LPS over a 28 hour period did not result in a significant change in SIRT1 mRNA expression although treatment with 50mM D-glucose appeared to result in a slight albeit non-significant increase in mRNA expression.
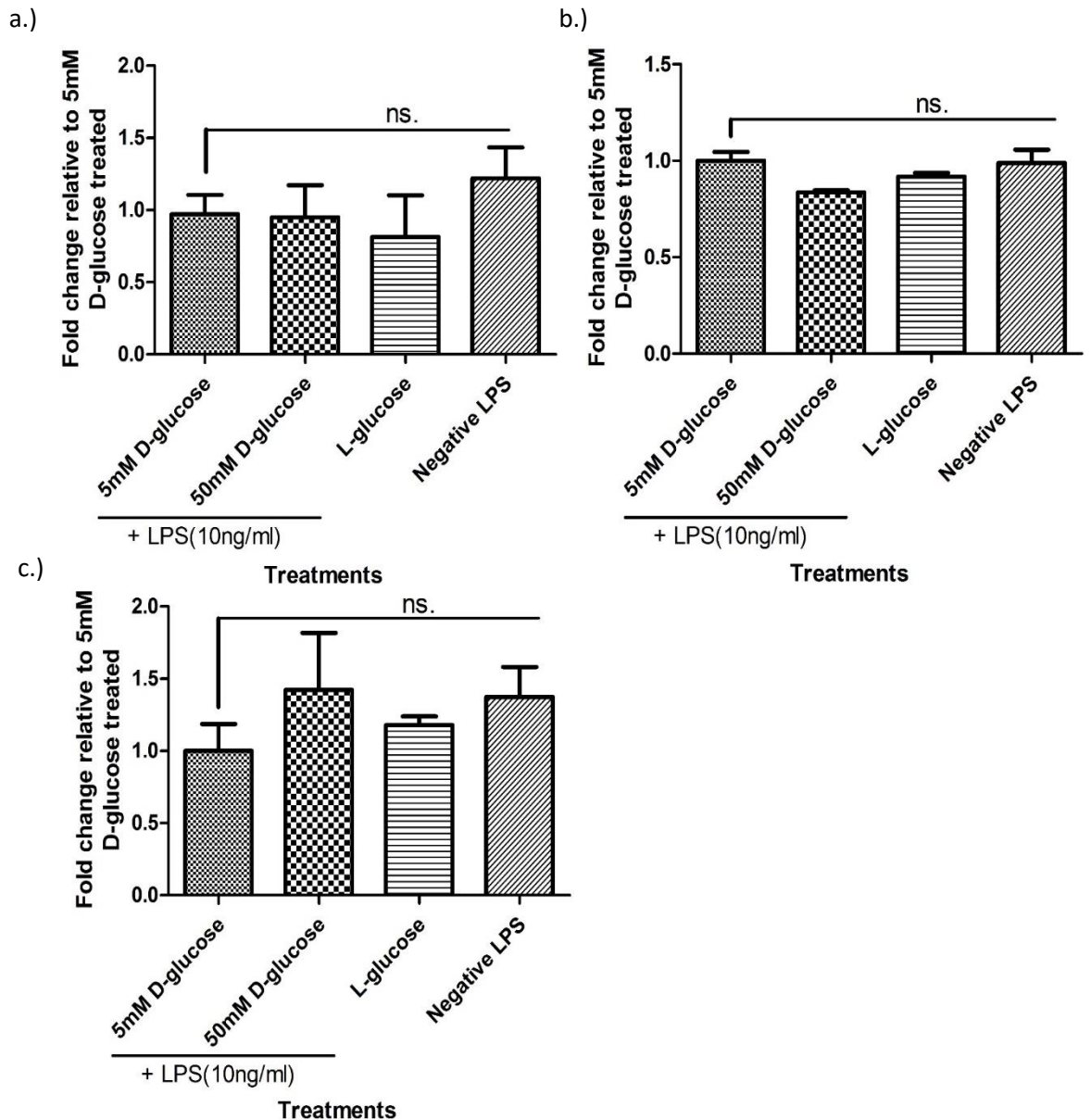
Figure 4.4.12: Treatment of THP-1 monocytes with increased concentrations of glucose had no significant effect on SIRT1 mRNA expression

THP-1 monocytes were treated with glucose at concentrations of either 5mM D-glucose, 50mM D-glucose or 5mM D-glucose with 45mM L-glucose for 4 hours prior to the addition of LPS (10ng/ml). The negative LPS treatment group were treated with 5mM D-glucose without LPS for the duration of the treatment. The monocytes were harvested by centrifugation, washed with PBS and lysed in Trizol reagent at 2 hours a.), 18 hours b.) and 24 hours c.) post LPS addition. The total RNA was extracted using Qiagen RNA extraction spin columns and the RNA quantity and quality assessed by nanodrop. The extracted RNA was reverse transcribed to cDNA and SIRT1 mRNA expression assessed by qPCR at the 2 hour, 18 hour and 24 hour post LPS addition time points. The ribosomal RNA 18S was used as a housekeeper gene. The results were analysed using the ΔΔCT method, whereby the results are expressed as a fold change (± standard error of the ΔCT) relative to the 5mM D-glucose treated monocytes. The results are the mean of 3 independent experiments (± the standard error of the mean). Significance was determined by ANOVA followed by Dunnett's post-test comparing treatments to the 5mM D-glucose treated cells, whereby (*), (**) and (***) represents $p < 0.05$, $p < 0.01$ and $p < 0.001$ respectively.

4.4.13 Treatment of THP-1 monocytes with 50mM D-glucose over a 6 hour period resulted in an increase in P65 acetylation at lysine 310

THP-1 monocytes were treated with increased concentrations of glucose over a 6 hour period and the cells subsequently lysed in order to determine the effect, if any, of high glucose on the acetylation status of the P65 subunit of the NF-κB complex. Immunoblot detection of acetylated (K310) P65 was normalised to total P65 and beta actin. Lysine 310 acetylation was assessed as it regulates P65 activity and is a target of SIRT1 deacetylation. Densitometry analysis of the immunoblots were analysed using Image J software and the acetylated P65 (K310) and total P65 blots normalised to the density of the beta actin blots. The densitometry results were expressed as fold change relative to 5mM D-glucose treated monocytes. When normalised to beta actin, P65 (K310) acetylation status was significantly increased ($p < 0.01$) in response to treatment with 50mM D-glucose over a 6 hour period (figure 4.4.13, b.)). Total P65 was then measured by immunoblot in order to be able to express acetylated P65 as a ratio of total P65. THP-1 monocytes treated with 50mM D-glucose and 5mM D-glucose with 45mM L-glucose over a 6 hour period resulted in a significant ($p < 0.01$) increase in expression of total P65 (figure4.4.13, c.)). As this result occurred in both treatment with 50mM D-glucose and 5mM D-glucose with 45mM L-glucose it appears to be as a result of the increased osmotic concentration. When these results (figures b.) and c.)) were expressed as a ratio of acetylated P65 to total P65 (figure 4.4.13, d.)) P65 acetylation was significantly increased ($p < 0.05$) in response to 50mM D-glucose. Treatment of THP-1 monocytes with 5mM D-glucose and 45mM L-glucose appeared to result in a trend to a decrease in P65 acetylation status relative to total P65 although this result was not statistically significant
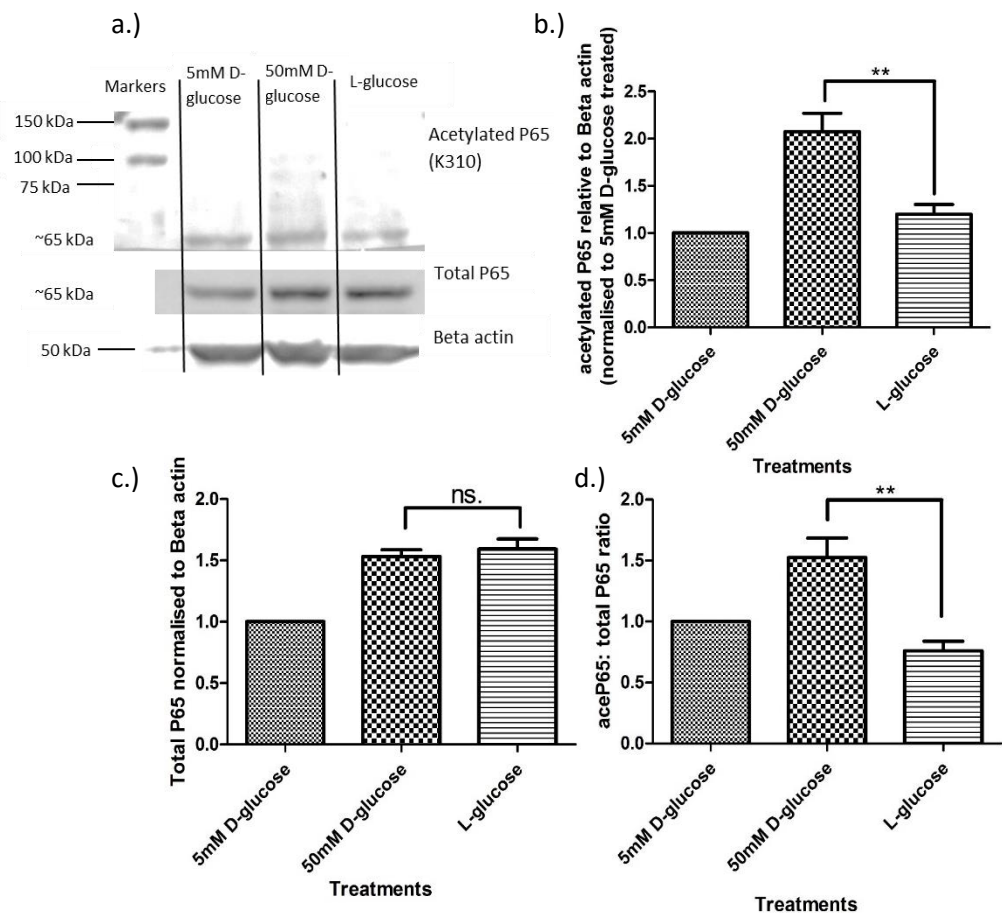
Figure 4.4.13: Treatment of THP-1 monocytes with increased concentrations of glucose over a 28 hour period resulted in increased P65 acetylation status (K310)

THP-1 monocytes were treated with glucose at concentrations of either 5mM D-glucose, 50mM D-glucose or 5mM D-glucose with 45mM L-glucose for a period of 6 hours. Subsequent to this the monocytes were harvested by centrifugation, washed with ice cold sterile PBS and lysed using a RIPA buffer. Protein concentration was determined by BCA assay. The extracted protein was separated by SDS electrophoresis on a 10% acrylamide gel prior to being transferred to PVDF membranes. The membranes were stained with antibodies against acetylated (K310) P65, total P65 and beta actin. The membranes were washed to remove excess antibody and incubated with HRP conjugated anti-IgG antibody. The blots were developed by incubating with an ECL solution and the produced chemiluminescence detected using a GBOX imaging system a.). Densitometry analysis was performed on the blots using Image J software, to compare acetylated P65 relative to the beta actin loading control b.), total P65 to beta actin c.) and to produce a ratio of acetylated P65 to total P65 d.). Results are the mean of 3 independent experiments (± the standard error of the mean). Significance was determined by ANOVA followed by Dunnett's post-test comparing treatments to the 5mM D-glucose, 45mML-glucose treated cells, whereby (*), (**) and (***) represents $p < 0.05$, $p < 0.01$ and $p < 0.001$ respectively.

138

4.5   Discussion

The purpose of the research presented in this chapter was to determine the effects of elevated glucose on monocyte cytokine secretion and to attempt to identify pathways through which any changes in expression might be occurring. Previous studies have primarily used the THP-1 monocyte cell line, which due to its proliferative nature is metabolically more active than primary monocytes. As THP-1 monocytes are frequently used as a model system in metabolic inflammation studies, it is important to assess how comparable the responses between THP-1 and primary monocytes treated with high concentrations of glucose are.

THP-1 monocytes are routinely cultured in high glucose (11mM), but here cells were treated with lower (5mM) and higher concentrations (20mM and 50mM) of either D-glucose or its metabolically inert isoform, L-glucose. Neither 5mM nor 50mM D-glucose affected TNFα secretion up to 24 hours. These result differ from previous reports where THP-1 monocytes treated with high glucose have been observed to increase secretion (Iwata, Soga et al. 2007, Wu, Wu et al. 2009) and mRNA expression of a number of inflammatory cytokines (Shanmugam, Reddy et al. 2003) including TNFα at 72 hours. The response observed at 72 hours may result from interaction between increased advanced glycation end products with their receptor (RAGE) which increases intracellular reactive oxygen species resulting in increased induction of an inflammatory response. Treatment of THP-1 monocytes over a 28 hour period with increased concentrations of D-glucose did not result in an increase in mitochondrial ROS generation as determined by MitoSOX staining. The generation of advanced glycation end products was not assessed in this thesis. Previous studies have failed to observe an increase in advanced glycation end products in endothelial cells treated with increased concentrations of glucose over a 24 hour period (Shinohara, Thornalley et al. 1998). In addition, the work presented in this chapter has shown that THP-1 monocytes treated with high glucose resulted in decreased secretion of a number of cytokines in response to either LPS or opsonised zymosan.

The cytokine IP-10 was the only cytokine observed to increase in THP-1 monocytes treated with high concentrations of D-glucose and LPS. The gene for the cytokine IP-10 has been mapped to chromosome 4, band q21, a locus strongly associated with monocytic leukaemia (Luster, Jhanwar et al. 1987, Liu, Guo et al. 2011). Increased secretion of IP-10 has also been associated with a variety of leukaemias (Olsnes, Motorin et al. 2006, Khandany, Hassanshahi et al. 2012). The strong association of the gene locus containing IP-10 with monocytic leukaemia cell lines (Domer, Fakharzadeh et al. 1993) could provide a reason for the increased expression of IP-10 observed in treated THP-1

monocytes. This increase in IP-10 secretion also supports the notion that the decreased secretion of the other cytokines are occurring independent of any osmotic toxicity effect.

LPS and opsonised zymosan induce an inflammatory response through interaction with the TLR4 or CR3 and TLR2 receptors respectively. As the same cytokine response to high glucose was observed with either stimulus it can be postulated that the decrease in cytokine secretion is not receptor mediated and is occurring downstream of receptor interaction. Decreased cytokine secretion was observed in response to treatment with either D- or L-glucose therefore it can be postulated that this effect is being caused by the increased osmotic concentration rather than an increase in glucose availability. The treatment of THP-1 monocytes with increased concentrations of either D- or L-glucose resulted in decreased expression of TNFα mRNA. The increased osmotic concentration, resulting from treatment with 50mM D-glucose or 5mM D-glucose with 45mM L-glucose could potentially have interfered with the ELISAs ability to detect THP-1 secreted TNFα. This could explain the decreased TNFα observed as a result of these treatments. Although this possibility can be discounted by the results obtained in figure 4.4.8, c.). THP-1 monocytes were treated with either 5mM D-glucose with 45mM L-glucose, 20mM D-glucose with 30mM L-glucose or 50mM D-glucose to create a constant osmotic concentration of 50mOsm with varying concentrations of D-glucose prior to stimulation with LPS. The ELISAs detected a greater concentration of TNFα present in the supernatants of THP-1 monocytes treated with higher concentrations of D-glucose at a constant osmotic concentration of 50 osmoles. This suggests that the increased osmotic concentration does not limit the ELISAs ability to detect secreted TNFα, rather the osmotic concentration affected the THP-1 monocytes ability to secrete TNFα in response to LPS. THP-1 monocytes treated with high concentrations of the sugar mannitol to produce an osmotic environment also showed reduced secretion of the cytokine TNFα in response to LPS. These results suggest that a high osmotic concentration irrespective of the source was resulting in a decrease in cytokine secretion and mRNA expression.

High osmolarity has been reported to interfere with secretory pathways blocking exocytosis from the endoplasmic reticulum and Golgi bodies to the cell surface in mammalian cell lines (Docherty and Snider 1991, Lee and Linstedt 1999, Wu, Zhao et al. 2003). The presence of hypertonic solutions has previously been observed to inhibit cellular mRNA transcription and protein expression (Robbins, Pederson et al. 1970, Petronini, Tramacere et al. 1986). The observed inhibition of monocyte cytokine secretion and mRNA expression in response to increased osmotic sugar concentration has also been observed in a study by Qiu, Campbell et al. (2002). The authors examined the effect increased concentrations of potassium ions had on monocyte cytokine response. To control for

osmotic concentration the monocytes were treated with the sugar, sucrose. Treatment with 30mM, 60mM and 90mM sucrose inhibited LPS-induced mRNA production and TNFα secretion in a dose-dependent manner with 90mM sucrose resulting in complete inhibition of TNFα secretion. The increased presence of inert osmolytes such as mannitol or xylitol has been found to reduce inflammatory response in several studies (Cuschieri, Gourlay et al. 2002, Suganuma, Miwa et al. 2010, Xiong, Wang et al. 2010). Rabbit macrophages pre-conditioned with either mannitol or NaCl at concentrations ranging from 40mM – 100mM for a period of 4 hours prior to the addition of LPS resulted in decreased secretion of TNFα (Cuschieri, Gourlay et al. 2002). The authors reported the increased osmotic concentration resulted in cell shrinkage leading to the inhibition of polymerisation of stress fibres in response to stimulation with LPS. The authors reported macrophage cell shrinkage in response to the hyperosmotic environment which resulted in decreased polymerisation of stress response fibres and decreased phosphorylation of extracellular signal-related kinase (ERK1/2) in response to LPS treatment. This response is consistent with in vitro models of endotoxin tolerance (Kraatz, Clair et al. 1999). The hyperosmotic environment had no effect on macrophage TNFα secretion after a 20 hour incubation period prior to treatment with LPS. This suggests that the cells adapt to the hyperosmotic environment restoring normal response to endotoxin. This may provide an explanation as to why examples in the literature of THP-1 monocytes treated with high concentrations of D-glucose over a longer time course result in increased secretion of pro-inflammatory cytokines such as TNFα. This response also potentially explains the decrease in secretion of multiple cytokines by THP-1 monocytes treated with increased concentrations of D- or L-glucose prior to LPS stimulation reported within this chapter.

These previous findings are supported by the work presented here which has shown that increasing D-glucose at a constant 50mOsM (from addition of L-glucose) resulted in increased secretion of the inflammatory cytokine TNFα from 50mM D-glucose relative to 5mM or 20mM D-glucose (with 45mM and 30mM L-glucose respectively). This suggests that high concentrations of D-glucose may stimulate secretion of the inflammatory cytokine TNFα over 24 hours when osmolarity effects are discounted.

To understand the biochemical mechanism that underpins the changes in cytokine mRNA expression, THP-1 monocytes treated with high concentrations of D-glucose over a 6 hour period were studied. Monocytes showed a decrease in the NAD^+:NADH ratio relative to cells treated with 5mM D-glucose or 5mM D-glucose with 45mM L-glucose. This result fits within the current literature where hyperglycaemic conditions have previously been observed to reduce the NAD^+:NADH ratio in a variety of different cell types, including monocytes (Travis, Morrison et al. 1971, Guha, Bai et al. 2000, Nyengaard, Ido et al. 2004, Fulco, Cen et al. 2008). A decrease in the NAD^+:NADH ratio in

response to treatment with high glucose was also seen as acutely as 2 hours in rat retinal cells (Nyengaard, Ido et al. 2004). Increased availability of glucose results in a greater amounts of glucose being shuttled through the polyol pathway to produce sorbitol and fructose (Travis, Morrison et al. 1971, Sango, Suzuki et al. 2006). This process results in cytosolic NAD^+ being reduced to NADH resulting in a decreased availability of available cytosolic NAD^+. The polyol pathway is dependent on the activity of the enzyme aldose reductase; the contribution of glucose entering the polyol pathway towards the observed results could be tested in the future through treating cells with aldose reductase inhibitors.

Here, THP-1 monocytes treated with increased concentrations of D-glucose over a 6 hour period exhibited a significant decrease in SIRT1 deacetylase activity relative to cells treated with 5mM D-glucose or 5mM D-glucose with 45mM L-glucose. These findings support other studies which have shown general histone deacetylase protein including SIRT1's deacetylase activities in response to hyperglycaemic conditions in a number of cell types. Yun, Jialal et al. (2011) observed a general decrease in total HDAC activity in THP-1 monocytes treated with high glucose over a 72 hour period. Zheng, Chen et al. (2012) and Mortuza, Chen et al. (2013) also observed a decrease in SIRT1 deacetylase activity in high glucose-treated endothelial cells over a longer time course of 3 weeks with 11 cellular passages. The decrease in SIRT1 deacetylase activity reported in this chapter occurred independent of changes in mRNA expression although protein translation of SIRT1 was not assessed, this could be examined in the future by western blot. A recent study by Ceolotto, De Kreutzenberg et al. (2014) reported that SIRT1 mRNA is stabilised for translation by the RNA binding protein HuR. The authors observed that participants exhibiting metabolic syndrome had significantly reduced binding of HuR to SIRT1 mRNA reducing mRNA stability and translation to protein. Decreased SIRT1 mRNA stability in response to high glucose could also represent a mechanism through which SIRT1 deacetylase activity is impaired. Studies assessing the effects of decreased SIRT1 deacetylase activity by pharmacological inhibition have described a number of adverse effects. Mortuza, Chen et al. (2013) reported a decrease in SIRT1 deacetylase to directly correlate with increased cellular senescence. In contrast, increased SIRT1 activity has also been shown to improve insulin sensitivity (Sun, Zhang et al. 2007) and decrease inflammatory response (Yoshizaki, Milne et al. 2009, Yang, Zhang et al. 2012). Inhibition of SIRT1 deacetylase activity results in increased acetylation of the NF-κB P65 subunit at lysine 310, leading to increased NF-κB-DNA binding and subsequently increased transcription of NF-κB regulated genes (Breitenstein, Stein et al. 2011).

In the present study, THP-1 monocytes treated with increased concentrations of D-glucose over a 6 hour period showed a significant increase in the ratio of acetylated P65 (K310) to total P65 relative to

monocytes treated with either 5mM D-glucose or 5mM D-glucose with 45mM L-glucose. These results support the current literature where a number of studies have observed increased P65 acetylation at lysine 310 in response to high concentrations of glucose. Kim, Kim et al. (2012), Kim, Lee et al. (2014) and Yun, Jialal et al. (2011) studied THP-1 monocytes over either a 48 or 72 hour period; within the present study, changes were observed within 6 hours, earlier than has previously been documented in the literature. Acetylation of P65 at lysine 310 has been shown to be an important regulator of NF-κB transcriptional activity; mutation of P65 lysine 310 to an arginine residue was observed to significantly reduce NF-κB transcriptional activity using luciferase assays (Chen, Mu et al. 2002). Acetylation of P65 at lysine 310 prevents methylation of lysine residues 314 and 315, a post translational modification that is required for the ubiquitination and degradation of DNA bound P65 (Yang, Huang et al. 2009, Yang, Tajkhorshid et al. 2010). According to the literature, the consequence of increased P65 acetylation appears to be increased and prolonged transcription of NF-κB regulated genes.

4.5.1 Strengths and limitations

A limitation of the results presented within this chapter is that the research was carried using the THP-1 monocytic leukaemia cell line rather than with primary human monocytes which may limit the applicability of the results to in vivo human monocytes. The use of the THP-1 monocyte cell line was chosen due to its wide use in numerous research studies as a model of monocyte function and due to the ease at which they are grown. The THP-1 cell line also provides easy access to large numbers of cells without which some of the experiments performed within this chapter would not have been possible. The THP-1 monocytes were routinely grown in RPMI media containing 11mM D-glucose as is recommended by the American Tissue Culture Collection (ATCC) and the ECACC. However, this concentration is much higher than the 5mM D-glucose used as the low glucose treatment, and the concentration observed in healthy non-diabetic individuals. This could have resulted in the THP-1 monocytes having an adaption to high concentrations of glucose prior to the treatment thereby perhaps limiting the responses observed.

The THP-1 monocytes also appeared to be very susceptible to the osmotic stress of the 50mOsm treatments (50mM D-glucose, 5mM D-glucose with 45mM L-glucose). This was observed by the apparent decreased cytokine response of the 50mM D-glucose and 5mM D-glucose with 45mM L-glucose treated THP-1 monocytes in response to LPS stimulation. This response to high osmolarity has been previously observed to inhibit cytokine response to LPS stimulation in rabbit macrophages (Cuschieri, Gourlay et al. 2002). Although a number of the results observed within this chapter did

occur independently of the osmolality control (5mM D-glucose, 45mM L-glucose) the validity of some of these results may be questioned due to the observed effects of high osmolarity on the cells.

The main strength of the results within this chapter are that a number of the changes observed in response to treatment with high concentrations of D-glucose are occurring over a much shorter time period than has previously been assessed within the literature.

5   Identifying mechanisms of inflammation during metabolic disturbances in primary human monocytes

5.1.1   Preface

Following on from the previous chapter, the aims of the research presented in this chapter were to investigate whether an acute treatment with high concentrations of glucose would induce an inflammatory response in primary human monocytes and whether the response would be comparable to treated THP-1 monocytes. The primary monocytes were collected from healthy participants and treated with up to 50mM D-glucose over a 6 or 28 hour period. High glucose induced cytokine secretion in the absence and presence of LPS was assessed and possible mechanisms of induced inflammatory response assessed.

5.2   Introduction

Immortalised leukemic monocytic cell lines such as the THP-1 and U937 cell lines have frequently been used to study metabolic and inflammatory diseases. However a number of studies have identified profound differences in inflammatory response and metabolic activity between immortalised leukemic cell lines and primary human cells. The use of monocytic cell lines has many advantages over primary human monocytes such as decreased variability due to a homogeneous genetic background (Rogers, Thornton et al. 2003), and relative ease of use; however these cell lines are derived from leukaemias, are highly proliferative and may behave differently to increased nutrient availability and inflammatory stimuli than primary human monocytes. These cell lines also represent relatively immature cells of the monocyte lineage, and have been shown to express a number of markers of monocyte immaturity not found on the cell surface of mature peripheral blood monocytes (Abrink, Gobl et al. 1994).

A number of studies have observed monocytic cell lines to be less responsive to inflammatory stimuli such as LPS than primary human monocytes. A study by Baek, Haas et al. (2009) reported U937 monocytes had lower basal expression of TNFα mRNA than primary human monocytes. The authors also identified the involvement of a number of novel genes in U937 cellular inflammation and differentiation not present in primary monocytes. A study by Schildberger, Rossmanith et al. (2013) reported that LPS stimulation of THP-1 and primary monocytes resulted in very different cytokine secretion profiles. The authors observed the LPS treated primary monocytes to secrete high levels of TNFα, IL-6 and IL-8 whereas the treated THP-1 monocytes secreted significantly less TNFα and IL-8

and did not secret detectable quantities of IL-6. Both THP-1 and U937 monocytes treated with trans-retinoic acid displayed increased expression of the integrins, CD11a/b/c, and CD18 whereas expression in treated primary monocytes decreased (Babina and Henz 2003). The authors suggest that this response may be due to considerable differences in the regulation of expression of these integrins between the cell lines and primary blood monocytes.

A number of leukaemias and cancers are highly proliferative and have been shown to have increased rates of metabolic activity and glycolysis (Gatenby and Gillies 2004, Herst, Howman et al. 2011). The THP-1 monocytes are highly proliferative and will therefore likely have a higher metabolic rate than mature non-proliferative primary human monocytes which could result in them having an altered response to high concentrations of D-glucose.

5.2.1   Aims and objectives
The aims of the research presented in this chapter were to assess the effect of acute exposure to high concentrations of glucose on primary monocyte inflammatory response; whether primary human monocytes treated with high concentrations of glucose would responds in similar ways to leukemic THP-1 monocytes.

The objectives were to identify whether treatment with high concentrations of D-glucose would modulate cytokine response alone or with co-treatment with LPS; to identify potential mechanisms through which high glucose may lead to induction of an inflammatory response and to compare responses observed in treated primary monocytes with THP-1 monocytes to determine differences in response

5.3 Methods

5.3.1 Collection of blood from participants

Whole blood was collected by venepuncture using 21 gauge butterfly needles from the antecubital vein of healthy volunteers. The blood was collected into potassium EDTA coated evacuated collection tubes; after collection the tubes were inverted repeatedly to ensure mixture of the EDTA. Study participants were fasted prior to blood collection to give accurate measurements of blood glucose, total cholesterol, HDL cholesterol and triglycerides using a Reflotron clinical analyser (Roche, UK). LDL cholesterol was subsequently determined using the Friedwald formula (Friedewald, Levy et al. 1972). Ethical approval for the study was granted by the Aston University Ethics Committee.

Table 5.1: Participant information

	Participants
Average Age	36.1 ± 13.42
Sex	M=5, F=4
Average resting glucose (mmol/L) ± SD	5.18 ± 0.67
Average Total cholesterol (mmol/L) ± SD	4.14 ± 0.97
Average total HDL cholesterol (mmol/L) ± SD	1.06 ± 0.39
Average total LDL cholesterol (mmol/L) ± SD	2.88 ± 0.76

5.3.2 Treatment of primary monocytes with increased concentrations of glucose prior to inflammatory stimulation

Primary monocytes were negatively isolated as previously described (methods chapter, section; 2.13) from whole blood taken from healthy participants. Their age and lipids profiles are described in Table 5.1. After isolation, the primary monocytes were pelleted by centrifugation at 350xg for 8 minutes and washed in a glucose free RPMI media previously supplemented with 10% FCS and 1% penicillin/streptomycin solution. The cells were counted by trypan blue staining and pelleted in again by centrifugation and re-suspended in fresh glucose-free RPMI media at a cell density of 5×10^5 cells/ml. Cells were transferred (100µl) to 96 well cell culture plates and subsequently treated with glucose stock solutions to give a final glucose concentration of either 5mM D-glucose, 50mM D-glucose or 5mM D-glucose with 45mM L-glucose. The final cell density was 2.5×10^5 cells/ml.

The concentration of LPS required to elicit the desired TNFα cytokine response was determined by treating primary monocytes incubated with 5mM D-glucose with concentrations of LPS ranging from 0 – 1µg/ml. A concentration of 250ng/ml was determined to induce the desired TNFα cytokine response.

Primary monocytes treated with the aforementioned glucose concentrations were incubated for 4 hours at 37°C prior to the addition of LPS (serotype- 0111:B4) at 250ng/ml. The cells were again incubated at 37°C for a further 2 or 24 hours after which supernatants, lysates and RNA were taken for analysis.
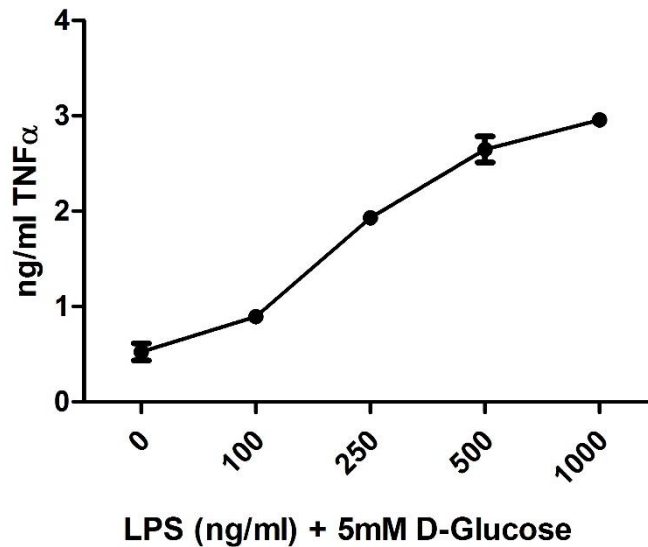
Figure 5.3.2: Optimisation of LPS concentration for the treatment of primary monocytes

Human primary monocytes were isolated from whole blood taken by venepuncture from healthy volunteers. The primary monocytes were treated ex vivo with 5mM D-glucose for 4 hours prior to the addition of LPS at concentrations ranging from 0ng/ml up to 1μg/ml. The treatments were incubated for a further 24 hours. Subsequent to treatment the supernatants were collected and TNFα (ng/ml) content was measured by ELISA. n=2.

5.3.3   Statistical analysis

The data reported within this chapter has been expressed as the mean± the standard error of the mean (SEM) of a minimum of three independent experiments. The data was collated using Graphpad software and statistically analysed by one-way analysis of variance (ANOVA) followed by Dunnett's post-test comparing treatments against 5mM D-glucose treated cells. The significance is reported where the p-value is less than 0.05 denoted by *, >0.01 denoted by ** and >0.001 denoted by ***.

5.4   Results

5.4.1   Treatment of whole blood with 50mM D-glucose and LPS (1µg/ml) over a 28 hour period results in increased TNFα secretion

Supplementation of whole blood over a 6 hour period with either 20mM or 50mM D-glucose had no significant effect on LPS-negative TNFα secretion relative to the 5mM D-glucose treated cells. Treatment of whole blood *ex vivo* with 500ng/ml LPS resulted in an increase in the TNFα content of plasma after 6 hours compared to LPS-negative treated cells although treatment with 20mM or 50mM D-glucose had no effect on LPS (500ng/ml)-induced secretion of TNFα. Treatment of whole blood over a 6 hour period with either 5mM D-glucose or 20mM D-glucose and 1µg/ml LPS did not result in any further increase in TNFα secretion compared to cells treated with 500ng/ml LPS. At this higher LPS concentration the addition of 50mM D-glucose appears to result in a slight increase in the mean TNFα secretion relative to 5mM D-glucose-treated cells although this increase was not large enough to be statistically significant.

Treatment of whole blood over a 28 hour period with 20mM or 50mM D-glucose had no effect on LPS-negative secretion of TNFα relative to 5mM D-glucose treated cells. Whole blood treated with 5mM or 20mM D-glucose and then stimulated with 500ng/ml of LPS did not display any change in TNFα secretion after a 28 hour period compared to the LPS-negative glucose-treated whole blood. Treatment of whole blood with 50mM D-glucose and stimulated with 500ng/ml LPS appeared to result in an increase in mean TNFα secretion compared to 5mM or 20mM cells treated with the same concentration of LPS, although this difference was not statistically significant so may be occurring due to chance. Stimulation of 5mM, 20mM and 50mM D-glucose treated whole blood with 1µg/ml LPS resulted in an increase in TNFα secretion over LPS-negative treated cells. Treatment of whole blood with 50mM D-glucose resulted in a significant increase ($p<0.01$) in TNFα secretion compared to 5mM and 20mM D-glucose treated cells when stimulated with LPS at 1µg/ml.
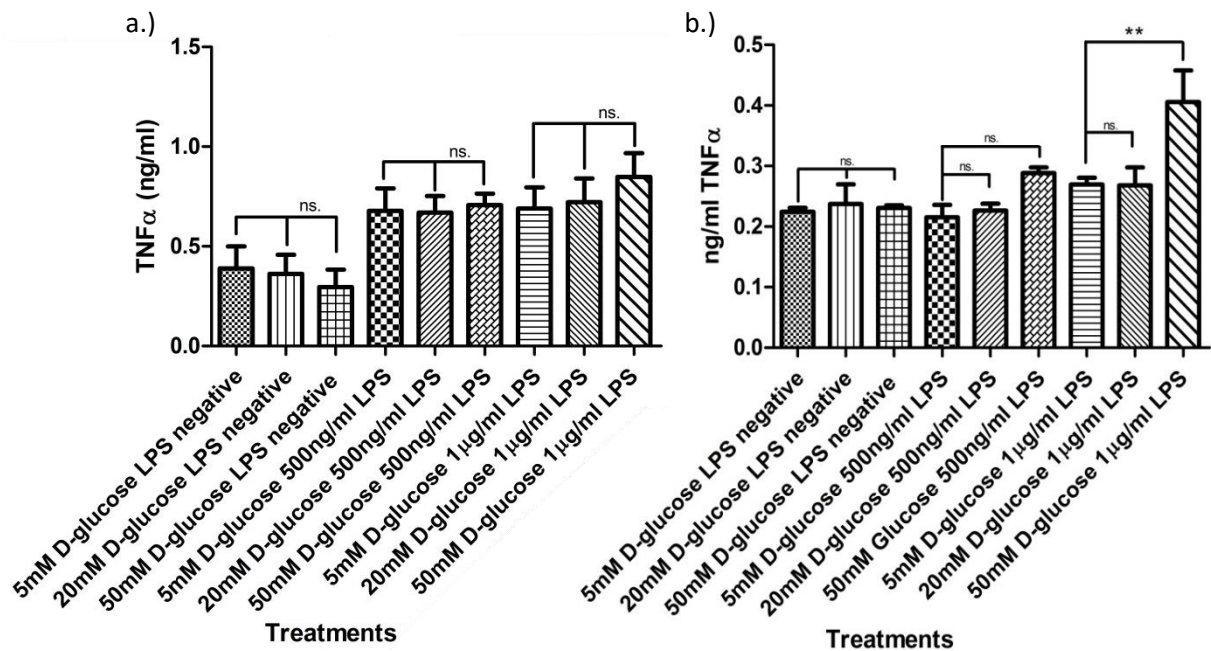
Figure 5.4.1: Treatment of whole blood with 50mM D-glucose results in increased TNFα secretion in response to stimulation with LPS at 1µg/ml over a 28 hour period.

Whole blood collected by venepuncture from healthy volunteers was treated ex vivo with either 5mM D-glucose, 20mM D-glucose or 50mM D-glucose for a period of 4 hours prior to the addition of LPS at either 500ng/ml or 1µg/ml. Plasma was collected by centrifugation and TNFα content assessed 2 hours a.) or 24 hours b.) post LPS addition by ELISA. Results are the mean of 3 independent experiments (± the standard error of the mean). Significance was determined by ANOVA followed by Dunnett's post-test comparing treatments to the 5mM D-glucose treated whole blood, whereby (*), (**) and (***) represents $p<0.05$, $p<0.01$ and $p<0.001$ respectively.

5.4.2 Treatment of primary monocytes with increased concentrations of D-glucose had no effect on cellular viability

Primary monocytes were isolated from whole blood taken from healthy volunteers and subsequently treated with varying concentrations of glucose for 4 hours prior to addition of LPS (250µg/ml). The treated cells were incubated for a further 24 hours after which cellular viability was determined by trypan blue staining. This was to determine whether treatment with increased concentrations of glucose or the accompanying increase in osmotic concentration would have an adverse effect on cellular viability.

Glucose-treated primary monocytes were stained with trypan blue and the unstained (alive) and stained (dead) cells counted and expressed as a percentage of viable to dead cells (figure, 5.4.2, a.). Primary monocytes incubated with increased concentrations of glucose in the presence of LPS produced no change in the percentage of viable and dead cells. There was no change in the total number of primary monocytes after incubation with increased concentrations of glucose in the presence of LPS (figure, 5.4.2, b.).
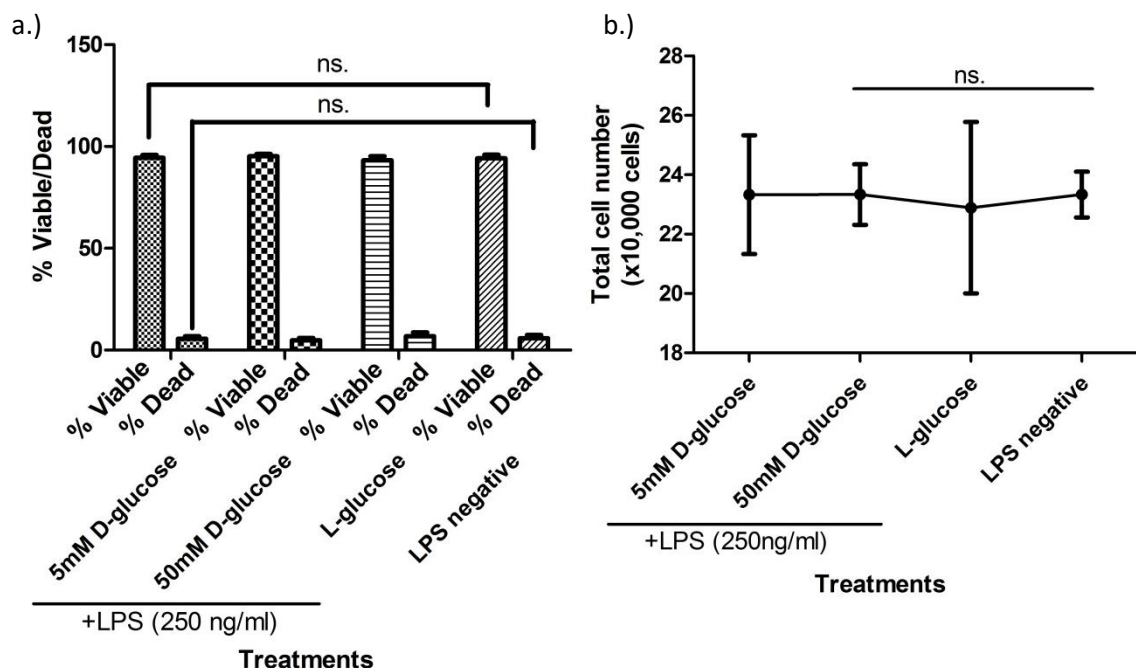
Figure 5.4.2: Treatment of primary monocytes with increased concentrations of D-glucose had no observable effect on cellular viability

Human primary monocytes were isolated from whole blood taken by venepuncture from healthy volunteers. The primary monocytes were treated ex vivo with either 5mM D-glucose, 50mM D-glucose or 5mM D-glucose with 45mM L-glucose for a period of 4 hours prior to the addition of LPS at 250ng/ml. The cells were incubated for a further 24 hours and cellular viability assessed by trypan blue staining. The results are expressed as a percentage of viable and dead cells a.) and as total cell number b.). Results are the mean of 3 independent experiments (± the standard error of the mean). Significance was determined by ANOVA followed by Dunnett's post-test comparing treatments to the 5mM D-glucose treated whole blood, whereby (*), (**) and (***) represents p<0.05, p<0.01 and p<0.001 respectively.

5.4.3 Primary monocytes treated with high concentrations of D-glucose sequestered an increased amount of glucose from the surrounding media

Glucose content of cell culture media after monocytes had been cultured for up to 28 hours was assessed using a glucose quantification assay purchased from Sigma; the final glucose measurement was subtracted from the initial value to determine the concentration of glucose removed by the cells from the media over the 28 hour period. This was investigated to determine whether primary monocytes incubated with a higher concentration of D-glucose would sequester more glucose from the media.

The results indicate that the treated primary monocytes incubated with 50mM D-glucose over a 28 hour period took up significantly more D-glucose over the time course compared to the 5mM treated and L-glucose-treated THP-1 monocytes.
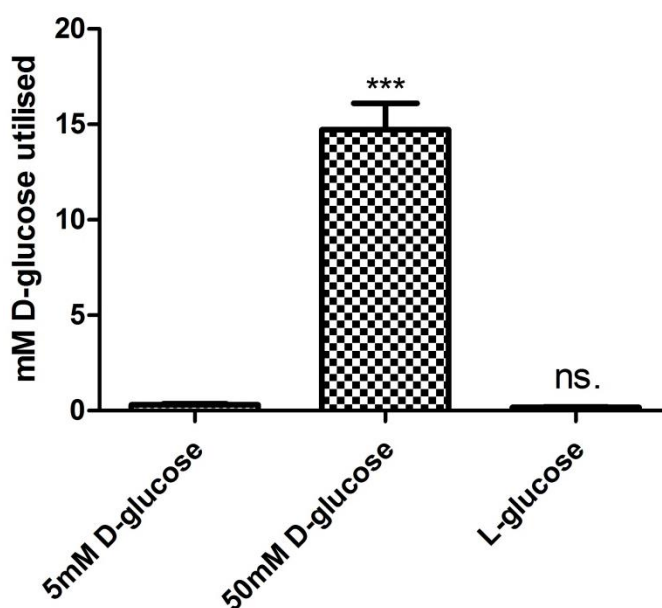
Figure 5.4.3: Treatment of primary monocytes with increased concentrations of D-glucose resulted in a significant increase in D-glucose removal from the media over a 28 hour period.

Human primary monocytes were isolated from whole blood taken by venepuncture from healthy volunteers. Glucose quantification assay performed on supernatants collected from primary monocytes treated with either 5mM D-glucose, 50mM D-glucose or 5mM D-glucose with 45mM L-glucose over a 28 hour period. Supernatants were collected at the start of the treatment and at the final time-point and the glucose concentration of these samples determined. Glucose utilisation from the media by the monocytes was calculated by subtracting the glucose concentration of the final time point from the concentration of the initial time point. Results are the mean of 3 independent experiments (± the standard error of the mean). Significance was determined by ANOVA followed by Dunnett's post-test comparing treatments to the 5mM D-glucose treated cells, whereby (*), (**) and (***) represents $p < 0.05$, $p < 0.01$ and $p < 0.001$ respectively.

5.4.4 Primary monocytes treated *ex vivo* with high concentrations of D-glucose and LPS increase TNFα secretion

LPS (1µg/ml) stimulation of whole blood presented in figure 5.4.1 subsequent to pre-treatment with 50mM D-glucose resulted in an increase in TNFα secretion compared to 5mM D-glucose pre-treated cells. Treatment of primary monocytes with glucose for 4 hours and LPS for a further 2 hours produced a trend to greater TNFα response upon LPS stimulation than pre-incubation with 5mM D-glucose. Treatment of the monocytes with 5mM D-glucose with 45mM L-glucose did not alter LPS-induced TNFα secretion compared to 5mM D-glucose treated cells. Primary monocytes incubated with 50mM D-glucose for 4 hours and LPS for a further 24 hours produced a significantly increased (p<0.01) TNFα response than 5mM D-glucose pre-treated primary monocytes. Treatment of primary monocytes with 5mM D-glucose with 45mM L-glucose did not alter LPS induced TNFα secretion compared to 5mM D-glucose treated cells after 28 hours. These results indicate that increased concentrations of D-glucose result in an increase in secretion of the pro-inflammatory cytokine TNFα upon LPS stimulation independent of the increased osmotic concentration.
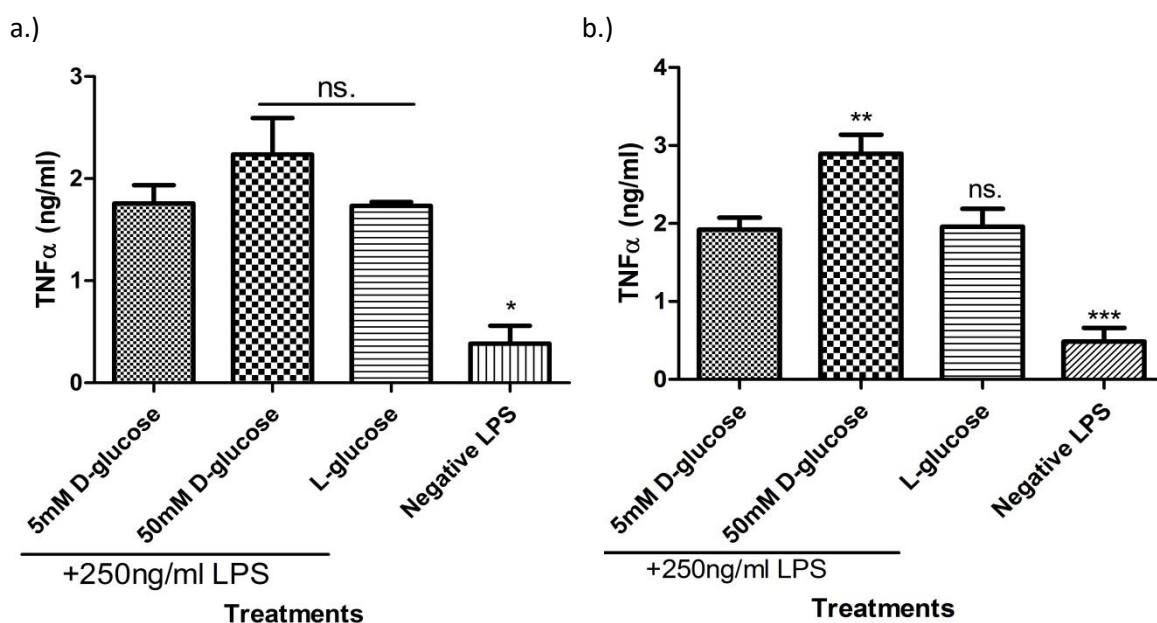
Figure 5.4.4: Treatment of primary monocytes with increased concentrations of D-glucose results in increased TNFα secretion in response to LPS stimulation

Human primary monocytes were isolated from whole blood taken by venepuncture from healthy volunteers. The primary monocytes were treated ex vivo with either 5mM D-glucose, 50mM D-glucose or 5mM D-glucose with 45mM L-glucose for a period of 4 hours prior to the addition of LPS at 250ng/ml. The negative LPS treatment group were treated with 5mM D-glucose without LPS for the duration of the treatment. Supernatants were collected and TNFα content assessed at either 2 hours a.) or 24 hours b.) post LPS addition by ELISA. Results are the means of n=3 and n=7 independent experiments respectively (± the standard error of the mean). Significance was determined by ANOVA followed by Dunnett's post-test comparing treatments to the 5mM D-glucose treated cells, whereby (*), (**) and (***) represents p<0.05, p<0.01 and p<0.001 respectively.

5.4.5 Primary monocytes treated *ex vivo* with 50mM D-glucose expressed increased levels of TNFα mRNA upon LPS stimulation

Primary monocytes were treated with high glucose ex vivo in order to determine any effect of glucose on LPS-induced inflammatory gene transcription. Treatment with 50mM D-glucose resulted in significant increases in TNFα mRNA transcription at both the 6 hour and 28 hour time points. After 6 hours with 50mM D-glucose, an approximate 1.8 fold increase ($p < 0.05$) in TNFα mRNA transcription was observed (Figure 5.4.5). At the 28 hour time point treatment with 50mM D-glucose resulted in an approximate 2.1 fold increase ($p < 0.05$) in TNFα mRNA transcription. At both times, 5mM D-glucose and 45mM L-glucose had no significant effect on TNFα mRNA transcription. This suggests that the changes induced by treatment with 50mM D-glucose are independent of increases in osmotic concentration. THP-1 monocytes treated with glucose and LPS over the 6 hour period displayed increased TNFα mRNA expression relative to the 5mM D-glucose negative LPS treated cells. THP-1 monocytes treated with either 5mM D-glucose or 5mM D-glucose with 45mM L-glucose displayed similar levels of TNFα mRNA expression to the 5mM D-glucose negative LPS treated cells. This indicates that in these treatments the LPS induced increase in TNFα mRNA transcription has returned to basal levels by 28 hours. However, the monocytes treated with 50mM D-glucose still have elevated TNFα mRNA expression indicating the high glucose is prolonging the inflammatory response.
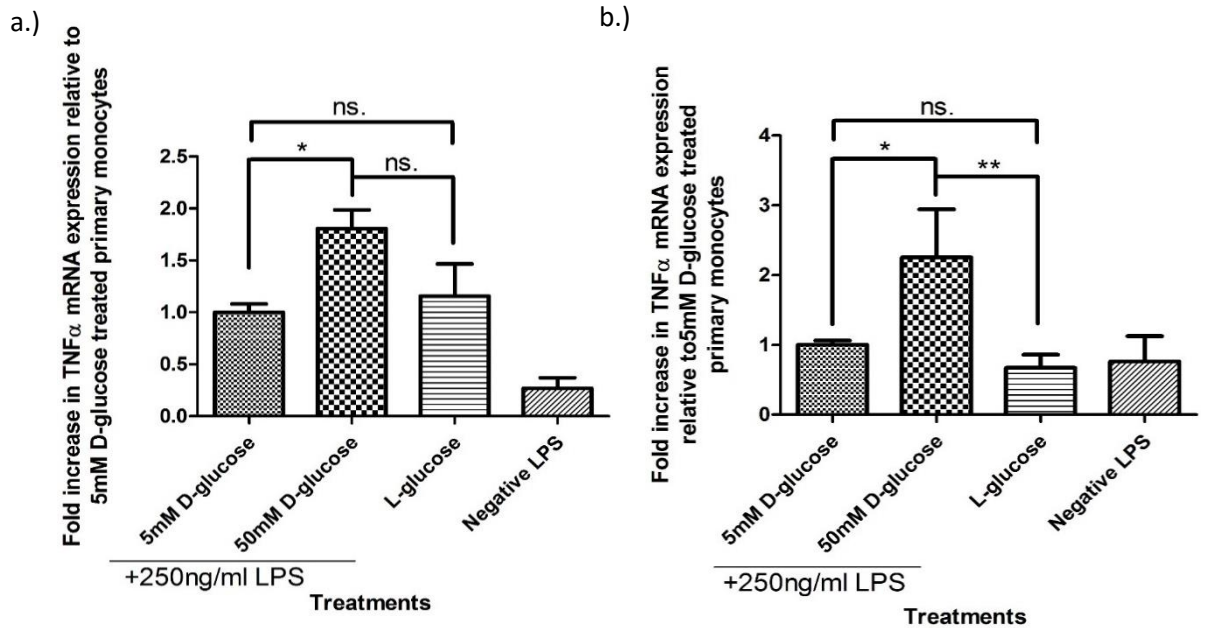
Figure 5.4.5: Primary monocytes treated with increased concentrations of D-glucose resulted in increased expression of TNFα mRNA in response to LPS stimulation

Human primary monocytes were isolated from whole blood taken by venepuncture from healthy volunteers. The primary monocytes were treated with 5mM D-glucose, 50mM D-glucose and 5mM D-glucose with 45mM L-glucose for 4 hours prior to the addition of LPS. The negative LPS treatment group were treated with 5mM D-glucose without LPS for the duration of the treatment. The monocytes were harvested by centrifugation, washed with PBS and lysed in Trizol reagent at 2 hours a.) and 24 hours b.) post LPS addition. The total RNA was extracted using Qiagen RNA extraction spin columns and the RNA quantity and quality assessed by nanodrop. The extracted RNA was reverse transcribed to cDNA and TNFα mRNA expression assessed by qPCR at the 2 hour a.) and 24 hour b.) post LPS addition time points. The ribosomal RNA 18S was used as a housekeeper gene. The results were analysed using the ΔΔCT method, whereby the results are expressed as a fold change (± standard error of the ΔCT) relative to the 5mM D-glucose treated monocytes. The results are the mean of 3 and 4 independent experiments respectively (± the standard error of the mean). Significance was determined by ANOVA followed by Dunnett's post-test comparing treatments to the 5mM D-glucose treated cells and the 5mM D-glucose and 45mM L-glucose treated cells, whereby (*), (**) and (***) represents p<0.05, p<0.01 and p<0.001 respectively.

5.4.6 Primary monocytes treated with increased concentrations of D-glucose over 24 hours resulted in a decrease in the intracellular NAD$^+$:NADH ratio

The ratio of NAD$^+$:NADH was assessed in order to determine whether treatment with increased concentrations of glucose would alter the intracellular NAD$^+$:NADH ratio in treated primary monocytes. This was to determine whether primary monocytes treated with high concentrations of glucose would display a decreased intracellular NAD$^+$: NADH ratio as was previously observed in treated THP-1 monocytes. Primary monocytes treated with 50mM D-glucose over a 24 hour period resulted in a significant decrease in the NAD$^+$: NADH ratio relative to monocytes treated with either 5mM D-glucose or 5mM D-glucose with 45mM L-glucose.
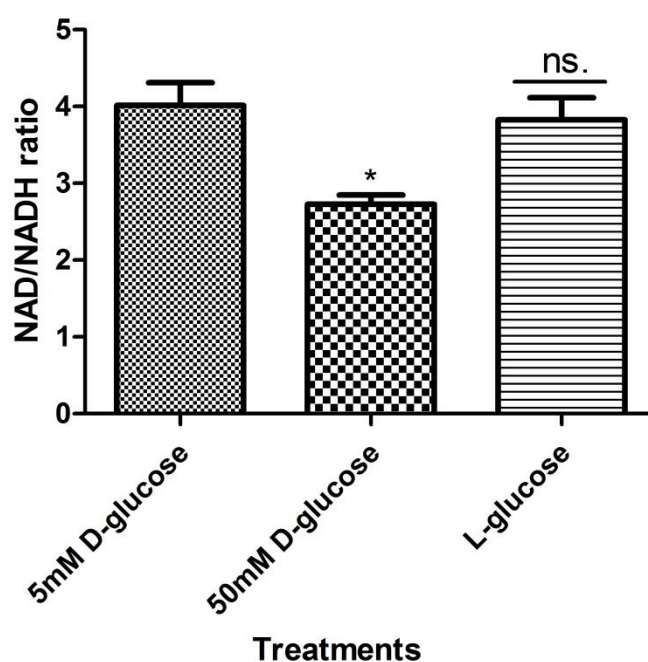
Figure 5.4.6: Treatment of primary monocytes with high concentrations of D-glucose over a 28 hour period results in a decrease in the NAD$^+$:NADH ratio

Human primary monocytes were isolated from whole blood taken by venepuncture from healthy volunteers. The primary monocytes were treated *ex vivo* with either 5mM D-glucose, 50mM D-glucose and 5mM D-glucose with 45mM L-glucose for a period of 28 hours. Subsequent to treatment the ratio of NAD$^+$: NADH was measured using a NAD$^+$: NADH quantification assay purchased from Abcam. The results are the mean of 3 independent experiments respectively (± the standard error of the mean). Significance was determined by ANOVA followed by Dunnett's post-test comparing treatments to the 5mM D-glucose treated cells, whereby (*), (**) and (***) represents $p < 0.05$, $p < 0.01$ and $p < 0.001$ respectively.

5.4.7 Treatment of primary monocytes with increased concentrations of D-glucose over a 28 hour period had no effect on SIRT1 mRNA expression

Expression of the SIRT1 gene was studied in the presence of high glucose in monocytes, as SIRT1 activity links metabolism and inflammation through altered acetylation. Treatment of primary monocytes with high concentrations of glucose and LPS over a 28 hour period produced no observable change in SIRT1 mRNA expression in the presence of LPS. Treatment with LPS alone at 5mM glucose appeared to result in a slight increase in SIRT1 mRNA expression.
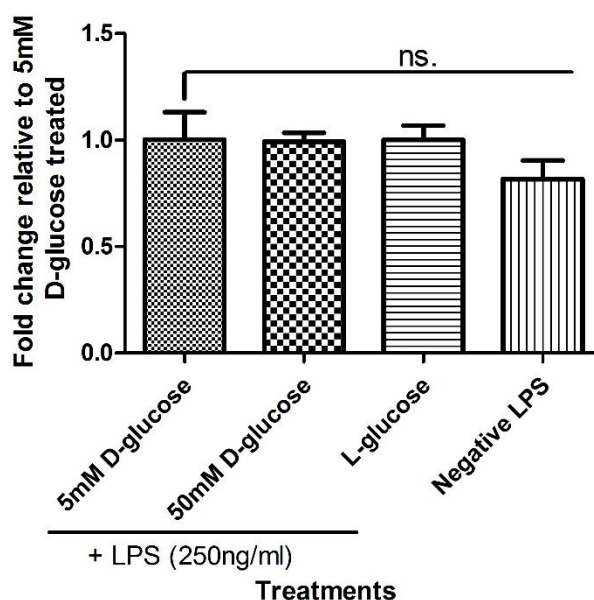
Figure 5.4.7: Treatment of primary monocytes with increased concentrations of D-glucose had no effect on SIRT1 mRNA expression

Human primary monocytes were isolated from whole blood taken by venepuncture from healthy volunteers. The primary monocytes were treated ex vivo with either 5mM D-glucose, 50mM D-glucose and 5mM D-glucose with 45mM L-glucose for 4 hours prior to the addition of LPS (250ng/ml). The negative LPS treatment group were treated with 5mM D-glucose without LPS for the duration of the treatment. The monocytes were harvested by centrifugation, washed with PBS and lysed in Trizol reagent 24 hours post LPS addition. The total RNA was extracted using Qiagen RNA extraction spin columns and the RNA quantity and quality assessed by nanodrop. The extracted RNA was reverse transcribed to cDNA and SIRT1 mRNA expression assessed by qPCR at the 24 hour post LPS addition time point. The ribosomal RNA 18S was used as a housekeeper gene. The results were analysed using the ΔΔCT method, whereby the results are expressed as a fold change (± standard error of the ΔCT) relative to the 5mM D-glucose treated monocytes. The results are the mean of 3 independent experiments respectively (± the standard error of the mean). Significance was determined by ANOVA followed by Dunnett's post-test comparing treatments to the 5mM D-glucose treated cells, whereby (*), (**) and (***) represents $p < 0.05$, $p < 0.01$ and $p < 0.001$ respectively.

5.4.8 Treatment of primary monocytes with 50mM D-glucose resulted in altered secretion of many inflammatory cytokines as determined by Luminex assay

The isolated monocytes were treated with either 5mM D-glucose, 50mM D-glucose or 5mM D-glucose with 45mM L-glucose for 28 hours and the supernatants collected. Due to the observed increases in both TNFα secretion and TNFα mRNA production in 50mM D-glucose- treated primary monocytes compared to 5mM D-glucose- and L-glucose-treated cells (Figures 5.4.4 and 5.4.5), further multiplex analysis of cytokine secretion was performed. Due to the inherent variation between individuals, the results are presented as fold change relative to the 5mM D-glucose treated-cells. The secretion of a number of cytokines was changed when the primary monocytes were incubated with 50mM D-glucose compared to 5mM D-glucose or the L-glucose (5mM D-glucose, 45mM L-glucose) control for osmotic concentration; inflammatory cytokines such as IL-6, IL-8 and TNFα increased whereas secretion of the anti-inflammatory cytokine IL-10 was decreased. Although there is some difference observed in the L-glucose treatment group compared to the 5mM D-glucose treated cells it is not significant, suggesting that the changes in cytokine secretion are occurring independent of changes in osmotic concentration.
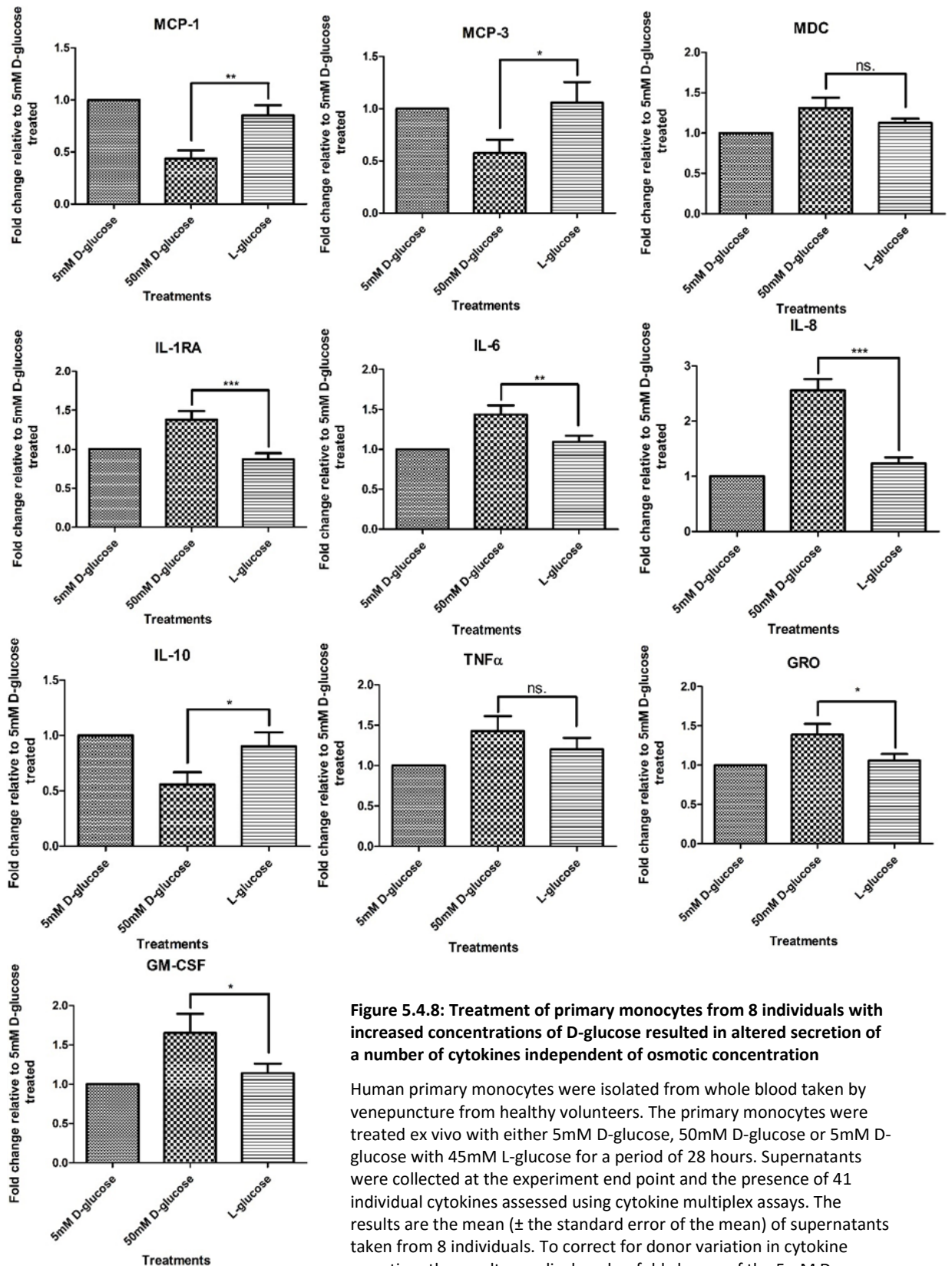
Figure 5.4.8: Treatment of primary monocytes from 8 individuals with increased concentrations of D-glucose resulted in altered secretion of a number of cytokines independent of osmotic concentration

Human primary monocytes were isolated from whole blood taken by venepuncture from healthy volunteers. The primary monocytes were treated ex vivo with either 5mM D-glucose, 50mM D-glucose or 5mM D-glucose with 45mM L-glucose for a period of 28 hours. Supernatants were collected at the experiment end point and the presence of 41 individual cytokines assessed using cytokine multiplex assays. The results are the mean (± the standard error of the mean) of supernatants taken from 8 individuals. To correct for donor variation in cytokine secretion, the results are displayed as fold change of the 5mM D-glucose treated values. Significance was determined by ANOVA followed by Dunnett's post-test comparing treatments to the 5mM D-glucose 45mM L-glucose treated monocytes, whereby (*), (**) and (***) represents $p < 0.05$, $p < 0.01$ and $p < 0.001$ respectively.

159

Table 5.2: Summary of multiplex (41-plex) cytokine assay of supernatants from primary monocytes treated with varying concentrations of glucose

Cytokine	Summary of change in cytokine secretion relative to 5mM D-glucose treated THP-1 monocytes	Cytokine	Summary of change in cytokine secretion relative to 5mM D-glucose treated THP-1 monocytes
EGF	Analyte concentration too low for detection	IL-10	Decrease secretion in response to 50mM D-glucose
Eotaxin	Analyte concentration too low for detection	IL-12(p40)	Analyte concentration too low for detection
FGF-2	Analyte concentration too low for detection	IL-12(p70)	Analyte concentration too low for detection
Flt-3L	Analyte concentration too low for detection	IL-13	Analyte concentration too low for detection
Fractalkine	Analyte concentration too low for detection	IL-15	Analyte concentration too low for detection
G-CSF	No change observed in response to treatment	IL-17	Analyte concentration too low for detection
GM-CSF	Increased secretion in response to 50mM D-glucose	IP-10	No change observed in response to treatment
GRO	Increased secretion in response to 50mM D-glucose	MCP-1	Decreased secretion in response to 50mM D-glucose
IFNα2	Increased secretion in response to 50mM D-glucose	MCP-3	Decreased secretion in response to 50mM D-glucose
IFN-γ	Analyte concentration too low for detection	MDC	No significant change in secretion
IL-1α	Analyte concentration too low for detection	MIP-1α	Analyte concentration too low for detection
IL-1β	Analyte concentration too low for detection	MIP-1β	Analyte concentration too low for detection
IL-1RA	Increased secretion in response to 50mM D-glucose	PDGF-AA	No change observed in response to treatment
IL-2	Analyte concentration too low for detection	PDGF-BB	No change observed in response to treatment
IL-3	Analyte concentration too low for detection	RANTES	No change observed in response to treatment
IL-4	Analyte concentration too low for detection	sCD40L	No change observed in response to treatment
IL-5	Analyte concentration too low for detection	TGFα	Analyte concentration too low for detection
IL-6	Increased secretion in response to 50mM D-glucose	TNFα	No significant change in secretion
IL-7	Analyte concentration too low for detection	TNFβ	Analyte concentration too low for detection
IL-8	Increased secretion in response to 50mM D-glucose	VEGF	No change observed in response to treatment
IL-9	Analyte concentration too low for detection		

5.4.9 Treatment of primary monocytes with 50mM D-glucose resulted in altered secretion of a number of LPS-induced cytokines as determined by Luminex assay

The secretion of a number of cytokines changed when the primary monocytes from 9 adults were incubated with 50mM D-glucose compared to 5mM D-glucose or the L-glucose (5mM D-glucose, 45mM L-glucose) osmolaric control and treated with LPS (250ng/ml). The secretion of inflammatory cytokines such as IL-6, IL-8 and TNFα increased whereas secretion of the anti-inflammatory and reparative cytokines IL-10 and TGFα was decreased. Due to the inherent variation between individuals, the results are presented as fold change relative to the 5mM D-glucose treated-cells. Although there is some difference observed in the L-glucose treatment group compared to the 5mM D-glucose treated cells it is not significant, suggesting that the changes in cytokine secretion are occurring independent of changes in osmolarity.
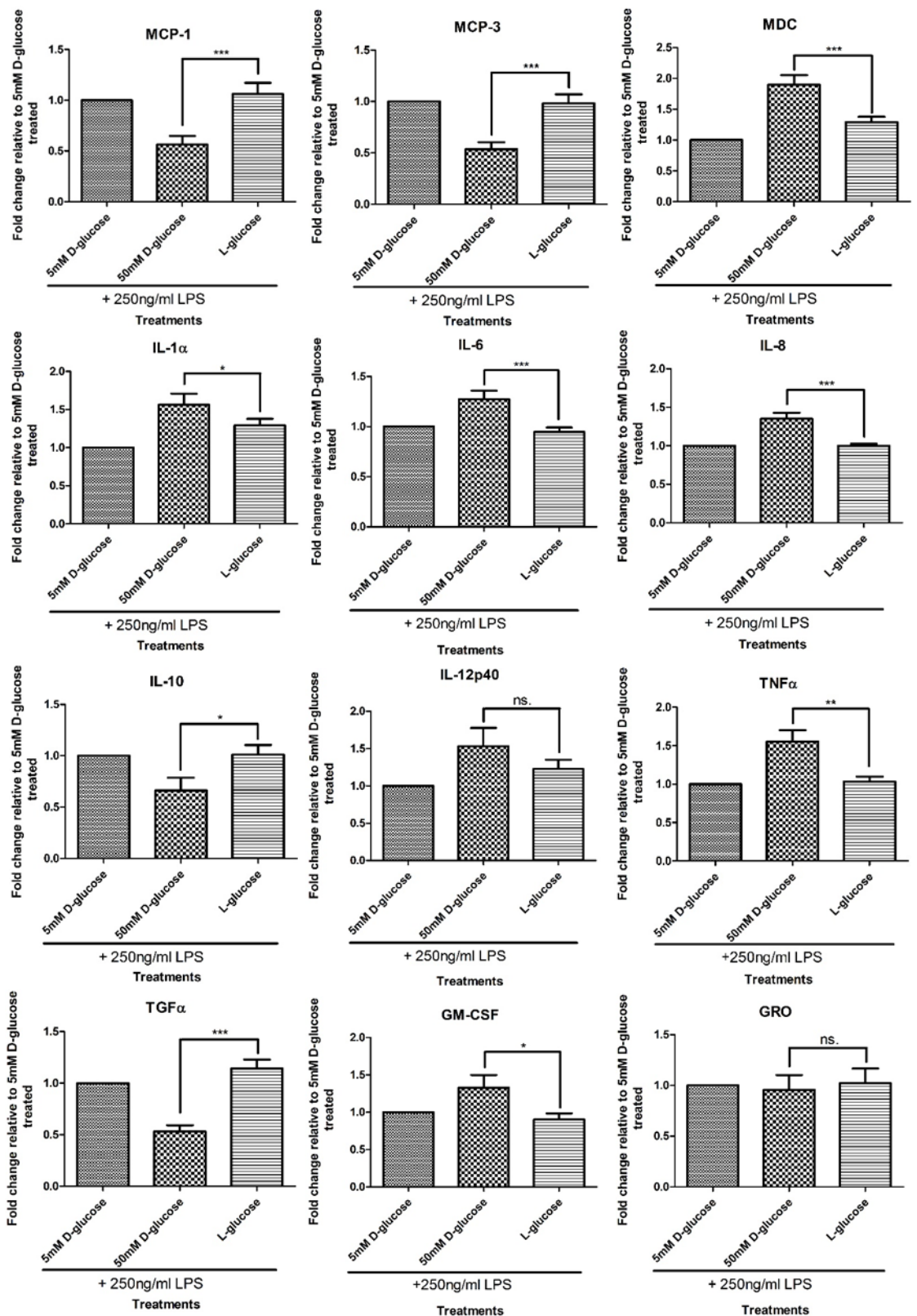
Figure 5.4.9: Treatment of primary monocytes, from 9 individuals with increased concentrations of D-glucose resulted in altered secretion of a number of cytokines in response to LPS stimulation

Human primary monocytes were isolated from whole blood taken by venepuncture from healthy volunteers. The primary monocytes were treated *ex vivo* with either 5mM D-glucose, 50mM D-glucose or 5mM D-glucose with 45mM L-glucose for a period of 4 hours prior to the addition of LPS at 250ng/ml. Supernatants were collected 24 hours post LPS addition and the presence of 41 individual cytokines assessed using cytokine multiplex assays. The results are the mean (± the standard error of the mean) of supernatants taken from 8 individuals. To correct for donor variation in cytokine secretion, the results are displayed as fold change of the 5mM D-glucose treated values. Significance was determined by ANOVA followed by Dunnett's post-test comparing treatments to the 5mM D-glucose, 45mM L-glucose treated monocytes, whereby (*), (**) and (***) represents $p<0.05$, $p<0.01$ and $p<0.001$ respectively.

Table 5.3: Summary table of multiplex (41-plex) cytokine assay of primary monocytes treated with varying concentrations of glucose with LPS

Cytokine	Summary of change in cytokine secretion relative to 5mM D-glucose treated THP-1 monocytes	Cytokine	Summary of change in cytokine secretion relative to 5mM D-glucose treated THP-1 monocytes
EGF	Analyte concentration too low for detection	IL-10	Decrease secretion in response to 50mM D-glucose
Eotaxin	Analyte concentration too low for detection	IL-12(p40)	Increased secretion in response to 50mM D-glucose
FGF-2	Analyte concentration too low for detection	IL-12(p70)	Analyte concentration too low for detection
Flt-3L	Analyte concentration too low for detection	IL-13	Analyte concentration too low for detection
Fractalkine	Analyte concentration too low for detection	IL-15	Analyte concentration too low for detection
G-CSF	No change observed in response to treatment	IL-17	Analyte concentration too low for detection
GM-CSF	Increased secretion in response to 50mM D-glucose	IP-10	No change observed in response to treatment
GRO	No change observed in response to treatment	MCP-1	Decreased secretion in response to 50mM D-glucose
IFNα2	Analyte concentration too low for detection	MCP-3	Decreased secretion in response to 50mM D-glucose
IFN-γ	Analyte concentration too low for detection	MDC	Increased secretion in response to 50mM D-glucose
IL-1α	Increased secretion in response to 50mM D-glucose	MIP-1α	No change observed in response to treatment
IL-1β	No change observed in response to treatment	MIP-1β	No change observed in response to treatment
IL-1RA	No change observed in response to treatment	PDGF-AA	No change observed in response to treatment
IL-2	Analyte concentration too low for detection	PDGF-BB	No change observed in response to treatment
IL-3	Analyte concentration too low for detection	RANTES	No change observed in response to treatment
IL-4	Analyte concentration too low for detection	sCD40L	No change observed in response to treatment
IL-5	Analyte concentration too low for detection	TGFα	Decreased secretion in response to 50mM D-glucose
IL-6	Increased secretion in response to 50mM D-glucose	TNFα	Increased secretion in response to 50mM D-glucose
IL-7	Analyte concentration too low for detection	TNFβ	Analyte concentration too low for detection
IL-8	Increased secretion in response to 50mM D-glucose	VEGF	No change observed in response to treatment
IL-9	Analyte concentration too low for detection		

5.4.10 Pathway analysis of multiplex cytokine assay results using Ingenuity Pathway Analysis software

The results of the multiplex cytokine assays shown in figures, 5.4.8 and 5.4.9 performed on supernatants from primary monocytes treated with 5mM D-glucose, 50mM D-glucose and 5mM D-glucose with 45mM L-glucose with or without the addition of LPS (250ng/ml) were uploaded into Ingenuity Pathway Analysis software. This was done in order to determine potential pathways or transcriptional regulators affected by the 50mM D-glucose treatment which may have resulted in the observed alteration in primary monocyte cytokine secretion. This allowed identification of potential targets for further investigation.

Tables 5.4 and 5.5 display the potential upstream regulators identified through pathway analysis of the changes in cytokine secretion in response to treatment with 50mM D-glucose in the absence and presence of LPS. The Ingenuity Pathway Analysis software identified a number of potential upstream regulators common in both tables such as the miRNAs 146a and 155, the secreted cytokine HMGB1 and the transcription factor NF-κB. This provided several potential targets for further investigation.

Table 5.4: Potential upstream regulators responsible for altered cytokine secretion observed in primary monocytes treated with high concentrations of glucose over a 28 hour period

Upstream regulator	Molecule type	p-value
mir-146a-5p	microRNA	3.32E-16
TRAF6	Enzyme	2.90E-15
CD14	Transmembrane receptor	3.27E-15
IL6R	Transmembrane receptor	1.56E-14
HMGB1	Transcription regulator	2.63E-14
CLEC7A	Transmembrane receptor	2.86E-14
NF-κB-RELA	Complex	3.65E-14
SPHK1	Kinase	2.18E-13
ERK1/2	Group	2.38E-13
SYK	Kinase	4.08E-13

Table 5.5: Potential upstream regulators responsible for altered cytokine secretion observed in primary monocytes treated with high concentrations of glucose and LPS over a 28 hour period

Upstream regulator	Molecule type	p-value
IL17a dimer	Complex	6.57E-19
CD14	Transmembrane receptor	3.27E-18
Lymphotoxin-α-1-β2	Complex	2.63E-17
NF-κB-RELA	Complex	8.81E-16
STAT3	Transcription regulator	1.79E-15
Ap1	Complex	2.90E-15
HMGB1	Transcription regulator	4.76E-15
RPSA	Transcription regulator	5.17E-15
miR-155-5p	microRNA	5.25E-15
miR-146a-5p	microRNA	2.02E-14

5.4.11 Treatment of primary monocytes with 50mM D-glucose resulted in altered secretion of HMGB1 over a 28 hour period

As HMGB1 may be an upstream regulator of glucose effects and is secreted by activated monocytes, the effect of high glucose on its secretion was studied. Primary monocytes treated with 50mM D-glucose over a 28 hour period without LPS (figure, 5.4.11 a.) showed a significant increase in HMGB1 secretion relative to 5mM D-glucose treated cells. Treatment of primary monocytes with 5mM D-glucose and 45mM L-glucose appeared to result in a slight increase in HMGB1 secretion relative to 5mM D-glucose, although this increase was not significant.

Primary monocytes treated with 50mM D-glucose in the presence of LPS (250ng/ml) over a 28 hour period (figure, 5.4.11 b.) showed a significant decrease in HMGB1 secretion relative to cells treated with 5mM D-glucose and LPS. When compared to the cells treated with 5mM D-glucose without LPS, treatment with 50mM D-glucose appears to reduce HMGB1 secretion to basal levels.
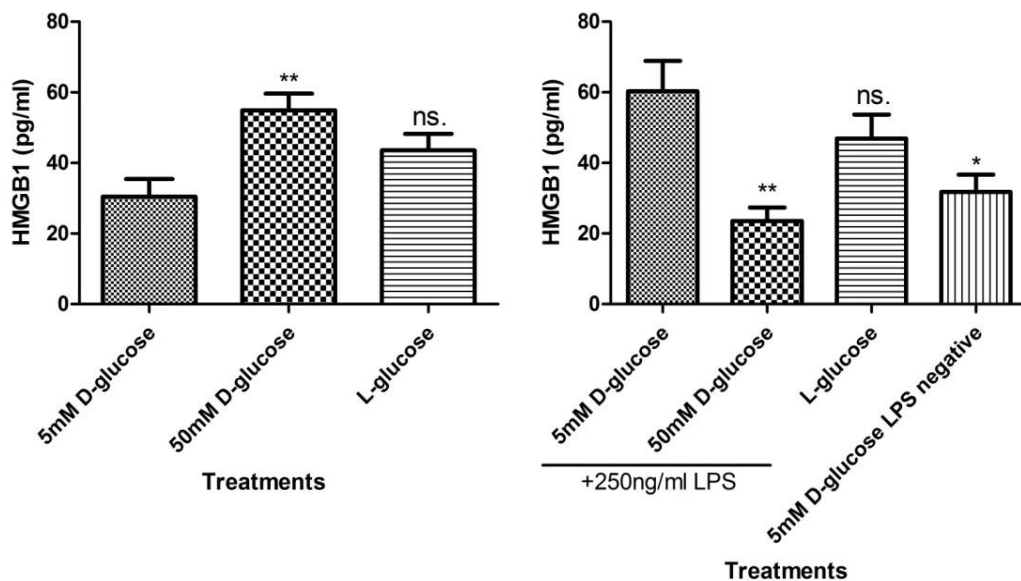
Figure 5.4.10: Treatment of primary monocytes with 50mM D-glucose alters HMGB1 secretion

Human primary monocytes were isolated from whole blood taken by venepuncture from healthy volunteers. Primary monocytes were treated ex vivo with either 5mM D-glucose, 50mM D-glucose or 5mM D-glucose with 45mM L-glucose for a period of 4 hours. The monocytes were incubated for a further 24 hours with or without the addition of LPS (250ng/ml). The supernatants were collected and HMGB1 secretion assessed by ELISA. The results are the mean (± the standard error of the mean) of supernatants taken from 5 and 7 individuals respectively. Significance was determined by ANOVA followed by Dunnett's post-test comparing treatments to the 5mM D-glucose treated monocytes, whereby (*), (**) and (***) represents $p < 0.05$, $p < 0.01$ and $p < 0.001$ respectively.

5.4.12 Treatment of primary monocytes with increased concentrations of D-glucose resulted in increased binding of acetylated P65 to the TNFα promoter region

Increased acetylated (K310) P65 was observed previously in high glucose treated THP-1 monocytes by western blot analysis. Treated primary monocytes were assessed for changes in P65 acetylation (K310) in order to confirm whether the same response would be observed. Due to limitations in cell number, assessment of acetylated (K310) P65 by immunoblot in treated primary monocytes proved insensitive. A chromatin immunoprecipitation method developed for use with low cell numbers, followed by quantitative PCR was used to assess the binding of acetylated P65 to the TNFα promoter region.

The chromatin sonication was performed using a Diagenode bioruptor. The sonication procedure was optimised to determine the number of sonication cycles necessary to achieve chromatin of between 200-500bps in length. Cells were sonicated for an increasing number of cycles, the DNA extracted by PCIA extraction and separated on agarose gels. A number of 10 sonication cycles (30 seconds on, 30 seconds off) was determined to produce chromatin of between 200-500bp in length.

Treatment of primary monocytes with 50mM D-glucose resulted in an increase in acetylated P65 (K310) binding to the TNFα promoter region relative to cells treated with either 5mM D-glucose or 5mM D- with 45mM L-glucose. Treatment of cells with 50mM D-glucose and LPS also resulted in an increase in binding of acetylated P65 to the TNFα promoter region. Glucose treatments to the primary monocytes with LPS resulted in an increase in acetylated P65 binding to the TNFα promoter relative to non-LPS, glucose-treated cells.

a.)

Number of sonication cycles

DNA ladder 0 2 4 6 8 10 12

1000bp
750bp
500bp
250bp

b.)

%input

ns.
ns.
ns.
ns.

0.25
0.20
0.15
0.10
0.05
0.00

5mM D-glucose
50mM D-glucose
L-glucose
5mM D-glucose
50mM D-glucose
L-glucose

+250ng/ml LPS
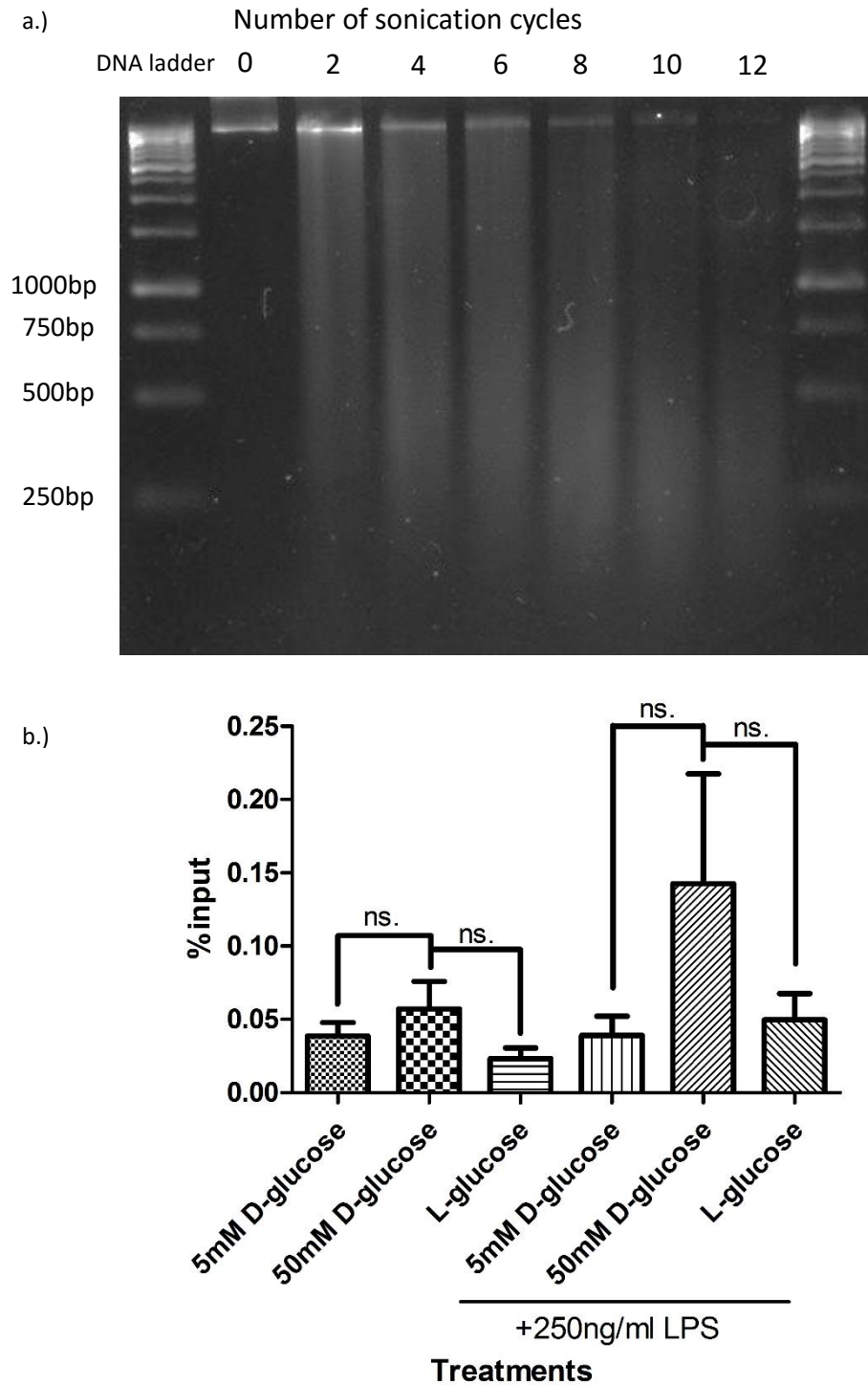
Treatments

Figure 5.4.9 Treatment of primary monocytes with 50mM D-glucose results in increased binding of acetylated P65 to the TNFα promoter region

Optimisation of DNA shearing by sonication, 1 x10^5 cells sheared by sonication, the DNA extracted and separated on 1% agarose gels stained with ethidium bromide a.). Primary monocytes were treated *ex vivo* with 5mM D-glucose, 50mM D-glucose and 5mM D-glucose with 45mM L-glucose for 4 hours. The cells were incubated for a further 2 hours with or without the addition of LPS (250ng/ml). The cells formaldehyde fixed, lysed and the DNA sheared by sonication. Acetylated P65 was immune-precipitated from the sheared DNA sample and the extracted DNA assessed for P65 binding region of the TNFα promoter by qPCR b.) Data is expressed as % of input (non-immuno-precipitated) sheared DNA samples. The data here represents the means (±SE) of 3 independent experiments. Significance was determined by ANOVA followed by Dunnett's post-test comparing treatments to the 5mM D-glucose treated monocytes, whereby (*), (**) and (***) represents p<0.05, p<0.01 and p<0.001 respectively.

5.4.13 Increased concentrations of D-glucose reduce the expression of miRNA 146a-5p in primary monocytes

Pathway analysis of the cytokine response to high concentrations of D-glucose both with and without the addition of LPS identified miR-146a-5p as potentially contributing to the response. For this reason, expression of miR-146a-5p in primary monocytes in the presence of high concentrations of D-glucose was assessed by qPCR.

Treatment of primary monocytes with 50mM D-glucose and LPS (250μg/ml) over a 6 hour period resulted in a significant decrease in the expression of miRNA 146a-5p relative to 5mM D-glucose treated cells. However, no observable change occurred in response to treatment with 5mM D-glucose with 45mM L-glucose relative to 5mM D-glucose treated cells, suggesting increased osmotic concentration had no effect on miRNA 146a-5p expression.

Treatment of primary monocytes with 50mM D-glucose or 5mM D-glucose with 45mM L-glucose and LPS (250ng/ml) over a 28 hour period produced no observable change in miRNA 146a-5p expression relative to 5mM D-glucose treated cells. This suggests that the expression of the miRNA 146a-5p in the presence of 50mM D-glucose has returned to basal levels after 28 hours.
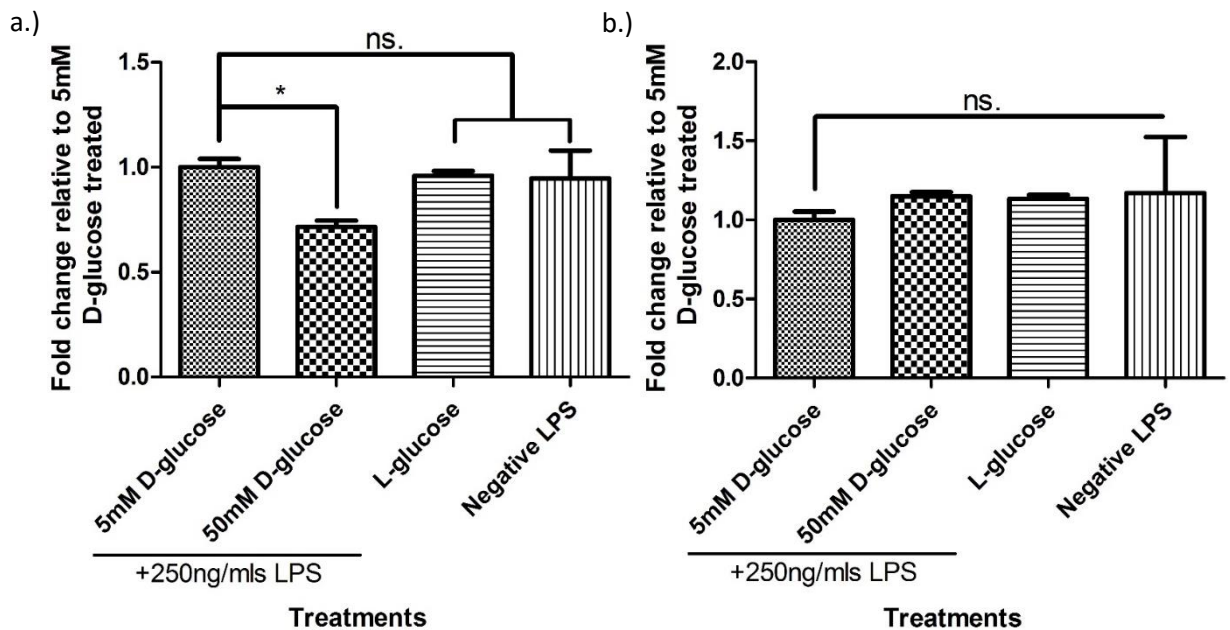
Figure 5.4.10: Treatment of primary monocytes with 50mM D-glucose over a 6 hour reduces expression of miR-146a-5p in the presence of LPS

Human primary monocytes were isolated from whole blood taken by venepuncture from healthy volunteers. The primary monocytes were treated with either 5mM D-glucose, 50mM D-glucose and 5mM D-glucose with 45mM L-glucose for 4 hours prior to the addition of LPS (250ng/ml). The negative LPS treatment group were treated with 5mM D-glucose without LPS for the duration of the treatment. The monocytes were harvested by centrifugation, washed with PBS and lysed in Trizol reagent at 2 hours a.) and 24 hours b.) post LPS addition. The total RNA was extracted using Qiagen RNA extraction spin columns and the RNA quantity and quality assessed by nanodrop. The extracted RNA was reverse transcribed and microRNA 146a-5p expression assessed by qPCR at the 2 hour a.) and 24 hour b.) post LPS addition time points. The microRNA miR-16 was used as a housekeeper gene. The results were analysed using the ΔΔCT method, whereby the results are expressed as a fold change (± standard error of the ΔCT) relative to the 5mM D-glucose treated monocytes. The results are the mean of 3 independent experiments respectively (± the standard error of the mean). Significance was determined by ANOVA followed by Dunnett's post-test comparing treatments to the 5mM D-glucose treated cells, whereby (*), (**) and (***) represents $p < 0.05$, $p < 0.01$ and $p < 0.001$ respectively.

5.4.14 Treatment with increased concentrations of D-glucose prevents LPS induction of miRNA 155-5p in primary monocytes

Pathway analysis of the cytokine response to high concentrations of D-glucose with and without addition of LPS both identified miR-155 as potentially contributing to the inflammatory response. For this reason, expression of miR-155 in response to high concentrations of D-glucose was assessed by qPCR.

Treatment of primary monocytes with 50mM D-glucose and LPS (250ng/ml) over a 6 hour period resulted in a decrease in the fold change expression of miRNA 155-5p relative to 5mM D-glucose and LPS treated cells, although this change was not statistically significant therefore cannot be confirmed to have occurred independent of chance. The expression of miR-155-5p in these 50mM D-glucose treated cells is approximately the same as the 5mM D-glucose negative LPS treatment group. This suggests that treatment with LPS resulted in increased expression of miR-155-5p in the 5mM D-glucose and 5mM D-glucose with 45mM L-glucose which treatment with 50mM D-glucose prevented.

Treatment of primary monocytes with 50mM D-glucose or 5mM D-glucose with 45mM L-glucose and LPS (250ng/ml) over a 28 hour period produced no observable change in miRNA 155-5p expression relative to 5mM D-glucose treated cells. This suggests that the increased expression of miRNA 155-5p induced by LPS in the 5mM D-glucose and 5mM D-glucose with 45mM L-glucose has returned to basal levels.
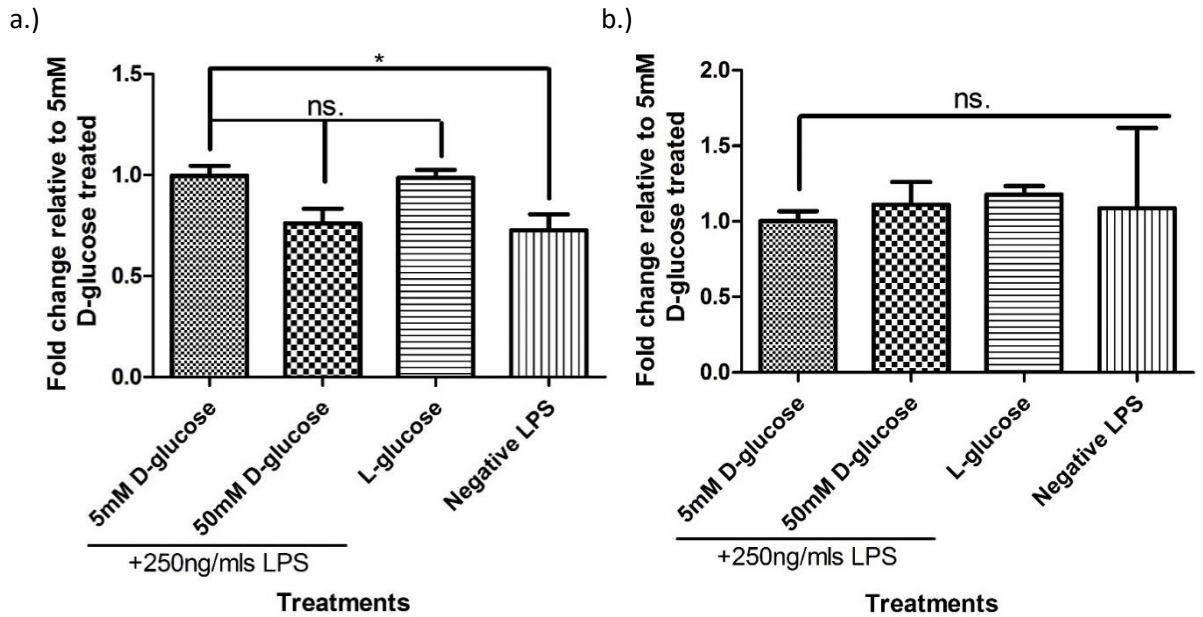
Figure 5.4.11: Assessment of miR-155-5p expression in primary monocytes treated *ex vivo* with LPS in the presence of elevated concentrations of D-glucose.

Human primary monocytes were isolated from whole blood taken by venepuncture from healthy volunteers. The primary monocytes were treated *ex vivo* with either 5mM D-glucose, 50mM D-glucose and 5mM D-glucose with 45mM L-glucose for 4 hours prior to the addition of LPS (250ng/ml). The negative LPS treatment group were treated with 5mM D-glucose without LPS for the duration of the treatment. The monocytes were harvested by centrifugation, washed with PBS and lysed in Trizol reagent at 2 hours a.) and 24 hours b.) post LPS addition. The total RNA was extracted using Qiagen RNA extraction spin columns and the RNA quantity and quality assessed by nanodrop. The extracted RNA was reverse transcribed and microRNA 155-5p expression assessed by qPCR at the 2 hour a.) and 24 hour b.) post LPS addition time points. The microRNA miR-16 was used as a housekeeper gene. The results were analysed using the ΔΔCT method, whereby the results are expressed as a fold change (± standard error of the ΔCT) relative to the 5mM D-glucose treated monocytes. The results are the mean of 3 independent experiments respectively (± the standard error of the mean). Significance was determined by ANOVA followed by Dunnett's post-test comparing treatments to the 5mM D-glucose treated cells, whereby (*), (**) and (***) represents $p<0.05$, $p<0.01$ and $p<0.001$ respectively.

5.4.15 Treatment with increased concentrations of D-glucose increases expression of miR-424-5p in primary monocytes

Treatment of primary monocytes with 50mM D-glucose and LPS (250ng/ml) over a 6 hour period resulted in a significant increase in the expression of miRNA 424-5p relative to 5mM D-glucose treated cells. However, no significant change in miRNA 424-5p expression occurred in response to treatment with 5mM D-glucose and 45mM L-glucose co-incubation relative to 5mM D-glucose treated cells, suggesting increased osmotic concentration had no effect on miRNA 424-5p expression.
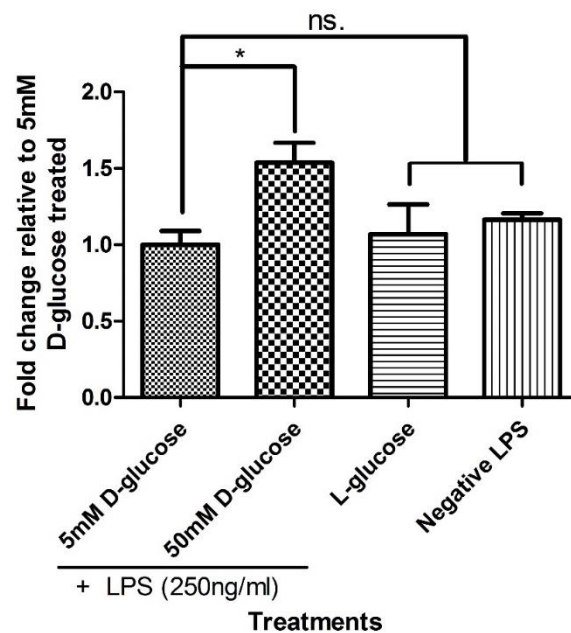
Figure 5.4.12: Treatment of primary monocytes with increased concentrations of glucose resulted in a significant increase in expression of miR-424-5p

Human primary monocytes were isolated from whole blood taken by venepuncture from healthy volunteers. The primary monocytes were treated ex vivo with either 5mM D-glucose, 50mM D-glucose and 5mM D-glucose with 45mM L-glucose for 4 hours prior to the addition of LPS (250ng/ml). The negative LPS treatment group were treated with 5mM D-glucose without LPS for the duration of the treatment. The monocytes were harvested by centrifugation, washed with PBS and lysed in Trizol reagent at 2 hours post LPS addition. The total RNA was extracted using Qiagen RNA extraction spin columns and the RNA quantity and quality assessed by nanodrop. The extracted RNA was reverse transcribed and microRNA 424-5p expression assessed by qPCR at the 2 hour post LPS addition time points. The microRNA, miR-16 was used as a housekeeper gene. The results were analysed using the $\Delta\Delta$CT method, whereby the results are expressed as a fold change (± standard error of the ΔCT) relative to the 5mM D-glucose treated monocytes. The results are the mean of 3 independent experiments respectively (± the standard error of the mean). Significance was determined by ANOVA followed by Dunnett's post-test comparing treatments to the 5mM D-glucose treated cells, whereby (*), (**) and (***) represents $p<0.05$, $p<0.01$ and $p<0.001$ respectively.

5.5   Discussion

Treatment of primary monocytes with increased concentrations of D-glucose with or without the addition of LPS over a 28 hour period resulted in altered secretion of a number of inflammatory cytokines. This included increased secretion of TNFα, IL-6 and IL-8 and decreased secretion of IL-10 and TGFα. These findings contrast to the response observed in high glucose treated THP-1 monocytes. No change in TNFα secretion was observed in THP-1 monocytes treated with high glucose alone but high D-glucose treated primary monocytes exhibited increased secretion of a number of inflammatory cytokines.

Previous studies have reported increased secretion and mRNA production of IL-6 and TNFα in high glucose treated primary monocytes (Morohoshi, Fujisawa et al. 1995, Morohoshi, Fujisawa et al. 1996). An additional study by Gonzalez, Herrera et al. (2012) observed that treatment of primary monocytes with high concentrations of glucose resulted in increased secretion of TNFα although they did not observe significant changes in secretion of IL-6, IL-8 or IL-1β. The authors of this paper treated the primary monocytes with 50mM D-glucose over a time period of 7 days which may have resulted in the cells becoming tolerant of the environment, reducing cytokine secretion back to control levels at later times. Further publications have also reported that treatment of PBMCs with high concentrations of glucose with LPS act synergistically to increase secretion of inflammatory cytokines (Hancu, Netea et al. 1998, Otto, Schindler et al. 2008). The results presented in this chapter are novel in that they examine the response of a wider variety of cytokines to treatment with high glucose with and without the addition of LPS. The benefit of a broader cytokine profile lies in the opportunity for pathway discovery.

The cytokine secretion profiles were inputted into Ingenuity Pathway Analysis software in order to determine predicted upstream regulators which may have contributed to the differences observed in response to incubation with high concentrations of D-glucose. The pathway analysis identified a number of potential upstream regulators including: NF-κB, STAT3, HMGB1, miR-146a-5p and miR-155-5p.

Treatment of primary monocytes over 28 hours with increased concentrations of D-glucose resulted in altered secretion of HMGB1. Primary monocytes treated with increased concentrations of D-glucose in the absence of LPS resulted in a significant increase in secretion of HMGB1 whereas in the presence of LPS high concentrations of D-glucose resulted in a significant decrease in secretion. HMGB1 is chromatin component that when secreted by activated monocytes or macrophages acts as a pro-inflammatory cytokine through interacting with RAGE (Luan, Zhang et al. 2010), TLR2 and TLR4

receptors (Park, Gamboni-Robertson et al. 2006). Secretion of HMGB1 has been previously reported to be increased in diabetic individuals (Abu El-Asrar, Nawaz et al. 2013) and in vitro treatments of endothelial cells with high concentrations of D-glucose (Mudaliar, Pollock et al. 2014). The observed increase in secretion of HMGB1 by primary human monocytes treated with high concentrations of D-glucose has not currently been reported in the literature. The translocation of HMGB1 from the nucleus to the cytoplasm and its secretion has been reported to be regulated by acetylation of HMGB1 at various lysine residues by the histone acetyltransferase enzymes (Bonaldi, Talamo et al. 2003). HMGB1 has been observed to be a target for deacetylation by SIRT1 which results in decreased cellular HMGB1 secretion (Rickenbacher, Jang et al. 2014, Rabadi, Xavier et al. 2015). The observed decrease in SIRT1 deacetylase activity and the previously reported increase in HAT activity in response to treatment with high concentrations of D-glucose could result in increased HMGB1 acetylation and secretion. The primary monocytes treated with increased concentrations of D-glucose with LPS resulted in a significant decrease in HMGB1 secretion over a 28 hour period. This response is not currently supported by the current literature where LPS has been observed to result in increased secretion of HMGB1 (El Gazzar 2007). Secretion of HMGB1 has been observed to be a late stage mediator of the inflammatory response; a study by (Wang, Bloom et al. 1999) reported that mice treated with endotoxin had increased serum levels of HMGB1 after 8 hours, peaking at 16 hours after which serum concentration remained high although it had started to decrease. The observed decrease in HMGB1 secretion of primary monocytes treated with high glucose and LPS after 28 hours could indicate that HMGB1 has reached its peak in secretion earlier than cells treated with high glucose alone. This could indicate an earlier resolution to the inflammatory response resulting in decreased secretion of HMGB1.

Although HMGB1 secretion by primary monocytes was increased in response to high glucose alone, the function of HMGB1 is dependent on the redox state of its three cysteine residues (Yang, Antoine et al. 2013). Further studies could seek to investigate the redox state of the secreted HMGB1 in order to contextualise the increased secretion.

Primary monocytes treated with increased concentrations of glucose over a 6 hour period decreased the expression of miR-146a-5p relative to cells treated with 5mM D-glucose. Expression of miR-146a-5p has been previously reported to decrease in response to incubation with high concentrations of D-glucose in endothelial cells (Feng, Chen et al. 2011, Wang, Huang et al. 2014); the observed decrease in miRNA 146a expression in response to high glucose reported in this chapter is the first time this effect has been observed in human primary monocytes. Expression of miR-146a-5p has been reported to be regulated by the binding of NF-κB to its gene promoter region (Taganov, Boldin et al.

2006). For this reason increased NF-κB activity induced in response to LPS has been observed to result in increased expression of miR-146a (Taganov, Boldin et al. 2006). Increased expression of miR-146a forms a negative feedback loop repressing TLR mediated inflammation and NF-κB transcriptional activity (Bhaumik, Scott et al. 2008).

Expression of miRNA 146a-5p has also been reported to be regulated by the histone acetyltransferase p300 (Feng, Chen et al. 2011). The authors observed that incubation with high concentrations of D-glucose increased activity of p300 and histone acetylation which resulted in decreased miR-146a expression. Treatment with p300-silencing RNA restored miR-146a expression in response to high concentrations of D-glucose suggesting increased p300 mediated acetylation regulates miR-146a expression. The expression and activity of p300 increased in response to treatment with high concentrations of glucose (Feng, Chen et al. 2011). Expression and activity of the p300 histone acetyltransferase has not been explored within this thesis although this could serve as the pathway resulting in increased miRNA 146a-5p expression. miRNA 146a-5p has a role in regulating the inflammatory response through disruption of the TLR4 signalling pathway by causing degradation of TRAF6 and IRAK1 mRNA (Gao, Wang et al. 2015, Lu, Cao et al. 2015). Decreased expression of miRNA 146a-5p has been observed to result in increased secretion of the inflammatory cytokines: IL-6 and IL-8 (Bhaumik, Scott et al. 2009) and may at least in part explain the increase in IL-6 and IL-8 observed here in primary monocytes during high glucose treatment.

Treatment of primary monocytes with increased concentrations of glucose resulted in a non-significant decrease, in the expression of miRNA 155-5p relative to cells treated with 5mM D-glucose and 5mM D-glucose with 45mM L-glucose. Within the literature, expression of miRNA 155-5p has been shown to be both increased and reduced in response to a hyperglycaemic environment. T2DM patients exhibited decreased expression of miRNA 155-5p in examined bone marrow-derived CD34 positive stem cells (Spinetti, Cordella et al. 2013). In diabetic rat and mouse models, increased expression of miRNA 155-5p has been observed (Kovacs, Lumayag et al. 2011, Lin, You et al. 2015). The exact role miR-155-5p plays in the regulation of inflammatory responses is also currently debated; reported in the literature as both pro- (Li, Tian et al. 2013) and anti-inflammatory (Tili, Michaille et al. 2007, Tang, Xiao et al. 2010). Li, Tian et al. (2013) identified miR-155-5p as having a pro-inflammatory role by targeting and inhibiting the expression of SOCS1 resulting in increased expression of TNFα and IL-1β. Tang, Xiao et al. (2010) identified miR-155-5p as having an anti-inflammatory role by targeting and inhibiting the expression of MyD88 which the authors observed to result in a significant decrease in IL-8 cytokine secretion. The role of miR-155-5p in the regulation of the inflammatory response may depend on the specific cell/tissue type or the circumstances of the

inflammatory response. Additional research appears to be required to further clarify the role of miR-155-5p in the inflammatory response.

Expression of the miR-424-5p was increased in primary monocytes treated with high concentrations of glucose. Expression of miR-424 in response to treatments with high concentrations of glucose has not currently been explored within the literature. Increased expression of miR-424-5p has been shown to be associated with increased monocyte differentiation to macrophages (Rosa, Ballarino et al. 2007). The authors observed that increased expression of miR-424 resulted in degradation of nuclear factor 1 A-type (NFIA) mRNA resulting in increased monocyte differentiation to macrophages. The expression of miR-424-5p has been reported to be regulated by the binding of the transcription factor PU.1 to the gene promoter region (Rosa, Ballarino et al. 2007). Expression of the PU.1 transcription factor and its activity has been observed to increase in response to obesity and diabetes (Nadler, Stoehr et al. 2000, Furukawa, Fujita et al. 2004). This known increase in PU.1 expression and activity in response to obesity and diabetes could explain the increased expression of miR-424-5p in high glucose treated primary monocytes. Expression of miR-424-5p has also been reported to be suppressed by a variety of histone deacetylase proteins (Zhou, Gong et al. 2013). The authors observed that mice treated with a number of histone deacetylase inhibitors for HDAC1, HDAC2 and SIRT1 had increased expression of miR-424-5p. This would suggest that decreased histone deacetylase activity, as has been previously reported in response to hyperglycaemia (Yun, Jialal et al. 2011), may result in increased expression of miR-424-5p.

The importance of these miRs in regulating the inflammatory response by monocytes to high glucose could be investigated further by treating cells with either anti-miRs or miR mimetics to either decrease or increase activity of specific miRs.

5.5.1 Strengths and limitations

A limitation of the research presented within this chapter is due to the monocyte isolation technique used. The isolation technique only isolated the CD14 positive, CD16 negative mon 1 monocyte subpopulation. The consequence of this being that the responses of the CD16 positive mon 2 and mon 3 populations to high concentrations of D-glucose and LPS remains unknown. This is of great significance when it is considered that the CD16 positive mon 2 and mon 3 populations have both been shown to secrete greater amounts of pro-inflammatory cytokines in response to TLR ligands. The mon 2 and mon 3 subpopulations have also been reported to expand in a number of

inflammatory conditions in addition to obesity and diabetes occurring either independently or simultaneously (Frankenberger, Sternsdorf et al. 1996, Belge, Dayyani et al. 2002, Cros, Cagnard et al. 2010, Poitou, Dalmas et al. 2011, Wong, Tai et al. 2011). This perhaps suggests a functional role of these populations in these inflammatory conditions. Further work could seek to isolate the total monocyte population and subsequently separate them by FACS to determine the responses of each subpopulation to treatment with elevated concentrations of glucose. Further work could also assess the effects of treatment with elevated glucose on mon 1 monocyte CD14 and CD16 expression by flow cytometry in order to determine whether exposure could promote mon 1 monocytes to shift to CD16 mon 2 or mon 3 populations. Although there are some advantages to only assessing a single monocyte subpopulation. Each of the individual subpopulations have been shown to have unique gene expression profile and role within the innate immune system (Wong, Tai et al. 2011), pooling the three populations together would potentially dilute and prevent observing significant changes in response to treatment.

A strength of the results presented within this chapter is that these experiments were performed using primary human monocytes treated *ex vivo*. By using primary human monocytes as opposed to a leukaemic monocyte cell line the results can be determined to be more applicable to human individuals with high plasma concentrations of D-glucose occurring as a result of diabetes. However, a consideration when treating and examining the responses of a single cell type in isolation is that *in vivo* the monocytes responses would be influenced by the variety of other cell types that reside in the blood. Using primary human monocytes also limited the available number of cells restricting some of the experiments that could be successfully performed. This meant that some of the responses from THP-1 monocytes treated with high concentrations of D-glucose presented in chapter four such as effect on SIRT1 deacetylase activity and P65 acetylation status could not be replicated in primary monocytes.

The *ex vivo* treatment of primary monocytes with high concentrations of D-glucose identified a number of novel responses not previously reported in the current literature; these include the increased secretion of HMGB1, acetylated P65 binding to the TNFα promotor and miR-424-5p expression in addition to decreased expression of miR-146a-5p.

6   Discussion

6.1   Summary of findings

The results of the study presented in chapter three identified a total of eight miRs that were dysregulated in monocytes of obese individuals awaiting bariatric surgery that returned to control levels of expression one year after the surgery. A number of the miRs identified, 146a-5p, 424-5p, 151a-5p and 199-5p, have previously been reported in the literature to play a role in the regulation of inflammatory signalling. As monocytes play a fundamental role in the induction of inflammatory responses, it is of note that miRs involved in the regulation of inflammation signalling are dysregulated in response to obesity. The dysregulation of these miRs could contribute to the chronic inflammatory phenotype observed in obese and diabetic individuals. The subsequent pathway analysis of the predicted miR target mRNAs which were identified using sequence prediction software appears to support the role of the dysregulated miRs in inflammatory signalling. The pathway analysis was performed on the top one hundred target mRNAs ranked in order of confidence of prediction for each miR; potential involvement in a number of inflammatory signalling pathways including IL-6, IL-10, toll-like receptor and NF-κB signalling was identified. Whilst the involvement in these pathways is likely to facilitate further investigation, it should be noted that this is based on the use of predictive software which should be considered when interpreting these results. The identification of these miRs represents a significant finding, adding to a currently limited knowledge base and could, with further investigation identify potential targets for intervention to limit obesity and diabetes associated inflammation and its complications. The study also showed that bariatric surgery and the resulting weight loss after one year was successful in restoring the dysregulated miRs towards control levels of expression.

The expression of miR-146a-5p and miR-424-5p was additionally altered in response to increased age; expression of miR-146a-5 was lower in older age and expression of miR-424 was higher. Human monocyte expression of these two miRs have not, at the time of writing been associated with age, although the trend in the change of expression of these two miRs has been observed in endothelial cells aged through increased cellular passages. The expression of both miR-146a-5p and miR-424-5p are both reportedly involved in the regulation of the inflammatory response. The dysregulation of these with increased age could contribute to the observed increase in serum inflammatory cytokines present with advancing age. The increased presence of inflammatory cytokines in response to dysregulation of these miRs could also contribute to the increased insulin resistance associated with

age. Alternatively these miRs could become dysregulated in response to age associated increases in insulin resistance, serum glucose and cholesterol concentrations. A longitudinal study would be necessary to determine whether alterations in expression of these miRs results from, or results in, the age associated changes in inflammatory response and metabolism.

The results of the study presented in chapter four identified the responses of THP-1 monocytes to incubation with increased concentrations of D-glucose with or without co-treatment with LPS. The results reported the effects of treatment with increased concentrations of D-glucose on THP-1 intracellular NAD^+:NADH ratio, SIRT1 deacetylase activity, P65 acetylation status, cytokine secretion and TNFα mRNA transcription in the presence or absence of LPS. Incubation with either increased concentrations of D-glucose or its osmotic control L-glucose reduced secretion of a number of cytokines and chemokines in response to LPS. Secretion of a total of 41 cytokines and chemokines were assessed by multiplex cytokine analysis; of all the cytokines detected, IP-10 was the single cytokine shown to increase in response to high concentrations of glucose in THP-1 monocytes. The increased osmotic concentration also reduced LPS-induced transcription of TNFα mRNA. Treatment of THP-1 monocytes with high concentrations of D-glucose was observed to decrease the NAD^+:NADH ratio. This response to increased glucose availability has been reported previously to occur in a variety of different cell types; the increased availability of glucose has been shown to result in increased sorbitol and fructose formation through the polyol pathway a process which utilises NAD^+ reducing it to NADH. Treatment of THP-1 monocytes with high concentrations of D-glucose was shown to result in decreased SIRT1 deacetylase activity independent of any significant changes in SIRT1 mRNA transcription. The current literature has described that incubation with increased concentrations of D-glucose to result in decreased SIRT1 deacetylase activity in a variety of cell types. This response is reported within the literature to be due to decreased availability of NAD^+, a co-factor required for SIRT1 deacetylase activity. However the assay used to assess deacetylase activity supplies NAD^+, so the observed decrease in SIRT1 activity seen here must be caused by alternative mechanisms, although its intracellular activity may be further reduced due to the observed decrease in the NAD^+:NADH ratio. SIRT1 mRNA stability has been observed to be decreased in individuals with metabolic syndrome which may not have an effect on levels of SIRT1 mRNA but may reduce translation to protein (Ceolotto, De Kreutzenberg et al. 2014). Treated THP-1 monocytes displayed an increased ratio of acetylated (K310) P65 to total P65 in response to treatment with increased concentrations of D-glucose. P65 acetylation status has been shown to be regulated by SIRT1 deacetylation. The increased P65 acetylation observed in treated THP-1 monocytes could be occurring as a result of the decrease in SIRT1 deacetylase activity. Increased P65 acetylation at lysine

310 has been observed to result in increased transcriptional activity and prolonged binding to sites of gene transcription resulting in increased NF-κB transcriptional activity.

The results reported in chapter five identified the responses of human primary monocytes from healthy volunteers to incubation with increased concentrations of D-glucose. This assessed the effects of treatment on NAD$^+$:NADH ratio, binding of acetylated P65 to the TNFα promoter, expression of the miRs 146a, 424 and 155, cytokine secretion and TNFα mRNA transcription in the presence or absence of LPS.

Incubation of primary monocytes with concentrations of D-glucose was observed to alter the secretion of a number of cytokines in either the presence or absence of LPS. A total of 41 individual cytokines from the supernatants of treated primary monocytes were assessed by multiplex cytokine assay. Treatment with increased concentrations of D-glucose in the absence or presence of LPS resulted in increased secretion of the inflammatory cytokines TNFα, IL-6, IL-8 and decreased secretion of IL-10 and TGFα. Treatment of primary monocytes with increased concentrations of D-glucose resulted in increased LPS induced expression of TNFα mRNA. The results from the cytokine panels were entered into Ingenuity Pathway Analysis software in order to determine predicted upstream regulators to direct further analysis. The results of the pathway analysis predicted that NF-κB, STAT3, HMGB1, miR-146a-5p and miR-155-5p were upstream regulators of the cytokine response. Treatment of primary human monocytes with high concentrations of D-glucose decreased the NAD$^+$:NADH ratio. This same response to high concentrations of D-glucose was observed in glucose treated THP-1 monocytes and has been reported previously in a variety of cells. Primary monocytes treated with increased concentrations of D-glucose resulted in increased binding of acetylated P65 (K310) to the TNFα promoter region. Increased P65 acetylation (K310) status has been reported to block SET9 mediated methylation of NF-κB, a process important for the ubiquitination and degradation of chromatin bound NF-κB which has been shown to result in increased and prolonged NF-κB transcriptional activity. Treatment with increased concentrations of D-glucose resulted in increased primary monocyte secretion of HMGB1; however, treatment with increased concentrations of D-glucose with the addition of LPS reduced the primary monocyte secretion of HMGB1. Increased serum levels of HMGB1 have been observed in diabetic individuals and secretion by endothelial cells increased in response to high concentrations of glucose. Secreted HMGB1 has been observed to perpetuate the inflammatory response by interacting with cell surface RAGE, TLR2 and TLR4. Treatment of primary monocytes taken from healthy volunteers, with high concentrations of D-glucose resulted in the decreased expression of miR-146a-5p and increased expression of miR-424-5p. Although decreased expression of miR-146a-5p in response to high

concentrations of D-glucose has been previously reported in the literature, this result represents the first time this response has been observed in treated primary human monocytes. Expression of miR-424-5p has not currently been explored in response to treatment with high concentrations of D-glucose; the observed increase in expression of miR-424-5p in primary human monocytes in response to high concentrations of D-glucose is a novel finding. The decreased expression of miR-146a-5p, a known negative regulator of TLR and NF-κB signalling, could potentially contribute towards the increased secretion of multiple inflammatory cytokines observed in high glucose-treated primary monocytes. This finding could indicate a potential mechanism through which high glucose availability results in increased inflammatory signalling and could represent a target for intervention during conditions such as T2 diabetes.

6.2   Implications of research

Gastric bypass surgery, which is associated with greater recovery from diabetes than other forms of bariatric surgery, has been shown to increase secretion of the gut hormone glucagon-like peptide-1 (GLP-1). GLP-1 secretion by intestinal L-cells increases pancreatic beta cell proliferation, survivability and glucose stimulated insulin secretion (Lim and Brubaker 2006). Secretion of, and beta cell sensitivity to GLP-1 has been previously reported to be reduced in obese and diabetic individuals (Xu, Kaneto et al. 2007, Calanna, Christensen et al. 2013). Rat models of gastric bypass surgery (Patriti, Facchiano et al. 2004, Rubino, Forgione et al. 2006) were shown to have an increased number of the cells responsible for secretion of GIP and GLP-1 (Speck, Cho et al. 2011). Treatment of the rats with exendin$_{9-39}$, a GLP-1 receptor antagonist (Serre, Dolci et al. 1998) neutralised the glucose reducing effects of gastric bypass surgery (Kindel, Yoder et al. 2009). Although administration of extendin$_{9-39}$ to gastric bypass patients had no significant effect on blood glucose concentrations (Jimenez, Casamitjana et al. 2013). Some restrictive bariatric surgeries such as sleeve gastrectomy have also been shown to increase GLP-1 secretion, this is believed to be caused by increased transit of gastrointestinal content (Jimenez, Casamitjana et al. 2012). This increased secretion of GLP-1 reportedly improves pancreatic beta cell function (Nannipieri, Baldi et al. 2013) an observation which was shown to be neutralised when treated with the GLP-1 antagonist exendin$_{9-39}$ (Salehi, Prigeon et al. 2011). A study by Shiraishi, Fujiwara et al. (2012) reported that increased GLP-1 resulted in increased STAT3 signalling and polarization of macrophages to a M2 anti-inflammatory phenotype. Both obesity and T2 diabetes are associated with an increased proportion of M1 pro-inflammatory macrophages (Satoh, Shimatsu et al. 2010, Kanter, Kramer et al. 2012). Bariatric surgery has been

shown to increase the proportion of M2 anti-inflammatory macrophages to M1 pro-inflammatory macrophages (Aron-Wisnewsky, Tordjman et al. 2009). The miR expression profiles of macrophages have been reported to alter depending on whether they are polarized towards a pro-inflammatory or anti-inflammatory phenotype (Graff, Dickson et al. 2012, Liu and Abraham 2013). Bariatric surgery could reduce circulating lipids and glucose in obesity contributing towards a shift in monocyte/macrophage polarization which could facilitate the change in miR expression towards control values post-surgery.

The monocyte expression of miR-146a-5p and miR-424-5p were observed to have similar trends in expression in response to obesity, age and treatment with high concentrations of D-glucose. In all of these conditions the expression of miR-146a-5p was decreased whilst the expression of miR-424-5p increased. The mid-life participants (>50 years old) had increased serum total cholesterol, LDL cholesterol HDL cholesterol and resting glucose compared to the younger participants (<30 years old). This is supported by previous studies which have shown mid-life (50-60 years old) to be associated with increased total cholesterol, LDL cholesterol (Heiss, Tamir et al. 1980, Moulopoulos, Adamopoulos et al. 1987, Heitmann 1992) and resting glucose (Ko, Wai et al. 2006). Potentially the increase in serum total cholesterol or resting glucose could lead to the observed changes in miR-146a-5p and miR-424-5p expression. Increased age has also been shown to result in decreased intracellular NAD^+:NADH ratio and decreased SIRT1 deacetylase activity in rats (Braidy, Guillemin et al. 2011). A response also observed in relation to obesity and type 2 diabetes (Gillum, Kotas et al. 2011, Yoshino, Mills et al. 2011, Mortuza, Chen et al. 2013). The obese patients awaiting bariatric surgery also displayed increased expression of miR-199b-5p which has been reported previously to target and reduce expression of SIRT1 (Saunders, Sharma et al. 2010). Although SIRT1 deacetylase activity was not assessed in the obese or midlife participants its activity was shown to decrease *in vitro* treatments of THP-1 monocytes with increased concentrations of D-glucose. Decreased SIRT1 deacetylase activity could provide a link between the observed changes in miR-146a-5p and miR-424-5p expression observed in obese and mid-life participants and primary monocytes treated ex vivo with high concentrations of glucose.

The dysregulation of these miRs whilst potentially having implications for monocyte function such as decreased regulation of inflammatory responses also may have implications for surrounding cells and tissues. A number of cells belonging to the innate immune system including monocytes have been observed to secrete miR containing exosomes (Matsumoto, Morisaki et al. 2004, Lemaire, Mkannez et al. 2013). Secreted exosomes containing miRs have been shown to affect the functioning of surrounding cells and tissues in a paracrine manner (Momen-Heravi, Bala et al. 2015, Zhang, Li et al.

2015). The dysregulation of monocyte miR expression in obesity could result in exosomes being secreted resulting in an adverse effect on the surrounding cells. Exosome secretion containing increased miR-424-5p, an identified promoter of monocyte differentiation, in the inflamed endothelium could result in increased macrophages perhaps contributing to the development of atherosclerosis. Exosomes being secreted containing lower levels of miR-146a-5p, an inhibitor of TLR induced inflammation could lead to dysregulation of inflammation in the surrounding cells.

The *in vitro* treatment of THP-1 and primary monocytes with increased concentrations of D-glucose resulted in differential cytokine secretion profiles and expression of TNFα mRNA. Treated THP-1 monocytes displayed decreased TNFα mRNA expression and secretion of a number of cytokines in response to LPS or opsonised zymosan. This response occurred in response to the increased osmotic concentration rather than the increased availability of D-glucose. A single cytokine, IP-10 was shown to increase in high glucose treated THP-1 monocytes, although this appeared to occur in response to the increased osmotic concentration. This response was considerably different to primary monocytes treated with increased concentrations of D-glucose and LPS which resulted in increased expression of TNFα mRNA and altered secretion of a number of cytokines independent of osmotic concentration. This appears to indicate that the THP-1 monocyte cell line is more sensitive to changes in osmotic pressure than primary human monocytes. Expression of aquaporin 5 mRNA has been observed to be increased in leukemic cell lines (K562, U937, EM-2, LAMA-84) relative to peripheral blood lymphocytes (Chae, Kang et al. 2008). Increased expression of cell surface aquaporins could result in increased flux of water across the cell membrane resulting in increased cell shrinkage in response to a hyperosmotic environment. Cuschieri, Gourlay et al. (2002) observed that preconditioning rabbit macrophages with increased osmotic concentrations reduced secretion of TNFα in response to LPS. The authors treated the macrophages for a period of 4 hours with mannitol or NaCl at concentrations of 40 – 100mM prior to the addition of LPS; this resulted in increased cell shrinkage which was observed to result in decreased activation of ERK1/2 leading to decreased TNFα secretion. This could represent the mechanism through which increased osmotic concentration reduces THP-1 cytokine secretion and TNFα mRNA expression in response to LPS or opsonised zymosan.

Treatment of THP-1 and primary human monocytes also produced a number of similar responses to high concentrations of D-glucose. Treatment of both primary human and THP-1 monocytes with increased concentrations of D-glucose resulted in a decreased NAD$^+$:NADH ratio. Treatment of THP-1 monocytes with high concentrations of D-glucose resulted in a significant decrease in SIRT1 deacetylase activity and increased ratio of acetylated (K310) P65 to total P65. Due to limitations in available cell numbers these findings could not be confirmed in treated primary monocytes, however

primary monocytes treated with increased concentrations of D-glucose displayed increased binding of acetylated P65 to the TNFα promotor. This result could indicate that the primary monocytes treated with high concentrations of D-glucose may also be displaying decreased SIRT1 deacetylase activity resulting in increased total P65 (K310) acetylation.

Acute treatments of primary and THP-1 monocytes with high concentrations of D-glucose resulted in a shift in the intracellular NAD^+:NADH ratio leading to decreased functioning of NAD^+ dependent enzymes such as SIRT1. The histone deacetylase SIRT1 displayed decreased deacetylase activity in response to high concentrations of glucose which could result in dysregulation of the balance between acetylation and deacetylation. This response was identified by the increased acetylation of P65 relative to total P65 observed in glucose treated monocytes, a modification reported to increase NF-κB transcriptional activity and duration. Although not explored within this thesis, alterations in the balance between acetylation and deacetylation could result in altered expression of multiple genes via altered acetylation of histone proteins. Some potential evidence for this exists in the expression profiles of the miR-146a-5p and miR-424-5p. Expression of miR-146a-5p was shown to decrease and miR-424-5p to increase in primary monocytes treated with high concentrations of glucose. Expression of miR-146a-5p has been shown to decrease and miR-424-5p increase in response to decreased deacetylation and increased acetylation. A number of these results occurred after only 6 hours of treatment with increased concentrations of glucose an earlier time point than has previously been assessed in monocytes. Assessment of treatment at these early time points also allowed for the identification of direct responses to increased availability of D-glucose independent of increased ROS. Changes occurring after 6 hours in response to high concentrations of glucose could have implications even for individuals with well controlled diabetes who may experience post-prandial hyperglycaemia occurring over short periods of time.
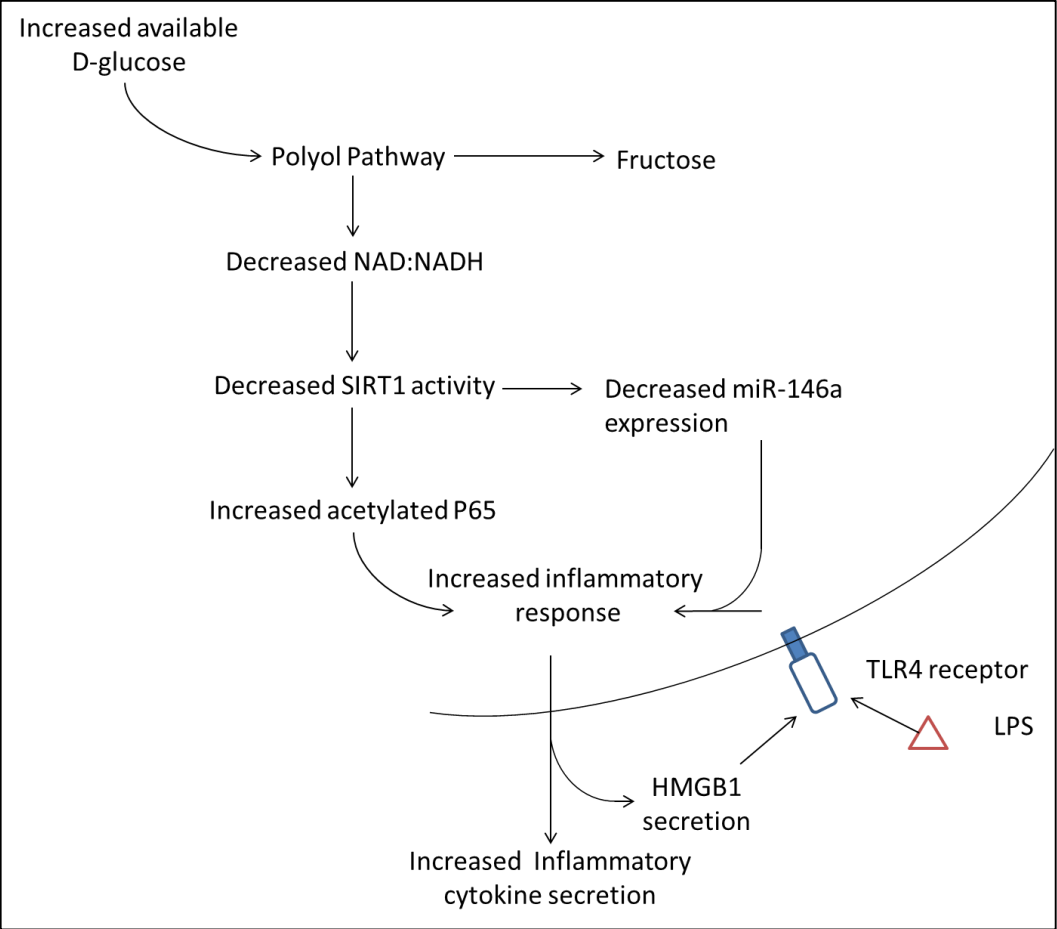
Figure 6.2.1: Schematic detailing a potential mechanism through which increased glucose availability induces inflammation

6.3   Strengths and limitations of research

The research presented in chapter 3 identified a number of novel miRs that were dysregulated in monocytes during obesity. The dysregulation of these miRs give possible insights into how differences in monocyte function and inflammatory response occur during obesity. Microarray analysis of miR expression, although shown in multiple publications to have a very good correlation with qPCR analysis, the latter has been shown to be the more sensitive and specific method of detection. The expression of these identified miRs should be confirmed in these samples by qPCR analysis to provide greater confidence in these results.

The *in vitro* treatments of THP-1 and primary human monocytes used 50mM D-glucose as the high glucose treatment. This concentration is higher than may be expected during diabetes although has been reported in individuals with unmanaged diabetes (Faxon, Creager et al. 2004) and been used as a high glucose treatment in various other studies (Fukuhara-Takaki, Sakai et al. 2005, Feng and Chou 2014, Jayakumar, Chang et al. 2014). This concentration was selected based on these previous publications and due to the acute nature of the treatments.

THP-1 monocytes appeared more sensitive than primary human monocytes to the increased osmotic concentration resulting from treatment with high concentrations of glucose. The high osmotic concentration affected THP-1 monocyte inflammatory response indicated through decreased expression of TNFα mRNA and secretion of multiple cytokines. This difference between THP-1 and primary monocytes may represent differential regulation of the inflammatory response occurring in THP-1 monocytes which may limit its usage in circumstances of high osmotic concentration.

The *in vitro* treatments of THP-1 and primary human monocytes with high concentrations of D-glucose produced a number of results previously reported in the literature such as decreased SIRT1 deacetylase activity and increased P65 acetylation; although the novelty of the work presented within this thesis is the identification of these changes in response to high concentrations of D-glucose occurring at earlier time points then had previously been reported.

The *in vitro* treatment of primary monocytes with high concentrations of D-glucose also identified a number of novel responses not previously reported in the current literature; these included the increased secretion of HMGB1, acetylated P65 binding to the TNFα promotor and miR-424-5p expression and decreased expression of miR-146a-5p and miR-155 in response to high concentrations of D-glucose.

A general limitation of assessing the expression of miRs is that so little is known about the specific target mRNAs of each miR. Target prediction software is required to attempt to determine which mRNAs may be affected by each miR. However, the results of target prediction and subsequent pathway analysis are based on predictions determined by sequence complementarity and may not reflect the actual function of the assessed miR. This should be taken into consideration when assessing these results.

As previously stated the research involving isolated primary monocytes detailed in chapters three and five is limited by the monocyte isolation technique chosen. The isolation technique only isolated CD14 positive and CD16 negative mon 1 monocytes leading to the loss of the CD16 positive mon 2 and mon 3 populations. Although these populations are relatively small relative to the mon 1 population these populations have been reported to expand during obesity, diabetes and a variety of chronic inflammatory conditions and have been suggested to play a role in disease development. The results can therefore only be applied to the mon 1 monocyte population.

6.4   Future work

Future work could seek to address some of the identified limitations of the research presented within this thesis. The obesity dysregulated miRs identified by microarray analysis could be confirmed by qPCR analysis, which is a more accurate and sensitive technique. The RNA extracted from the obese and control individuals could be subjected to transcriptome analysis by either RNA sequencing or microarray. This would provide information on the specific genes being transcribed which could be paired with the already assessed miRs in order to determine which predicted target mRNAs were being affected by the dysregulated miRs. This would provide greater detail on the effects dysregulation of these miRs would have on monocyte function in obesity and diabetes.

Future work could additionally seek to assess to contribution of increased glucose entering the polyol pathway on the reduction of intracellular NAD^+:NADH ratio and the responses observed in THP-1 and primary monocytes to high concentrations of D-glucose. Treatment of primary monocytes with inhibitors of aldose reductase an enzyme required for glucose to enter the polyol pathway in conjunction with high concentrations of D-glucose could also be investigated to further understand the mechanism and as a potential target for modulating inflammation with age and obesity.

Investigation of high glucose induced inflammatory response in treated THP-1 monocytes showed high sensitivity to the increased osmotic concentration within 24 hours. Further work could treat

THP-1 monocytes with high concentrations of D-glucose subsequent to being adapted to an increased osmotic environment. Cuschieri, Gourlay et al. (2002) reported that after incubation for 20 hours in a high osmotic environment rabbit macrophages secreted the same quantities of TNFα as macrophages incubated in an isosmotic environment. THP-1 monocytes could be treated with an equivalent osmotic concentration over a 24 hour period to allow adjustment, the media replaced and the cells treated with the high concentrations of glucose.

Further work could also explore the dysregulated miRs in *in vitro* treatments using specific miR inhibitors and mimetics. This could be done in order to assess the contribution of these miRs towards the inflammatory response to the high glucose conditions reported within this thesis.

Finally, the microarray analysis of monocyte miRs dysregulated in obesity identified a number of miRs that could be assessed in the in vitro treatments of primary monocytes with increased concentrations of D-glucose.

6.5   Conclusion

The results presented within this thesis identified a number of novel miR dysregulated in obesity in addition to highlighting the benefits of bariatric surgery to reduce these changes towards control values. Some of these results were replicated in older individuals and by *in vitro* treatments of primary monocytes with high concentrations of D-glucose, specifically alterations in expression of miRs 146a-5p and 424-5p. *In vitro* treatments of THP-1 monocytes did not induce an inflammatory response over 24 hours due to an apparent sensitivity to hyper-osmolality. However these treatments did significantly shift the intracellular NAD^+:NADH availability, SIRT1 deacetylase activity and P65 acetylation status. These results suggest that increased glucose availability impairs SIRT1 mediated deacetylation leading to increased inflammatory cytokine secretion and expression of pro-inflammatory miRs. These changes may contribute to, and perpetuate the inflammatory response observed with increased age, obesity and diabetes, playing a role in the development of long term complications.

7   References

Abrink, M., A. E. Gobl, R. Huang, K. Nilsson and L. Hellman (1994). "Human cell lines U-937, THP-1 and Mono Mac 6 represent relatively immature cells of the monocyte-macrophage cell lineage." Leukemia **8**(9): 1579-1584.

Abu El-Asrar, A. M., M. I. Nawaz, M. M. Siddiquei, A. S. Al-Kharashi, D. Kangave and G. Mohammad (2013). "High-mobility group box-1 induces decreased brain-derived neurotrophic factor-mediated neuroprotection in the diabetic retina." Mediators Inflamm **2013**: 863036.

Ach, R. A., H. Wang and B. Curry (2008). "Measuring microRNAs: comparisons of microarray and quantitative PCR measurements, and of different total RNA prep methods." BMC Biotechnol **8**: 69.

Alexopoulou, L., A. C. Holt, R. Medzhitov and R. A. Flavell (2001). "Recognition of double-stranded RNA and activation of NF-kappaB by Toll-like receptor 3." Nature **413**(6857): 732-738.

Alipour, M. R., A. M. Khamaneh, N. Yousefzadeh, D. Mohammad-nejad and F. G. Soufi (2013). "Upregulation of microRNA-146a was not accompanied by downregulation of pro-inflammatory markers in diabetic kidney." Mol Biol Rep **40**(11): 6477-6483.

Amos, A. F., D. J. McCarty and P. Zimmet (1997). "The rising global burden of diabetes and its complications: estimates and projections to the year 2010." Diabet Med **14 Suppl 5**: S1-85.

Antal-Szalmas, P., J. A. Strijp, A. J. Weersink, J. Verhoef and K. P. Van Kessel (1997). "Quantitation of surface CD14 on human monocytes and neutrophils." J Leukoc Biol **61**(6): 721-728.

Arkan, M. C., A. L. Hevener, F. R. Greten, S. Maeda, Z. W. Li, J. M. Long, A. Wynshaw-Boris, G. Poli, J. Olefsky and M. Karin (2005). "IKK-beta links inflammation to obesity-induced insulin resistance." Nat Med **11**(2): 191-198.

Aron-Wisnewsky, J., J. Tordjman, C. Poitou, F. Darakhshan, D. Hugol, A. Basdevant, A. Aissat, M. Guerre-Millo and K. Clement (2009). "Human adipose tissue macrophages: m1 and m2 cell surface markers in subcutaneous and omental depots and after weight loss." J Clin Endocrinol Metab **94**(11): 4619-4623.

Asirvatham, A. J., C. J. Gregorie, Z. Hu, W. J. Magner and T. B. Tomasi (2008). "MicroRNA targets in immune genes and the Dicer/Argonaute and ARE machinery components." Mol Immunol **45**(7): 1995-2006.

Avruch, J. (1998). "Insulin signal transduction through protein kinase cascades." Mol Cell Biochem **182**(1-2): 31-48.

Babaev, V. R., L. A. Gleaves, K. J. Carter, H. Suzuki, T. Kodama, S. Fazio and M. F. Linton (2000). "Reduced atherosclerotic lesions in mice deficient for total or macrophage-specific expression of scavenger receptor-A." Arterioscler Thromb Vasc Biol **20**(12): 2593-2599.

Babina, M. and B. M. Henz (2003). "All-trans retinoic acid down-regulates expression and function of beta2 integrins by human monocytes: opposite effects on monocytic cell lines." Eur J Immunol **33**(3): 616-625.

Baek, Y. S., S. Haas, H. Hackstein, G. Bein, M. Hernandez-Santana, H. Lehrach, S. Sauer and H. Seitz (2009). "Identification of novel transcriptional regulators involved in macrophage differentiation and activation in U937 cells." BMC Immunol **10**: 18.

Baillie, A. G., C. T. Coburn and N. A. Abumrad (1996). "Reversible binding of long-chain fatty acids to purified FAT, the adipose CD36 homolog." J Membr Biol **153**(1): 75-81.

Balasubramanyam, M., S. Aravind, K. Gokulakrishnan, P. Prabu, C. Sathishkumar, H. Ranjani and V. Mohan (2011). "Impaired miR-146a expression links subclinical inflammation and insulin resistance in Type 2 diabetes." Mol Cell Biochem **351**(1-2): 197-205.

Baldeon, R. L., K. Weigelt, H. de Wit, B. Ozcan, A. van Oudenaren, F. Sempertegui, E. Sijbrands, L. Grosse, W. Freire, H. A. Drexhage and P. J. Leenen (2014). "Decreased Serum Level of miR-146a as Sign of Chronic Inflammation in Type 2 Diabetic Patients." PLoS One **9**(12): e115209.

Baldeon, R. L., K. Weigelt, H. de Wit, B. Ozcan, A. van Oudenaren, F. Sempertegui, E. Sijbrands, L. Grosse, A. J. van Zonneveld, H. A. Drexhage and P. J. Leenen (2015). "Type 2 Diabetes Monocyte

MicroRNA and mRNA Expression: Dyslipidemia Associates with Increased Differentiation-Related Genes but Not Inflammatory Activation." PLoS One **10**(6): e0129421.

Bao, J. and M. N. Sack (2010). "Protein deacetylation by sirtuins: delineating a post-translational regulatory program responsive to nutrient and redox stressors." Cell Mol Life Sci **67**(18): 3073-3087.

Bekkering, S., J. Quintin, L. A. B. Joosten, J. W. M. van der Meer, M. G. Netea and N. P. Riksen (2014). "Oxidized Low-Density Lipoprotein Induces Long-Term Proinflammatory Cytokine Production and Foam Cell Formation via Epigenetic Reprogramming of Monocytes." Arteriosclerosis, Thrombosis, and Vascular Biology **34**(8): 1731-1738.

Belge, K. U., F. Dayyani, A. Horelt, M. Siedlar, M. Frankenberger, B. Frankenberger, T. Espevik and L. Ziegler-Heitbrock (2002). "The proinflammatory CD14+CD16+DR++ monocytes are a major source of TNF." J Immunol **168**(7): 3536-3542.

Benjamini, Y. and Y. Hochberg (1995). "Controlling the False Discovery Rate: A Practical and Powerful Approach to Multiple Testing." Journal of the Royal Statistical Society. Series B (Methodological) **57**(1): 289-300.

Berger, S. L., T. Kouzarides, R. Shiekhattar and A. Shilatifard (2009). "An operational definition of epigenetics." Genes Dev **23**(7): 781-783.

Berrington de Gonzalez, A., P. Hartge, J. R. Cerhan, A. J. Flint, L. Hannan, R. J. MacInnis, S. C. Moore, G. S. Tobias, H. Anton-Culver, L. B. Freeman, W. L. Beeson, S. L. Clipp, D. R. English, A. R. Folsom, D. M. Freedman, G. Giles, N. Hakansson, K. D. Henderson, J. Hoffman-Bolton, J. A. Hoppin, K. L. Koenig, I. M. Lee, M. S. Linet, Y. Park, G. Pocobelli, A. Schatzkin, H. D. Sesso, E. Weiderpass, B. J. Willcox, A. Wolk, A. Zeleniuch-Jacquotte, W. C. Willett and M. J. Thun (2010). "Body-mass index and mortality among 1.46 million white adults." N Engl J Med **363**(23): 2211-2219.

Bhaumik, D., G. K. Scott, S. Schokrpur, C. K. Patil, J. Campisi and C. C. Benz (2008). "Expression of microRNA-146 suppresses NF-kappaB activity with reduction of metastatic potential in breast cancer cells." Oncogene **27**(42): 5643-5647.

Bhaumik, D., G. K. Scott, S. Schokrpur, C. K. Patil, A. V. Orjalo, F. Rodier, G. J. Lithgow and J. Campisi (2009). "MicroRNAs miR-146a/b negatively modulate the senescence-associated inflammatory mediators IL-6 and IL-8." Aging (Albany NY) **1**(4): 402-411.

Bird, A. (2007). "Perceptions of epigenetics." Nature **447**(7143): 396-398.

Bird, A. (2007). "Perceptions of epigenetics." Nature **447**(7143): 396-398.

Bird, A. P. (1980). "DNA methylation and the frequency of CpG in animal DNA." Nucleic Acids Res **8**(7): 1499-1504.

Bojsen-Moller, K. N., C. Dirksen, N. B. Jorgensen, S. H. Jacobsen, A. K. Serup, P. H. Albers, D. L. Hansen, D. Worm, L. Naver, V. B. Kristiansen, J. F. Wojtaszewski, B. Kiens, J. J. Holst, E. A. Richter and S. Madsbad (2014). "Early enhancements of hepatic and later of peripheral insulin sensitivity combined with increased postprandial insulin secretion contribute to improved glycemic control after Roux-en-Y gastric bypass." Diabetes **63**(5): 1725-1737.

Bonaldi, T., F. Talamo, P. Scaffidi, D. Ferrera, A. Porto, A. Bachi, A. Rubartelli, A. Agresti and M. E. Bianchi (2003). "Monocytic cells hyperacetylate chromatin protein HMGB1 to redirect it towards secretion." Embo j **22**(20): 5551-5560.

Boney, C. M., A. Verma, R. Tucker and B. R. Vohr (2005). "Metabolic syndrome in childhood: association with birth weight, maternal obesity, and gestational diabetes mellitus." Pediatrics **115**(3): e290-296.

Borchert, G. M., W. Lanier and B. L. Davidson (2006). "RNA polymerase III transcribes human microRNAs." Nat Struct Mol Biol **13**(12): 1097-1101.

Borisenko, O., D. Adam, P. Funch-Jensen, A. R. Ahmed, R. Zhang, Z. Colpan and J. Hedenbro (2015). "Bariatric Surgery can Lead to Net Cost Savings to Health Care Systems: Results from a Comprehensive European Decision Analytic Model." Obes Surg.

Boutet, S. C., T. H. Cheung, N. L. Quach, L. Liu, S. L. Prescott, A. Edalati, K. Iori and T. A. Rando (2012). "Alternative polyadenylation mediates microRNA regulation of muscle stem cell function." Cell Stem Cell **10**(3): 327-336.

Boyum, A. (1968). "Separation of leukocytes from blood and bone marrow." <u>Scand J Clin Lab Invest Suppl</u> **97**: 7.

Braidy, N., G. J. Guillemin, H. Mansour, T. Chan-Ling, A. Poljak and R. Grant (2011). "Age related changes in NAD+ metabolism oxidative stress and Sirt1 activity in wistar rats." <u>PLoS One</u> **6**(4): e19194.

Breitenstein, A., S. Stein, E. W. Holy, G. G. Camici, C. Lohmann, A. Akhmedov, R. Spescha, P. J. Elliott, C. H. Westphal, C. M. Matter, T. F. Luscher and F. C. Tanner (2011). "Sirt1 inhibition promotes in vivo arterial thrombosis and tissue factor expression in stimulated cells." <u>Cardiovasc Res</u> **89**(2): 464-472.

Brenseke, B., M. R. Prater, J. Bahamonde and J. C. Gutierrez (2013). "Current thoughts on maternal nutrition and fetal programming of the metabolic syndrome." <u>J Pregnancy</u> **2013**: 368461.

Brethauer, S. A., A. Aminian, H. Romero-Talamas, E. Batayyah, J. Mackey, L. Kennedy, S. R. Kashyap, J. P. Kirwan, T. Rogula, M. Kroh, B. Chand and P. R. Schauer (2013). "Can diabetes be surgically cured? Long-term metabolic effects of bariatric surgery in obese patients with type 2 diabetes mellitus." <u>Ann Surg</u> **258**(4): 628-636; discussion 636-627.

Brownlee, M. (2005). "The pathobiology of diabetic complications: a unifying mechanism." <u>Diabetes</u> **54**(6): 1615-1625.

Brunet, A., L. B. Sweeney, J. F. Sturgill, K. F. Chua, P. L. Greer, Y. Lin, H. Tran, S. E. Ross, R. Mostoslavsky, H. Y. Cohen, L. S. Hu, H. L. Cheng, M. P. Jedrychowski, S. P. Gygi, D. A. Sinclair, F. W. Alt and M. E. Greenberg (2004). "Stress-dependent regulation of FOXO transcription factors by the SIRT1 deacetylase." <u>Science</u> **303**(5666): 2011-2015.

Buchwald, H., Y. Avidor, E. Braunwald, M. D. Jensen, W. Pories, K. Fahrbach and K. Schoelles (2004). "Bariatric surgery: a systematic review and meta-analysis." <u>Jama</u> **292**(14): 1724-1737.

Bull, P. C., G. R. Thomas, J. M. Rommens, J. R. Forbes and D. W. Cox (1993). "The Wilson disease gene is a putative copper transporting P-type ATPase similar to the Menkes gene." <u>Nat Genet</u> **5**(4): 327-337.

Calanna, S., M. Christensen, J. J. Holst, B. Laferrere, L. L. Gluud, T. Vilsboll and F. K. Knop (2013). "Secretion of glucagon-like peptide-1 in patients with type 2 diabetes mellitus: systematic review and meta-analyses of clinical studies." <u>Diabetologia</u> **56**(5): 965-972.

Calin, G. A., C. D. Dumitru, M. Shimizu, R. Bichi, S. Zupo, E. Noch, H. Aldler, S. Rattan, M. Keating, K. Rai, L. Rassenti, T. Kipps, M. Negrini, F. Bullrich and C. M. Croce (2002). "Frequent deletions and down-regulation of micro- RNA genes miR15 and miR16 at 13q14 in chronic lymphocytic leukemia." <u>Proc Natl Acad Sci U S A</u> **99**(24): 15524-15529.

Caricilli, A. M., P. H. Nascimento, J. R. Pauli, D. M. Tsukumo, L. A. Velloso, J. B. Carvalheira and M. J. Saad (2008). "Inhibition of toll-like receptor 2 expression improves insulin sensitivity and signaling in muscle and white adipose tissue of mice fed a high-fat diet." <u>J Endocrinol</u> **199**(3): 399-406.

Ceolotto, G., S. V. De Kreutzenberg, A. Cattelan, A. S. Fabricio, E. Squarcina, M. Gion, A. Semplicini, G. P. Fadini and A. Avogaro (2014). "Sirtuin 1 stabilization by HuR represses TNF-alpha- and glucose-induced E-selectin release and endothelial cell adhesiveness in vitro: relevance to human metabolic syndrome." <u>Clin Sci (Lond)</u> **127**(7): 449-461.

Chae, Y. K., S. K. Kang, M. S. Kim, J. Woo, J. Lee, S. Chang, D. W. Kim, M. Kim, S. Park, I. Kim, B. Keam, J. Rhee, N. H. Koo, G. Park, S. H. Kim, S. E. Jang, I. Y. Kweon, D. Sidransky and C. Moon (2008). "Human AQP5 plays a role in the progression of chronic myelogenous leukemia (CML)." <u>PLoS One</u> **3**(7): e2594.

Chang, T. W. (1983). "Binding of cells to matrixes of distinct antibodies coated on solid surface." <u>J Immunol Methods</u> **65**(1-2): 217-223.

Chen, C. W. and C. A. Thomas, Jr. (1980). "Recovery of DNA segments from agarose gels." <u>Anal Biochem</u> **101**(2): 339-341.

Chen, J., F. M. Ghazawi and Q. Li (2010). "Interplay of bromodomain and histone acetylation in the regulation of p300-dependent genes." <u>Epigenetics</u> **5**(6): 509-515.

Chen, L. F., Y. Mu and W. C. Greene (2002). "Acetylation of RelA at discrete sites regulates distinct nuclear functions of NF-kappaB." <u>Embo j</u> **21**(23): 6539-6548.

Chen, L. F., S. A. Williams, Y. Mu, H. Nakano, J. M. Duerr, L. Buckbinder and W. C. Greene (2005). "NF-kappaB RelA phosphorylation regulates RelA acetylation." Mol Cell Biol **25**(18): 7966-7975.

Chen, Y., J. A. Gelfond, L. M. McManus and P. K. Shireman (2009). "Reproducibility of quantitative RT-PCR array in miRNA expression profiling and comparison with microarray analysis." BMC Genomics **10**: 407.

Chendrimada, T. P., K. J. Finn, X. Ji, D. Baillat, R. I. Gregory, S. A. Liebhaber, A. E. Pasquinelli and R. Shiekhattar (2007). "MicroRNA silencing through RISC recruitment of eIF6." Nature **447**(7146): 823-828.

Chesnutt, B. C., D. F. Smith, N. A. Raffler, M. L. Smith, E. J. White and K. Ley (2006). "Induction of LFA-1-dependent neutrophil rolling on ICAM-1 by engagement of E-selectin." Microcirculation **13**(2): 99-109.

Cheung, A. T., D. Ree, J. K. Kolls, J. Fuselier, D. H. Coy and M. Bryer-Ash (1998). "An in vivo model for elucidation of the mechanism of tumor necrosis factor-alpha (TNF-alpha)-induced insulin resistance: evidence for differential regulation of insulin signaling by TNF-alpha." Endocrinology **139**(12): 4928-4935.

Cheung, A. T., J. Wang, D. Ree, J. K. Kolls and M. Bryer-Ash (2000). "Tumor necrosis factor-alpha induces hepatic insulin resistance in obese Zucker (fa/fa) rats via interaction of leukocyte antigen-related tyrosine phosphatase with focal adhesion kinase." Diabetes **49**(5): 810-819.

Chomczynski, P. and N. Sacchi (1987). "Single-step method of RNA isolation by acid guanidinium thiocyanate-phenol-chloroform extraction." Anal Biochem **162**(1): 156-159.

Christou, N. V., D. Look and L. D. Maclean (2006). "Weight gain after short- and long-limb gastric bypass in patients followed for longer than 10 years." Ann Surg **244**(5): 734-740.

Clement, K., C. Vaisse, N. Lahlou, S. Cabrol, V. Pelloux, D. Cassuto, M. Gourmelen, C. Dina, J. Chambaz, J. M. Lacorte, A. Basdevant, P. Bougneres, Y. Lebouc, P. Froguel and B. Guy-Grand (1998). "A mutation in the human leptin receptor gene causes obesity and pituitary dysfunction." Nature **392**(6674): 398-401.

Cornwell, W., M. Vega and T. Rogers (2013). Monocyte Populations Which Participate in Chronic Lung Inflammation. Smoking and Lung Inflammation. T. J. Rogers, G. J. Criner and W. D. Cornwell, Springer New York**:** 29-58.

Cros, J., N. Cagnard, K. Woollard, N. Patey, S. Y. Zhang, B. Senechal, A. Puel, S. K. Biswas, D. Moshous, C. Picard, J. P. Jais, D. D'Cruz, J. L. Casanova, C. Trouillet and F. Geissmann (2010). "Human CD14dim monocytes patrol and sense nucleic acids and viruses via TLR7 and TLR8 receptors." Immunity **33**(3): 375-386.

Cuschieri, J., D. Gourlay, I. Garcia, S. Jelacic and R. V. Maier (2002). "Hypertonic preconditioning inhibits macrophage responsiveness to endotoxin." J Immunol **168**(3): 1389-1396.

Dahl, J. A. and P. Collas (2009). "MicroChIP: chromatin immunoprecipitation for small cell numbers." Methods Mol Biol **567**: 59-74.

Dandona, P., A. Aljada and A. Bandyopadhyay (2004). "Inflammation: the link between insulin resistance, obesity and diabetes." Trends Immunol **25**(1): 4-7.

Dasu, M. R., S. Devaraj, L. Zhao, D. H. Hwang and I. Jialal (2008). "High glucose induces toll-like receptor expression in human monocytes: mechanism of activation." Diabetes **57**(11): 3090-3098.

Dasu, M. R. and I. Jialal (2011). "Free fatty acids in the presence of high glucose amplify monocyte inflammation via Toll-like receptors." Am J Physiol Endocrinol Metab **300**(1): E145-154.

Davis, B. J. and L. Ornstein (1959). "A new high resolution electrophoresis method." Delivered at The Society for the Study of Blood at the New York Academy of Medicine.

Decker, T. and P. Kovarik (2000). "Serine phosphorylation of STATs." Oncogene **19**(21): 2628-2637.

Deiuliis, J. A. (2015). "MicroRNAs as regulators of metabolic disease: Pathophysiologic significance and emerging role as biomarkers and therapeutics." Int J Obes (Lond).

Devitt, A. and C. Gregory (2008). Innate immune mechanisms in the resolution of inflammation. The Resolution of Inflammation. A. Rossi and D. Sawatzky, Birkhäuser Basel**:** 39-56.

Devitt, A., S. Pierce, C. Oldreive, W. H. Shingler and C. D. Gregory (2003). "CD14-dependent clearance of apoptotic cells by human macrophages: the role of phosphatidylserine." Cell Death Differ **10**(3): 371-382.

DiLella, A. G., S. C. M. Kwok, F. D. Ledley, J. Marvit and S. L. C. Woo (1986). "Molecular structure and polymorphic map of the human phenylalanine hydroxylase gene." Biochemistry **25**(4): 743-749.

Dixon, J. B., P. E. O'Brien, J. Playfair, L. Chapman, L. M. Schachter, S. Skinner, J. Proietto, M. Bailey and M. Anderson (2008). "Adjustable gastric banding and conventional therapy for type 2 diabetes: a randomized controlled trial." Jama **299**(3): 316-323.

Docherty, P. A. and M. D. Snider (1991). "Effects of hypertonic and sodium-free medium on transport of a membrane glycoprotein along the secretory pathway in cultured mammalian cells." J Cell Physiol **146**(1): 34-42.

Dokmanovic, M., C. Clarke and P. A. Marks (2007). "Histone deacetylase inhibitors: overview and perspectives." Mol Cancer Res **5**(10): 981-989.

Domer, P. H., S. S. Fakharzadeh, C. S. Chen, J. Jockel, L. Johansen, G. A. Silverman, J. H. Kersey and S. J. Korsmeyer (1993). "Acute mixed-lineage leukemia t(4;11)(q21;q23) generates an MLL-AF4 fusion product." Proc Natl Acad Sci U S A **90**(16): 7884-7888.

Dunne, J. L., C. M. Ballantyne, A. L. Beaudet and K. Ley (2002). "Control of leukocyte rolling velocity in TNF-alpha-induced inflammation by LFA-1 and Mac-1." Blood **99**(1): 336-341.

El Gazzar, M. (2007). "HMGB1 modulates inflammatory responses in LPS-activated macrophages." Inflamm Res **56**(4): 162-167.

ElSharawy, A., A. Keller, F. Flachsbart, A. Wendschlag, G. Jacobs, N. Kefer, T. Brefort, P. Leidinger, C. Backes, E. Meese, S. Schreiber, P. Rosenstiel, A. Franke and A. Nebel (2012). "Genome-wide miRNA signatures of human longevity." Aging Cell **11**(4): 607-616.

Endemann, G., L. W. Stanton, K. S. Madden, C. M. Bryant, R. T. White and A. A. Protter (1993). "CD36 is a receptor for oxidized low density lipoprotein." J Biol Chem **268**(16): 11811-11816.

Erbel, C., G. Rupp, G. Domschke, F. Linden, M. Akhavanpoor, A. O. Doesch, H. A. Katus and C. A. Gleissner (2016). "Differential regulation of aldose reductase expression during macrophage polarization depends on hyperglycemia." Innate Immun **22**(3): 230-237.

Fabian, M. R., N. Sonenberg and W. Filipowicz (2010). "Regulation of mRNA translation and stability by microRNAs." Annu Rev Biochem **79**: 351-379.

Fang, Z. and N. Rajewsky (2011). "The impact of miRNA target sites in coding sequences and in 3'UTRs." PLoS One **6**(3): e18067.

Faxon, D. P., M. A. Creager, S. C. Smith, R. C. Pasternak, J. W. Olin, M. A. Bettmann, M. H. Criqui, R. V. Milani, J. Loscalzo, J. A. Kaufman, D. W. Jones and W. H. Pearce (2004). "Atherosclerotic Vascular Disease Conference: Executive Summary: Atherosclerotic Vascular Disease Conference Proceeding for Healthcare Professionals From a Special Writing Group of the American Heart Association." Circulation **109**(21): 2595-2604.

Febbraio, M., E. A. Podrez, J. D. Smith, D. P. Hajjar, S. L. Hazen, H. F. Hoff, K. Sharma and R. L. Silverstein (2000). "Targeted disruption of the class B scavenger receptor CD36 protects against atherosclerotic lesion development in mice." J Clin Invest **105**(8): 1049-1056.

Federation, I. D. (2014). DF Diabetes Atlas update poster. I. D. Federation. Brussels, Belgium. **6th edn**.

Feng, B., S. Chen, K. McArthur, Y. Wu, S. Sen, Q. Ding, R. D. Feldman and S. Chakrabarti (2011). "miR-146a-Mediated extracellular matrix protein production in chronic diabetes complications." Diabetes **60**(11): 2975-2984.

Feng, C.-L. and H.-C. Chou (2014). "Hyperglycemia initiates N-cadherin rearrangement and diabetic monocytes promote inflammatory responses in human microvascular endothelial cells." Biomarkers and Genomic Medicine **6**(4): 175-179.

Feng, D., J. A. Nagy, K. Pyne, H. F. Dvorak and A. M. Dvorak (1998). "Neutrophils emigrate from venules by a transendothelial cell pathway in response to FMLP." J Exp Med **187**(6): 903-915.

Feng, J., J. Han, S. F. Pearce, R. L. Silverstein, A. M. Gotto, Jr., D. P. Hajjar and A. C. Nicholson (2000). "Induction of CD36 expression by oxidized LDL and IL-4 by a common signaling pathway dependent on protein kinase C and PPAR-gamma." J Lipid Res **41**(5): 688-696.

Fischer-Posovszky, P., J. B. Funcke and M. Wabitsch (2015). "Biologically inactive leptin and early-onset extreme obesity." N Engl J Med **372**(13): 1266-1267.

Fischer, S., A. J. Paul, A. Wagner, S. Mathias, M. Geiss, F. Schandock, M. Domnowski, J. Zimmermann, R. Handrick, F. Hesse and K. Otte (2015). "miR-2861 as novel HDAC5 inhibitor in CHO cells enhances productivity while maintaining product quality." Biotechnol Bioeng.

Flegal, K. M., B. K. Kit, H. Orpana and B. I. Graubard (2013). "Association of all-cause mortality with overweight and obesity using standard body mass index categories: a systematic review and meta-analysis." Jama **309**(1): 71-82.

Fleit, H. B. and C. D. Kobasiuk (1991). "The human monocyte-like cell line THP-1 expresses Fc gamma RI and Fc gamma RII." J Leukoc Biol **49**(6): 556-565.

Franceschi, C., M. Bonafe, S. Valensin, F. Olivieri, M. De Luca, E. Ottaviani and G. De Benedictis (2000). "Inflamm-aging. An evolutionary perspective on immunosenescence." Ann N Y Acad Sci **908**: 244-254.

Franceschi, C., M. Capri, D. Monti, S. Giunta, F. Olivieri, F. Sevini, M. P. Panourgia, L. Invidia, L. Celani, M. Scurti, E. Cevenini, G. C. Castellani and S. Salvioli (2007). "Inflammaging and anti-inflammaging: a systemic perspective on aging and longevity emerged from studies in humans." Mech Ageing Dev **128**(1): 92-105.

Frankenberger, M., T. Sternsdorf, H. Pechumer, A. Pforte and H. W. Ziegler-Heitbrock (1996). "Differential cytokine expression in human blood monocyte subpopulations: a polymerase chain reaction analysis." Blood **87**(1): 373-377.

Frenkel, O., E. Shani, I. Ben-Bassat, F. Brok-Simoni, E. Shinar and D. Danon (2001). "Activation of human monocytes/macrophages by hypo-osmotic shock." Clin Exp Immunol **124**(1): 103-109.

Friedewald, W. T., R. I. Levy and D. S. Fredrickson (1972). "Estimation of the Concentration of Low-Density Lipoprotein Cholesterol in Plasma, Without Use of the Preparative Ultracentrifuge." Clinical Chemistry **18**(6): 499-502.

Fu, X., B. Dong, Y. Tian, P. Lefebvre, Z. Meng, X. Wang, F. Pattou, W. Han, X. Wang, F. Lou, R. Jove, B. Staels, D. D. Moore and W. Huang (2015). "MicroRNA-26a regulates insulin sensitivity and metabolism of glucose and lipids." J Clin Invest **125**(6): 2497-2509.

Fukuhara-Takaki, K., M. Sakai, Y. Sakamoto, M. Takeya and S. Horiuchi (2005). "Expression of class A scavenger receptor is enhanced by high glucose in vitro and under diabetic conditions in vivo: one mechanism for an increased rate of atherosclerosis in diabetes." J Biol Chem **280**(5): 3355-3364.

Fulco, M., Y. Cen, P. Zhao, E. P. Hoffman, M. W. McBurney, A. A. Sauve and V. Sartorelli (2008). "Glucose restriction inhibits skeletal myoblast differentiation by activating SIRT1 through AMPK-mediated regulation of Nampt." Dev Cell **14**(5): 661-673.

Furukawa, S., T. Fujita, M. Shimabukuro, M. Iwaki, Y. Yamada, Y. Nakajima, O. Nakayama, M. Makishima, M. Matsuda and I. Shimomura (2004). "Increased oxidative stress in obesity and its impact on metabolic syndrome." J Clin Invest **114**(12): 1752-1761.

Gagnon, A., S. Lau and A. Sorisky (2001). "Rapamycin-sensitive phase of 3T3-L1 preadipocyte differentiation after clonal expansion." J Cell Physiol **189**(1): 14-22.

Gao, M., X. Wang, X. Zhang, T. Ha, H. Ma, L. Liu, J. H. Kalbfleisch, X. Gao, R. L. Kao, D. L. Williams and C. Li (2015). "Attenuation of Cardiac Dysfunction in Polymicrobial Sepsis by MicroRNA-146a Is Mediated via Targeting of IRAK1 and TRAF6 Expression." J Immunol.

Gao, Z., X. Zhang, A. Zuberi, D. Hwang, M. J. Quon, M. Lefevre and J. Ye (2004). "Inhibition of insulin sensitivity by free fatty acids requires activation of multiple serine kinases in 3T3-L1 adipocytes." Mol Endocrinol **18**(8): 2024-2034.

Gatenby, R. A. and R. J. Gillies (2004). "Why do cancers have high aerobic glycolysis?" Nat Rev Cancer **4**(11): 891-899.

Gatineau Mary, H. C., Holman Naomi, Outhwaite Helen, Oldridge Lorraine, Christie Anna and Ells Louisa (2014). Adult obesity and type 2 diabetes. P. H. England. Oxford.

Ghattas, A., H. R. Griffiths, A. Devitt, G. Y. Lip and E. Shantsila (2013). "Monocytes in coronary artery disease and atherosclerosis: where are we now?" J Am Coll Cardiol 62(17): 1541-1551.

Ghosh, H. S., M. McBurney and P. D. Robbins (2010). "SIRT1 negatively regulates the mammalian target of rapamycin." PLoS One 5(2): e9199.

Gillum, M. P., M. E. Kotas, D. M. Erion, R. Kursawe, P. Chatterjee, K. T. Nead, E. S. Muise, J. J. Hsiao, D. W. Frederick, S. Yonemitsu, A. S. Banks, L. Qiang, S. Bhanot, J. M. Olefsky, D. D. Sears, S. Caprio and G. I. Shulman (2011). "SirT1 Regulates Adipose Tissue Inflammation." Diabetes 60(12): 3235-3245.

Giulietti, A., E. van Etten, L. Overbergh, K. Stoffels, R. Bouillon and C. Mathieu (2007). "Monocytes from type 2 diabetic patients have a pro-inflammatory profile. 1,25-Dihydroxyvitamin D(3) works as anti-inflammatory." Diabetes Res Clin Pract 77(1): 47-57.

Godfrey, K. M., A. Sheppard, P. D. Gluckman, K. A. Lillycrop, G. C. Burdge, C. McLean, J. Rodford, J. L. Slater-Jefferies, E. Garratt, S. R. Crozier, B. S. Emerald, C. R. Gale, H. M. Inskip, C. Cooper and M. A. Hanson (2011). "Epigenetic gene promoter methylation at birth is associated with child's later adiposity." Diabetes 60(5): 1528-1534.

Gonzalez-Gay, M. A., J. M. De Matias, C. Gonzalez-Juanatey, C. Garcia-Porrua, A. Sanchez-Andrade, J. Martin and J. Llorca (2006). "Anti-tumor necrosis factor-alpha blockade improves insulin resistance in patients with rheumatoid arthritis." Clin Exp Rheumatol 24(1): 83-86.

Gonzalez, Y., M. T. Herrera, G. Soldevila, L. Garcia-Garcia, G. Fabian, E. M. Perez-Armendariz, K. Bobadilla, S. Guzman-Beltran, E. Sada and M. Torres (2012). "High glucose concentrations induce TNF-alpha production through the down-regulation of CD33 in primary human monocytes." BMC Immunol 13: 19.

Gordon, E. S. (1960). "Non-Esterified Fatty Acids in the Blood of Obese and Lean Subjects." The American Journal of Clinical Nutrition 8(5): 740-747.

Graff, J. W., A. M. Dickson, G. Clay, A. P. McCaffrey and M. E. Wilson (2012). "Identifying functional microRNAs in macrophages with polarized phenotypes." J Biol Chem 287(26): 21816-21825.

Greco, S., P. Fasanaro, S. Castelvecchio, Y. D'Alessandra, D. Arcelli, M. Di Donato, A. Malavazos, M. C. Capogrossi, L. Menicanti and F. Martelli (2012). "MicroRNA dysregulation in diabetic ischemic heart failure patients." Diabetes 61(6): 1633-1641.

Grimshaw, C. E. (1986). "Direct measurement of the rate of ring opening of D-glucose by enzyme-catalyzed reduction." Carbohydr Res 148(2): 345-348.

Guha, M., W. Bai, J. L. Nadler and R. Natarajan (2000). "Molecular mechanisms of tumor necrosis factor alpha gene expression in monocytic cells via hyperglycemia-induced oxidant stress-dependent and -independent pathways." J Biol Chem 275(23): 17728-17739.

Guo, J. U., Y. Su, C. Zhong, G. L. Ming and H. Song (2011). "Hydroxylation of 5-methylcytosine by TET1 promotes active DNA demethylation in the adult brain." Cell 145(3): 423-434.

Haigis, M. C. and D. A. Sinclair (2010). "Mammalian sirtuins: biological insights and disease relevance." Annu Rev Pathol 5: 253-295.

Hales, C. N. and D. J. Barker (1992). "Type 2 (non-insulin-dependent) diabetes mellitus: the thrifty phenotype hypothesis." Diabetologia 35(7): 595-601.

Hamada, Y., N. Araki, S. Horiuchi and N. Hotta (1996). "Role of polyol pathway in nonenzymatic glycation." Nephrol Dial Transplant 11 Suppl 5: 95-98.

Han, J., D. P. Hajjar, M. Febbraio and A. C. Nicholson (1997). "Native and modified low density lipoproteins increase the functional expression of the macrophage class B scavenger receptor, CD36." J Biol Chem 272(34): 21654-21659.

Han, J., Y. Lee, K. H. Yeom, Y. K. Kim, H. Jin and V. N. Kim (2004). "The Drosha-DGCR8 complex in primary microRNA processing." Genes Dev 18(24): 3016-3027.

Hancu, N., M. G. Netea and I. Baciu (1998). "High glucose concentrations increase the tumor necrosis factor-alpha production capacity by human peripheral blood mononuclear cells." Rom J Physiol 35(3-4): 325-330.

Harrison, D. E., R. Strong, Z. D. Sharp, J. F. Nelson, C. M. Astle, K. Flurkey, N. L. Nadon, J. E. Wilkinson, K. Frenkel, C. S. Carter, M. Pahor, M. A. Javors, E. Fernandez and R. A. Miller (2009). "Rapamycin fed late in life extends lifespan in genetically heterogeneous mice." Nature 460(7253): 392-395.

Hashimoto, C., K. L. Hudson and K. V. Anderson (1988). "The Toll gene of Drosophila, required for dorsal-ventral embryonic polarity, appears to encode a transmembrane protein." Cell 52(2): 269-279.

Hayashi, F., K. D. Smith, A. Ozinsky, T. R. Hawn, E. C. Yi, D. R. Goodlett, J. K. Eng, S. Akira, D. M. Underhill and A. Aderem (2001). "The innate immune response to bacterial flagellin is mediated by Toll-like receptor 5." Nature 410(6832): 1099-1103.

Heiss, G., I. Tamir, C. E. Davis, H. A. Tyroler, B. M. Rifkand, G. Schonfeld, D. Jacobs and I. D. Frantz, Jr. (1980). "Lipoprotein-cholesterol distributions in selected North American populations: the lipid research clinics program prevalence study." Circulation 61(2): 302-315.

Heitmann, B. L. (1992). "The effects of gender and age on associations between blood lipid levels and obesity in Danish men and women aged 35-65 years." J Clin Epidemiol 45(7): 693-702.

Herst, P. M., R. A. Howman, P. J. Neeson, M. V. Berridge and D. S. Ritchie (2011). "The level of glycolytic metabolism in acute myeloid leukemia blasts at diagnosis is prognostic for clinical outcome." J Leukoc Biol 89(1): 51-55.

Hex, N., C. Bartlett, D. Wright, M. Taylor and D. Varley (2012). "Estimating the current and future costs of Type 1 and Type 2 diabetes in the UK, including direct health costs and indirect societal and productivity costs." Diabet Med 29(7): 855-862.

Ho, B. C., I. S. Yu, L. F. Lu, A. Rudensky, H. Y. Chen, C. W. Tsai, Y. L. Chang, C. T. Wu, L. Y. Chang, S. R. Shih, S. W. Lin, C. N. Lee, P. C. Yang and S. L. Yu (2014). "Inhibition of miR-146a prevents enterovirus-induced death by restoring the production of type I interferon." Nat Commun 5: 3344.

Hofer, T. P., A. M. Zawada, M. Frankenberger, K. Skokann, A. A. Satzl, W. Gesierich, M. Schuberth, J. Levin, A. Danek, B. Rotter, G. H. Heine and L. Ziegler-Heitbrock (2015). "slan-defined subsets of CD16-positive monocytes: impact of granulomatous inflammation and M-CSF receptor mutation." Blood 126(24): 2601-2610.

Hulsmans, M., D. De Keyzer and P. Holvoet (2011). "MicroRNAs regulating oxidative stress and inflammation in relation to obesity and atherosclerosis." Faseb j 25(8): 2515-2527.

Huszar, D., C. A. Lynch, V. Fairchild-Huntress, J. H. Dunmore, Q. Fang, L. R. Berkemeier, W. Gu, R. A. Kesterson, B. A. Boston, R. D. Cone, F. J. Smith, L. A. Campfield, P. Burn and F. Lee (1997). "Targeted disruption of the melanocortin-4 receptor results in obesity in mice." Cell 88(1): 131-141.

Ideraabdullah, F. Y., S. Vigneau and M. S. Bartolomei (2008). "Genomic imprinting mechanisms in mammals." Mutat Res 647(1-2): 77-85.

Illingworth, R. S. and A. P. Bird (2009). "CpG islands--'a rough guide'." FEBS Lett 583(11): 1713-1720.

Inagaki, K., I. Miwa and J. Okuda (1982). "Affinity purification and glucose specificity of aldose reductase from bovine lens." Arch Biochem Biophys 216(1): 337-344.

Isbell, J. M., R. A. Tamboli, E. N. Hansen, J. Saliba, J. P. Dunn, S. E. Phillips, P. A. Marks-Shulman and N. N. Abumrad (2010). "The importance of caloric restriction in the early improvements in insulin sensitivity after Roux-en-Y gastric bypass surgery." Diabetes Care 33(7): 1438-1442.

Iwata, H., Y. Soga, M. Meguro, S. Yoshizawa, Y. Okada, Y. Iwamoto, A. Yamashita, S. Takashiba and F. Nishimura (2007). "High glucose up-regulates lipopolysaccharide-stimulated inflammatory cytokine production via c-jun N-terminal kinase in the monocytic cell line THP-1." J Endotoxin Res 13(4): 227-234.

Jayakumar, T., C. C. Chang, S. L. Lin, Y. K. Huang, C. M. Hu, A. R. Elizebeth, S. C. Lin and C. S. Choy (2014). "Brazilin ameliorates high glucose-induced vascular inflammation via inhibiting ROS and CAMs production in human umbilical vein endothelial cells." Biomed Res Int 2014: 403703.

Jenny, N. S. (2012). "Inflammation in aging: cause, effect, or both?" Discov Med 13(73): 451-460.

Jimenez, A., R. Casamitjana, L. Flores, J. Viaplana, R. Corcelles, A. Lacy and J. Vidal (2012). "Long-term effects of sleeve gastrectomy and Roux-en-Y gastric bypass surgery on type 2 diabetes mellitus in morbidly obese subjects." Ann Surg 256(6): 1023-1029.

Jimenez, A., R. Casamitjana, J. Viaplana-Masclans, A. Lacy and J. Vidal (2013). "GLP-1 action and glucose tolerance in subjects with remission of type 2 diabetes after gastric bypass surgery." Diabetes Care **36**(7): 2062-2069.

Jung, S. H., H. S. Park, K. S. Kim, W. H. Choi, C. W. Ahn, B. T. Kim, S. M. Kim, S. Y. Lee, S. M. Ahn, Y. K. Kim, H. J. Kim, D. J. Kim and K. W. Lee (2008). "Effect of weight loss on some serum cytokines in human obesity: increase in IL-10 after weight loss." J Nutr Biochem **19**(6): 371-375.

Kahn, S. E., R. L. Hull and K. M. Utzschneider (2006). "Mechanisms linking obesity to insulin resistance and type 2 diabetes." Nature **444**(7121): 840-846.

Kanda, H., S. Tateya, Y. Tamori, K. Kotani, K. Hiasa, R. Kitazawa, S. Kitazawa, H. Miyachi, S. Maeda, K. Egashira and M. Kasuga (2006). "MCP-1 contributes to macrophage infiltration into adipose tissue, insulin resistance, and hepatic steatosis in obesity." J Clin Invest **116**(6): 1494-1505.

Kanety, H., R. Feinstein, M. Z. Papa, R. Hemi and A. Karasik (1995). "Tumor necrosis factor alpha-induced phosphorylation of insulin receptor substrate-1 (IRS-1). Possible mechanism for suppression of insulin-stimulated tyrosine phosphorylation of IRS-1." J Biol Chem **270**(40): 23780-23784.

Kansas, G. S. (1996). "Selectins and their ligands: current concepts and controversies." Blood **88**(9): 3259-3287.

Kanter, J. E., F. Kramer, S. Barnhart, M. M. Averill, A. Vivekanandan-Giri, T. Vickery, L. O. Li, L. Becker, W. Yuan, A. Chait, K. R. Braun, S. Potter-Perigo, S. Sanda, T. N. Wight, S. Pennathur, C. N. Serhan, J. W. Heinecke, R. A. Coleman and K. E. Bornfeldt (2012). "Diabetes promotes an inflammatory macrophage phenotype and atherosclerosis through acyl-CoA synthetase 1." Proc Natl Acad Sci U S A **109**(12): E715-724.

Kato, H., F. Hayase, D. B. Shin, M. Oimomi and S. Baba (1989). "3-Deoxyglucosone, an intermediate product of the Maillard reaction." Prog Clin Biol Res **304**: 69-84.

Kawai, T., O. Adachi, T. Ogawa, K. Takeda and S. Akira (1999). "Unresponsiveness of MyD88-deficient mice to endotoxin." Immunity **11**(1): 115-122.

Kawai, T., O. Takeuchi, T. Fujita, J. Inoue, P. F. Muhlradt, S. Sato, K. Hoshino and S. Akira (2001). "Lipopolysaccharide stimulates the MyD88-independent pathway and results in activation of IFN-regulatory factor 3 and the expression of a subset of lipopolysaccharide-inducible genes." J Immunol **167**(10): 5887-5894.

Kelly, A. S., D. R. Jacobs, Jr., A. R. Sinaiko, A. Moran, L. M. Steffen and J. Steinberger (2010). "Relation of circulating oxidized LDL to obesity and insulin resistance in children." Pediatr Diabetes **11**(8): 552-555.

Kern, P. A., S. Ranganathan, C. Li, L. Wood and G. Ranganathan (2001). "Adipose tissue tumor necrosis factor and interleukin-6 expression in human obesity and insulin resistance." Am J Physiol Endocrinol Metab **280**(5): E745-751.

Khandany, B. K., G. Hassanshahi, H. Khorramdelazad, Z. Balali, A. Shamsizadeh, M. K. Arababadi, H. Ostadebrahimi, A. Fatehi, M. Rezazadeh, Z. Ahmadi and M. N. Karimabad (2012). "Evaluation of circulating concentrations of CXCL1 (Gro-alpha), CXCL10 (IP-10) and CXCL12 (SDF-1) in ALL patients prior and post bone marrow transplantation." Pathol Res Pract **208**(10): 615-619.

Khaodhiar, L., P. R. Ling, G. L. Blackburn and B. R. Bistrian (2004). "Serum levels of interleukin-6 and C-reactive protein correlate with body mass index across the broad range of obesity." JPEN J Parenter Enteral Nutr **28**(6): 410-415.

Kim, H. J., S. H. Kim and J. M. Yun (2012). "Fisetin inhibits hyperglycemia-induced proinflammatory cytokine production by epigenetic mechanisms." Evid Based Complement Alternat Med **2012**: 639469.

Kim, H. J., W. Lee and J. M. Yun (2014). "Luteolin inhibits hyperglycemia-induced proinflammatory cytokine production and its epigenetic mechanism in human monocytes." Phytother Res **28**(9): 1383-1391.

Kim, S. J., Y. Choi, Y. H. Choi and T. Park (2012). "Obesity activates toll-like receptor-mediated proinflammatory signaling cascades in the adipose tissue of mice." J Nutr Biochem **23**(2): 113-122.

Kindel, T. L., S. M. Yoder, R. J. Seeley, D. A. D'Alessio and P. Tso (2009). "Duodenal-jejunal exclusion improves glucose tolerance in the diabetic, Goto-Kakizaki rat by a GLP-1 receptor-mediated mechanism." J Gastrointest Surg **13**(10): 1762-1772.

Ko, G. T., H. P. Wai and J. S. Tang (2006). "Effects of age on plasma glucose levels in non-diabetic Hong Kong Chinese." Croat Med J **47**(5): 709-713.

Komura, T., Y. Sakai, M. Honda, T. Takamura, K. Matsushima and S. Kaneko (2010). "CD14+ monocytes are vulnerable and functionally impaired under endoplasmic reticulum stress in patients with type 2 diabetes." Diabetes **59**(3): 634-643.

Koscianska, E., J. Starega-Roslan and W. J. Krzyzosiak (2011). "The role of Dicer protein partners in the processing of microRNA precursors." PLoS One **6**(12): e28548.

Kovacs, B., S. Lumayag, C. Cowan and S. Xu (2011). "MicroRNAs in early diabetic retinopathy in streptozotocin-induced diabetic rats." Invest Ophthalmol Vis Sci **52**(7): 4402-4409.

Kraatz, J., L. Clair, J. L. Rodriguez and M. A. West (1999). "Macrophage TNF secretion in endotoxin tolerance: role of SAPK, p38, and MAPK." J Surg Res **83**(2): 158-164.

Kuchibhotla, S., D. Vanegas, D. J. Kennedy, E. Guy, G. Nimako, R. E. Morton and M. Febbraio (2008). "Absence of CD36 protects against atherosclerosis in ApoE knock-out mice with no additional protection provided by absence of scavenger receptor A I/II." Cardiovascular Research **78**(1): 185-196.

Kunjathoor, V. V., M. Febbraio, E. A. Podrez, K. J. Moore, L. Andersson, S. Koehn, J. S. Rhee, R. Silverstein, H. F. Hoff and M. W. Freeman (2002). "Scavenger receptors class A-I/II and CD36 are the principal receptors responsible for the uptake of modified low density lipoprotein leading to lipid loading in macrophages." J Biol Chem **277**(51): 49982-49988.

Lakowski, B. and S. Hekimi (1998). "The genetics of caloric restriction in Caenorhabditis elegans." Proc Natl Acad Sci U S A **95**(22): 13091-13096.

Landthaler, M., A. Yalcin and T. Tuschl (2004). "The human DiGeorge syndrome critical region gene 8 and Its D. melanogaster homolog are required for miRNA biogenesis." Curr Biol **14**(23): 2162-2167.

Laplante, M. and D. M. Sabatini (2012). "mTOR signaling in growth control and disease." Cell **149**(2): 274-293.

Lee, R. C., R. L. Feinbaum and V. Ambros (1993). "The C. elegans heterochronic gene lin-4 encodes small RNAs with antisense complementarity to lin-14." Cell **75**(5): 843-854.

Lee, T. H. and A. D. Linstedt (1999). "Osmotically induced cell volume changes alter anterograde and retrograde transport, Golgi structure, and COPI dissociation." Mol Biol Cell **10**(5): 1445-1462.

Lee, Y., C. Ahn, J. Han, H. Choi, J. Kim, J. Yim, J. Lee, P. Provost, O. Radmark, S. Kim and V. N. Kim (2003). "The nuclear RNase III Drosha initiates microRNA processing." Nature **425**(6956): 415-419.

Lee, Y., M. Kim, J. Han, K. H. Yeom, S. Lee, S. H. Baek and V. N. Kim (2004). "MicroRNA genes are transcribed by RNA polymerase II." Embo j **23**(20): 4051-4060.

Lemaire, J., G. Mkannez, F. Z. Guerfali, C. Gustin, H. Attia, R. M. Sghaier, K. Dellagi, D. Laouini and P. Renard (2013). "MicroRNA expression profile in human macrophages in response to Leishmania major infection." PLoS Negl Trop Dis **7**(10): e2478.

Lemaitre, B., E. Nicolas, L. Michaut, J. M. Reichhart and J. A. Hoffmann (1996). "The dorsoventral regulatory gene cassette spatzle/Toll/cactus controls the potent antifungal response in Drosophila adults." Cell **86**(6): 973-983.

Lewis, B. P., C. B. Burge and D. P. Bartel (2005). "Conserved seed pairing, often flanked by adenosines, indicates that thousands of human genes are microRNA targets." Cell **120**(1): 15-20.

Li, H., H. Xie, W. Liu, R. Hu, B. Huang, Y. F. Tan, K. Xu, Z. F. Sheng, H. D. Zhou, X. P. Wu and X. H. Luo (2009). "A novel microRNA targeting HDAC5 regulates osteoblast differentiation in mice and contributes to primary osteoporosis in humans." J Clin Invest **119**(12): 3666-3677.

Li, J., C. Zhou, J. Li, Z. Su, H. Sang, E. Jia and D. Si (2015). "Global correlation analysis for microRNA and gene expression profiles in human obesity." Pathol Res Pract **211**(5): 361-368.

Li, Q. J., J. Chau, P. J. Ebert, G. Sylvester, H. Min, G. Liu, R. Braich, M. Manoharan, J. Soutschek, P. Skare, L. O. Klein, M. M. Davis and C. Z. Chen (2007). "miR-181a is an intrinsic modulator of T cell sensitivity and selection." <u>Cell</u> **129**(1): 147-161.

Li, X., F. Tian and F. Wang (2013). "Rheumatoid arthritis-associated microRNA-155 targets SOCS1 and upregulates TNF-alpha and IL-1beta in PBMCs." <u>Int J Mol Sci</u> **14**(12): 23910-23921.

Lim, E. L., K. G. Hollingsworth, B. S. Aribisala, M. J. Chen, J. C. Mathers and R. Taylor (2011). "Reversal of type 2 diabetes: normalisation of beta cell function in association with decreased pancreas and liver triacylglycerol." <u>Diabetologia</u> **54**(10): 2506-2514.

Lim, G. E. and P. L. Brubaker (2006). "Glucagon-Like Peptide 1 Secretion by the L-Cell: The View From Within." <u>Diabetes</u> **55**(Supplement 2): S70-S77.

Lim, L. P., N. C. Lau, P. Garrett-Engele, A. Grimson, J. M. Schelter, J. Castle, D. P. Bartel, P. S. Linsley and J. M. Johnson (2005). "Microarray analysis shows that some microRNAs downregulate large numbers of target mRNAs." <u>Nature</u> **433**(7027): 769-773.

Lin, S. J., M. Kaeberlein, A. A. Andalis, L. A. Sturtz, P. A. Defossez, V. C. Culotta, G. R. Fink and L. Guarente (2002). "Calorie restriction extends Saccharomyces cerevisiae lifespan by increasing respiration." <u>Nature</u> **418**(6895): 344-348.

Lin, X., Y. You, J. Wang, Y. Qin, P. Huang and F. Yang (2015). "MicroRNA-155 deficiency promotes nephrin acetylation and attenuates renal damage in hyperglycemia-induced nephropathy." <u>Inflammation</u> **38**(2): 546-554.

Lipman, R. D., D. E. Smith, J. B. Blumberg and R. T. Bronson (1998). "Effects of caloric restriction or augmentation in adult rats: longevity and lesion biomarkers of aging." <u>Aging (Milano)</u> **10**(6): 463-470.

Lirun, K., M. Sewe and W. Yong (2015). "A Pilot Study: The Effect of Roux-en-Y Gastric Bypass on the Serum MicroRNAs of the Type 2 Diabetes Patient." <u>Obes Surg</u>.

Liu, G. and E. Abraham (2013). "MicroRNAs in immune response and macrophage polarization." <u>Arterioscler Thromb Vasc Biol</u> **33**(2): 170-177.

Liu, M., S. Guo, J. M. Hibbert, V. Jain, N. Singh, N. O. Wilson and J. K. Stiles (2011). "CXCL10/IP-10 in infectious diseases pathogenesis and potential therapeutic implications." <u>Cytokine Growth Factor Rev</u> **22**(3): 121-130.

Livak, K. J. and T. D. Schmittgen (2001). "Analysis of relative gene expression data using real-time quantitative PCR and the 2(-Delta Delta C(T)) Method." <u>Methods</u> **25**(4): 402-408.

Lo, S. K., S. Lee, R. A. Ramos, R. Lobb, M. Rosa, G. Chi-Rosso and S. D. Wright (1991). "Endothelial-leukocyte adhesion molecule 1 stimulates the adhesive activity of leukocyte integrin CR3 (CD11b/CD18, Mac-1, alpha m beta 2) on human neutrophils." <u>J Exp Med</u> **173**(6): 1493-1500.

Locke, A. E., B. Kahali, S. I. Berndt, A. E. Justice, T. H. Pers, F. R. Day, C. Powell, S. Vedantam, M. L. Buchkovich, J. Yang, D. C. Croteau-Chonka, T. Esko, T. Fall, T. Ferreira, S. Gustafsson, Z. Kutalik, J. Luan, R. Magi, J. C. Randall, T. W. Winkler, A. R. Wood, T. Workalemahu, J. D. Faul, J. A. Smith, J. Hua Zhao, W. Zhao, J. Chen, R. Fehrmann, A. K. Hedman, J. Karjalainen, E. M. Schmidt, D. Absher, N. Amin, D. Anderson, M. Beekman, J. L. Bolton, J. L. Bragg-Gresham, S. Buyske, A. Demirkan, G. Deng, G. B. Ehret, B. Feenstra, M. F. Feitosa, K. Fischer, A. Goel, J. Gong, A. U. Jackson, S. Kanoni, M. E. Kleber, K. Kristiansson, U. Lim, V. Lotay, M. Mangino, I. Mateo Leach, C. Medina-Gomez, S. E. Medland, M. A. Nalls, C. D. Palmer, D. Pasko, S. Pechlivanis, M. J. Peters, I. Prokopenko, D. Shungin, A. Stancakova, R. J. Strawbridge, Y. Ju Sung, T. Tanaka, A. Teumer, S. Trompet, S. W. van der Laan, J. van Setten, J. V. Van Vliet-Ostaptchouk, Z. Wang, L. Yengo, W. Zhang, A. Isaacs, E. Albrecht, J. Arnlov, G. M. Arscott, A. P. Attwood, S. Bandinelli, A. Barrett, I. N. Bas, C. Bellis, A. J. Bennett, C. Berne, R. Blagieva, M. Bluher, S. Bohringer, L. L. Bonnycastle, Y. Bottcher, H. A. Boyd, M. Bruinenberg, I. H. Caspersen, Y. D. Ida Chen, R. Clarke, E. W. Daw, A. J. de Craen, G. Delgado, M. Dimitriou, A. S. Doney, N. Eklund, K. Estrada, E. Eury, L. Folkersen, R. M. Fraser, M. E. Garcia, F. Geller, V. Giedraitis, B. Gigante, A. S. Go, A. Golay, A. H. Goodall, S. D. Gordon, M. Gorski, H. J. Grabe, H. Grallert, T. B. Grammer, J. Grassler, H. Gronberg, C. J. Groves, G. Gusto, J. Haessler, P. Hall, T. Haller, G. Hallmans, C. A. Hartman, M. Hassinen, C. Hayward, N. L. Heard-Costa, Q. Helmer, C. Hengstenberg, O. Holmen, J. J. Hottenga, A. L. James, J. M. Jeff, A. Johansson, J. Jolley, T. Juliusdottir, L. Kinnunen, W. Koenig, M. Koskenvuo, W.

Kratzer, J. Laitinen, C. Lamina, K. Leander, N. R. Lee, P. Lichtner, L. Lind, J. Lindstrom, K. Sin Lo, S. Lobbens, R. Lorbeer, Y. Lu, F. Mach, P. K. Magnusson, A. Mahajan, W. L. McArdle, S. McLachlan, C. Menni, S. Merger, E. Mihailov, L. Milani, A. Moayyeri, K. L. Monda, M. A. Morken, A. Mulas, G. Muller, M. Muller-Nurasyid, A. W. Musk, R. Nagaraja, M. M. Nothen, I. M. Nolte, S. Pilz, N. W. Rayner, F. Renstrom, R. Rettig, J. S. Ried, S. Ripke, N. R. Robertson, L. M. Rose, S. Sanna, H. Scharnagl, S. Scholtens, F. R. Schumacher, W. R. Scott, T. Seufferlein, J. Shi, A. Vernon Smith, J. Smolonska, A. V. Stanton, V. Steinthorsdottir, K. Stirrups, H. M. Stringham, J. Sundstrom, M. A. Swertz, A. J. Swift, A. C. Syvanen, S. T. Tan, B. O. Tayo, B. Thorand, G. Thorleifsson, J. P. Tyrer, H. W. Uh, L. Vandenput, F. C. Verhulst, S. H. Vermeulen, N. Verweij, J. M. Vonk, L. L. Waite, H. R. Warren, D. Waterworth, M. N. Weedon, L. R. Wilkens, C. Willenborg, T. Wilsgaard, M. K. Wojczynski, A. Wong, A. F. Wright, Q. Zhang, E. P. Brennan, M. Choi, Z. Dastani, A. W. Drong, P. Eriksson, A. Franco-Cereceda, J. R. Gadin, A. G. Gharavi, M. E. Goddard, R. E. Handsaker, J. Huang, F. Karpe, S. Kathiresan, S. Keildson, K. Kiryluk, M. Kubo, J. Y. Lee, L. Liang, R. P. Lifton, B. Ma, S. A. McCarroll, A. J. McKnight, J. L. Min, M. F. Moffatt, G. W. Montgomery, J. M. Murabito, G. Nicholson, D. R. Nyholt, Y. Okada, J. R. Perry, R. Dorajoo, E. Reinmaa, R. M. Salem, N. Sandholm, R. A. Scott, L. Stolk, A. Takahashi, T. Tanaka, F. M. Van't Hooft, A. A. Vinkhuyzen, H. J. Westra, W. Zheng, K. T. Zondervan, A. C. Heath, D. Arveiler, S. J. Bakker, J. Beilby, R. N. Bergman, J. Blangero, P. Bovet, H. Campbell, M. J. Caulfield, G. Cesana, A. Chakravarti, D. I. Chasman, P. S. Chines, F. S. Collins, D. C. Crawford, L. A. Cupples, D. Cusi, J. Danesh, U. de Faire, H. M. den Ruijter, A. F. Dominiczak, R. Erbel, J. Erdmann, J. G. Eriksson, M. Farrall, S. B. Felix, E. Ferrannini, J. Ferrieres, I. Ford, N. G. Forouhi, T. Forrester, O. H. Franco, R. T. Gansevoort, P. V. Gejman, C. Gieger, O. Gottesman, V. Gudnason, U. Gyllensten, A. S. Hall, T. B. Harris, A. T. Hattersley, A. A. Hicks, L. A. Hindorff, A. D. Hingorani, A. Hofman, G. Homuth, G. K. Hovingh, S. E. Humphries, S. C. Hunt, E. Hypponen, T. Illig, K. B. Jacobs, M. R. Jarvelin, K. H. Jockel, B. Johansen, P. Jousilahti, J. W. Jukema, A. M. Jula, J. Kaprio, J. J. Kastelein, S. M. Keinanen-Kiukaanniemi, L. A. Kiemeney, P. Knekt, J. S. Kooner, C. Kooperberg, P. Kovacs, A. T. Kraja, M. Kumari, J. Kuusisto, T. A. Lakka, C. Langenberg, L. Le Marchand, T. Lehtimaki, V. Lyssenko, S. Mannisto, A. Marette, T. C. Matise, C. A. McKenzie, B. McKnight, F. L. Moll, A. D. Morris, A. P. Morris, J. C. Murray, M. Nelis, C. Ohlsson, A. J. Oldehinkel, K. K. Ong, P. A. Madden, G. Pasterkamp, J. F. Peden, A. Peters, D. S. Postma, P. P. Pramstaller, J. F. Price, L. Qi, O. T. Raitakari, T. Rankinen, D. C. Rao, T. K. Rice, P. M. Ridker, J. D. Rioux, M. D. Ritchie, I. Rudan, V. Salomaa, N. J. Samani, J. Saramies, M. A. Sarzynski, H. Schunkert, P. E. Schwarz, P. Sever, A. R. Shuldiner, J. Sinisalo, R. P. Stolk, K. Strauch, A. Tonjes, D. A. Tregouet, A. Tremblay, E. Tremoli, J. Virtamo, M. C. Vohl, U. Volker, G. Waeber, G. Willemsen, J. C. Witteman, M. C. Zillikens, L. S. Adair, P. Amouyel, F. W. Asselbergs, T. L. Assimes, M. Bochud, B. O. Boehm, E. Boerwinkle, S. R. Bornstein, E. P. Bottinger, C. Bouchard, S. Cauchi, J. C. Chambers, S. J. Chanock, R. S. Cooper, P. I. de Bakker, G. Dedoussis, L. Ferrucci, P. W. Franks, P. Froguel, L. C. Groop, C. A. Haiman, A. Hamsten, J. Hui, D. J. Hunter, K. Hveem, R. C. Kaplan, M. Kivimaki, D. Kuh, M. Laakso, Y. Liu, N. G. Martin, W. Marz, M. Melbye, A. Metspalu, S. Moebus, P. B. Munroe, I. Njolstad, B. A. Oostra, C. N. Palmer, N. L. Pedersen, M. Perola, L. Perusse, U. Peters, C. Power, T. Quertermous, R. Rauramaa, F. Rivadeneira, T. E. Saaristo, D. Saleheen, N. Sattar, E. E. Schadt, D. Schlessinger, P. E. Slagboom, H. Snieder, T. D. Spector, U. Thorsteinsdottir, M. Stumvoll, J. Tuomilehto, A. G. Uitterlinden, M. Uusitupa, P. van der Harst, M. Walker, H. Wallaschofski, N. J. Wareham, H. Watkins, D. R. Weir, H. E. Wichmann, J. F. Wilson, P. Zanen, I. B. Borecki, P. Deloukas, C. S. Fox, I. M. Heid, J. R. O'Connell, D. P. Strachan, K. Stefansson, C. M. van Duijn, G. R. Abecasis, L. Franke, T. M. Frayling, M. I. McCarthy, P. M. Visscher, A. Scherag, C. J. Willer, M. Boehnke, K. L. Mohlke, C. M. Lindgren, J. S. Beckmann, I. Barroso, K. E. North, E. Ingelsson, J. N. Hirschhorn, R. J. Loos and E. K. Speliotes (2015). "Genetic studies of body mass index yield new insights for obesity biology." Nature **518**(7538): 197-206.

Loos, R. J., C. M. Lindgren, S. Li, E. Wheeler, J. H. Zhao, I. Prokopenko, M. Inouye, R. M. Freathy, A. P. Attwood, J. S. Beckmann, S. I. Berndt, K. B. Jacobs, S. J. Chanock, R. B. Hayes, S. Bergmann, A. J. Bennett, S. A. Bingham, M. Bochud, M. Brown, S. Cauchi, J. M. Connell, C. Cooper, G. D. Smith, I. Day, C. Dina, S. De, E. T. Dermitzakis, A. S. Doney, K. S. Elliott, P. Elliott, D. M. Evans, I. Sadaf Farooqi, P. Froguel, J. Ghori, C. J. Groves, R. Gwilliam, D. Hadley, A. S. Hall, A. T. Hattersley, J. Hebebrand, I. M.

Heid, C. Lamina, C. Gieger, T. Illig, T. Meitinger, H. E. Wichmann, B. Herrera, A. Hinney, S. E. Hunt, M. R. Jarvelin, T. Johnson, J. D. Jolley, F. Karpe, A. Keniry, K. T. Khaw, R. N. Luben, M. Mangino, J. Marchini, W. L. McArdle, R. McGinnis, D. Meyre, P. B. Munroe, A. D. Morris, A. R. Ness, M. J. Neville, A. C. Nica, K. K. Ong, S. O'Rahilly, K. R. Owen, C. N. Palmer, K. Papadakis, S. Potter, A. Pouta, L. Qi, J. C. Randall, N. W. Rayner, S. M. Ring, M. S. Sandhu, A. Scherag, M. A. Sims, K. Song, N. Soranzo, E. K. Speliotes, H. E. Syddall, S. A. Teichmann, N. J. Timpson, J. H. Tobias, M. Uda, C. I. Vogel, C. Wallace, D. M. Waterworth, M. N. Weedon, C. J. Willer, Wraight, X. Yuan, E. Zeggini, J. N. Hirschhorn, D. P. Strachan, W. H. Ouwehand, M. J. Caulfield, N. J. Samani, T. M. Frayling, P. Vollenweider, G. Waeber, V. Mooser, P. Deloukas, M. I. McCarthy, N. J. Wareham, I. Barroso, K. B. Jacobs, S. J. Chanock, R. B. Hayes, C. Lamina, C. Gieger, T. Illig, T. Meitinger, H. E. Wichmann, P. Kraft, S. E. Hankinson, D. J. Hunter, F. B. Hu, H. N. Lyon, B. F. Voight, M. Ridderstrale, L. Groop, P. Scheet, S. Sanna, G. R. Abecasis, G. Albai, R. Nagaraja, D. Schlessinger, A. U. Jackson, J. Tuomilehto, F. S. Collins, M. Boehnke and K. L. Mohlke (2008). "Common variants near MC4R are associated with fat mass, weight and risk of obesity." Nat Genet **40**(6): 768-775.

Lu, Y., L. Cao, B. C. Jiang, T. Yang and Y. J. Gao (2015). "MicroRNA-146a-5p attenuates neuropathic pain via suppressing TRAF6 signaling in the spinal cord." Brain Behav Immun.

Lu, Y. C., W. C. Yeh and P. S. Ohashi (2008). "LPS/TLR4 signal transduction pathway." Cytokine **42**(2): 145-151.

Luan, Z. G., H. Zhang, P. T. Yang, X. C. Ma, C. Zhang and R. X. Guo (2010). "HMGB1 activates nuclear factor-kappaB signaling by RAGE and increases the production of TNF-alpha in human umbilical vein endothelial cells." Immunobiology **215**(12): 956-962.

Lumeng, C. N., S. M. Deyoung, J. L. Bodzin and A. R. Saltiel (2007). "Increased inflammatory properties of adipose tissue macrophages recruited during diet-induced obesity." Diabetes **56**(1): 16-23.

Lumeng, C. N., S. M. Deyoung and A. R. Saltiel (2007). "Macrophages block insulin action in adipocytes by altering expression of signaling and glucose transport proteins." Am J Physiol Endocrinol Metab **292**(1): E166-174.

Lund, E. and J. E. Dahlberg (2006). "Substrate selectivity of exportin 5 and Dicer in the biogenesis of microRNAs." Cold Spring Harb Symp Quant Biol **71**: 59-66.

Luster, A. D., S. C. Jhanwar, R. S. Chaganti, J. H. Kersey and J. V. Ravetch (1987). "Interferon-inducible gene maps to a chromosomal band associated with a (4;11) translocation in acute leukemia cells." Proc Natl Acad Sci U S A **84**(9): 2868-2871.

Lye, E., C. Mirtsos, N. Suzuki, S. Suzuki and W. C. Yeh (2004). "The role of interleukin 1 receptor-associated kinase-4 (IRAK-4) kinase activity in IRAK-4-mediated signaling." J Biol Chem **279**(39): 40653-40658.

Lytle, J. R., T. A. Yario and J. A. Steitz (2007). "Target mRNAs are repressed as efficiently by microRNA-binding sites in the 5' UTR as in the 3' UTR." Proc Natl Acad Sci U S A **104**(23): 9667-9672.

Ma, J. B., K. Ye and D. J. Patel (2004). "Structural basis for overhang-specific small interfering RNA recognition by the PAZ domain." Nature **429**(6989): 318-322.

Magnusson, P. K. and F. Rasmussen (2002). "Familial resemblance of body mass index and familial risk of high and low body mass index. A study of young men in Sweden." Int J Obes Relat Metab Disord **26**(9): 1225-1231.

Manduteanu, I., M. Voinea, G. Serban and M. Simionescu (1999). "High glucose induces enhanced monocyte adhesion to valvular endothelial cells via a mechanism involving ICAM-1, VCAM-1 and CD18." Endothelium **6**(4): 315-324.

Manigrasso, M. R., P. Ferroni, F. Santilli, T. Taraborelli, M. T. Guagnano, N. Michetti and G. Davi (2005). "Association between circulating adiponectin and interleukin-10 levels in android obesity: effects of weight loss." J Clin Endocrinol Metab **90**(10): 5876-5879.

Marko, M. A., R. Chipperfield and H. C. Birnboim (1982). "A procedure for the large-scale isolation of highly purified plasmid DNA using alkaline extraction and binding to glass powder." Anal Biochem **121**(2): 382-387.

Mathonnet, G., M. R. Fabian, Y. V. Svitkin, A. Parsyan, L. Huck, T. Murata, S. Biffo, W. C. Merrick, E. Darzynkiewicz, R. S. Pillai, W. Filipowicz, T. F. Duchaine and N. Sonenberg (2007). "MicroRNA inhibition of translation initiation in vitro by targeting the cap-binding complex eIF4F." Science **317**(5845): 1764-1767.

Matsumoto, K., T. Morisaki, H. Kuroki, M. Kubo, H. Onishi, K. Nakamura, C. Nakahara, H. Kuga, E. Baba, M. Nakamura, K. Hirata, M. Tanaka and M. Katano (2004). "Exosomes secreted from monocyte-derived dendritic cells support in vitro naive CD4+ T cell survival through NF-(kappa)B activation." Cell Immunol **231**(1-2): 20-29.

Maus, U., S. Henning, H. Wenschuh, K. Mayer, W. Seeger and J. Lohmeyer (2002). "Role of endothelial MCP-1 in monocyte adhesion to inflamed human endothelium under physiological flow." Am J Physiol Heart Circ Physiol **283**(6): H2584-2591.

McEver, R. P. and R. D. Cummings (1997). "Perspectives series: cell adhesion in vascular biology. Role of PSGL-1 binding to selectins in leukocyte recruitment." J Clin Invest **100**(3): 485-491.

Meister, G., M. Landthaler, A. Patkaniowska, Y. Dorsett, G. Teng and T. Tuschl (2004). "Human Argonaute2 mediates RNA cleavage targeted by miRNAs and siRNAs." Mol Cell **15**(2): 185-197.

Meng, L., J. Park, Q. Cai, L. Lanting, M. A. Reddy and R. Natarajan (2010). "Diabetic conditions promote binding of monocytes to vascular smooth muscle cells and their subsequent differentiation." Am J Physiol Heart Circ Physiol **298**(3): H736-745.

Mindell, R. C. a. J. (2014). Health Survey for England 2013. T. H. a. S. C. I. Centre. London.

Mingrone, G., S. Panunzi, A. De Gaetano, C. Guidone, A. Iaconelli, L. Leccesi, G. Nanni, A. Pomp, M. Castagneto, G. Ghirlanda and F. Rubino (2012). "Bariatric surgery versus conventional medical therapy for type 2 diabetes." N Engl J Med **366**(17): 1577-1585.

Momen-Heravi, F., S. Bala, K. Kodys and G. Szabo (2015). "Exosomes derived from alcohol-treated hepatocytes horizontally transfer liver specific miRNA-122 and sensitize monocytes to LPS." Sci Rep **5**: 9991.

Montague, C. T., I. S. Farooqi, J. P. Whitehead, M. A. Soos, H. Rau, N. J. Wareham, C. P. Sewter, J. E. Digby, S. N. Mohammed, J. A. Hurst, C. H. Cheetham, A. R. Earley, A. H. Barnett, J. B. Prins and S. O'Rahilly (1997). "Congenital leptin deficiency is associated with severe early-onset obesity in humans." Nature **387**(6636): 903-908.

Moreira-Tabaka, H., J. Peluso, J. L. Vonesch, D. Hentsch, P. Kessler, J. M. Reimund, S. Dumont and C. D. Muller (2012). "Unlike for human monocytes after LPS activation, release of TNF-alpha by THP-1 cells is produced by a TACE catalytically different from constitutive TACE." PLoS One **7**(3): e34184.

Morgan, H. D., W. Dean, H. A. Coker, W. Reik and S. K. Petersen-Mahrt (2004). "Activation-induced cytidine deaminase deaminates 5-methylcytosine in DNA and is expressed in pluripotent tissues: implications for epigenetic reprogramming." J Biol Chem **279**(50): 52353-52360.

Morohoshi, M., K. Fujisawa, I. Uchimura and F. Numano (1995). "The effect of glucose and advanced glycosylation end products on IL-6 production by human monocytes." Ann N Y Acad Sci **748**: 562-570.

Morohoshi, M., K. Fujisawa, I. Uchimura and F. Numano (1996). "Glucose-dependent interleukin 6 and tumor necrosis factor production by human peripheral blood monocytes in vitro." Diabetes **45**(7): 954-959.

Mortuza, R., S. Chen, B. Feng, S. Sen and S. Chakrabarti (2013). "High glucose induced alteration of SIRTs in endothelial cells causes rapid aging in a p300 and FOXO regulated pathway." PLoS One **8**(1): e54514.

Mosmann, T. (1983). "Rapid colorimetric assay for cellular growth and survival: application to proliferation and cytotoxicity assays." J Immunol Methods **65**(1-2): 55-63.

Moulopoulos, S. D., P. N. Adamopoulos, E. I. Diamantopoulos, S. N. Nanas, L. N. Anthopoulos and M. Iliadi-Alexandrou (1987). "Coronary heart disease risk factors in a random sample of Athenian adults. The Athens Study." Am J Epidemiol **126**(5): 882-892.

Mudaliar, H., C. Pollock, J. Ma, H. Wu, S. Chadban and U. Panchapakesan (2014). "The role of TLR2 and 4-mediated inflammatory pathways in endothelial cells exposed to high glucose." PLoS One **9**(10): e108844.

Mukherjee, S. P., M. Behar, H. A. Birnbaum, A. Hoffmann, P. E. Wright and G. Ghosh (2013). "Analysis of the RelA:CBP/p300 interaction reveals its involvement in NF-kappaB-driven transcription." PLoS Biol **11**(9): e1001647.

Murray, P. J., J. E. Allen, S. K. Biswas, E. A. Fisher, D. W. Gilroy, S. Goerdt, S. Gordon, J. A. Hamilton, L. B. Ivashkiv, T. Lawrence, M. Locati, A. Mantovani, F. O. Martinez, J. L. Mege, D. M. Mosser, G. Natoli, J. P. Saeij, J. L. Schultze, K. A. Shirey, A. Sica, J. Suttles, I. Udalova, J. A. van Ginderachter, S. N. Vogel and T. A. Wynn (2014). "Macrophage activation and polarization: nomenclature and experimental guidelines." Immunity **41**(1): 14-20.

Nadler, S. T., J. P. Stoehr, K. L. Schueler, G. Tanimoto, B. S. Yandell and A. D. Attie (2000). "The expression of adipogenic genes is decreased in obesity and diabetes mellitus." Proc Natl Acad Sci U S A **97**(21): 11371-11376.

Nagy, L., P. Tontonoz, J. G. Alvarez, H. Chen and R. M. Evans (1998). "Oxidized LDL regulates macrophage gene expression through ligand activation of PPARgamma." Cell **93**(2): 229-240.

Nan, X., F. J. Campoy and A. Bird (1997). "MeCP2 is a transcriptional repressor with abundant binding sites in genomic chromatin." Cell **88**(4): 471-481.

Nandy, D., R. Janardhanan, D. Mukhopadhyay and A. Basu (2011). "Effect of hyperglycemia on human monocyte activation." J Investig Med **59**(4): 661-667.

Nannipieri, M., S. Baldi, A. Mari, D. Colligiani, D. Guarino, S. Camastra, E. Barsotti, R. Berta, D. Moriconi, R. Bellini, M. Anselmino and E. Ferrannini (2013). "Roux-en-Y gastric bypass and sleeve gastrectomy: mechanisms of diabetes remission and role of gut hormones." J Clin Endocrinol Metab **98**(11): 4391-4399.

Netto, B. D., S. C. Bettini, A. P. Clemente, J. P. Ferreira, K. Boritza, F. Souza Sde, M. E. Von der Heyde, C. P. Earthman and A. R. Damaso (2015). "Roux-en-Y gastric bypass decreases pro-inflammatory and thrombotic biomarkers in individuals with extreme obesity." Obes Surg **25**(6): 1010-1018.

NICE (2014). Obesity: identification, assessment and management of overweight and obesity in children, young people and adults. T. N. I. f. H. a. C. Excellence.

Nie, Y., D. M. Erion, Z. Yuan, M. Dietrich, G. I. Shulman, T. L. Horvath and Q. Gao (2009). "STAT3 inhibition of gluconeogenesis is downregulated by SirT1." Nat Cell Biol **11**(4): 492-500.

Njajou, O. T., A. M. Kanaya, P. Holvoet, S. Connelly, E. S. Strotmeyer, T. B. Harris, S. R. Cummings and W. C. Hsueh (2009). "Association between oxidized LDL, obesity and type 2 diabetes in a population-based cohort, the Health, Aging and Body Composition Study." Diabetes Metab Res Rev **25**(8): 733-739.

Noren Hooten, N., M. Fitzpatrick, W. H. Wood, 3rd, S. De, N. Ejiogu, Y. Zhang, J. A. Mattison, K. G. Becker, A. B. Zonderman and M. K. Evans (2013). "Age-related changes in microRNA levels in serum." Aging (Albany NY) **5**(10): 725-740.

Nyengaard, J. R., Y. Ido, C. Kilo and J. R. Williamson (2004). "Interactions between hyperglycemia and hypoxia: implications for diabetic retinopathy." Diabetes **53**(11): 2931-2938.

Oh, D. Y., H. Morinaga, S. Talukdar, E. J. Bae and J. M. Olefsky (2012). "Increased macrophage migration into adipose tissue in obese mice." Diabetes **61**(2): 346-354.

Olsnes, A. M., D. Motorin, A. Ryningen, A. Y. Zaritskey and O. Bruserud (2006). "T lymphocyte chemotactic chemokines in acute myelogenous leukemia (AML): local release by native human AML blasts and systemic levels of CXCL10 (IP-10), CCL5 (RANTES) and CCL17 (TARC)." Cancer Immunol Immunother **55**(7): 830-840.

Otto, N. M., R. Schindler, A. Lun, O. Boenisch, U. Frei and M. Oppert (2008). "Hyperosmotic stress enhances cytokine production and decreases phagocytosis in vitro." Crit Care **12**(4): R107.

Painter, R. C., S. R. de Rooij, P. M. Bossuyt, T. A. Simmers, C. Osmond, D. J. Barker, O. P. Bleker and T. J. Roseboom (2006). "Early onset of coronary artery disease after prenatal exposure to the Dutch famine." The American Journal of Clinical Nutrition **84**(2): 322-327.

Panning, B. (2008). "X-chromosome inactivation: the molecular basis of silencing." J Biol **7**(8): 30.

Paredes-Turrubiarte, G., A. Gonzalez-Chavez, R. Perez-Tamayo, B. Y. Salazar-Vazquez, V. S. Hernandez, N. Garibay-Nieto, J. M. Fragoso and G. Escobedo (2015). "Severity of non-alcoholic fatty

liver disease is associated with high systemic levels of tumor necrosis factor alpha and low serum interleukin 10 in morbidly obese patients." Clin Exp Med.

Park, H., X. Huang, C. Lu, M. S. Cairo and X. Zhou (2015). "MicroRNA-146a and microRNA-146b regulate human dendritic cell apoptosis and cytokine production by targeting TRAF6 and IRAK1 proteins." J Biol Chem **290**(5): 2831-2841.

Park, J. S., F. Gamboni-Robertson, Q. He, D. Svetkauskaite, J. Y. Kim, D. Strassheim, J. W. Sohn, S. Yamada, I. Maruyama, A. Banerjee, A. Ishizaka and E. Abraham (2006). "High mobility group box 1 protein interacts with multiple Toll-like receptors." Am J Physiol Cell Physiol **290**(3): C917-924.

Patriti, A., E. Facchiano and A. Donini (2004). "Effect of duodenal-jejunal exclusion in a non-obese animal model of type 2 diabetes: a new perspective for an old disease." Ann Surg **240**(2): 388-389; author reply 389-391.

Pauley, K. M., M. Satoh, A. L. Chan, M. R. Bubb, W. H. Reeves and E. K. Chan (2008). "Upregulated miR-146a expression in peripheral blood mononuclear cells from rheumatoid arthritis patients." Arthritis Res Ther **10**(4): R101.

Petronini, P. G., M. Tramacere, J. E. Kay and A. F. Borghetti (1986). "Adaptive response of cultured fibroblasts to hyperosmolarity." Exp Cell Res **165**(1): 180-190.

Picot, J., J. Jones, J. L. Colquitt, E. Gospodarevskaya, E. Loveman, L. Baxter and A. J. Clegg (2009). "The clinical effectiveness and cost-effectiveness of bariatric (weight loss) surgery for obesity: a systematic review and economic evaluation." Health Technol Assess **13**(41): 1-190, 215-357, iii-iv.

Pillai, R. S., C. G. Artus and W. Filipowicz (2004). "Tethering of human Ago proteins to mRNA mimics the miRNA-mediated repression of protein synthesis." Rna **10**(10): 1518-1525.

Pina, T., S. Armesto, R. Lopez-Mejias, F. Genre, B. Ubilla, M. A. Gonzalez-Lopez, M. C. Gonzalez-Vela, A. Corrales, R. Blanco, M. T. Garcia-Unzueta, J. L. Hernandez, J. Llorca and M. A. Gonzalez-Gay (2015). "Anti-TNF-alpha therapy improves insulin sensitivity in non-diabetic patients with psoriasis: a 6-month prospective study." J Eur Acad Dermatol Venereol **29**(7): 1325-1330.

Poehlmann, H., J. C. Schefold, H. Zuckermann-Becker, H. D. Volk and C. Meisel (2009). "Phenotype changes and impaired function of dendritic cell subsets in patients with sepsis: a prospective observational analysis." Crit Care **13**(4): R119.

Poitou, C., E. Dalmas, M. Renovato, V. Benhamo, F. Hajduch, M. Abdennour, J. F. Kahn, N. Veyrie, S. Rizkalla, W. H. Fridman, C. Sautes-Fridman, K. Clement and I. Cremer (2011). "CD14dimCD16+ and CD14+CD16+ monocytes in obesity and during weight loss: relationships with fat mass and subclinical atherosclerosis." Arterioscler Thromb Vasc Biol **31**(10): 2322-2330.

Polak, P., N. Cybulski, J. N. Feige, J. Auwerx, M. A. Ruegg and M. N. Hall (2008). "Adipose-specific knockout of raptor results in lean mice with enhanced mitochondrial respiration." Cell Metab **8**(5): 399-410.

Poltorak, A., X. He, I. Smirnova, M. Y. Liu, C. Van Huffel, X. Du, D. Birdwell, E. Alejos, M. Silva, C. Galanos, M. Freudenberg, P. Ricciardi-Castagnoli, B. Layton and B. Beutler (1998). "Defective LPS signaling in C3H/HeJ and C57BL/10ScCr mice: mutations in Tlr4 gene." Science **282**(5396): 2085-2088.

Pradervand, S., J. Weber, F. Lemoine, F. Consales, A. Paillusson, M. Dupasquier, J. Thomas, H. Richter, H. Kaessmann, E. Beaudoing, O. Hagenbuchle and K. Harshman (2010). "Concordance among digital gene expression, microarrays, and qPCR when measuring differential expression of microRNAs." Biotechniques **48**(3): 219-222.

Pradervand, S., J. Weber, J. Thomas, M. Bueno, P. Wirapati, K. Lefort, G. P. Dotto and K. Harshman (2009). "Impact of normalization on miRNA microarray expression profiling." Rna **15**(3): 493-501.

Qatanani, M. and M. A. Lazar (2007). "Mechanisms of obesity-associated insulin resistance: many choices on the menu." Genes Dev **21**(12): 1443-1455.

Qin, B., W. Qiu, R. K. Avramoglu and K. Adeli (2007). "Tumor necrosis factor-alpha induces intestinal insulin resistance and stimulates the overproduction of intestinal apolipoprotein B48-containing lipoproteins." Diabetes **56**(2): 450-461.

Qiu, M. R., T. J. Campbell and S. N. Breit (2002). "A potassium ion channel is involved in cytokine production by activated human macrophages." Clin Exp Immunol **130**(1): 67-74.

Rabadi, M. M., S. Xavier, R. Vasko, K. Kaur, M. S. Goligorksy and B. B. Ratliff (2015). "High-mobility group box 1 is a novel deacetylation target of Sirtuin1." Kidney Int **87**(1): 95-108.

Rai, K., I. J. Huggins, S. R. James, A. R. Karpf, D. A. Jones and B. R. Cairns (2008). "DNA demethylation in zebrafish involves the coupling of a deaminase, a glycosylase, and gadd45." Cell **135**(7): 1201-1212.

Rana, T. M. (2007). "Illuminating the silence: understanding the structure and function of small RNAs." Nat Rev Mol Cell Biol **8**(1): 23-36.

Randle, P. J., P. B. Garland, C. N. Hales and E. A. Newsholme (1963). "The glucose fatty-acid cycle. Its role in insulin sensitivity and the metabolic disturbances of diabetes mellitus." Lancet **1**(7285): 785-789.

Raymond, S. and L. Weintraub (1959). "Acrylamide gel as a supporting medium for zone electrophoresis." Science **130**(3377): 711.

Reaven, E. P., G. Gold and G. M. Reaven (1979). "Effect of age on glucose-stimulated insulin release by the beta-cell of the rat." J Clin Invest **64**(2): 591-599.

Reaven, G. M., C. Hollenbeck, C. Y. Jeng, M. S. Wu and Y. D. Chen (1988). "Measurement of plasma glucose, free fatty acid, lactate, and insulin for 24 h in patients with NIDDM." Diabetes **37**(8): 1020-1024.

Richard Dobbs, C. S., Fraser Thompson, James Manyika, Jonathan Woetzel, Peter Child, Sorcha McKenna, Angela Spatharou (2014). Overcoming obesity: An initial economic analysis, McKinsey Global Institute.

Rickenbacher, A., J. H. Jang, P. Limani, U. Ungethum, K. Lehmann, C. E. Oberkofler, A. Weber, R. Graf, B. Humar and P. A. Clavien (2014). "Fasting protects liver from ischemic injury through Sirt1-mediated downregulation of circulating HMGB1 in mice." J Hepatol **61**(2): 301-308.

Robbins, E., T. Pederson and P. Klein (1970). "Comparison of mitotic phenomena and effects induced by hypertonic solutions in HeLa cells." J Cell Biol **44**(2): 400-416.

Rodgers, J. T., C. Lerin, W. Haas, S. P. Gygi, B. M. Spiegelman and P. Puigserver (2005). "Nutrient control of glucose homeostasis through a complex of PGC-1alpha and SIRT1." Nature **434**(7029): 113-118.

Rogers, P. D., J. Thornton, K. S. Barker, D. O. McDaniel, G. S. Sacks, E. Swiatlo and L. S. McDaniel (2003). "Pneumolysin-dependent and -independent gene expression identified by cDNA microarray analysis of THP-1 human mononuclear cells stimulated by Streptococcus pneumoniae." Infect Immun **71**(4): 2087-2094.

Rosa, A., M. Ballarino, A. Sorrentino, O. Sthandier, F. G. De Angelis, M. Marchioni, B. Masella, A. Guarini, A. Fatica, C. Peschle and I. Bozzoni (2007). "The interplay between the master transcription factor PU.1 and miR-424 regulates human monocyte/macrophage differentiation." Proc Natl Acad Sci U S A **104**(50): 19849-19854.

Rossol, M., S. Kraus, M. Pierer, C. Baerwald and U. Wagner (2012). "The CD14(bright) CD16+ monocyte subset is expanded in rheumatoid arthritis and promotes expansion of the Th17 cell population." Arthritis Rheum **64**(3): 671-677.

Rowe, J. W., K. L. Minaker, J. A. Pallotta and J. S. Flier (1983). "Characterization of the insulin resistance of aging." J Clin Invest **71**(6): 1581-1587.

Rubino, F., A. Forgione, D. E. Cummings, M. Vix, D. Gnuli, G. Mingrone, M. Castagneto and J. Marescaux (2006). "The mechanism of diabetes control after gastrointestinal bypass surgery reveals a role of the proximal small intestine in the pathophysiology of type 2 diabetes." Ann Surg **244**(5): 741-749.

Saiki, R. K., D. H. Gelfand, S. Stoffel, S. J. Scharf, R. Higuchi, G. T. Horn, K. B. Mullis and H. A. Erlich (1988). "Primer-directed enzymatic amplification of DNA with a thermostable DNA polymerase." Science **239**(4839): 487-491.

Saiki, R. K., S. Scharf, F. Faloona, K. B. Mullis, G. T. Horn, H. A. Erlich and N. Arnheim (1985). "Enzymatic amplification of beta-globin genomic sequences and restriction site analysis for diagnosis of sickle cell anemia." Science **230**(4732): 1350-1354.

Salas, A., M. Shimaoka, A. N. Kogan, C. Harwood, U. H. von Andrian and T. A. Springer (2004). "Rolling adhesion through an extended conformation of integrin alphaLbeta2 and relation to alpha I and beta I-like domain interaction." Immunity **20**(4): 393-406.

Salehi, M., R. L. Prigeon and D. A. D'Alessio (2011). "Gastric bypass surgery enhances glucagon-like peptide 1-stimulated postprandial insulin secretion in humans." Diabetes **60**(9): 2308-2314.

Salser, W. (1978). "Globin mRNA sequences: analysis of base pairing and evolutionary implications." Cold Spring Harb Symp Quant Biol **42 Pt 2**: 985-1002.

Sango, K., T. Suzuki, H. Yanagisawa, S. Takaku, H. Hirooka, M. Tamura and K. Watabe (2006). "High glucose-induced activation of the polyol pathway and changes of gene expression profiles in immortalized adult mouse Schwann cells IMS32." J Neurochem **98**(2): 446-458.

Sato, S., H. Sanjo, K. Takeda, J. Ninomiya-Tsuji, M. Yamamoto, T. Kawai, K. Matsumoto, O. Takeuchi and S. Akira (2005). "Essential function for the kinase TAK1 in innate and adaptive immune responses." Nat Immunol **6**(11): 1087-1095.

Sato, T., X. Liu, A. Nelson, M. Nakanishi, N. Kanaji, X. Wang, M. Kim, Y. Li, J. Sun, J. Michalski, A. Patil, H. Basma, O. Holz, H. Magnussen and S. I. Rennard (2010). "Reduced miR-146a increases prostaglandin E(2)in chronic obstructive pulmonary disease fibroblasts." Am J Respir Crit Care Med **182**(8): 1020-1029.

Satoh, N., A. Shimatsu, A. Himeno, Y. Sasaki, H. Yamakage, K. Yamada, T. Suganami and Y. Ogawa (2010). "Unbalanced M1/M2 phenotype of peripheral blood monocytes in obese diabetic patients: effect of pioglitazone." Diabetes Care **33**(1): e7.

Saunders, L. R., A. D. Sharma, J. Tawney, M. Nakagawa, K. Okita, S. Yamanaka, H. Willenbring and E. Verdin (2010). "miRNAs regulate SIRT1 expression during mouse embryonic stem cell differentiation and in adult mouse tissues." Aging (Albany NY) **2**(7): 415-431.

Schakel, K., R. Kannagi, B. Kniep, Y. Goto, C. Mitsuoka, J. Zwirner, A. Soruri, M. von Kietzell and E. Rieber (2002). "6-Sulfo LacNAc, a novel carbohydrate modification of PSGL-1, defines an inflammatory type of human dendritic cells." Immunity **17**(3): 289-301.

Schalkwijk, C. G., C. D. Stehouwer and V. W. van Hinsbergh (2004). "Fructose-mediated non-enzymatic glycation: sweet coupling or bad modification." Diabetes Metab Res Rev **20**(5): 369-382.

Schanne, F. A., A. B. Kane, E. E. Young and J. L. Farber (1979). "Calcium dependence of toxic cell death: a final common pathway." Science **206**(4419): 700-702.

Schauer, P. R., S. R. Kashyap, K. Wolski, S. A. Brethauer, J. P. Kirwan, C. E. Pothier, S. Thomas, B. Abood, S. E. Nissen and D. L. Bhatt (2012). "Bariatric surgery versus intensive medical therapy in obese patients with diabetes." N Engl J Med **366**(17): 1567-1576.

Schildberger, A., E. Rossmanith, T. Eichhorn, K. Strassl and V. Weber (2013). "Monocytes, peripheral blood mononuclear cells, and THP-1 cells exhibit different cytokine expression patterns following stimulation with lipopolysaccharide." Mediators Inflamm **2013**: 697972.

Schmittgen, T. D. and K. J. Livak (2008). "Analyzing real-time PCR data by the comparative C(T) method." Nat Protoc **3**(6): 1101-1108.

Schwandner, R., R. Dziarski, H. Wesche, M. Rothe and C. J. Kirschning (1999). "Peptidoglycan- and lipoteichoic acid-induced cell activation is mediated by toll-like receptor 2." J Biol Chem **274**(25): 17406-17409.

Schwende, H., E. Fitzke, P. Ambs and P. Dieter (1996). "Differences in the state of differentiation of THP-1 cells induced by phorbol ester and 1,25-dihydroxyvitamin D3." J Leukoc Biol **59**(4): 555-561.

Serre, V., W. Dolci, E. Schaerer, L. Scrocchi, D. Drucker, S. Efrat and B. Thorens (1998). "Exendin-(9-39) is an inverse agonist of the murine glucagon-like peptide-1 receptor: implications for basal intracellular cyclic adenosine 3',5'-monophosphate levels and beta-cell glucose competence." Endocrinology **139**(11): 4448-4454.

Shanmugam, N., M. A. Reddy, M. Guha and R. Natarajan (2003). "High glucose-induced expression of proinflammatory cytokine and chemokine genes in monocytic cells." Diabetes **52**(5): 1256-1264.

Shanthi Mendis, T. A., Douglas Bettcher, Francesco Branca, Jeremy Lauer, and S. M. Cecile Mace, Vladimir Poznyak, Leanne Riley, Vera Da Costa E Silva, Gretchen Stevens (2014). Global Status Report on noncommunicable diseases 2014. Switzerland, World Health Organisation.

Shantsila, E., B. Wrigley, L. Tapp, S. Apostolakis, S. Montoro-Garcia, M. T. Drayson and G. Y. Lip (2011). "Immunophenotypic characterization of human monocyte subsets: possible implications for cardiovascular disease pathophysiology." J Thromb Haemost **9**(5): 1056-1066.

Shi, Y. and F. B. Hu (2014). "The global implications of diabetes and cancer." The Lancet **383**(9933): 1947-1948.

Shinohara, M., P. J. Thornalley, I. Giardino, P. Beisswenger, S. R. Thorpe, J. Onorato and M. Brownlee (1998). "Overexpression of glyoxalase-I in bovine endothelial cells inhibits intracellular advanced glycation endproduct formation and prevents hyperglycemia-induced increases in macromolecular endocytosis." J Clin Invest **101**(5): 1142-1147.

Shiraishi, D., Y. Fujiwara, Y. Komohara, H. Mizuta and M. Takeya (2012). "Glucagon-like peptide-1 (GLP-1) induces M2 polarization of human macrophages via STAT3 activation." Biochem Biophys Res Commun **425**(2): 304-308.

Shoelson, S. E., J. Lee and A. B. Goldfine (2006). "Inflammation and insulin resistance." J Clin Invest **116**(7): 1793-1801.

Sikes, M. L., J. M. Bradshaw, W. T. Ivory, J. L. Lunsford, R. E. McMillan and C. R. Morrison (2009). "A streamlined method for rapid and sensitive chromatin immunoprecipitation." J Immunol Methods **344**(1): 58-63.

Sinclair, D. A. and L. Guarente (1997). "Extrachromosomal rDNA circles--a cause of aging in yeast." Cell **91**(7): 1033-1042.

Sjostrom, L., A. K. Lindroos, M. Peltonen, J. Torgerson, C. Bouchard, B. Carlsson, S. Dahlgren, B. Larsson, K. Narbro, C. D. Sjostrom, M. Sullivan and H. Wedel (2004). "Lifestyle, diabetes, and cardiovascular risk factors 10 years after bariatric surgery." N Engl J Med **351**(26): 2683-2693.

Sjostrom, L., K. Narbro, C. D. Sjostrom, K. Karason, B. Larsson, H. Wedel, T. Lystig, M. Sullivan, C. Bouchard, B. Carlsson, C. Bengtsson, S. Dahlgren, A. Gummesson, P. Jacobson, J. Karlsson, A. K. Lindroos, H. Lonroth, I. Naslund, T. Olbers, K. Stenlof, J. Torgerson, G. Agren and L. M. Carlsson (2007). "Effects of bariatric surgery on mortality in Swedish obese subjects." N Engl J Med **357**(8): 741-752.

Smith, P. K., R. I. Krohn, G. T. Hermanson, A. K. Mallia, F. H. Gartner, M. D. Provenzano, E. K. Fujimoto, N. M. Goeke, B. J. Olson and D. C. Klenk (1985). "Measurement of protein using bicinchoninic acid." Anal Biochem **150**(1): 76-85.

Song, M. J., K. H. Kim, J. M. Yoon and J. B. Kim (2006). "Activation of Toll-like receptor 4 is associated with insulin resistance in adipocytes." Biochem Biophys Res Commun **346**(3): 739-745.

Sonkoly, E., T. Wei, P. C. Janson, A. Saaf, L. Lundeberg, M. Tengvall-Linder, G. Norstedt, H. Alenius, B. Homey, A. Scheynius, M. Stahle and A. Pivarcsi (2007). "MicroRNAs: novel regulators involved in the pathogenesis of psoriasis?" PLoS One **2**(7): e610.

Speck, M., Y. M. Cho, A. Asadi, F. Rubino and T. J. Kieffer (2011). "Duodenal-jejunal bypass protects GK rats from {beta}-cell loss and aggravation of hyperglycemia and increases enteroendocrine cells coexpressing GIP and GLP-1." Am J Physiol Endocrinol Metab **300**(5): E923-932.

Spinetti, G., D. Cordella, O. Fortunato, E. Sangalli, S. Losa, A. Gotti, F. Carnelli, F. Rosa, S. Riboldi, F. Sessa, E. Avolio, A. P. Beltrami, C. Emanueli and P. Madeddu (2013). "Global remodeling of the vascular stem cell niche in bone marrow of diabetic patients: implication of the microRNA-155/FOXO3a signaling pathway." Circ Res **112**(3): 510-522.

Stewart, C. R., L. M. Stuart, K. Wilkinson, J. M. van Gils, J. Deng, A. Halle, K. J. Rayner, L. Boyer, R. Zhong, W. A. Frazier, A. Lacy-Hulbert, J. El Khoury, D. T. Golenbock and K. J. Moore (2010). "CD36 ligands promote sterile inflammation through assembly of a Toll-like receptor 4 and 6 heterodimer." Nat Immunol **11**(2): 155-161.

Stunkard, A. J., T. I. Sorensen, C. Hanis, T. W. Teasdale, R. Chakraborty, W. J. Schull and F. Schulsinger (1986). "An adoption study of human obesity." N Engl J Med **314**(4): 193-198.

Suganuma, K., H. Miwa, N. Imai, M. Shikami, M. Gotou, M. Goto, S. Mizuno, M. Takahashi, H. Yamamoto, A. Hiramatsu, M. Wakabayashi, M. Watarai, I. Hanamura, A. Imamura, H. Mihara and M. Nitta (2010). "Energy metabolism of leukemia cells: glycolysis versus oxidative phosphorylation." Leuk Lymphoma **51**(11): 2112-2119.

Sun, C., F. Zhang, X. Ge, T. Yan, X. Chen, X. Shi and Q. Zhai (2007). "SIRT1 improves insulin sensitivity under insulin-resistant conditions by repressing PTP1B." Cell Metab **6**(4): 307-319.

Sutherland, B. W., J. Toews and J. Kast (2008). "Utility of formaldehyde cross-linking and mass spectrometry in the study of protein-protein interactions." J Mass Spectrom **43**(6): 699-715.

Suzuki, H., Y. Kurihara, M. Takeya, N. Kamada, M. Kataoka, K. Jishage, O. Ueda, H. Sakaguchi, T. Higashi, T. Suzuki, Y. Takashima, Y. Kawabe, O. Cynshi, Y. Wada, M. Honda, H. Kurihara, H. Aburatani, T. Doi, A. Matsumoto, S. Azuma, T. Noda, Y. Toyoda, H. Itakura, Y. Yazaki, T. Kodama and et al. (1997). "A role for macrophage scavenger receptors in atherosclerosis and susceptibility to infection." Nature **386**(6622): 292-296.

Suzuki, N., S. Suzuki, G. S. Duncan, D. G. Millar, T. Wada, C. Mirtsos, H. Takada, A. Wakeham, A. Itie, S. Li, J. M. Penninger, H. Wesche, P. S. Ohashi, T. W. Mak and W. C. Yeh (2002). "Severe impairment of interleukin-1 and Toll-like receptor signalling in mice lacking IRAK-4." Nature **416**(6882): 750-756.

Taganov, K. D., M. P. Boldin, K. J. Chang and D. Baltimore (2006). "NF-kappaB-dependent induction of microRNA miR-146, an inhibitor targeted to signaling proteins of innate immune responses." Proc Natl Acad Sci U S A **103**(33): 12481-12486.

Takamura, Y., T. Tomomatsu, E. Kubo, S. Tsuzuki and Y. Akagi (2008). "Role of the polyol pathway in high glucose-induced apoptosis of retinal pericytes and proliferation of endothelial cells." Invest Ophthalmol Vis Sci **49**(7): 3216-3223.

Tang, B., B. Xiao, Z. Liu, N. Li, E. D. Zhu, B. S. Li, Q. H. Xie, Y. Zhuang, Q. M. Zou and X. H. Mao (2010). "Identification of MyD88 as a novel target of miR-155, involved in negative regulation of Helicobacter pylori-induced inflammation." FEBS Lett **584**(8): 1481-1486.

Taniguchi, C. M., B. Emanuelli and C. R. Kahn (2006). "Critical nodes in signalling pathways: insights into insulin action." Nat Rev Mol Cell Biol **7**(2): 85-96.

Tencerova, M., J. Kracmerova, E. Krauzova, L. Malisova, Z. Kovacova, Z. Wedellova, M. Siklova, V. Stich and L. Rossmeislova (2015). "Experimental hyperglycemia induces an increase of monocyte and T-lymphocyte content in adipose tissue of healthy obese women." PLoS One **10**(3): e0122872.

Tennant, J. R. (1964). "EVALUATION OF THE TRYPAN BLUE TECHNIQUE FOR DETERMINATION OF CELL VIABILITY." Transplantation **2**: 685-694.

Terranova, L., L. Busetto, A. Vestri and M. A. Zappa (2012). "Bariatric surgery: cost-effectiveness and budget impact." Obes Surg **22**(4): 646-653.

Tili, E., J. J. Michaille, A. Cimino, S. Costinean, C. D. Dumitru, B. Adair, M. Fabbri, H. Alder, C. G. Liu, G. A. Calin and C. M. Croce (2007). "Modulation of miR-155 and miR-125b levels following lipopolysaccharide/TNF-alpha stimulation and their possible roles in regulating the response to endotoxin shock." J Immunol **179**(8): 5082-5089.

Tobias, D. K. and F. B. Hu (2013). "Does being overweight really reduce mortality?" Obesity (Silver Spring) **21**(9): 1746-1749.

Tontonoz, P., L. Nagy, J. G. Alvarez, V. A. Thomazy and R. M. Evans (1998). "PPARgamma promotes monocyte/macrophage differentiation and uptake of oxidized LDL." Cell **93**(2): 241-252.

Travis, S. F., A. D. Morrison, R. S. Clements, Jr., A. I. Winegrad and F. A. Oski (1971). "Metabolic alterations in the human erythrocyte produced by increases in glucose concentration. The role of the polyol pathway." J Clin Invest **50**(10): 2104-2112.

Tsuchiya, S., Y. Kobayashi, Y. Goto, H. Okumura, S. Nakae, T. Konno and K. Tada (1982). "Induction of maturation in cultured human monocytic leukemia cells by a phorbol diester." Cancer Res **42**(4): 1530-1536.

Tsuchiya, S., M. Yamabe, Y. Yamaguchi, Y. Kobayashi, T. Konno and K. Tada (1980). "Establishment and characterization of a human acute monocytic leukemia cell line (THP-1)." Int J Cancer **26**(2): 171-176.

Tsukumo, D. M., M. A. Carvalho-Filho, J. B. Carvalheira, P. O. Prada, S. M. Hirabara, A. A. Schenka, E. P. Araujo, J. Vassallo, R. Curi, L. A. Velloso and M. J. Saad (2007). "Loss-of-function mutation in Toll-like receptor 4 prevents diet-induced obesity and insulin resistance." Diabetes **56**(8): 1986-1998.

Turula, M., J. Kaprio, A. Rissanen and M. Koskenvuo (1990). "Body weight in the Finnish Twin Cohort." Diabetes Res Clin Pract **10 Suppl 1**: S33-36.

Vaisse, C., K. Clement, B. Guy-Grand and P. Froguel (1998). "A frameshift mutation in human MC4R is associated with a dominant form of obesity." Nat Genet **20**(2): 113-114.

Vanden Berghe, W., K. De Bosscher, E. Boone, S. Plaisance and G. Haegeman (1999). "The nuclear factor-kappaB engages CBP/p300 and histone acetyltransferase activity for transcriptional activation of the interleukin-6 gene promoter." J Biol Chem **274**(45): 32091-32098.

Vasa-Nicotera, M., H. Chen, P. Tucci, A. L. Yang, G. Saintigny, R. Menghini, C. Mahe, M. Agostini, R. A. Knight, G. Melino and M. Federici (2011). "miR-146a is modulated in human endothelial cell with aging." Atherosclerosis **217**(2): 326-330.

Vaziri, H., S. K. Dessain, E. Ng Eaton, S. I. Imai, R. A. Frye, T. K. Pandita, L. Guarente and R. A. Weinberg (2001). "hSIR2(SIRT1) functions as an NAD-dependent p53 deacetylase." Cell **107**(2): 149-159.

Verreck, F. A., T. de Boer, D. M. Langenberg, L. van der Zanden and T. H. Ottenhoff (2006). "Phenotypic and functional profiling of human proinflammatory type-1 and anti-inflammatory type-2 macrophages in response to microbial antigens and IFN-gamma- and CD40L-mediated costimulation." J Leukoc Biol **79**(2): 285-293.

Voll, R. E., M. Herrmann, E. A. Roth, C. Stach, J. R. Kalden and I. Girkontaite (1997). "Immunosuppressive effects of apoptotic cells." Nature **390**(6658): 350-351.

Waddington, C. H. (1942). "The epigenotype. 1942." Int J Epidemiol **41**(1): 10-13.

Wang, H., O. Bloom, M. Zhang, J. M. Vishnubhakat, M. Ombrellino, J. Che, A. Frazier, H. Yang, S. Ivanova, L. Borovikova, K. R. Manogue, E. Faist, E. Abraham, J. Andersson, U. Andersson, P. E. Molina, N. N. Abumrad, A. Sama and K. J. Tracey (1999). "HMG-1 as a late mediator of endotoxin lethality in mice." Science **285**(5425): 248-251.

Wang, H. J., Y. L. Huang, Y. Y. Shih, H. Y. Wu, C. T. Peng and W. Y. Lo (2014). "MicroRNA-146a decreases high glucose/thrombin-induced endothelial inflammation by inhibiting NAPDH oxidase 4 expression." Mediators Inflamm **2014**: 379537.

Wang, L., B. Balas, C. Y. Christ-Roberts, R. Y. Kim, F. J. Ramos, C. K. Kikani, C. Li, C. Deng, S. Reyna, N. Musi, L. Q. Dong, R. A. DeFronzo and F. Liu (2007). "Peripheral disruption of the Grb10 gene enhances insulin signaling and sensitivity in vivo." Mol Cell Biol **27**(18): 6497-6505.

Wang, R., P. Cherukuri and J. Luo (2005). "Activation of Stat3 sequence-specific DNA binding and transcription by p300/CREB-binding protein-mediated acetylation." J Biol Chem **280**(12): 11528-11534.

Wang, S., A. B. Aurora, B. A. Johnson, X. Qi, J. McAnally, J. A. Hill, J. A. Richardson, R. Bassel-Duby and E. N. Olson (2008). "The endothelial-specific microRNA miR-126 governs vascular integrity and angiogenesis." Dev Cell **15**(2): 261-271.

Wantha, S., J. E. Alard, R. T. Megens, A. M. van der Does, Y. Doring, M. Drechsler, C. T. Pham, M. W. Wang, J. M. Wang, R. L. Gallo, P. von Hundelshausen, L. Lindbom, T. Hackeng, C. Weber and O. Soehnlein (2013). "Neutrophil-derived cathelicidin promotes adhesion of classical monocytes." Circ Res **112**(5): 792-801.

Wardle, J., S. Carnell, C. M. Haworth and R. Plomin (2008). "Evidence for a strong genetic influence on childhood adiposity despite the force of the obesogenic environment." Am J Clin Nutr **87**(2): 398-404.

Weindruch, R., R. L. Walford, S. Fligiel and D. Guthrie (1986). "The retardation of aging in mice by dietary restriction: longevity, cancer, immunity and lifetime energy intake." J Nutr **116**(4): 641-654.

Weisberg, S. P., D. Hunter, R. Huber, J. Lemieux, S. Slaymaker, K. Vaddi, I. Charo, R. L. Leibel and A. W. Ferrante, Jr. (2006). "CCR2 modulates inflammatory and metabolic effects of high-fat feeding." J Clin Invest **116**(1): 115-124.

Weisberg, S. P., D. McCann, M. Desai, M. Rosenbaum, R. L. Leibel and A. W. Ferrante, Jr. (2003). "Obesity is associated with macrophage accumulation in adipose tissue." J Clin Invest **112**(12): 1796-1808.

White, M. F. (1997). "The insulin signalling system and the IRS proteins." Diabetologia **40 Suppl 2**: S2-17.

Wiechelman, K. J., R. D. Braun and J. D. Fitzpatrick (1988). "Investigation of the bicinchoninic acid protein assay: identification of the groups responsible for color formation." Anal Biochem **175**(1): 231-237.

Wieczorek, M., T. Ginter, P. Brand, T. Heinzel and O. H. Kramer (2012). "Acetylation modulates the STAT signaling code." Cytokine Growth Factor Rev **23**(6): 293-305.

Wijesinghe, P. and A. S. Bhagwat (2012). "Efficient deamination of 5-methylcytosines in DNA by human APOBEC3A, but not by AID or APOBEC3G." Nucleic Acids Res **40**(18): 9206-9217.

Wilcox, G. (2005). "Insulin and insulin resistance." Clin Biochem Rev **26**(2): 19-39.

Willett, W. C., F. B. Hu and M. Thun (2013). "Overweight, obesity, and all-cause mortality." Jama **309**(16): 1681.

Williams, M. D. and G. M. Mitchell (2012). "MicroRNAs in Insulin Resistance and Obesity." Experimental Diabetes Research **2012**: 8.

Winter, J., S. Jung, S. Keller, R. I. Gregory and S. Diederichs (2009). "Many roads to maturity: microRNA biogenesis pathways and their regulation." Nat Cell Biol **11**(3): 228-234.

Wong, K. L., J. J. Tai, W. C. Wong, H. Han, X. Sem, W. H. Yeap, P. Kourilsky and S. C. Wong (2011). "Gene expression profiling reveals the defining features of the classical, intermediate, and nonclassical human monocyte subsets." Blood **118**(5): e16-31.

World Health Organisation, I. D. F. (2006). Definition and diagnosis of diabetes mellitus and intermediate hyperglycaemia. W. IDF.

Wormser, D., S. Kaptoge, E. Di Angelantonio, A. M. Wood, L. Pennells, A. Thompson, N. Sarwar, J. R. Kizer, D. A. Lawlor, B. G. Nordestgaard, P. Ridker, V. Salomaa, J. Stevens, M. Woodward, N. Sattar, R. Collins, S. G. Thompson, G. Whitlock and J. Danesh (2011). "Separate and combined associations of body-mass index and abdominal adiposity with cardiovascular disease: collaborative analysis of 58 prospective studies." Lancet **377**(9771): 1085-1095.

Wu, C. H., C. F. Wu, H. W. Huang, Y. C. Jao and G. C. Yen (2009). "Naturally occurring flavonoids attenuate high glucose-induced expression of proinflammatory cytokines in human monocytic THP-1 cells." Mol Nutr Food Res **53**(8): 984-995.

Wu, Q., J. V. Li, F. Seyfried, C. W. le Roux, H. Ashrafian, T. Athanasiou, W. Fenske, A. Darzi, J. K. Nicholson, E. Holmes and N. J. Gooderham (2015). "Metabolic phenotype-microRNA data fusion analysis of the systemic consequences of Roux-en-Y gastric bypass surgery." Int J Obes (Lond) **39**(7): 1126-1134.

Wu, X., X. Zhao, R. Puertollano, J. S. Bonifacino, E. Eisenberg and L. E. Greene (2003). "Adaptor and clathrin exchange at the plasma membrane and trans-Golgi network." Mol Biol Cell **14**(2): 516-528.

Xiao, C., L. Srinivasan, D. P. Calado, H. C. Patterson, B. Zhang, J. Wang, J. M. Henderson, J. L. Kutok and K. Rajewsky (2008). "Lymphoproliferative disease and autoimmunity in mice with increased miR-17-92 expression in lymphocytes." Nat Immunol **9**(4): 405-414.

Xiao, F., J. Yu, B. Liu, Y. Guo, K. Li, J. Deng, J. Zhang, C. Wang, S. Chen, Y. Du, Y. Lu, Y. Xiao, Z. Zhang and F. Guo (2014). "A novel function of microRNA 130a-3p in hepatic insulin sensitivity and liver steatosis." Diabetes **63**(8): 2631-2642.

Xiong, Y., G. F. Wang, J. Y. Zhang, S. Y. Wu, W. Xu, J. J. Zhang, S. G. Wu and J. J. Rao (2010). "[Naringin inhibits monocyte adhesion to high glucose-induced human umbilical vein endothelial cells]." Nan Fang Yi Ke Da Xue Xue Bao **30**(2): 321-325.

Xu, G., H. Kaneto, D. R. Laybutt, V. F. Duvivier-Kali, N. Trivedi, K. Suzuma, G. L. King, G. C. Weir and S. Bonner-Weir (2007). "Downregulation of GLP-1 and GIP receptor expression by hyperglycemia: possible contribution to impaired incretin effects in diabetes." Diabetes **56**(6): 1551-1558.

Xu, H., G. T. Barnes, Q. Yang, G. Tan, D. Yang, C. J. Chou, J. Sole, A. Nichols, J. S. Ross, L. A. Tartaglia and H. Chen (2003). "Chronic inflammation in fat plays a crucial role in the development of obesity-related insulin resistance." J Clin Invest **112**(12): 1821-1830.

Yan, S. T., C. L. Li, H. Tian, J. Li, Y. Pei, Y. Liu, Y. P. Gong, F. S. Fang and B. R. Sun (2014). "MiR-199a is overexpressed in plasma of type 2 diabetes patients which contributes to type 2 diabetes by targeting GLUT4." Mol Cell Biochem **397**(1-2): 45-51.

Yang, H., D. J. Antoine, U. Andersson and K. J. Tracey (2013). "The many faces of HMGB1: molecular structure-functional activity in inflammation, apoptosis, and chemotaxis." J Leukoc Biol **93**(6): 865-873.

Yang, H., W. Zhang, H. Pan, H. G. Feldser, E. Lainez, C. Miller, S. Leung, Z. Zhong, H. Zhao, S. Sweitzer, T. Considine, T. Riera, V. Suri, B. White, J. L. Ellis, G. P. Vlasuk and C. Loh (2012). "SIRT1 activators suppress inflammatory responses through promotion of p65 deacetylation and inhibition of NF-kappaB activity." PLoS One **7**(9): e46364.

Yang, K., Y. S. He, X. Q. Wang, L. Lu, Q. J. Chen, J. Liu, Z. Sun and W. F. Shen (2011). "MiR-146a inhibits oxidized low-density lipoprotein-induced lipid accumulation and inflammatory response via targeting toll-like receptor 4." FEBS Lett **585**(6): 854-860.

Yang, X. D., B. Huang, M. Li, A. Lamb, N. L. Kelleher and L. F. Chen (2009). "Negative regulation of NF-kappaB action by Set9-mediated lysine methylation of the RelA subunit." Embo j **28**(8): 1055-1066.

Yang, X. D., E. Tajkhorshid and L. F. Chen (2010). "Functional interplay between acetylation and methylation of the RelA subunit of NF-kappaB." Mol Cell Biol **30**(9): 2170-2180.

Yang, Y. (2011). "Structure, function and regulation of the melanocortin receptors." Eur J Pharmacol **660**(1): 125-130.

Yeung, F., J. E. Hoberg, C. S. Ramsey, M. D. Keller, D. R. Jones, R. A. Frye and M. W. Mayo (2004). "Modulation of NF-kappaB-dependent transcription and cell survival by the SIRT1 deacetylase." Embo j **23**(12): 2369-2380.

Yi, R., Y. Qin, I. G. Macara and B. R. Cullen (2003). "Exportin-5 mediates the nuclear export of pre-microRNAs and short hairpin RNAs." Genes Dev **17**(24): 3011-3016.

Yoo, J. K., C. H. Kim, H. Y. Jung, D. R. Lee and J. K. Kim (2014). "Discovery and characterization of miRNA during cellular senescence in bone marrow-derived human mesenchymal stem cells." Exp Gerontol **58**: 139-145.

Yoshino, J., K. F. Mills, M. J. Yoon and S. Imai (2011). "Nicotinamide mononucleotide, a key NAD(+) intermediate, treats the pathophysiology of diet- and age-induced diabetes in mice." Cell Metab **14**(4): 528-536.

Yoshizaki, T., J. C. Milne, T. Imamura, S. Schenk, N. Sonoda, J. L. Babendure, J. C. Lu, J. J. Smith, M. R. Jirousek and J. M. Olefsky (2009). "SIRT1 exerts anti-inflammatory effects and improves insulin sensitivity in adipocytes." Mol Cell Biol **29**(5): 1363-1374.

Yu, C., Y. Chen, G. W. Cline, D. Zhang, H. Zong, Y. Wang, R. Bergeron, J. K. Kim, S. W. Cushman, G. J. Cooney, B. Atcheson, M. F. White, E. W. Kraegen and G. I. Shulman (2002). "Mechanism by Which Fatty Acids Inhibit Insulin Activation of Insulin Receptor Substrate-1 (IRS-1)-associated Phosphatidylinositol 3-Kinase Activity in Muscle." Journal of Biological Chemistry **277**(52): 50230-50236.

Yuan, M., N. Konstantopoulos, J. Lee, L. Hansen, Z. W. Li, M. Karin and S. E. Shoelson (2001). "Reversal of obesity- and diet-induced insulin resistance with salicylates or targeted disruption of Ikkbeta." Science **293**(5535): 1673-1677.

Yuan, Z. L., Y. J. Guan, D. Chatterjee and Y. E. Chin (2005). "Stat3 dimerization regulated by reversible acetylation of a single lysine residue." Science **307**(5707): 269-273.

Yun, J. M., I. Jialal and S. Devaraj (2011). "Epigenetic regulation of high glucose-induced proinflammatory cytokine production in monocytes by curcumin." J Nutr Biochem **22**(5): 450-458.

Zeng, Y. and B. R. Cullen (2004). "Structural requirements for pre-microRNA binding and nuclear export by Exportin 5." Nucleic Acids Res **32**(16): 4776-4785.

Zentner, G. E. and S. Henikoff (2013). "Regulation of nucleosome dynamics by histone modifications." Nat Struct Mol Biol **20**(3): 259-266.

Zernecke, A., K. Bidzhekov, H. Noels, E. Shagdarsuren, L. Gan, B. Denecke, M. Hristov, T. Koppel, M. N. Jahantigh, E. Lutgens, S. Wang, E. N. Olson, A. Schober and C. Weber (2009). "Delivery of microRNA-126 by apoptotic bodies induces CXCL12-dependent vascular protection." Sci Signal **2**(100): ra81.

Zhang, H. H., J. Huang, K. Duvel, B. Boback, S. Wu, R. M. Squillace, C. L. Wu and B. D. Manning (2009). "Insulin stimulates adipogenesis through the Akt-TSC2-mTORC1 pathway." PLoS One **4**(7): e6189.

Zhang, J. (2007). "The direct involvement of SirT1 in insulin-induced insulin receptor substrate-2 tyrosine phosphorylation." J Biol Chem **282**(47): 34356-34364.

Zhang, J., S. Li, L. Li, M. Li, C. Guo, J. Yao and S. Mi (2015). "Exosome and exosomal microRNA: trafficking, sorting, and function." Genomics Proteomics Bioinformatics **13**(1): 17-24.

Zhao, Z., M. C. de Beer, L. Cai, R. Asmis, F. C. de Beer, W. J. S. de Villiers and D. R. van der Westhuyzen (2005). "Low-Density Lipoprotein From Apolipoprotein E-Deficient Mice Induces Macrophage Lipid Accumulation in a CD36 and Scavenger Receptor Class A-Dependent Manner." Arteriosclerosis, Thrombosis, and Vascular Biology **25**(1): 168-173.

Zheng, Z., H. Chen, J. Li, T. Li, B. Zheng, Y. Zheng, H. Jin, Y. He, Q. Gu and X. Xu (2012). "Sirtuin 1-mediated cellular metabolic memory of high glucose via the LKB1/AMPK/ROS pathway and therapeutic effects of metformin." Diabetes **61**(1): 217-228.

Zhong, H., R. E. Voll and S. Ghosh (1998). "Phosphorylation of NF-kappa B p65 by PKA stimulates transcriptional activity by promoting a novel bivalent interaction with the coactivator CBP/p300." Mol Cell **1**(5): 661-671.

Zhou, B., S. Wang, C. Mayr, D. P. Bartel and H. F. Lodish (2007). "miR-150, a microRNA expressed in mature B and T cells, blocks early B cell development when expressed prematurely." Proc Natl Acad Sci U S A **104**(17): 7080-7085.

Zhou, R., A. Y. Gong, D. Chen, R. E. Miller, A. N. Eischeid and X. M. Chen (2013). "Histone deacetylases and NF-kB signaling coordinate expression of CX3CL1 in epithelial cells in response to microbial challenge by suppressing miR-424 and miR-503." PLoS One **8**(5): e65153.

Zu, Y., L. Liu, M. Y. Lee, C. Xu, Y. Liang, R. Y. Man, P. M. Vanhoutte and Y. Wang (2010). "SIRT1 promotes proliferation and prevents senescence through targeting LKB1 in primary porcine aortic endothelial cells." Circ Res **106**(8): 1384-1393.

8 Appendix

8.1 Ethics approval 1

Aston University

MEMORANDUM

DATE: 8th November 2011

TO: Dr Srikanth Bellary,
Life & Health Sciences

FROM: John Walter,
Academic Registrar

SUBJECT: **Project 444: 'Metabolic regulation of cellular ageing in obese/diabetic subjects'**

I am writing to inform you that the Chair of the University's Ethics Committee has approved the above project proposals as amended in the light of the Ethics Sub-Group's comments.

The details of the investigation will be placed on file. You should notify me of any difficulties experienced by the volunteer subjects, and any significant changes which may be planned for this project in the future.

J.G.Walter

Secretary to the Ethics Committee

8.2 Ethics approval 2

06 June 2012

Professor Helen R Griffiths
Executive Dean
Aston University
Aston Triangle
Birmingham
B4 7ET

Dear Professor Griffiths

Study title:	Effects of bariatic surgery on insulin resistance with a focus on the metabolism-sensitive epigenome in the monocyte.
REC reference:	12/WM/0145
Protocol number:	CH-2011-0792

The Research Ethics Committee reviewed the above application at the meeting held on 30 May 2012. Thank you for sending Dr Bellary and Stuart Bennett to discuss the application with the Committee.

Ethical opinion
- The Committee advised the researchers that the study read very well.
- The Committee asked the Researchers about the control group and whether they had thought of using an obese control group. The researchers advised they had considered it previously but thought it would be better if they were their own control group to enable them to see the effects of time.
- The Committee asked whether the participant's partner would also be obese as they were likely to have the same diet. The researchers explained it was likely but not always the case. The Researchers explained that the control may be a partner from a patient at their weight management clinic.
- The Researchers were asked about the involvement of Unilever. The Researchers advised they have provided funding for some of the analysis. The Researchers confirmed that most of the analysis would be done at Aston University.
- The Committee advised they would have been interested to see the peer review. The Researchers explained they were asked not to disclose it as there was likely to be a lot of interest.
- The Committee explained there needs to be a mechanism to complain within the Participant Information Sheet. The Researchers asked who this normally would be. The Committee advised generally it would be PALS.
- The Committee advised there are a number of grammatical errors within the Participant Information sheet.
- The Researchers were asked why they are excluding Non English speakers. They explained that they do not have the resources to translate the documents.
- The Researchers advised that funding had already started for the study and as such they were keen to start as soon as possible.
- The Committee asked why travel expenses had been capped at £6. The Researchers accepted it was a small sum and will change it to cover reasonable

expenses. The researchers advised they will try and coordinate the visits to fit in with their other appointments so as to limit the amount of extra trips.

- The Researchers were advised that the consent form should have initial boxes not tick boxes

The members of the Committee present gave a favourable ethical opinion of the above research on the basis described in the application form, protocol and supporting documentation, subject to the conditions specified below.

Ethical review of research sites

NHS Sites

The favourable opinion applies to all NHS sites taking part in the study, subject to management permission being obtained from the NHS/HSC R&D office prior to the start of the study (see "Conditions of the favourable opinion" below).

Conditions of the favourable opinion

The favourable opinion is subject to the following conditions being met prior to the start of the study.

Management permission or approval must be obtained from each host organisation prior to the start of the study at the site concerned.

Management permission ("R&D approval") should be sought from all NHS organisations involved in the study in accordance with NHS research governance arrangements.

Guidance on applying for NHS permission for research is available in the Integrated Research Application System or at http://www.rdforum.nhs.uk.

Where a NHS organisation's role in the study is limited to identifying and referring potential participants to research sites ("participant identification centre"), guidance should be sought from the R&D office on the information it requires to give permission for this activity.

For non-NHS sites, site management permission should be obtained in accordance with the procedures of the relevant host organisation.

Sponsors are not required to notify the Committee of approvals from host organisations

- The Participant information Sheet should be proof read and any grammatical errors corrected.
- There should be a mechanism to complain within the Participant Information Sheet; generally this would be the Patient Advice and Liaison Service (PALS).
- The Participant Information Sheet should be revised to state that reasonable travel expenses will be paid.

It is responsibility of the sponsor to ensure that all the conditions are complied with before the start of the study or its initiation at a particular site (as applicable).

You should notify the REC in writing once all conditions have been met (except for site approvals from host organisations) and provide copies of any revised documentation with updated version numbers. Confirmation should also be provided to host organisations together with relevant documentation

With the Committee's best wishes for the success of this project

Yours sincerely
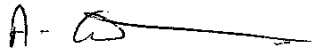
Dr Helen Brittain
Chair

Email: Andrea.Graham@nottspct.nhs.uk

Enclosures: *List of names and professions of members who were present at the meeting and those who submitted written comments*
"After ethical review – guidance for researchers" [SL-AR2]

Copy to: *Dr Nichola Seare*
Ms Elizabeth Adey, Heart of England NHS Foundation Trust

8.3 List of experimentally observed miRNA target mRNA inputted into ingenuity pathway analysis software

ID	Source	Confidence	Symbol
hsa-miR-199b-5p	TargetScan Human,miRecords	Experimentally Observed	SIRT1
hsa-miR-199b-5p	miRecords	Experimentally Observed	SET
hsa-miR-199b-5p	TarBase,miRecords	Experimentally Observed	LAMC2
hsa-miR-199b-5p	Ingenuity Expert Findings,TargetScan Human,miRecords	Experimentally Observed	HIF1A
hsa-miR-199b-5p	Ingenuity Expert Findings,TargetScan Human	Experimentally Observed	ETS1
hsa-miR-199b-5p	Ingenuity Expert Findings	Experimentally Observed	DYRK1A
hsa-miR-199b-5p	miRecords	Experimentally Observed	ALOX5AP
hsa-miR-424-5p	Ingenuity Expert Findings,TargetScan Human	Experimentally Observed	ZYX
hsa-miR-424-5p	TarBase,TargetScan Human	Experimentally Observed	ZNF622
hsa-miR-424-5p	miRecords	Experimentally Observed	ZNF559
hsa-miR-424-5p	TarBase	Experimentally Observed	YIF1B
hsa-miR-424-5p	miRecords	Experimentally Observed	WT1
hsa-miR-424-5p	Ingenuity Expert Findings,TargetScan Human	Experimentally Observed	WNT3A
hsa-miR-424-5p	miRecords	Experimentally Observed	WIPF1
hsa-miR-424-5p	Ingenuity Expert Findings,TargetScan Human	Experimentally Observed	WEE1
hsa-miR-424-5p	TarBase,TargetScan Human	Experimentally Observed	VTI1B
hsa-miR-424-5p	miRecords	Experimentally Observed	VPS45
hsa-miR-424-5p	TargetScan Human,miRecords	Experimentally Observed	VEGFA
hsa-miR-424-5p	TarBase	Experimentally Observed	UTP15
hsa-miR-424-5p	miRecords	Experimentally Observed	UGP2
hsa-miR-424-5p	miRecords	Experimentally Observed	UGDH
hsa-miR-424-5p	Ingenuity Expert Findings,TargetScan Human	Experimentally Observed	UCP2
hsa-miR-424-5p	TarBase,TargetScan Human	Experimentally Observed	UBE4A

hsa-miR-424-5p	TarBase	Experimentally Observed	UBE2S
hsa-miR-424-5p	TarBase,TargetScan Human	Experimentally Observed	TXN2
hsa-miR-424-5p	miRecords	Experimentally Observed	TRMT13
hsa-miR-424-5p	TarBase,TargetScan Human,miRecords	Experimentally Observed	TPPP3
hsa-miR-424-5p	TarBase,TargetScan Human	Experimentally Observed	TPM3
hsa-miR-424-5p	miRecords	Experimentally Observed	TPI1
hsa-miR-424-5p	TarBase	Experimentally Observed	TOMM34
hsa-miR-424-5p	TarBase,TargetScan Human	Experimentally Observed	TNFSF9
hsa-miR-424-5p	TarBase,TargetScan Human	Experimentally Observed	TMEM43
hsa-miR-424-5p	miRecords	Experimentally Observed	TMEM251
hsa-miR-424-5p	TarBase,TargetScan Human	Experimentally Observed	TMEM189-UBE2V1
hsa-miR-424-5p	TarBase	Experimentally Observed	TMEM109
hsa-miR-424-5p	miRecords	Experimentally Observed	TIA1
hsa-miR-424-5p	TarBase,TargetScan Human	Experimentally Observed	SRPRB
hsa-miR-424-5p	TarBase,TargetScan Human	Experimentally Observed	SRPR
hsa-miR-424-5p	TarBase	Experimentally Observed	SQSTM1
hsa-miR-424-5p	TarBase,TargetScan Human	Experimentally Observed	SPTLC1
hsa-miR-424-5p	Ingenuity Expert Findings	Experimentally Observed	SPI1
hsa-miR-424-5p	TarBase	Experimentally Observed	SNX15
hsa-miR-424-5p	TarBase,TargetScan Human	Experimentally Observed	SLC7A1
hsa-miR-424-5p	TarBase	Experimentally Observed	SLC38A5
hsa-miR-424-5p	TarBase	Experimentally Observed	SLC38A1
hsa-miR-424-5p	miRecords	Experimentally Observed	SLC35B3
hsa-miR-424-5p	miRecords	Experimentally Observed	SLC35A1
hsa-miR-424-5p	TarBase,TargetScan Human	Experimentally Observed	SLC25A22
hsa-miR-424-5p	TarBase	Experimentally Observed	SLC16A3
hsa-miR-424-5p	TarBase,TargetScan Human,miRecords	Experimentally Observed	SLC12A2
hsa-miR-424-5p	miRecords	Experimentally Observed	SKAP2
hsa-miR-424-5p	TarBase,TargetScan Human	Experimentally Observed	SHOC2

hsa-miR-424-5p	TarBase	Experimentally Observed	SERPINE2
hsa-miR-424-5p	TarBase,TargetScan Human	Experimentally Observed	SEC24A
hsa-miR-424-5p	TarBase,TargetScan Human	Experimentally Observed	RTN4
hsa-miR-424-5p	miRecords	Experimentally Observed	RNASEL
hsa-miR-424-5p	miRecords	Experimentally Observed	RHOT1
hsa-miR-424-5p	TarBase	Experimentally Observed	RFT1
hsa-miR-424-5p	TargetScan Human,miRecords	Experimentally Observed	RECK
hsa-miR-424-5p	TarBase	Experimentally Observed	RARS
hsa-miR-424-5p	miRecords	Experimentally Observed	RAD51C
hsa-miR-424-5p	TargetScan Human,miRecords	Experimentally Observed	RAB9B
hsa-miR-424-5p	TarBase	Experimentally Observed	RAB30
hsa-miR-424-5p	miRecords	Experimentally Observed	RAB21
hsa-miR-424-5p	miRecords	Experimentally Observed	PWWP2A
hsa-miR-424-5p	Ingenuity Expert Findings,TarBase,TargetScan Human	Experimentally Observed	PURA
hsa-miR-424-5p	TarBase	Experimentally Observed	PTGS2
hsa-miR-424-5p	TarBase,TargetScan Human	Experimentally Observed	PSAT1
hsa-miR-424-5p	miRecords	Experimentally Observed	PRIMPOL
hsa-miR-424-5p	miRecords	Experimentally Observed	PRIM1
hsa-miR-424-5p	TarBase,TargetScan Human	Experimentally Observed	PPP2R5C
hsa-miR-424-5p	TarBase,TargetScan Human	Experimentally Observed	PPIF
hsa-miR-424-5p	TarBase,TargetScan Human	Experimentally Observed	PNP
hsa-miR-424-5p	miRecords	Experimentally Observed	PNN
hsa-miR-424-5p	miRecords	Experimentally Observed	PMS1
hsa-miR-424-5p	TarBase	Experimentally Observed	PLK1
hsa-miR-424-5p	TargetScan Human,miRecords	Experimentally Observed	PLAG1
hsa-miR-424-5p	TarBase,TargetScan Human	Experimentally Observed	PISD
hsa-miR-424-5p	TarBase	Experimentally Observed	PHLDB2
hsa-miR-424-5p	miRecords	Experimentally Observed	PHKB

hsa-miR-424-5p	TargetScan Human,miRecords	Experimentally Observed	PDCD6IP
hsa-miR-424-5p	TargetScan Human,miRecords	Experimentally Observed	PDCD4
hsa-miR-424-5p	TarBase	Experimentally Observed	PANX1
hsa-miR-424-5p	TarBase,TargetScan Human	Experimentally Observed	PAFAH1B2
hsa-miR-424-5p	miRecords	Experimentally Observed	OSGEPL1
hsa-miR-424-5p	miRecords	Experimentally Observed	OMA1
hsa-miR-424-5p	miRecords	Experimentally Observed	NT5DC1
hsa-miR-424-5p	TarBase	Experimentally Observed	NPR3
hsa-miR-424-5p	TarBase,TargetScan Human	Experimentally Observed	NOTCH2
hsa-miR-424-5p	miRecords	Experimentally Observed	NIPAL2
hsa-miR-424-5p	Ingenuity Expert Findings,miRecords	Experimentally Observed	NFIA
hsa-miR-424-5p	TarBase,TargetScan Human	Experimentally Observed	NAPG
hsa-miR-424-5p	TarBase,TargetScan Human	Experimentally Observed	NAA15
hsa-miR-424-5p	TargetScan Human,miRecords	Experimentally Observed	MYB
hsa-miR-424-5p	miRecords	Experimentally Observed	MSH2
hsa-miR-424-5p	TarBase	Experimentally Observed	MRPL20
hsa-miR-424-5p	TarBase	Experimentally Observed	MLLT1
hsa-miR-424-5p	Ingenuity Expert Findings	Experimentally Observed	mir-9
hsa-miR-424-5p	miRecords	Experimentally Observed	MCL1
hsa-miR-424-5p	Ingenuity Expert Findings	Experimentally Observed	MAPK3
hsa-miR-424-5p	TargetScan Human,miRecords	Experimentally Observed	MAP2K4
hsa-miR-424-5p	TargetScan Human,miRecords	Experimentally Observed	MAP2K1
hsa-miR-424-5p	TarBase,TargetScan Human	Experimentally Observed	LYPLA2
hsa-miR-424-5p	TarBase,TargetScan Human	Experimentally Observed	LUZP1
hsa-miR-424-5p	TarBase	Experimentally Observed	LAMTOR5
hsa-miR-424-5p	TarBase,TargetScan Human	Experimentally Observed	LAMTOR3
hsa-miR-424-5p	TarBase,TargetScan Human	Experimentally Observed	LAMC1
hsa-miR-424-5p	TarBase,TargetScan Human	Experimentally Observed	KPNA3

hsa-miR-424-5p	Ingenuity Expert Findings,TargetScan Human	Experimentally Observed	KIF23
hsa-miR-424-5p	TarBase,TargetScan Human	Experimentally Observed	KCNN4
hsa-miR-424-5p	miRecords	Experimentally Observed	JUN
hsa-miR-424-5p	TarBase,TargetScan Human	Experimentally Observed	ITGA2
hsa-miR-424-5p	TarBase	Experimentally Observed	IPO4
hsa-miR-424-5p	TarBase,TargetScan Human	Experimentally Observed	IGF2R
hsa-miR-424-5p	TarBase,TargetScan Human	Experimentally Observed	IFRD1
hsa-miR-424-5p	TarBase	Experimentally Observed	HYAL3
hsa-miR-424-5p	TarBase,TargetScan Human,miRecords	Experimentally Observed	HSPA1A/HSPA1B
hsa-miR-424-5p	miRecords	Experimentally Observed	HSP90B1
hsa-miR-424-5p	TargetScan Human,miRecords	Experimentally Observed	HSDL2
hsa-miR-424-5p	miRecords	Experimentally Observed	HRSP12
hsa-miR-424-5p	TarBase	Experimentally Observed	HMOX1
hsa-miR-424-5p	TargetScan Human,miRecords	Experimentally Observed	HMGA1
hsa-miR-424-5p	TargetScan Human,miRecords	Experimentally Observed	HERC6
hsa-miR-424-5p	miRecords	Experimentally Observed	HDHD2
hsa-miR-424-5p	TarBase	Experimentally Observed	HARS
hsa-miR-424-5p	miRecords	Experimentally Observed	HACE1
hsa-miR-424-5p	miRecords	Experimentally Observed	H3F3A/H3F3B
hsa-miR-424-5p	miRecords	Experimentally Observed	GTF2H1
hsa-miR-424-5p	TarBase	Experimentally Observed	GSTM4
hsa-miR-424-5p	TarBase	Experimentally Observed	GPAM
hsa-miR-424-5p	miRecords	Experimentally Observed	GOLPH3L
hsa-miR-424-5p	miRecords	Experimentally Observed	GOLGA5
hsa-miR-424-5p	TarBase	Experimentally Observed	GNL3L
hsa-miR-424-5p	TarBase	Experimentally Observed	GFPT1
hsa-miR-424-5p	TarBase	Experimentally Observed	GFM1
hsa-miR-424-5p	TarBase,TargetScan Human	Experimentally Observed	GALNT7
hsa-miR-424-5p	TarBase,TargetScan Human	Experimentally Observed	FNDC3B

hsa-miR-424-5p	Ingenuity Expert Findings,TargetScan Human,miRecords	Experimentally Observed	FGFR1
hsa-miR-424-5p	Ingenuity Expert Findings,TargetScan Human	Experimentally Observed	FGF7
hsa-miR-424-5p	Ingenuity Expert Findings,TarBase,TargetScan Human	Experimentally Observed	FGF2
hsa-miR-424-5p	miRecords	Experimentally Observed	FAM69A
hsa-miR-424-5p	TargetScan Human,miRecords	Experimentally Observed	FAM122C
hsa-miR-424-5p	TarBase	Experimentally Observed	F2
hsa-miR-424-5p	TarBase,TargetScan Human	Experimentally Observed	EIF4E
hsa-miR-424-5p	TarBase	Experimentally Observed	EGFR
hsa-miR-424-5p	TargetScan Human,miRecords	Experimentally Observed	ECHDC1
hsa-miR-424-5p	TargetScan Human,miRecords	Experimentally Observed	E2F3
hsa-miR-424-5p	TarBase	Experimentally Observed	DTD1
hsa-miR-424-5p	TarBase,TargetScan Human	Experimentally Observed	DNAJB4
hsa-miR-424-5p	TarBase,TargetScan Human,miRecords	Experimentally Observed	DMTF1
hsa-miR-424-5p	miRecords	Experimentally Observed	CSHL1
hsa-miR-424-5p	miRecords	Experimentally Observed	CRHBP
hsa-miR-424-5p	miRecords	Experimentally Observed	CREBL2
hsa-miR-424-5p	TargetScan Human,miRecords	Experimentally Observed	CLDN12
hsa-miR-424-5p	TarBase,TargetScan Human	Experimentally Observed	CHORDC1
hsa-miR-424-5p	Ingenuity Expert Findings,TargetScan Human	Experimentally Observed	CHEK1
hsa-miR-424-5p	miRecords	Experimentally Observed	CFL2
hsa-miR-424-5p	miRecords	Experimentally Observed	CEP63
hsa-miR-424-5p	miRecords	Experimentally Observed	CENPJ
hsa-miR-424-5p	TargetScan Human,miRecords	Experimentally Observed	CDK6
hsa-miR-424-5p	TarBase	Experimentally Observed	CDK5RAP1
hsa-miR-424-5p	Ingenuity Expert Findings,TargetScan Human	Experimentally Observed	CDC25A
hsa-miR-424-5p	TargetScan Human,miRecords	Experimentally Observed	CDC14B

hsa-miR-424-5p	Ingenuity Expert Findings,TargetScan Human	Experimentally Observed	CDC14A
hsa-miR-424-5p	Ingenuity Expert Findings	Experimentally Observed	CCNF
hsa-miR-424-5p	Ingenuity Expert Findings,TargetScan Human,miRecords	Experimentally Observed	CCNE1
hsa-miR-424-5p	TargetScan Human,miRecords	Experimentally Observed	CCND3
hsa-miR-424-5p	Ingenuity Expert Findings,TargetScan Human,miRecords	Experimentally Observed	CCND1
hsa-miR-424-5p	miRecords	Experimentally Observed	CARD8
hsa-miR-424-5p	TargetScan Human,miRecords	Experimentally Observed	CAPRIN1
hsa-miR-424-5p	miRecords	Experimentally Observed	CADM1
hsa-miR-424-5p	TarBase	Experimentally Observed	CACNA2D1
hsa-miR-424-5p	TarBase,TargetScan Human	Experimentally Observed	CA12
hsa-miR-424-5p	miRecords	Experimentally Observed	C4orf27
hsa-miR-424-5p	miRecords	Experimentally Observed	C2orf74
hsa-miR-424-5p	miRecords	Experimentally Observed	C2orf43
hsa-miR-424-5p	TarBase	Experimentally Observed	C1orf56
hsa-miR-424-5p	miRecords	Experimentally Observed	C17orf80
hsa-miR-424-5p	miRecords	Experimentally Observed	BMI1
hsa-miR-424-5p	TargetScan Human,miRecords	Experimentally Observed	BDNF
hsa-miR-424-5p	Ingenuity Expert Findings,TargetScan Human,miRecords	Experimentally Observed	BCL2L2
hsa-miR-424-5p	Ingenuity Expert Findings,TarBase,TargetScan Human,miRecords	Experimentally Observed	BCL2
hsa-miR-424-5p	TarBase,TargetScan Human	Experimentally Observed	ATG9A
hsa-miR-424-5p	Ingenuity Expert Findings,TargetScan Human	Experimentally Observed	ATF6
hsa-miR-424-5p	miRecords	Experimentally Observed	ASXL2
hsa-miR-424-5p	TargetScan Human,miRecords	Experimentally Observed	ARL2
hsa-miR-424-5p	TarBase,TargetScan Human	Experimentally Observed	ARHGDIA
hsa-miR-424-5p	Ingenuity Expert Findings,TargetScan Human	Experimentally Observed	ANLN
hsa-miR-424-5p	miRecords	Experimentally	ANAPC16

		Observed	
hsa-miR-424-5p	TarBase	Experimentally Observed	ADSS
hsa-miR-424-5p	TargetScan Human,miRecords	Experimentally Observed	ACTR1A
hsa-miR-424-5p	TarBase	Experimentally Observed	ACP2
hsa-miR-424-5p	TarBase	Experimentally Observed	ABHD10
hsa-miR-424-5p	TarBase	Experimentally Observed	ABCF2
hsa-miR-146a-5p	miRecords	Experimentally Observed	VWCE
hsa-miR-146a-5p	TargetScan Human,miRecords	Experimentally Observed	UHRF1
hsa-miR-146a-5p	miRecords	Experimentally Observed	TRIM14
hsa-miR-146a-5p	Ingenuity Expert Findings,TargetScan Human	Experimentally Observed	TRAF6
hsa-miR-146a-5p	miRecords	Experimentally Observed	TMSB15A
hsa-miR-146a-5p	Ingenuity Expert Findings	Experimentally Observed	TLR9
hsa-miR-146a-5p	Ingenuity Expert Findings	Experimentally Observed	TLR4
hsa-miR-146a-5p	Ingenuity Expert Findings	Experimentally Observed	TLR10
hsa-miR-146a-5p	Ingenuity Expert Findings	Experimentally Observed	TLR1
hsa-miR-146a-5p	TargetScan Human,miRecords	Experimentally Observed	TIMELESS
hsa-miR-146a-5p	Ingenuity Expert Findings,TargetScan Human	Experimentally Observed	SYT1
hsa-miR-146a-5p	miRecords	Experimentally Observed	STAT1
hsa-miR-146a-5p	Ingenuity Expert Findings	Experimentally Observed	SFTPD
hsa-miR-146a-5p	miRecords	Experimentally Observed	SDCBP2
hsa-miR-146a-5p	Ingenuity Expert Findings	Experimentally Observed	S100A12
hsa-miR-146a-5p	miRecords	Experimentally Observed	RAD54L
hsa-miR-146a-5p	Ingenuity Expert Findings	Experimentally Observed	PTGES2
hsa-miR-146a-5p	Ingenuity Expert Findings	Experimentally Observed	PTAFR
hsa-miR-146a-5p	miRecords	Experimentally Observed	PRR15
hsa-miR-146a-5p	miRecords	Experimentally Observed	POLE2
hsa-miR-146a-5p	miRecords	Experimentally Observed	PLEKHA4
hsa-miR-146a-5p	Ingenuity Expert Findings	Experimentally Observed	PGLYRP2
hsa-miR-146a-5p	Ingenuity Expert Findings	Experimentally Observed	PGLYRP1

hsa-miR-146a-5p	miRecords	Experimentally Observed	PEX11G
hsa-miR-146a-5p	miRecords	Experimentally Observed	PDIK1L
hsa-miR-146a-5p	TargetScan Human,miRecords	Experimentally Observed	PBLD
hsa-miR-146a-5p	miRecords	Experimentally Observed	PA2G4
hsa-miR-146a-5p	Ingenuity Expert Findings,TargetScan Human	Experimentally Observed	NOVA1
hsa-miR-146a-5p	Ingenuity Expert Findings	Experimentally Observed	NOS2
hsa-miR-146a-5p	Ingenuity Expert Findings	Experimentally Observed	NLGN1
hsa-miR-146a-5p	TargetScan Human,miRecords	Experimentally Observed	NFIX
hsa-miR-146a-5p	miRecords	Experimentally Observed	MR1
hsa-miR-146a-5p	TargetScan Human,miRecords	Experimentally Observed	MMP16
hsa-miR-146a-5p	miRecords	Experimentally Observed	METTL7A
hsa-miR-146a-5p	miRecords	Experimentally Observed	MCPH1
hsa-miR-146a-5p	miRecords	Experimentally Observed	MCM10
hsa-miR-146a-5p	Ingenuity Expert Findings	Experimentally Observed	LTF
hsa-miR-146a-5p	miRecords	Experimentally Observed	LTB
hsa-miR-146a-5p	Ingenuity Expert Findings	Experimentally Observed	LBP
hsa-miR-146a-5p	Ingenuity Expert Findings	Experimentally Observed	LALBA
hsa-miR-146a-5p	miRecords	Experimentally Observed	KIF22
hsa-miR-146a-5p	miRecords	Experimentally Observed	IRF5
hsa-miR-146a-5p	miRecords	Experimentally Observed	IRAK2
hsa-miR-146a-5p	TargetScan Human,miRecords	Experimentally Observed	IRAK1
hsa-miR-146a-5p	Ingenuity Expert Findings	Experimentally Observed	IL37
hsa-miR-146a-5p	Ingenuity Expert Findings	Experimentally Observed	IL36RN
hsa-miR-146a-5p	Ingenuity Expert Findings	Experimentally Observed	IL36G
hsa-miR-146a-5p	Ingenuity Expert Findings	Experimentally Observed	IL36B
hsa-miR-146a-5p	Ingenuity Expert Findings	Experimentally Observed	IL36A
hsa-miR-146a-5p	Ingenuity Expert Findings	Experimentally Observed	IL1RL2
hsa-miR-146a-5p	Ingenuity Expert Findings	Experimentally Observed	IL1RAPL2
hsa-miR-146a-5p	Ingenuity Expert Findings	Experimentally Observed	IL1RAP

hsa-miR-146a-5p	Ingenuity Expert Findings	Experimentally Observed	IL1R1
hsa-miR-146a-5p	Ingenuity Expert Findings	Experimentally Observed	IL1F10
hsa-miR-146a-5p	Ingenuity Expert Findings	Experimentally Observed	IL12RB2
hsa-miR-146a-5p	Ingenuity Expert Findings	Experimentally Observed	IL10
hsa-miR-146a-5p	Ingenuity Expert Findings	Experimentally Observed	IFNB1
hsa-miR-146a-5p	Ingenuity Expert Findings	Experimentally Observed	IFNA1/IFNA13
hsa-miR-146a-5p	miRecords	Experimentally Observed	FADD
hsa-miR-146a-5p	Ingenuity Expert Findings	Experimentally Observed	DMBT1
hsa-miR-146a-5p	miRecords	Experimentally Observed	CXCR4
hsa-miR-146a-5p	Ingenuity Expert Findings	Experimentally Observed	CXCL8
hsa-miR-146a-5p	Ingenuity Expert Findings	Experimentally Observed	CRP
hsa-miR-146a-5p	miRecords	Experimentally Observed	COL13A1
hsa-miR-146a-5p	Ingenuity Expert Findings	Experimentally Observed	CHUK
hsa-miR-146a-5p	Ingenuity Expert Findings,TargetScan Human,miRecords	Experimentally Observed	CFH
hsa-miR-146a-5p	miRecords	Experimentally Observed	CDKN3
hsa-miR-146a-5p	Ingenuity Expert Findings	Experimentally Observed	CD40
hsa-miR-146a-5p	Ingenuity Expert Findings	Experimentally Observed	CD1D
hsa-miR-146a-5p	Ingenuity Expert Findings	Experimentally Observed	CCR3
hsa-miR-146a-5p	miRecords	Experimentally Observed	CCNA2
hsa-miR-146a-5p	miRecords	Experimentally Observed	CCL8
hsa-miR-146a-5p	Ingenuity Expert Findings	Experimentally Observed	CAMP
hsa-miR-146a-5p	Ingenuity Expert Findings	Experimentally Observed	C8A
hsa-miR-146a-5p	miRecords	Experimentally Observed	BRCA1
hsa-miR-146a-5p	miRecords	Experimentally Observed	BLMH
hsa-miR-146a-5p	miRecords	Experimentally Observed	ATOH8
hsa-miR-130a-3p	TargetScan Human,miRecords	Experimentally Observed	ZFPM2
hsa-miR-130a-3p	TarBase	Experimentally Observed	TAC1
hsa-miR-130a-3p	Ingenuity Expert Findings,TargetScan Human	Experimentally Observed	SMAD4

hsa-miR-130a-3p	TarBase,TargetScan Human,miRecords	Experimentally Observed	MEOX2
hsa-miR-130a-3p	TarBase,TargetScan Human,miRecords	Experimentally Observed	MAFB
hsa-miR-130a-3p	TarBase,TargetScan Human,miRecords	Experimentally Observed	HOXA5
hsa-miR-130a-3p	Ingenuity Expert Findings,TargetScan Human	Experimentally Observed	DICER1
hsa-miR-130a-3p	TarBase,TargetScan Human,miRecords	Experimentally Observed	CSF1
hsa-miR-130a-3p	Ingenuity Expert Findings,TargetScan Human	Experimentally Observed	ATG2B
hsa-miR-151a-5p	TarBase	Experimentally Observed	E2F6
hsa-miR-151a-5p	TarBase	Experimentally Observed	MPL
hsa-miR-151a-5p	TarBase	Experimentally Observed	N4BP1
hsa-miR-151a-5p	TarBase	Experimentally Observed	ARHGDIA
hsa-miR-582-5p	TarBase	Experimentally Observed	MCL1
hsa-miR-638	TarBase	Experimentally Observed	OSCP1
has-miR-2861	(Li, Xie et al. 2009, Fischer, Paul et al. 2015)	Experimentally Observed	HDAC5